F 1503/3

BULETINUL INSTITUTULUI POLITEHNIC DIN IAŞI

Tomul XXXVI (XL)

Fasc. 1–2

Secţia III

ELECTROTEHNICĂ
ENERGETICĂ
ELECTRONICĂ
AUTOMATIZĂRI

1990

BULETINUL INSTITUTULUI POLITEHNIC DIN IAŞI

BIBLIOTECA CENTRALĂ UNIVERSITARĂ

Tomul XXXVI (XL)

Fasc. 1–2

Secţia III ELECTROTEHNICĂ
ENERGETICĂ
ELECTRONICĂ
AUTOMATIZĂRI

1990

EDITORIAL STAFF

Prof dr. ing. **VITALIE BELOUSOV** (President)

Prof. dr. doc. **D. I. MANGERON** (Honorary President)

Conf. dr. ing. **MIRCEA MANOLOVICI** (Secretary)

Conf. dr. ing. **MATEI MACOVEANU**

Prof. dr. doc. **ALFRED BRAIER** (Editor)

Prof. dr. ing. **HUGO ROSMAN** (Editor)

Prof. dr. ing. **MIHAIL VOICU** (Head of the Exchange Service)

Prof. dr. **AUREL BEJANCU**

Prof. dr. ing. **VICTOR BULACOVSCHI**

Prof. dr. ing. **MIHAI LUCANU**

Prof. dr. ing. **SPIRIDON CREȚU**

Prof. dr. ing. **ADRIAN RADU**

Prof. dr. ing. **AURELIA GRIGORIU**

BULETINUL INSTITUTULUI POLITEHNIC DIN IAŞI
BULLETIN OF THE POLYTECHNIC INSTITUTE OF JASSY
ИЗВЕСТИЯ ЯССКОГО ПОЛИТЕХНИЧЕСКОГО ИНСТИТУТА
Tomul XXVXI (XL), Fasc. 1–2 1990

Secţia III

ELECTROTEHNICĂ ENERGETICĂ. ELECTRONICĂ. AUTOMATIZĂRI

SUMAR

Pag.

F. TRIFAN şi C. PETRESCU, Studiul cîmpului magnetic creat de un tub omogen dielectric în mişcare uniformă într-un cîmp electric omogen (engl., rez. rom.) . . . 1
H. ROSMAN, O generalizare a teoremei lui Schérer relativă la cuadripoli generali liniari neautonomi în regim permanent armonic (franc., rez. rom.) . . . 7
S. MITREA şi A. ADĂSCĂLIŢEI, Asupra determinării curentului de magnetizare necesar pentru evitarea ferorezonanţei serie (engl., rez. rom.) . . . 13
V. GRIGORAŞ, Filtrarea numerică a semnalelor codate prin predicţie liniară (engl., rez. rom.) . . . 17
M. VOICU, Condiţii suficiente de existenţă a ciclurilor limită (engl., rez. rom.). 23
D. BALAN şi T. BALAN, Asupra pierderilor de energie în miezurile magnetice din ferită ale bobinelor liniare în regim periodic permanent nesinusoidal (franc., rez. rom.) . . . 27
A. BARABOI şi M. ADAM, Încălzirea în regim permanent a piesei de grafit din construcţia unui contact electric punctiform de tip alunecător (franc., rez. rom.) . . . 33
E. HNATIUC, Cu privire la funcţionarea electromagneţilor monofazaţi de curent alternativ de tip E–I prevăzuţi cu două spire în scurtcircuit (franc., rez. rom.) . . . 39
I.-C. TEŞU, O. PĂSTRĂVANU, D. ŞTIURCĂ şi T. GANCIU, Extragerea parametrilor Gummel-Poon pentru aplicaţii în proiectarea asistată de calculator cu SPICE (engl., rez. rom.) . . . 43
M. ANTONESCU, I. ANTONESCU, P. DUMA şi E. BANU, Asupra problemelor de software legate de realizarea unui calculator de bord destinat urmăririi unor parametri de deplasare ai autovehiculelor şi ai motoarelor (germ., rez. rom.) . . . 55
L. BRENIUC, M. CREŢU şi C. SĂRMĂŞANU, Convertor analog–numeric cu rezoluţie programabilă (franc., rez. rom.) . . . 61
M. FLOREA, AL. LAZĂR şi C. POŞA, Consideraţii privind un invertor tranzistoriza tmonofazat caracterizat printr-o tensiune joasă de alimentare şi de o undă cu conţinut bogat în fundamentală (engl., rez. rom.) . . . 67
I. POPESCU, I. ZAHARIA şi C. PETRESCU, Regimuri de rezonanţă pe armonici în reţele care alimentează staţii de tracţiune electrică feroviară (engl., rez. rom.) . . . 73
GH. CÎRŢINĂ, Influenţa erorilor informaţiei asupra calculului regimurilor sistemelor electroenergetice (franc., rez. rom.) . . . 79
|GHEORGHE VASILIU| (H. Rosman) . . . 83
RECENZII . . . 85

BULETINUL INSTITUTULUI POLITEHNIC DIN IAŞI
BULLETIN OF THE POLYTECHNIC INSTITUTE OF JASSY
ИЗВЕСТИЯ ЯССКОГО ПОЛИТЕХНИЧЕСКОГО ИНСТИТУТА
Tome XXXVI (XL), Fasc. 1–2 1990

Section III

ELECTROTECHNICS ENERGETICS. ELECTRONICS. AUTOMATION

CONTENTS

Pp.

F. TRIFAN and C. PETRESCU, Study of the Magnetic Field Created by a Dielectric Tube Moving Uniformly in an Homogeneous Electric Field (English, Romanian summary) 1

H. ROSMAN, Une généralisation du théorème de Schérer relatif aux quadripôles générals linéaires nonautonomes, en régime permanent harmonique (French, Romanian summary) 7

S. MITREA and A. ADĂSCĂLIŢEI, Upon the Determination of Magnetizing current to Prevent Series Ferroresonance (English, Romanian summary) 13

V. GRIGORAŞ, Digital Filtering of Linear Predictive Coded Signals (English, Romanian summary) 17

M. VOICU, Sufficient Existence Conditions of Limit Cycles (English, Romanian summary) 23

D. BALAN et T. BALAN, Sur les pertes d'énergie dans les noyaux magnétiques de ferrite des bobines linéaires en régime permanent périodique nonsinusoïdal (French, Romanian summary) 27

A. BARABOI et M. ADAM, L'échauffement en régime permanent de la pièce en graphite d'un contact électrique glissant (French, Romanian summary)

E. HNATIUC, Sur le fonctionnement des électro-aimants monophasés à courant alternatif de type E–I ayant deux bagues de déphasage (French, Romanian summary) 33 39

I.-C. TEŞU, O. PĂSTRĂVANU, D. ŞTIURCĂ and T. GANCIU, Gummel-Poon Parameters Optimal Extraction for Computer-aided Design with SPICE (English, Romanian summary) 43

M. ANTONESCU, I. ANTONESCU, P. DUMA und E. BANU, Über Softwarefragen die sich auf die Realisierung eines Bordrechners zur Überwachung einiger Bewegungsparametern der Fahrzeugen unde deren Motoren beziehen (German, Romanian summary) 55

L. BRENIUC, M. CREŢU et C. SĂRMĂŞANU, Convertisseur analogique–digital avec résolution en programme (French, Romanian summary) 61

M. FLOREA, AL. LAZĂR and C. POŞA, Considerations concerning a Transistorised Monophase Inverter Characterised by Low Voltage Power Supply and a Wave with High Content in Fundamental (English, Romanian summary) 67

I. POPESCU, I. ZAHARIA and C. PETRESCU, Harmonic Resonance Effects on Electric Networks Supplying Electrical Traction Stations (English, Romanian summary) 73

GH. CÎRŢINĂ, L'influence des erreurs de l'information sur les calculs des régimes des systèmes électroénergetiques (French, Romanian summary) 79

GHEORGHE VASILIU (H. Rosman) 83

BOOK REVIEWS 85

BULETINUL INSTITUTULUI POLITEHNIC DIN IAȘI
Tomul XXXVI (XL) Fasc. 1—2, 1990
Secția III
ELECTROTEHNICĂ. ENERGETICĂ. ELECTRONICĂ. AUTOMATIZĂRI

D.C. 538.12

STUDY OF THE MAGNETIC FIELD CREATED BY A DIELECTRIC TUBE MOVING UNIFORMLY IN AN HOMOGENEOUS ELECTRIC FIELD

BY

FLORENTINA TRIFAN and CAMELIA PETRESCU

1. Introduction

The aim of this paper is to determine the magnetic field created by a dielectric tube moving uniformly in air with a constant velocity, v, in axial direction in an homogeneous electric field. The length of the tube being large as compared to its radius, the problem has a translational symmetry, so that both the electric and magnetic fields may be studied in a plane transversal to the tube axis. A cross-section of the dielectric tube is represented in Fig. 1.

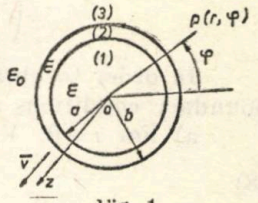

Fig. 1

2. Computation of the Electric Field Intensity

If the field is stationary or quasi-stationary the variation of the magnetic flux density, $\partial\mathcal{B}/\partial t$, may be considered equal to zero, so that the electric field is irotational. In this problem the electric field has no sources, and cnnsequently the scalar electric potential satisfies L a p l a c e's equation :

$$\Delta V=0. \tag{1}$$

The boundary conditions for this problem concern the electric field which is uniform and finite at infinity, $\mathbf{E}_0$. Due to the geometrical symmetry of the field, Eq. (1) must be treated in polar coordinates. The general solution for Eq. (1) in such coordinates is [1] :

$$V(r,\varphi)=(A_0\ln r+B_0)(C_0\varphi+D_0)+\sum_{k=1}^{\infty}(A_kr^k+B_kr^{-k})(C_k\sin k\varphi+D_k\cos k\varphi). \tag{2}$$

The function $V(r,\varphi)$ is even with respect to φ so that :

$$C_0=C_k=0. \tag{3}$$

For $r=0$, $V(0,0)=$finite and consequently

$$A_0=0. \tag{4}$$

We conclude that :

$$V(r, \varphi)=\sum_{k=1}^{\infty}(A_k r^k+B_k r^{-k})\cos k\varphi. \tag{5}$$

Since $\mathbf{E}$ must be finite everywhere and taking into account that :

$$\begin{aligned}\mathbf{E}&=-\operatorname{grad} V=-\frac{\partial V}{\partial r}\mathbf{u}_r-\frac{1}{r}\cdot\frac{\partial V}{\partial \varphi}\mathbf{u}_\varphi=\\ &=-\sum_{k=1}^{\infty}(kA_k r^{k-1}-kB_k r^{-k-1})\cos k\varphi\,\mathbf{u}_r-\frac{1}{r}\cdot\frac{\partial V}{\partial \varphi}\mathbf{u}_\varphi,\end{aligned} \tag{6}$$

we conclude that necessarily $k=1$.

Finally, relations (3) ... (6) give :

$$\begin{cases} V_1(r, \varphi)=\left(A_1 r+\dfrac{B_1}{r}\right)\cos\varphi, & r<a,\\ V_2(r, \varphi)=\left(A_2 r+\dfrac{B_2}{r}\right)\cos\varphi, & a<r<b,\\ V_3(r, \varphi)=\left(A_3 r+\dfrac{B_3}{r}\right)\cos\varphi, & r>b. \end{cases} \tag{7}$$

In order to obtain the constants A_1, B_1, A_2, B_2, A_3, B_3 the following boundary conditions are used :

a) For $r=0$, V_1 is finite so that :

$$B_1=0. \tag{8}$$

b) For $r\to\infty$, $\mathbf{E}_3\to\mathbf{E}_0$ and

$$\mathbf{E}_3=-\operatorname{grad} V_3=-\left(A_3-\frac{B_3}{r^2}\right)\cos\varphi\,\mathbf{u}_r+\left(A_3+\frac{B_3}{r^2}\right)\sin\varphi\,\mathbf{u}_\varphi \tag{9}$$

and consequently

$$\lim_{r\to\infty} E_r=E_0\cos\varphi=-A_3\cos\varphi. \tag{10}$$

In conclusion it results that

$$A_3=-E_0. \tag{11}$$

e) For $r=a$ and $r=b$, respectively, the normal components of the electric flux density and tangential components of the electric field intensity are continuous :

$$\begin{cases} \left.\dfrac{\partial V_1}{\partial r}\right|_{r=a}=\varepsilon_r\left.\dfrac{\partial V_2'}{\partial r}\right|_{r=a}, & \varepsilon_r\left.\dfrac{\partial V_2}{\partial r}\right|_{r=b}=\left.\dfrac{\partial V_3}{\partial r}\right|_{r=b};\\ \left.\dfrac{\partial V_2'}{\partial \varphi}\right|_{r=a}=\left.\dfrac{\partial V_1}{\partial \varphi}\right|_{r=a}, & \left.\dfrac{\partial V_2}{\partial \varphi}\right|_{r=b}=\left.\dfrac{\partial V_3}{\partial \varphi}\right|_{r=b}. \end{cases} \tag{12}$$

Using relations (7) and (12) the following expressions for A_1, A_2, B_2, B_3, are obtained :

$$(13)\quad \begin{cases} A_1 = \dfrac{4E_0\varepsilon_r b^2}{a^2(1-\varepsilon_r)^2 - b^2(1+\varepsilon_r)^2}, & A_2 = \dfrac{2E_0 b^2(\varepsilon_r+1)}{a^2(1-\varepsilon_r)^2 - b^2(1+\varepsilon_r)^2}, \\ B_2 = \dfrac{2E_0 a^2 b^2(\varepsilon_r-1)}{a^2(1-\varepsilon_r)^2 - b^2(1+\varepsilon_r)^2}, & B_3 = \dfrac{E_0 b^2(1-\varepsilon_r^2)(a^2-b^2)}{b^2(1+\varepsilon_r)^2 - a^2(1-\varepsilon_r)^2}. \end{cases}$$

The final expressions for the electric potential in the three regions are :

$$(14)\quad \begin{cases} V_1(r,\varphi) = \dfrac{4E_0\varepsilon_r b^2}{a^2(1-\varepsilon_r)^2 - b^2(1+\varepsilon_r)^2} r\cos\varphi, \quad r<a; \\ V_2(r,\varphi) = \left[\dfrac{2E_0 b^2(\varepsilon_r+1)}{a^2(1-\varepsilon_r)^2 - b^2(1+\varepsilon_r)^2} r + \dfrac{2E_0 a^2 b^2(\varepsilon_r-1)}{a^2(1-\varepsilon_r)^2 - b^2(1+\varepsilon_r)^2}\cdot\dfrac{1}{r}\right]\cos\varphi, \\ \qquad\qquad a<r<b; \\ V_3(r,\varphi) = \left[-E_0 r + \dfrac{E_0 b^2(1-\varepsilon_r^2)(a^2-b^2)}{b^2(1+\varepsilon_r)^2 - a^2(1-\varepsilon_r)^2}\cdot\dfrac{1}{r}\right]\cos\varphi, \quad r>b \end{cases}$$

3. Computation of the Polarization Charge

The dielectric tube is polarized by the electric field ; this fact leads to the appearance of polarization charges.

The volume polarization charge density is zero because :

$$(15)\qquad \rho_{pv} = -\operatorname{div}\mathbf{P} = -\operatorname{div}(\varepsilon-\varepsilon_0)\mathbf{E} = (\varepsilon-\varepsilon_0)\Delta V = 0.$$

The surface densities of the polarization charge are :

$$(16)\quad \begin{cases} \rho_{ps}\Big|_{r=a} = -\operatorname{div}_s\mathbf{P} = -\mathbf{Pn} = (\varepsilon_0-\varepsilon)E_r = (\varepsilon-\varepsilon_0)\dfrac{\partial V_2}{\partial r}\Big|_{r=a}; \\ \rho_{ps}\Big|_{r=b} = (\varepsilon_0-\varepsilon)\left(A_2 - \dfrac{B_2}{b^2}\right)\cos\varphi, \end{cases}$$

or, using, relations (13) :

$$(17)\quad \begin{cases} \rho_{ps}\Big|_{r=a} = \dfrac{4E_0 b^2(\varepsilon-\varepsilon_0)}{a^2(1-\varepsilon_r)^2 - b^2(1+\varepsilon_r)^2}\cos\varphi, \\ \rho_{ps}\Big|_{r=b} = \dfrac{2E_0(\varepsilon_0-\varepsilon)[\varepsilon_r(b^2-a^2)+a^2+b^2]}{a^2(1-\varepsilon_r)^2 - b^2(1+\varepsilon_r)^2}\cos\varphi. \end{cases}$$

4. Computation of the Magnetic Field Created by the Temporary Polarized Dielectric Tube, Moving in Axial Direction

The polarized dilectric tube moving in axial direction is equivalent to two Röntgen surface currents placed on the surfaces of the tube ($r=a$ and $r=b$). The Röntgen surface current densities are computed by means of the following relations :

$$(18)\quad \begin{cases} \mathbf{J}^{(ex)}_{l_{R_a}} = \operatorname{rot},\ (\mathbf{P}\times\mathbf{v}) = \mathbf{n}_{12}\times(\mathbf{P}_2\times\mathbf{v}_2 - \mathbf{P}_1\times\mathbf{v}_1) = \mathbf{n}_{12}\times(\mathbf{P}_2\times\mathbf{v}) = \\ \qquad\qquad = -P_{2r}v\mathbf{k}|_{r=a} = -\rho_{ps}|_{r=a}\mathbf{v}, \\ \mathbf{J}^{(ex)}_{l_{R_b}} = P_{2r}v\mathbf{k}|_{r=b} = \rho_{ps}|_{r=b}\mathbf{v}. \end{cases}$$

Using relations (17) for the surface polarization charge density, relations (18) become :

$$(19)\quad \begin{cases} \mathbf{J}^{(ex)}_{l_{R_a}} = \dfrac{4(\varepsilon-\varepsilon_0)E_0b^2\mathbf{v}}{a^2(1-\varepsilon_r)^2 - b^2(1+\varepsilon_r)^2}\cos\varphi = \mathbf{k}_1\cos\varphi, \\ \mathbf{J}^{(ex)}_{l_{R_b}} = \dfrac{2E_0(\varepsilon_0-\varepsilon_1)[\varepsilon_r(b^2-a^2)+a^2+b^2]}{a^2(1-\varepsilon_r)^2 - b^2(1+\varepsilon_r)^2}\cos\varphi\ \mathbf{v} = \mathbf{k}_2\cos\varphi, \end{cases}$$

where

$$(20)\quad \mathbf{k}_1 = \frac{4(\varepsilon-\varepsilon_0)E_0b^2\mathbf{v}}{a^2(1-\varepsilon_r)^2 - b^2(1+\varepsilon_r)^2},\quad \mathbf{k}_2 = \frac{2E_0(\varepsilon_0-\varepsilon_1)[\varepsilon_r(b^2-a^2)+a^2+b^2]}{a^2(1-\varepsilon_r)^2 - b^2(1+\varepsilon_r)^2}\mathbf{v}.$$

Due to the dependence of $\mathbf{J}^{(ex)}_{l_{Ra}}$ and $\mathbf{J}^{(ex)}_{l_{Rb}}$ w.r.t. variable φ, the computation of the magnetic field intensity using the magnetic circuit law is not adequate. In order to obtain the magnetic field intensity, the superposition of effects principle may be used namely : the elementary magnetic fields $\mathbf{dH}_1$ and $\mathbf{dH}_2$ produced by long, straight conductors with the infinitesimal width $a\,\mathrm{d}\varphi$ and $b\,\mathrm{d}\varphi$, respectively, are superposed in a given point $P(r_0,\ \varphi_0)$ to obtain the resultant field $\mathbf{H}$. Using the notations from Fig. 2, $\mathrm{d}H_1$ and $\mathrm{d}H_2$ are :

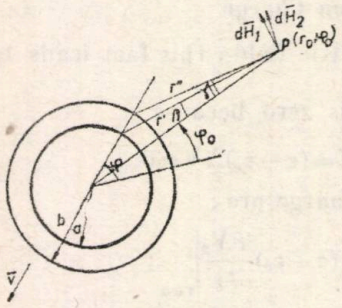

Fig. 2

$$(21)\quad \mathrm{d}H_1 = \frac{J^{(ex)}_{l_{Ra}}\,a\,\mathrm{d}\varphi}{2\pi r'},\quad \mathrm{d}H_2 = -\frac{J^{(ex)}_{l_{Rb}}\,b\,\mathrm{d}\varphi}{2\pi r''},$$

where r' and r'', the distances between $P(r_0,\ \varphi_0)$ and the two conductors, are given by the relations :

$$(22)\quad r' = \sqrt{a^2+r_0^2-2ar_0\cos(\varphi-\varphi_0)},\qquad r'' = \sqrt{b^2+r_0^2-2br_0\cos(\varphi-\varphi_0)}.$$

The projections of the two elementary fields $\mathrm{d}H_1$ and $\mathrm{d}H_2$ on the x- and y-axis are :

$$(23)\quad \begin{cases} \mathrm{d}H_{1x} = -\mathrm{d}H_1\sin(\varphi_0-\beta), & \mathrm{d}H_{2x} = -\mathrm{d}H_2\sin(\varphi_0-\gamma), \\ \mathrm{d}H_{1y} = \mathrm{d}H_1\cos(\varphi_0-\beta), & \mathrm{d}H_{2y} = \mathrm{d}H_2\cos(\gamma-\varphi_0), \end{cases}$$

where :

$$(24)\quad \beta = \arcsin\left[\frac{a}{r'}\sin(\varphi-\varphi_0)\right],\quad \gamma = \arcsin\left[\frac{b}{r''}\sin(\varphi-\varphi_0)\right].$$

Relations (21) ... (24) give the final expressions for H_x and H_y, the two components of the magnetic field in $P(r_0,\ \varphi_0)$:

$$(25)\quad \begin{cases} H_x = -\dfrac{k_1 a}{2\pi}\displaystyle\int_0^{2\pi} \frac{\cos\varphi \sin(\varphi_0-\beta)}{r'}\,d\varphi + \frac{k_2 b}{2\pi}\int_0^{2\pi} \frac{\cos\varphi \sin(\gamma-\varphi_0)}{r''}\,d\varphi, \\ H_y = \dfrac{k_1 a}{2\pi}\displaystyle\int_0^{2\pi} \frac{\cos\varphi \cos(\varphi_0-\beta)}{r'}\,d\varphi + \frac{k_2 b}{2\pi}\int_0^{2\pi} \frac{\cos\varphi \cos(\gamma-\varphi_0)}{r''}\,d\varphi. \end{cases}$$

Direct integration of relations (25) is difficult so that the numerical integration approach is almost inevitable. The S i m p s o n algorithm [2] was used in order to integrate rel. (25) and a BASIC program was written for this algoritm. The program permits to compute the two components H_x and H_y in many points (nodes in a net) for different values of r_0 and φ_0.

5. Numerical Example

In view to draw the spectrum of the magnetic field created by the Röntgen surface currents, the following numerical values have been considered: $E_0 = 20{,}000$ V/m; $a = 2.25$ cm;

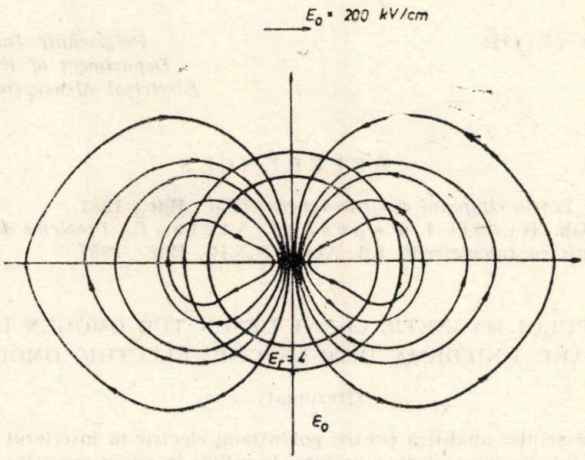

Fig. 3

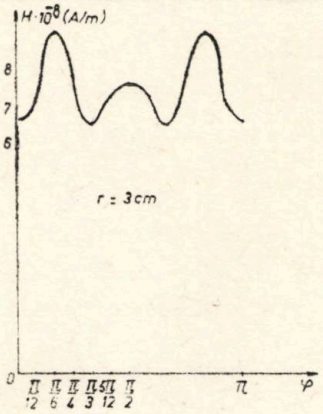

Fig. 4

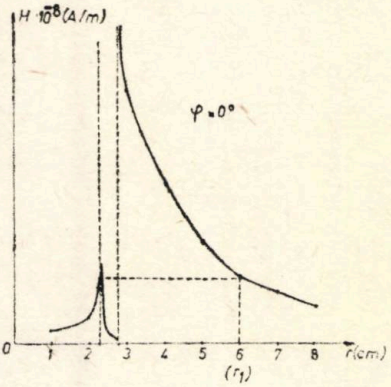

Fig. 5

$b=2.75$ cm ; $\varepsilon_r=4$. The obtained spectrum in represented in Fig. 3 ; it exhibits the symmetry of the magnetic field lines w.r.t the Oy axis. The magnetic field intensity for $r<a$ is smaller than that for $b<r<r_1$, (s. Fig. 5); for $r>b$ the magnetic field intensity decreases with r, while for $r<a$ it inceases with r (in both cases for $\varphi=$const.). If $r=$const., the strongest magnetic field is obtained for $\varphi=\pi/6$, $5\pi/6$, $7\pi/6$, $11\pi/6$. The curves $H(\varphi)$ for $r=3$ cm and $H(r)$ for $\varphi=0$ are plotted in Figs. 4 and 5 respectively.

It may be observed that the values of the magnetic field intensity are very small.

6. Conclusions

To compute the magnetic field produced by a dielectric tube shifting uniformly in air with a constant velocity, in axial direction, in an homogeneous and stationary electric field, it is necessary firstly to determine the scalar electric potential by integration of Laplace's equation. Secondly it may be obtained the polarization charge and after that, the Röntgen surface current densities. Finally it is possible to compute the magnetic field intensity using numerical methods.

An analogous problem concerning a dielectric tube rotating uniformly in an homogeneous and stationary electric field will be studied in a subsequent paper.

Received, September 25, 1989

Polytechnic Institute, Jassy,
Department of Electrotechnics and
Electrical Measurement and Machines

REFERENCES

1. Mocanu C.I., *Teoria cîmpului electromagnetic*, EDP, Buc., 1981.
2. Marinescu Gh., Rizoli I., Popescu I., Ştefan C., *Probleme de analiză numerică rezolvate cu calculatorul*. Ed. Acad. R.S.R., Buc., 1987.

STUDIUL CÎMPULUI MAGNETIC CREAT DE UN TUB OMOGEN DIELECTRIC ÎN MIŞCARE UNIFORMĂ ÎNTR-UN CÎMP ELECTRIC OMOGEN

(Rezumat)

Se determină soluţia analitică pentru potenţialul electric în interiorul şi exteriorul unui tub dielectric aflat într-un cîmp electric uniform la infinit în regim cvasistaţionar amagnetic şi apoi se determină cîmpul magnetic creat de tubul în mişcare axială uniformă folosind o metodă de integrare numerică.

BULETINUL INSTITUTULUI POLITEHNIC DIN IAŞI
Tomul XXXVI (XL) Fasc. 1—2, 1990
Secţia III
ELECTROTEHNICĂ. ENERGETICĂ. ELECTRONICĂ. AUTOMATIZĂRI

C.D. 621.392.5

UNE GÉNÉRALISATION DU THÉORÈME DE SCHÉRER RELATIF AUX QUADRIPÔLES GÉNÉRALS LINÉAIRES NONAUTONOMES, EN RÉGIME PERMANENT HARMONIQUE

PAR

HUGO ROSMAN

1. Introduction

En 1951, J. Schérer a établi le suivant théorème [1] : *si l'impédance du récepteur d'un quadripôle biporte linéaire nonautonome décrit, en régime permanent harmonique, une droite, alors l'impédance équivalente à la porte d'entrée du quadripôle décrit une cercle.*

Une généralisation de ce théorème a constitué l'objet d'une Note publieé en 1967 [2]. À savoir on a montré que *si l'impédance du récepteur d'un quadripôle biporte linéaire nonautonome, qui fonctionne en régime permanent harmonique, décrit le diagramme ayant l'équation :*

$$\underline{Z}_2(\lambda) = \frac{\sum_{k=0}^{n} \underline{M}_k \lambda^k}{\sum_{k=0}^{n} N_k \lambda^k}, \qquad \lambda \in [0, \infty), \tag{1}$$

alors l'impédance équivalente à la porte d'entrée du quadripôle, les coefficients de transfert de la tension et du courant de même que l'impédance de transfert décrivent des diagrammes du même type.

Le but prioritaire de cette Note c'est de fournir une extension de la généralisation ci-dessus du théoreme de Schérer, valable pour le cas d'un quadripôle général linéaire nonautonome, en régime permanent harmonique.

2. La généralisation du théoreme de Schérer

On considère un quadripôle général linéaire nonautonome (QGLN), qui fonctionne en régime permanent harmonique, ayant les equations [3], [4] (Fig. 1) :

$$\begin{bmatrix} \underline{U}_1 \\ \underline{I}_1 \\ \underline{U}_3 \end{bmatrix} = \begin{bmatrix} \underline{A}_{11} & \underline{A}_{12} & \underline{A}_{13} \\ \underline{A}_{21} & \underline{A}_{22} & \underline{A}_{23} \\ \underline{A}_{31} & \underline{A}_{32} & \underline{A}_{33} \end{bmatrix} \begin{bmatrix} \underline{U}_2 \\ \underline{I}_2 \\ \underline{I}_3 \end{bmatrix}, \tag{2}$$

où $\underline{A}_{ij}$, $(i, j = 1, 2, 3)$, sont les paramètres fondamentaux du quadripôle.

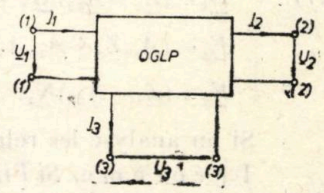

Fig. 1

Si l'on définit par :

$$\underline{Z}_{e1} \triangleq \frac{\underline{U}_1}{\underline{I}_1}, \quad \underline{k}_U \triangleq \frac{\underline{U}_2}{\underline{U}_1}, \quad \underline{k}_I \triangleq \frac{\underline{I}_2}{\underline{I}_1}, \quad \underline{Z}_m \triangleq \frac{\underline{U}_2}{\underline{I}_1} \tag{3}$$

l'impédance équivalente à la porte d'entrée, le coefficient de transmission de la tension, le coefficient de transmission du courant et, respectivement, l'impédance de transfert et l'on tient compte que

$$\underline{Z}_2 = R_2 + jX_2, \qquad \underline{Z}_3 = R_3 + jX_3, \tag{4}$$

en se basant sur les équations (1) on peut déduire les expressions :

$$\begin{cases} \underline{Z}_{e1} = \dfrac{(\underline{A}_{11}\underline{Z}_3 + \underline{A}_{13}\underline{A}_{31} - \underline{A}_{11}\underline{A}_{33})\underline{Z}_2 + \underline{A}_{12}\underline{Z}_3 + \underline{A}_{13}\underline{A}_{32} - \underline{A}_{12}\underline{A}_{33}}{(\underline{A}_{21}\underline{Z}_3 + \underline{A}_{23}\underline{A}_{31} - \underline{A}_{21}\underline{A}_{33})\underline{Z}_2 + \underline{A}_{22}\underline{Z}_3 + \underline{A}_{23}\underline{A}_{32} - \underline{A}_{22}\underline{A}_{33}}, \\ \underline{k}_U = \dfrac{(\underline{Z}_3 - \underline{A}_{33})\underline{Z}_2}{(\underline{A}_{11}\underline{Z}_3 + \underline{A}_{13}\underline{A}_{31} - \underline{A}_{11}\underline{A}_{33})\underline{Z}_2 + \underline{A}_{12}\underline{Z}_3 - \underline{A}_{12}\underline{A}_{33} + \underline{A}_{13}\underline{A}_{32}}, \\ \underline{k}_I = \dfrac{\underline{Z}_3 - \underline{A}_{33}}{(\underline{A}_{21}\underline{Z}_3 + \underline{A}_{23}\underline{A}_{31} - \underline{A}_{21}\underline{A}_{33})\underline{Z}_2 + \underline{A}_{22}\underline{Z}_3 + \underline{A}_{23}\underline{A}_{32} - \underline{A}_{22}\underline{A}_{33}}, \\ \underline{Z}_m = \dfrac{(\underline{Z}_3 - \underline{A}_{33})\underline{Z}_2}{(\underline{A}_{21}\underline{Z}_3 + \underline{A}_{23}\underline{A}_{31}) - \underline{A}_{21}\underline{A}_{33})\underline{Z}_2 + \underline{A}_{22}\underline{Z}_3 + \underline{A}_{23}\underline{A}_{32} - \underline{A}_{22}\underline{A}_{33}}. \end{cases} \tag{5}$$

Dans tous les cas où l'impedance du récepteur décrit le diagramme (1) les relations (5) conduisent à :

$$\begin{cases} \underline{Z}_{e1} = \dfrac{\sum\limits_{k=0}^{n} \underline{B}_k \lambda^k}{\sum\limits_{k=0}^{n} \underline{C}_k \lambda^k}, \qquad \underline{k}_U = \dfrac{\sum\limits_{k=0}^{n} \underline{D}_k \lambda^k}{\sum\limits_{k=0}^{n} \underline{E}_k \lambda^k}, \\ \underline{k}_I = \dfrac{\sum\limits_{k=0}^{n} \underline{F}_k \lambda^k}{\sum\limits_{k=0}^{n} \underline{C}_k \lambda^k}, \qquad \underline{Z}_m = \dfrac{\sum\limits_{k=0}^{n} \underline{D}_k \lambda^k}{\sum\limits_{k=0}^{n} \underline{C}_k \lambda^k}, \end{cases} \tag{6}$$

avec

$$\begin{cases} \underline{B}_k = (\underline{A}_{11}\underline{Z}_3 + \underline{A}_{13}\underline{A}_{31} - \underline{A}_{11}\underline{A}_{33})\underline{M}_k + (\underline{A}_{12}\underline{Z}_3 + \underline{A}_{13}\underline{A}_{32} - \underline{A}_{12}\underline{A}_{33})\underline{N}_k, \\ \underline{C}_k = (\underline{A}_{21}\underline{Z}_3 + \underline{A}_{23}\underline{A}_{31} - \underline{A}_{21}\underline{A}_{33})\underline{M}_k + (\underline{A}_{22}\underline{Z}_3 + \underline{A}_{23}\underline{A}_{32} - \underline{A}_{22}\underline{A}_{33})\underline{N}_k, \\ \underline{D}_k = (\underline{Z}_3 - \underline{A}_{33})\underline{M}_k + \underline{N}_k, \\ \underline{E}_k = (\underline{A}_{11}\underline{Z}_3 + \underline{A}_{13}\underline{A}_{31} - \underline{A}_{11}\underline{A}_{33})\underline{M}_k + (\underline{A}_{12}\underline{Z}_3 - \underline{A}_{12}\underline{A}_{33} + \underline{A}_{13}\underline{A}_{32})\underline{N}_k, \\ \underline{F}_k = (\underline{Z}_3 - \underline{A}_{33})\underline{N}_k. \end{cases} \tag{7}$$

Si on analyse les relations (1) et (6) il s'ensuit le suivant

T h é o r è m e. *Si l'impédance du récepteur d'un quadripôle général non-autonome, qui fonctionne en régime permanent harmonique, décrit le diagramme ayant l'equation (1), alors l'impédance équivalente à la porte d'entrée du quadripôle, les coefficients de transfert de la tension et du courant de même que l'impédance de transfert décrivent, chacun, un diagramme du même type.*

Dans le cas particulier lorsque $n=1$, $\underline{N}_1=0$, considéré par S c h é r e r, les diagrammes $\underline{Z}_{e1}(\lambda)$, $\underline{k}_U(\lambda)$, $\underline{k}_I(\lambda)$ et $\underline{Z}_m(\lambda)$ sont des cercles.

3. Les diagrammes des coefficients de transfert dans les régimes qui réalisent la résonance à la porte d'entrée

Afin de déterminer les équation de ces diagrammes il s'avère avantageux à exprimer $\underline{Z}_{e1}$, $\underline{k}_U$, $\underline{k}_I$ et $\underline{Z}_m$ en fonction de l'impédance équivalente, $\underline{Z}_{e1}$, à la porte d'entrée du QGLN, qui dans les régimes qui réalisent la résonance à cette porte a la forme

$$\underline{Z}_{e1}=\lambda \underline{R}_{e1*},\quad \lambda\in[0,\infty). \tag{8}$$

Dans un tel régime l'impédance du récepteur est donnée par l'expression [5] :

$$\underline{Z}_2=\frac{\underline{A}_{12}\underline{Z}_3+\underline{A}_{13}\underline{A}_{32}-\underline{A}_{12}\underline{A}_{33}-\lambda(\underline{A}_{22}\underline{Z}_3+\underline{A}_{23}\underline{A}_{32}-\underline{A}_{22}\underline{A}_{33})\underline{R}_{e1*}}{-\underline{A}_{11}\underline{Z}_3-\underline{A}_{13}\underline{A}_{31}+\underline{A}_{11}\underline{A}_{33}+\lambda(\underline{A}_{21}\underline{Z}_3+\underline{A}_{23}\underline{A}_{31}-\underline{A}_{21}\underline{A}_{33})\underline{R}_{e1*}}. \tag{9}$$

Si l'on substitue dans (5_2) ... (5_4) l'impédance $\underline{Z}_2$ par (9), tous calculs effectués on obtient :

$$\underline{k}_U(\mu)=\underline{G}-\mu\frac{\underline{H}}{\underline{R}_{e1*}},\quad \underline{k}_I(\lambda)=\underline{I}-\lambda\underline{J}\underline{R}_{e1*},\quad \underline{Z}_m(\lambda)=-\underline{H}+\lambda\underline{G}\underline{R}_{e1*}, \tag{10}$$

où

$$\mu=\frac{1}{\lambda} \tag{11}$$

et

$$\begin{cases} \underline{G}=\dfrac{\underline{a}_1\underline{Z}_3^2+\underline{a}_2\underline{Z}_3+\underline{a}_3}{\underline{a}_4\underline{Z}_3^2+\underline{a}_5\underline{Z}_3+\underline{a}_6}, \quad \underline{H}=\dfrac{\underline{a}_7\underline{Z}_3^2+\underline{a}_8\underline{Z}_3+\underline{a}_9}{\underline{a}_{10}\underline{Z}_3^2+\underline{a}_{11}\underline{Z}_3+\underline{a}_{12}}, \\ \underline{I}=-\dfrac{\underline{a}_{10}\underline{Z}_3^2+\underline{a}_{11}\underline{Z}_3+\underline{a}_{12}}{\underline{a}_4\underline{Z}_3^2+\underline{a}_5\underline{Z}_3+\underline{a}_6}, \quad \underline{J}=-\dfrac{\underline{a}_{13}\underline{Z}_3^2+\underline{a}_{14}\underline{Z}_3+\underline{a}_{15}}{\underline{a}_4\underline{Z}_3^2+\underline{a}_5\underline{Z}_3+\underline{a}_6}, \end{cases} \tag{12}$$

avec

$$\begin{cases} \underline{a}_1=\underline{A}_{22},\ \underline{a}_2=\underline{A}_{23}\underline{A}_{32}-2\underline{A}_{22}\underline{A}_{33},\ \underline{a}_3=\underline{A}_{33}(\underline{A}_{22}\underline{A}_{33}-\underline{A}_{23}\underline{A}_{32}), \\ \underline{a}_4=\underline{A}_{11}\underline{A}_{22}-\underline{A}_{12}\underline{A}_{21}, \\ \underline{a}_5=\underline{A}_{31}(\underline{A}_{13}\underline{A}_{22}-\underline{A}_{12}\underline{A}_{23})-2\underline{A}_{33}(\underline{A}_{11}\underline{A}_{22}-\underline{A}_{12}\underline{A}_{21})+\underline{A}_{32}(\underline{A}_{11}\underline{A}_{23}-\underline{A}_{13}\underline{A}_{21}), \\ \underline{a}_6=\underline{A}_{33}^2(\underline{A}_{11}\underline{A}_{22}-\underline{A}_{12}\underline{A}_{21})-\underline{A}_{23}\underline{A}_{33}(\underline{A}_{11}\underline{A}_{32}-\underline{A}_{12}\underline{A}_{31})-\underline{A}_{11}\underline{A}_{33}(\underline{A}_{22}\underline{A}_{31}-\underline{A}_{21}\underline{A}_{32}), \\ \underline{a}_7=\underline{A}_{12},\ \underline{a}_8=\underline{A}_{13}\underline{A}_{32}-2\underline{A}_{12}\underline{A}_{33},\ \underline{a}_9=\underline{A}_{33}(\underline{A}_{12}\underline{A}_{33}-\underline{A}_{13}\underline{A}_{32}), \\ \underline{a}_{10}=-\underline{A}_{11},\ \underline{a}_{11}=2\underline{A}_{11}\underline{A}_{33}-\underline{A}_{13}\underline{A}_{31},\ \underline{a}_{12}=\underline{A}_{33}(\underline{A}_{11}\underline{A}_{33}-\underline{A}_{13}\underline{A}_{31}), \\ \underline{a}_{13}=-\underline{A}_{21},\ \underline{a}_{14}=\underline{A}_{23}\underline{A}_{31}-2\underline{A}_{21}\underline{A}_{33},\ \underline{a}_{15}=\underline{A}_{33}(\underline{A}_{23}\underline{A}_{31}-\underline{A}_{21}\underline{A}_{33}). \end{cases} \tag{13}$$

Dans les cas où le QGLN est *réciproque*, ses paramètres fondamentaux satisfont aux relations [3], [4] :

(14) $$|\underline{A}|=1,\ \underline{A}_{12}\underline{A}_{23}-\underline{A}_{13}\underline{A}_{22}=\underline{A}_{32},\ \underline{A}_{11}\underline{A}_{32}-\underline{A}_{12}\underline{A}_{31}=-\underline{A}_{13}$$

de sorte que

(15) $$\underline{a}_5=-\underline{A}_{33}(\underline{A}_{11}\underline{A}_{22}-\underline{A}_{12}\underline{A}_{21})-1,\quad \underline{a}_6=\underline{A}_{33}$$

Si on analyse les relations (10) on aboutit à la conclusion que *les diagrammes des coefficients de transfert d'un QGLN, dans les régimes qui réalisent la résonance à la porte d'entrée de celui-ci, sont des droites.* Compte tenu que dans tous les cas où de tels régimes sont réalisés avec des recepteurs passifs les coefficients de transfert d'un QGLN ont des valeurs situées seulement dans certains domaines (d'existence) [5], en général finis, les diagrammes de ces coefficients sont des *segments* des droites (10) situés à l'intérieur des domaines d'existence ($\mathcal{D}_{\underline{k}_U}$, $\mathcal{D}_{\underline{k}_I}$, $\mathcal{D}_{\underline{Z}_m}$).

4. Les diagrammes des coefficients de transfert dans les régimes qui réalisent la résonance à la porte de sortie

Dans les régimes qui réalisent la résonance à la porte de sortie

(16) $$\underline{Z}_2=\sigma R_{2*},\ \sigma\in[0,\infty),$$

de sorte que les coefficients de transfert du quadripôle, donnés par les relations (6), deviennent :

(17) $$\underline{k}_U(\tau)=\frac{\underline{K}R_{2*}}{\underline{L}+\tau\underline{M}},\quad \underline{k}_I(\sigma)=\frac{\underline{K}}{\underline{N}+\sigma\underline{T}},\quad \underline{Z}_m(\sigma)=\frac{\underline{K}R_{2*}}{\underline{T}+\tau\underline{N}},$$

où

(18) $$\begin{cases}\underline{K}=\underline{Z}_3-\underline{A}_{33},\ \underline{L}=(\underline{A}_{11}\underline{Z}_3+\underline{A}_{13}\underline{A}_{31}-\underline{A}_{11}\underline{A}_{33})R_{2*},\\ \underline{M}=\underline{A}_{12}\underline{Z}_3-\underline{A}_{12}\underline{A}_{33}+\underline{A}_{13}\underline{A}_{32},\\ \underline{N}=\underline{A}_{22}\underline{Z}_3+\underline{A}_{23}\underline{A}_{32}-\underline{A}_{22}\underline{A}_{33},\ \underline{T}=(\underline{A}_{21}\underline{Z}_2+\underline{A}_{23}\underline{A}_{31}-\underline{A}_{21}\underline{A}_{33})R_{2*}\end{cases}$$

et

(19) $$\tau=\frac{1}{\sigma}.$$

On constate aisément que *les diagrammes des coeficients de transfert d'un QGLN, dans les régimes de résonance à la porte d'entrée du quadripôle, sont des cercles qui passent par l'origine.* Lorsque ces régimes sont réalisés avec des récepteurs passifs les coefficients de transfert ont des valeurs situées seulement dans certains domaines d'existence [5], en général finis, de sorte que les diagrammes ci-dessus sont des arcs de cercle contenus à l'intérieur des domaines $\mathcal{D}_{\underline{k}_U}$, $\mathcal{D}_{\underline{k}_I}$, $\mathcal{D}_{\underline{Z}_m}$. Ces arcs de cercle séparent, en fait, à l'intérieur de ces domaines, les sous-domaines qui correspondent à des récepteurs passifs de nature inductive, de ceux de nature capacitive. Les équations de ces arcs de cercle, en coordonnées k'_U, k''_U ; k'_I, k''_I, respectivement R_m, X_m ont été établies dans une Note précédente [5].

5. Conclusions

1. On établit un théorème relatif au diagrammes décrites par l'impédance équivalente à la porte d'entrée et les coefficients de transfert d'un quadripôle général linéaire nonautonome lorsque l'impédance du récepteur décrit le diagramme ayant l'equation (1) ; les résultats acquis représentent une généralisation du théorème de S c h é r e r relatif aux quadripôles biportes linéaires nonautonomes.

2. On aboutit à la conclusion que les diagrammes des coefficients de transfert d'un quadripôle général linéaire nonautonome sont : a) des segments de droite, dans les régimes qui réalisent à l'aide des récepteurs passifs la résonance à la porte d'entrée : b) des arcs de cercle, dans les régimes qui réalisent, de même à l'aide des récepteurs passifs, la résonance à la porte de sortie.

Reçue le 18 mai 1989

Institut Polytechnique, Jassy,
Chaire d'Électrotechnique, Machines et Mesures électriques

BIBLIOGRAPHIE

1. S c h é r e r J., *Étude graphique des quadripôles à fréquence constante.* RGÉ, **60**, *9*, 359 (1951).
2. R o s m a n H., *Diagramele loc-geometric ale coeficienţilor de transfer ai unui cuadripol diport liniar, pasiv şi reciproc, în regimurile rezonante.* Bu. Inst. polit., Iaşi, **XIII (XVII)**, *1*—2, 381—388 (1967).
3. С и г о р с к и й В. П., *Общая теория четырёхполюсников.* Изд. АН УССР, Киев, 1955.
4. Ş o r a C., *Cuadripolul electric.* Ed. Tehn., Buc., 1964.
5. R o s m a n H., *Les domaines d'existence des coefficients de transfert d'un quadripôle général linéaire nonautonome en régime permanent harmonique.* Mem. secţ. şt. Acad. R.S.R., s. IV, **XII** (1989) (sous presse).

O GENERALIZARE A TEOREMEI LUI SCHÉRER RELATIVĂ LA CUADRIPOLI GENERALI LINIARI NEAUTONOMI ÎN REGIM PERMANENT ARMONIC

(Rezumat)

Se stabileşte o teoremă relativă la diagramele loc-geometric descrise de impedanţa echivalentă la poarta de intrare şi coeficienţii de transfer ai unui cuadripol general liniar neautonom, atunci cînd impedanţa receptorului descrie diagrama loc-geometric (1); rezultatul obţinut constituie o generalizare a teoremei lui S c h é r e r [1] relativă la cuadripoli diporţi liniari neautonomi.

Se demonstrează că diagramele loc geometric ale coeficienţilor de transfer ai unui cuadripol general liniar neautonom sînt : a) segmente de dreaptă în regimurile care realizează, cu receptoare pasive, rezonanţa la poarta de intrare ; b) arce de cerc în cele în care are loc, de asemenea cu receptoare pasive, rezonanţa la poarta de ieşire.

BULETINUL INSTITUTULUI POLITEHNIC DIN IAŞI
Tomul XXXVI (XL) Fasc. 1—2, 1990
Secţia III
ELECTROTEHNICĂ. ENERGETICĂ. ELECTRONICĂ. AUTOMATIZĂRI

D.C. 538.551.25

UPON THE DETERMINATION OF MAGNETIZING CURRENT TO PREVENT SERIES FERRORESONANCE

BY

SAVEL MITREA and ADRIAN ADĂSCĂLIŢEI

1. Introduction

Series ferroresonance is an undesired phenomenon occurring especially in the single-phase switching of unloaded three-phase distribution transformer banks [1]. As shown in [2] the piecewise-linear model of ferroresonant circuit using the magnetic characteristic in Fig. 1 is an effective representation of the real circuit. The characteristic in Fig. 1 leads to the representation of series ferroresonant circuit in Fig. 2.

It is known that input—output amplitude characteristic of the circuit ressembles a parabola presenting a minimum input voltage (V_{min}) bellow which ferroresonance cannot be sustained. V_{min} strongly depends on the magnetizing current I_m. The authors present a simple way to determine I_m for which the series ferroresonance cannot be sustained when nominal voltage is applied.

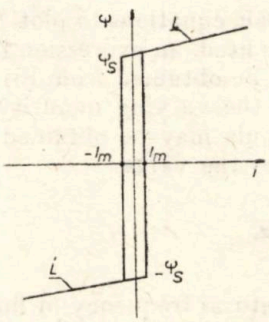

Fig. 1

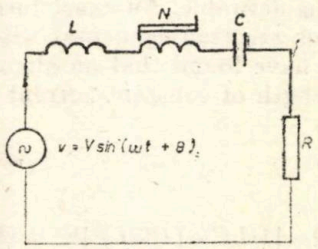

Fig. 2

2. Determination of Minimum Voltage to Sustain Ferroresonance

Fig. 3 shows the steady-state voltage waveform across the capacitor. The circuit is described on the constant-current interval $\tau \in (0, \tau_1)$ as flux linkage changes from Ψ_s to $-\Psi_s$, by the equations :

$$(1) \qquad v_c = V_{c0} - \frac{1}{C} I_m t, \qquad (2) \qquad \frac{d\Psi}{dt} + v_c = V \sin(\omega t + \theta).$$

On the varying-current interval $\tau\in(\tau_1, \tau_2)$ the circuit is described by the equations :

$$(3)\qquad LC\frac{d^2v_c}{dt^2}+RC\frac{dv_c}{dt}+v_c=V\sin(\omega t+\theta),\qquad (4)\qquad i=C\frac{dv_c}{dt}.$$

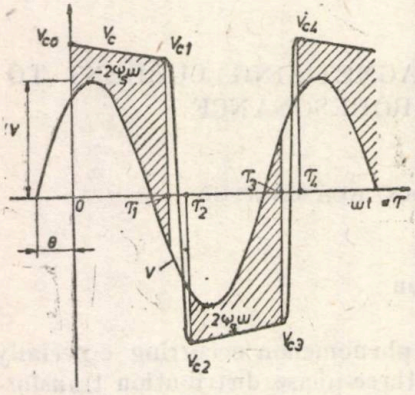

Fig. 3

By using the adimensional variable $\omega t=\tau$ and considering $\Psi_0=\Psi_s$ at $\tau=0$, the quantities $\Psi(\tau)$, $v_c(\tau)$, $i(\tau)$ are found by means of linear circuit theory. Then, setting the periodicity conditions $V_{c2}=-V_{c0}$ and $\tau_2=\pi$, one obtains steady-state equations describing the response waveform. The equations can be written in a linear form as :

$$(5)\qquad \sum_{j=1}^{3}a_{ij}x_i=b_i,\qquad (i=1, 2, 3),$$

where : $x_1=V\sin\theta$, $x_2=V\cos\theta$, $x_3=V_{c0}$, $a_{ij}=f_{ij}(\tau_1, R, L, C, \omega)$, $b_i=f_i(I_m, \Psi_s, R, L, C, \omega)$. τ_1 is a parameter taking values on the interval $[0, \pi]$. Given a value for τ_1 on the above interval, the resulting quantities $V(x_1^2+x_2^2)^{1/2}$, $\theta=\tan^{-1}(x_1/x_2)$ and V_{c0} are valid if the condition $v_c(\tau)>v(\tau)$ is fulfilled for all $\tau\in(0, \tau_1)$.

Exact value for $V_{\min}$ is found on the imput—output amplitude characteristic $V=f(V_{c0})$, that is obtained by repeatedly solving (5) for different values assigned to τ_1. By applying the above procedure for different values of I_m the curve $V_{\min}=f(I_m)$ can be plotted. If $V_{\min}$ is greater than amplitude of nominal voltage (V_{nom}) series ferroresonance cannot be sustained.

Although repeatedly solving linear algebraic equations to plot amplitude characteristics is not a problem if a computer is used, an expression for $V_{\min}=f(I_m)$ is desirable. An exact formula cannot be obtained from (5) since the equations are transcendental with respect to the varying quantity τ_1. The authors have found that an almost exact formula may be obtained from (5) if the length of constant-current interval takes the value

$$(6)\qquad \tau_1=\pi\left(1-\frac{\omega}{\Omega}\right)\triangleq\alpha,$$

where $\Omega=[1/LC-(R/2L)^2]^{1/2}$ is the damped natural frequency of linear *RLC* branch of the circuit in Fig. 2. By using (6), coefficients a_{ij} and right-hand terms b_i of (5) become :

$$(7)\qquad \begin{cases} a_{12}=1-\cos\alpha,\ a_{13}=-\alpha,\ a_{21}=\exp(\delta/2)\sin\varphi+\sin(\alpha-\varphi),\\ a_{22}=\exp(\delta/2)\cos\varphi-\cos(\alpha-\varphi),\ a_{23}=ZC\omega[\exp(\delta/2)-1],\\ a_{31}=-a_{22},\ a_{32}=a_{21},\ a_{33}=0,\\ b_1=-2\omega\Psi_s-\dfrac{1}{2\omega C}\alpha^2I_m,\ b_2=\alpha ZI_m,\ b_3=2I_m[\exp(\delta/2)-1]. \end{cases}$$

Other notations used in the above expressions are :

$$\delta=\pi R/L\omega,\quad Z=\sqrt{R^2+(L\omega-1/C\omega)^2},\quad \varphi=\tan^{-1}\left[\frac{1}{R}(L\omega-1/C\omega)\right].$$

The linear form of (5) permits to write the expression for $V_{\min}=f(I_m)$ as

$$V_{\min}(I_m)=\frac{1}{|\Delta|}\sqrt{\Delta_1^2(I_m)+\Delta_2^2(I_m)}. \tag{8}$$

3. Application

In order to see whether the approximate expression (8) is of practical use we consider a circuit having the parameters : $R=25\ \Omega$, $C=10\ \mu F$, $L=35$ mH. The dependence of exact $V_{\min}$ vs. magnetizing current I_m is shown in Fig. 4. The curve is plotted in per volt units. It comes out that it can be represented graphically by a straight line. The approximate values obtained by (8) differ very little from the exact ones. Thus, $V_{\min}/V_{\min_a}=0.967$ for $I_m=0$ and 0.997 for $I_m=2$. There is no need to extend the curve in Fig. 4 beyond the above value for I_m since one can see that the normalized input voltage for $I_m=2$ is greater than the nominal one.

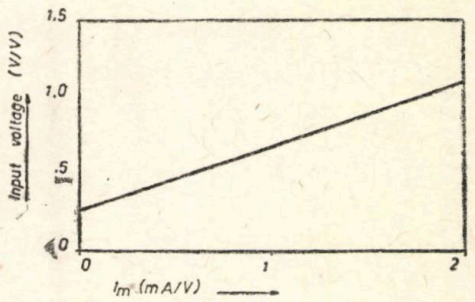

Fig. 4

4. Conclusions

It has been shown in the literature [2] that the piecewise-linear model we use in this paper provides an effective description of ferroresonance. A drawback of the model consists in that, generally, it involves solution of transcendental equations to find periodic response. It is found by the authors that the portion of input—output amplitude characteristic which is of interest from the practice point of view can be obtained by aid of a set of three linear algebraic equations. This permits to express the approximate minimum voltage to sustain ferroresonance in a closed form. It is found that this expression produces results that are in good agreement to the exact ones.

Received, November 13, 1989

Polytechnic Institute, Jassy,
Department of Electrotechnics, Electrical Measurements and Machines

REFERENCES

1. Hopkinson R.H., *Ferroresonant Overvoltage Control Based on TNA Tests on Three-Phase Delta-Wye Transformer Banks.* I.E.E.E. Trans., **PAS-86**, *10*, 1 258—1 265 (1967).
2. Feldman J.M., Capabianca A.L., *On the Accuracy and Utility of Piecewise-Linear Model of Ferroresonance.* I.E.E.E. Tans., **PAS-97**, *2*, 469—477 (1978).

ASUPRA DETERMINĂRII CURENTULUI DE MAGNETIZARE NECESAR PENTRU EVITAREA FEROREZONANȚEI SERIE

(Rezumat)

În literatura de specialitate se arată că modelul circuitului ferorezonant serie bazat pe liniarizarea pe porțiuni a caracteristicii de magnetizare reprezintă o descriere efectivă a circuitului real. Un dezavantaj important al acestui model constă în faptul că pentru a descrie regimul permanent este necesară, în general, rezolvarea unui sistem de ecuații transcendente. Se arată că porțiunea din caracteristica de amplitudine intrare— ieșire, care prezintă interes pentru practică, poate fi descrisă cu ajutorul unui sistem de trei ecuații algebrice liniare. Aceasta permite obținerea unei expresii aproximative pentru valoarea tensiunii de intrare sub nivelul căreia ferorezonanța serie nu este posibilă. Se constată că rezultatele obținute cu această expresie diferă foarte puțin de cele exacte.

BULETINUL INSTITUTULUI POLITEHNIC DIN IAŞI
Tomul XXXVI (XL) Fasc. 1—2, 1990
Secţia III
ELECTROTEHNICĂ. ENERGETICĂ. ELECTRONICĂ. AUTOMATIZĂRI

D.C. 621.318.7

DIGITAL FILTERING OF LINEAR PREDICTIVE CODED SIGNALS

BY

VICTOR GRIGORAŞ

1. Introduction

Linear shift invariant digital filtering is a common and very useful digital processing tool [1]. For real time processing, programable or dedicated digital signal processors are used to implement digital filtering algorithms. In order to reduce the complexity of signal processors and to increase their speed, the representation on a reduced number of bits is recommended for both signal samples and filter coefficients. The reduction of the number of bits for the coefficients representation was treated, e.g. in [2] ; the reduction of the number of bits for the representation of the signal samples, in the general case, would mean a reduced precision. If we restrict the class of input signals, coding the samples of the input signal on a reduced number of bits is possible without any sacrifice on precision. Such a solution is given in [3], reducing the memory capacity in look-up tables, for functions with bounded first derivative :

$$B_1 < f'(x) < B_u.$$

In other papers (e.g. [4]) the particular case of digital filtering delta modulated signals is treated, with focus on half band filters.

This paper reports a generalisation of the preceeding results to linear predictive coding of the input signal of any digital filter. Restrictions imposed to the discrete signal, as well as the analog one, are given in both time and frequency domain. The special case of differential modulation is discussed as an example.

2. Principle of Operation

The principle for reducing the number of bits of the filter processor is based on cascading a linear predictive coder, the linear shift invariant digital filter and the corresponding linear predictive decoder. This is possible if the statistic properties of the input and output signals were known.

If the linear prediction filter has the transfer function $H_{lpf}(z)$, then the coder and the decoder will have the transfer functions :

$$H_{lpc}(z) = 1 - H_{lpf}(z), \qquad (2)$$

$$H_{lpd}(z) = \frac{1}{1 - H_{lpf}(z)}. \qquad (3)$$

By virtue of the linearity of the linear predictive coder, digital filter and linear predictive decoder, the system obtained by cascading the three operators has a transfer function identical to that of the original digital filter, $H_f(z)$. If some of the factors in $H_f(z)$ are identical to those in $H_{lpc}(z)$, they

may be simplified with $H_{lpd}^{1}(z)$, reducing the computational complexity of the system.

Such a generalized approach might offer a better reduction of the number of bits of the signal processor, at the expense of increased complexity of the coder and decoder. From the practical point of view linear predictive coding would be acceptable only if the coefficients of the predictive filter were simple enough (e.g. $+/-1$ or the powers of 2) to eliminate the need of an extra multiplier.

3. Conditions Imposed to the Signal

If we denote by $x[n]$ and $y[n]$ the input and, respectively, the output signals of a digital filter and consider them represented on J bits, our purpose is to reduce the representation of $x_c[n]$ and $y_c[n]$, the corresponding coded versions, to I bits, with :

$$I<J. \tag{4}$$

In this case the following relations must stand true, in order to avoid any loss of accuracy :

$$\frac{X_{max}}{2^J}=\frac{X_{cmax}}{2^I}; \tag{5}$$

$$\frac{Y_{max}}{2^J}=\frac{Y_{cmax}}{2^I}, \tag{6}$$

where we denoted by X_{max} and Y_{max} the amplitudes of the discrete input and output signals and by X_{cmax} and Y_{cmax} the maximum values of the linear predictive coded input and output signals.

Hence, in the time domain, the conditions imposed to both input and output signals for the effectiveness of the proposed method are :

$$|x_c[n]|<X_{cmax}=2^{I-J}X_{max}, \tag{7}$$

$$|Y_c[n]|<Y_{cmax}=2^{I-J}X_{max} \tag{8}$$

To obtain a frequency domain condition, we must compute the Z-transform of the input sequence :

$$X(z)=\sum_{k=0}^{\infty}x(k)z^{-k}. \tag{9}$$

For causal input signals, taking into account condition (7), we deduce :

$$|X(z)|<|H_{lpd}|X_{cmax}\sum_{k=0}^{\infty}|z|^{-k}. \tag{10}$$

For :

$$|z|<1 \tag{11}$$

the series in the right side of the inequality (10) converges, and the final result is :

$$|X(z)|<2^{I-J}X_{max}|H_{lpd}(z)|\frac{z}{z-1} \tag{12}$$

and, for the output signal :

$$|Y(z)|<2^{I-J}Y_{max}|H_{lpc}(z)|\frac{z}{z-1}. \tag{13}$$

It is worth noting that imposing similar conditions to both input and output signals of the digital filter, imposes restrictions on its transfer function too.

By the way of deduction, it is obvious that (12) and (13) are sufficient but not necessary conditions.

Similar conditions can be deduced for the analog input signal, before A/D conversion, and analog output signal, after D/A conversion, respectively $x(t)$ and $y(t)$. These signals must, first of all, obey the Shannon sampling theorem :

$$X_a(\omega)=Y_a(\omega)=0 \quad \text{for} \quad \omega>-\frac{\pi}{T} \text{ and } \omega<\frac{\pi}{T}. \tag{14}$$

Conditions, similar to (7), (8), (12) and (13), can be deduced, taking into account that :

$$x[n]=Tx(nT), \tag{15}$$

$$y[n]=Ty(nT), \tag{16}$$

$$X_a(\omega)=X(e^{j\omega T}), \tag{17}$$

$$Y_a(\omega)=Y(e^{j\omega T}), \tag{18}$$

where $X_a(\omega)$ and $Y_a(\omega)$ are the Fourier transforms of $x(t)$ and $y(t)$ respectivelly, and T is the sampling period. It follows that :

$$\left|\sum_{n=0}^{N} a_n x(nT)\right| < \frac{2^{I-J}X_{\max}}{T}, \tag{19}$$

$$\left|\sum_{n=0}^{N} a_n y(nT)\right| < \frac{2^{I-J}Y_{\max}}{T}, \tag{20}$$

$$|X_a(\omega)| < \frac{2^{I-J}X_{\max}|H_{lpd}(e^{j\omega T})|}{|e^{j\omega T}-1|}, \tag{21}$$

$$|Y_a(\omega)| < \frac{2^{I-J}Y_{\max}|H_{lpd}(e^{j\omega T})|}{|e^{j\omega T}-1|}, \tag{22}$$

4. The Case of Differential Modulation

Considering that differential modulation is a particular case of linear predictive coding, with a linear prediction filter :

$$H_{lpf}(z)=z^{-1}, \tag{23}$$

we must compute the transfer function of the differential coder :

$$H_c(z)=\frac{z-1}{z} \tag{24}$$

and decoder :

$$H_d(z)=\frac{z}{z-1}. \tag{25}$$

The conditions imposed to the discrete time signals remain the same ((7) and (8)) with the particular interpretation for the coded samples as being differences of two successive samples. The frequency domain conditions, (12) and (13), however become :

$$|X(z)| < \frac{X_{c\max}|z^2|}{|z-1|^2}, \tag{26}$$

$$|Y(z)| < \frac{Y_{c\max}|z^2|}{|z-1|^2}. \tag{27}$$

Similarly, for the analog signals, the particular relations are :

$$(28) \qquad |X_a(\omega)| = \frac{2^{I-J} X_{max}}{|e^{j\omega T} - 1|^2}, \qquad (29) \qquad |Y_a(\omega)| = \frac{2^{I-J} Y_{max}}{|e^{j\omega t} - 1|^2},$$

for :

$$-\frac{\pi}{T} < \omega < \frac{\pi}{T}.$$

Relations (28) and (29) may be further refined, to obtain :

$$(30) \qquad |X_a(\omega)| = \frac{2^{I-J} X_{max}}{4 \sin^2(\omega T/2)}, \qquad (31) \qquad |Y_a(\omega)| = \frac{2^{I-J} Y_{max}}{4 \sin^2(\omega T/2)}.$$

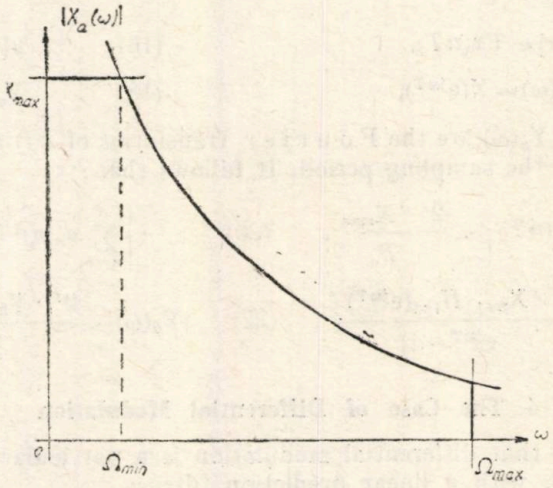

Fig. 1. — Graphical representation of the conditions imposed to the amplitude spectrum of the signal to be differentially coded on a reduced number of bits.

These conditions may be graphically represented as in Fig. 1; it may be observed that in order to be properly sampled, A/D converted and differentially coded, the analog input signal must have a spectrum limited in frequency by the S h a n n o n sampling theorem at :

$$(32) \qquad \Omega_{max} = \frac{\pi}{T},$$

limited in amplitude at frequencies lower than :

$$(33) \qquad \Omega_{min} = \frac{2}{T} \text{ arc } \sin(2^{I/2-J/2-1}),$$

by the dynamic range of the A/D and D/A converters at X_{max}, Y_{max} and, at frequencies between Ω_{min} and Ω_{max} limited in amplitude by relations (30) or(31).

5. Conclusions

The reported method reduces the number of bits coding the samples of a discrete signal, by means of a scalar quantizer of the linear predictive type (in particular differential coder). The main goal of the method is to reduce the complexity of the processor performing a digital filtering task. The possibility of using the same filtering algorithm, as well as the restrictions imposed to the input and output signal are demonstrated.

A k n o w l e d g e m e n t. The author wishes to express his gratitude to dr. Liviu G o r a ș and eng. Florin G r i g o r a ș for their extremly useful suggestions and comments.

Received, November 11, 1989

Polytechnic Institute, Jassy,
Department of Applied Electronics

REFERENCES

1. B o s e N.K., *Digital Filter, Theory and Applications*. Elsevier Science Publishing Co. Inc., New York, 1985.
2. V a n g C h i n g L i m, *Predictive Coding for FIR Filter Wordlength Prediction*. I.E.E.E. Trans., **CAS,—32**, *4*, (1985).
3. S t a s i n s k i R., *Memory Savings in Look-up Tables for Functions with Bounded First Derivative*. Proc. European Conf. on Circuit Theory and Design, Academia Publishing House, Prague, 1985.
4. A n a s t a s o p o u l u s V., D e l i y a n i s T., *A Method for Designing Half Band FIR Bandpass Filters for D.M. Signals*. Proc. European Conf. on Circuit Theory and Design, Academia Publishing House, Prague, 1985.

FILTRAREA NUMERICĂ A SEMNALELOR CODATE PRIN PREDICȚIE LINIARĂ

(Rezumat)

Se stabilesc condițiile ce urmează a fi impuse unui semnal discret, precum și semnalului analogic din care provine, pentru a putea fi codat predictiv pe un număr redus și impus de biți. Este demonstrată posibilitatea filtrării numerice a semnalului codat, cu același algoritm de filtrare.

BULETINUL INSTITUTULUI POLITEHNIC DIN IAŞI
Tomul XXXVI (XL) Fasc. 1—2, 1990
Secţia III
ELECTROTEHNICĂ. ENERGETICĂ. ELECTRONICĂ. AUTOMATIZĂRI

D.C. 621.—501.1(021)

SUFFICIENT EXISTENCE CONDITIONS OF LIMIT CYCLES

BY

M. VOICU

1. Introduction

Consider the nonlinear continuous-time dynamical system :

$$\dot{x}=f(t, x),\ t\in R_+,\ x\in R^n, \tag{1}$$

where x is the state and f is a vector function.

According to the usually specified attributes of a dynamical system we assume that $f: T\times X\to R^n$ is a continuous and locally Lipschitzian function on some open set $T\times X\subseteq R_+\times R^n$, i.e. for each $(t_0, x_0)\in T\times X$ system (1) has a unique C a u c h y solution :

$$x(t)=\varphi(t\,;\, t_0, x_0), \tag{2}$$

with

$$x(t_0)=x_0, \tag{3}$$

defined on a maximal time interval (depending on (t_0, x_0)) $T_0\triangleq(t_1, t_2)\subseteq T$, with $t_0\in T_0$.

It is well-known that for certain f and $(t_0, x_0)\in T\times X$ solution (2) may be a time periodic function, that corresponds to a closed trajectory in the state space or, in other words, to a *limit cycle*.

Taking into account the significance of the limit cycles for the system stability characterization and the lack of some general and practically efficient conditions for their existence, it is easily to understand that this celebrated problem remained among of the perennial ones in the theory of nonlinear dynamical systems.

This Note is devoted to the derivation of some efficient sufficiency conditions for the existence of limit cycles by applying the flow-invariance method, [1] ... [5].

2. Main Result

For the sake of intelligibility of our developments we first remind some known results.

D e f i n i t i o n 1 [1], [2]. A time-dependent set $D(t)\subset X$, $t\in T$, is called *positively flow-invariant* with respect to system (1) if for each $(t_0, x_0)\in T\times D(t_0)$ the following condition is satisfied :

$$x(t)\in D(t),\ t\in[t_0, t_2). \tag{4}$$ ■

T h e o r e m 1 [2]. *Assume that $D(t)$ is closed. Then $D(t)$ is positively flow-invariant with respect to system (1) on T if and only if*

(5) $$\liminf_{h\searrow 0} h^{-1}d(x+hf(t, x)\ ;\ D(t+h))=0$$

for each $(t, x)\in T\times D(t)$. ■

In relation (5) d denotes the distance in R^n and $d(v, V)$ is the distance from $v\in R^n$ to the set $V\subset R^n$.

Subtangential condition (5) is to be treated in applications as an equation. If $f(t, x)$ is given, then $D(t)$ is the unknown. Lacking a general method for solving equation (5), the choice of $D(t)$ depends upon the possibilities of subsequent conversion of equation (5) into transparent and tractable forms.

Such a choice, which proved to be fertile in the evolution characterization and design of control systems, [3] ... [8], and which opens a real possibility for our developments, is the time-dependent curved box :

(6) $$B(t)\triangleq\{x\in R^n\ ;\ \underline{a}(t)\leqslant p(x)\leqslant\bar{a}(t)\}\subset X,\quad t\in T,$$

where $p : X\to X$ is an invertible and derivable vector function (having the inverse $p^{-1} : X\to X$ and the Jacobian $J(x)=\partial p/\partial x$), and $\underline{a} : T\to X$, $\bar{a} : T\to X$ are two differentiable functions satisfying $\underline{a}(t)\leqslant\bar{a}(t)$, $t\in T$, „$\leqslant$" denoting the componentwise inequality of two vectors.

For the convenience of statement of the next result let us introduce now some notations. Let $V\subset R^n$ be a compact subset and $\psi : V\to R^n$ be a continuous function with the components ψ_i, and let $z\triangleq(z_1, ..., z_n)$ be a certain point in V. We denote by $\mathcal{C}_v^z$ the operator which „caches" $\psi(v)$ at $z\in V$ in a diagonal manner, i.e. $\mathcal{C}_v^z\{\psi(v)\}\triangleq[\psi_1(z_1, v_2, ..., v_n), ..., \psi_i(v_1, ..., z_i, ..., v_n), ..., \psi_n(v_1, ..., v_{n-1}, z_n)]'$, where $[\ ]'$ symbolizes the vector transposition. We also denote by $\operatorname{ext}\mathcal{C}_v^z\{\psi(v)\}$, where ext may be min or max, the vector with the components $\operatorname{ext}\psi_i(v_1, ..., z_i, ..., v_n)$, $(i=1, 2, ..., n)$.

In compliance with a possible state transformation defined by $\tilde{x}=p(x)$ and regarding its use for transforming system (1) we introduce the following notation :

(7) $$\tilde{f}(t, \cdot)\triangleq J(p^{-1}(\cdot))f(t, p^{-1}(\cdot)).$$

Theorem 2 [5]. *$B(t)$ defined by (6) is positively flow-invariant with respect to system (1) on T if and only if*

(8) $$\min_{T\times B}[\mathcal{C}_v^{\underline{a}}\{\tilde{f}(t, v)\}-\dot{\underline{a}}(t)]\geqslant 0,$$ (9) $$\max_{T\times B}[\mathcal{C}_v^{\bar{a}}\{\tilde{f}(t, v)\}-\dot{\bar{a}}(t)]\leqslant 0.$$ ■

Remark 1. In order to deal with the problem of limit cycles existence, let us assume for the remainder of this note that $\sup T=+\infty$, $\sup T_0=+\infty$. ■

Under these circumstances the next step of our approach is the following

Theorem 3 (Poincaré-Bendixson). *If solution (2) with (3) is contained in a bounded subset of X for all $t\geqslant t_0$, then this solution approaches an equilibrium point or a limit cycle as t approaches infinity.*

Obviously, according to Theorem 3, Definition 1 and Theorems 1, 2, one may state the following results concerning our purpose:

Theorem 4. *A bounded subset $D(t)\subseteq X$ contains a limit cycle of system (1) if it is positively flow-invariant with respect to system (1)* (under Remark 1) *and it does not contain any equilibrium point of system (1).* ■

Theorem 5. *A bounded subset $D(t)\subseteq X$ contains a limit cycle of system (1) if it satisfies condition (5)* (under Remark 1) *and it does not contain any equilibrium point of system (1).* ■

Theorem 6. *Curved box* (6) *contains a limit cycle of system* (1) *if it satisfies conditions* (8) *and* (9) (under Remark 1) *and it does not contain any equilibrium point of system* (1). ■

Remark 2. Generally speaking, by using Theorems 5 and 6 (which provide effectually applicable conditions) one cannot ascertain anything about the number and the nature (i.e. stable, unstable or semistable) of limit cycles contained in a positively flow-invariant subset because these questions lie entierely with subset form and scope. Concerning the second problem the ambiguity is explainable by considering the case when the flow-invariant subset is precisely a limit cycle. For all of that in many applications even the particular form and scope of the considered subset allow to characterize the limit cycle nature (s · §3). ■

Now, in view of the effective using of Theorem 6 the cardinal problem is that of the adequate choosing of p in definition of curved box (6). The simplest possibility is to express p via the polar coordinate transformation.

In the case $n=2$ and $X=R^2$ (state plane) one may define p^{-1} by :

$$x_1=a_1+\alpha_1 r\cos\theta, \qquad x_2=a_2+\alpha_2 r\sin\theta, \tag{10}$$

where $(x_1, x_2)\triangleq x$, $(r, \theta)\triangleq\tilde{x}$; (a_1, a_2) defines a translation of the origin in R^2, and $\alpha_1>0$, $\alpha_2>0$ are two scale coefficients.

Using (10) and for $f\triangleq(f_1, f_2)$ and $\tilde{f}\triangleq(\tilde{f}_1, \tilde{f}_2)$ we obtain:

$$\begin{cases} \tilde{f}_1(t, r, \theta)=\alpha_1^{-1}f_1(t, a_1+\alpha_1 r\cos\theta,\ a_2+\alpha_2 r\sin\theta)\cos\theta+ \\ \qquad +\alpha_2^{-1}f_2(t, a_1+\alpha_1 r\cos\theta,\ a_2+\alpha_2 r\sin\theta)\sin\theta, \\ \tilde{f}_2(t, r, \theta)=r^{-1}[-\alpha_1^{-1}f_1(t, a_1+\alpha_1 r\cos\theta,\ a_2+\alpha_2\ r\sin\theta)\sin\theta+ \\ \qquad +\alpha_2^{-1}f_2(t, a_1+\alpha_1 r\cos\theta,\ a_2+\alpha_2\ r\sin\theta)\cos\theta]. \end{cases} \tag{11}$$

Further, the chosen form of p allows to adopt a positively flow-invariant set having the following ringshaped form :

$$\begin{aligned} B_R(t)\triangle\{x\in R^2 ;\ r_1^2(t)\leqslant\alpha_1^{-2}(x_1-a_1)^2+\alpha_2^{-2}(x_2-a_2)^2\leqslant r_2^2(t)\}= \\ =\{\tilde{x}\in R_+\times R ;\ r_1(t)\leqslant r\leqslant r_2(t)\},\quad t\in R_+, \end{aligned} \tag{12}$$

where $r_1 : R_+\to R_+$, $r_2 : R_+\to R_+$ are two differentiable functions, and (a_1, a_2) may eventually be an equilibrium point of the system to be analysed.

Corollary 6.1. *Ringshaped subset* (12) *contains a limit cycle of system* (1) *with* $n=2$ *if*

$$\min_{R_+\times R}[\tilde{f}_1(t, r_1(t), \theta)-\dot{r}_1(t)]\geqslant 0, \tag{13}$$

$$\max_{R_+\times R}[\tilde{f}_2(t, r_2(t), \theta)-\dot{r}_2(t)]\leqslant 0, \tag{14}$$

for $\theta\in R$, *and it does not contain any equilibrium point of system* (1). ■

Obviously, similar corollaries may be also stated for $n\geqslant 3$ by using suitable forms of the polar coordinate transformation.

3. Example

Consider a nonlinear oscillator described by

$$\dot{x}_1=x_2, \quad \dot{x}_2=-\omega_n^2 x_1-(2\zeta\omega_n+ax_1^2+b\omega_n^{-2}x_2^2)x_2 \tag{15}$$

where $\omega_n>0$, $a\geqslant b>0$ are given constants. Determine $\zeta\in R$ such that system (15) have a limit cycle.

Since for sistem (15) the origin is the unique equilibrium point, we shall use transformation (10) with $a_1=a_2=0$. By adopting $\alpha_1=1$, $\alpha_2=\omega_n$ it results:

$$\tilde{f}_1(t,\ r,\ \theta)=-r(2\zeta\omega_n-ar^2\cos^2\theta+br^2\sin^2\theta)\sin^2\theta. \tag{16}$$

For $r_1=\text{const.}$, $r_2=\text{const.}$, with $r_2\geqslant r_1>0$, according to Corollary 6.1, to (16) and to the fact that $r^2\sin^2\theta\geqslant 0$ and $\min\limits_{\theta\in R}[-2\zeta\omega_n-r^2(a\cos^2\theta+b\sin^2\theta)]=-2\zeta\omega_n-ar^2$, $\max\limits_{\theta\in R}[-2\zeta\omega_n-r^2(a\cos^2\theta+b\sin^2\theta)]=-2\zeta\omega_n-br^2$, it results that, under the necessary condition $\zeta<0$, system (15) has a limit cycle contained in a ringshaped subset $\{(r,\theta)\in R_+\times R\,;\ r_1\leqslant r\leqslant r_2\}$ with $r_1\leqslant\sqrt{2|\zeta|\omega_n/a}$ and $r_2\geqslant\sqrt{2|\zeta|\omega_n/b}$. As a consequence of even this fact, it follows that the limit cycle is stable (s. Remark 2).

Finally, one may remark that for $a=b$ the ringshaped subset may be taken precisely the limit cycle which is an ellipse described by the equation $x_1^2+\omega_n^{-2}x_2^2=2|\zeta|\omega_n a^{-1}$. For $b=0$ system (15) represents the well-known Van der Pol oscillator and in this case $r_2=+\infty$. Being not essentially different, the case $b>a\geqslant 0$ leads to similar results.

4. Concluding Remarks

The limit cycles existence may be analysed by applying Theorems 4, 5 and 6. Metatheoretically characterizing, these theorems evidence a simultaneous and gradual increasing of the „if parts" strongness and application effectiveness. For a given system the successfull using of Theorem 6 depends on the choosing of an adequate function p which actually defines a coordinate transformation in the state space. In this respect the simplest possibility seems to be the polar coordinate transformation which led to Corollary 6.1.

Received, October 31, 1989

Polytechnic Institute, Jassy,
Department of Automations
and Electric Utilizations

REFERENCES

1. Bhatia P.N., Szegö P.G., *Stability Theory of Dynamical Systems.* Springer-Verlag, Berlin, 1970.
2. Pavel H.N., *Differential Equations, Flow-Invariance and Applications.* Pitman, Boston, 1984.
3. Voicu M., *Free Response Characterization via Flow-Invariance.* 9-th World Congress of IFAC, Budapest, July 2—6, 1984; Preprints, **V**, 12—17.
4. Voicu M., *Componentwise Asymptotic Stability of Linear Constant Dynamical Systems.* I.E.E.E. Trans. on Aut. Control, **AC-29**, *10*, 937—939 (1984).
5. Voicu M., *On the Application of the Flow-Invariance Method in Control Theory and Design.* 10-th World Congress of IFAC, Munich, July 26—31, 1987; Preprints, **8**, 364—369.
6. Voicu M., *Structural Properties of the Spatial Manipulating Systems in Connection with the State and Control Constraints.* IFAC Symp. on Robot Control (SYROCO), Barcelona, November 6—8, 1985; Preprints, 425—428.
7. Voicu M., *Observing the State with Componentwise Decaying Error.* Systems & Control Letters, **9**, 33—42 (1987).
8. Voicu M., Moroșan B.-I., *State Space Flow Structure Induced by Sliding Motion Control.* Bul. Inst. polit., Iași, **XXXV (XXXIX)**, *3—4*, s. III, 25—29 (1989).

CONDIȚII SUFICIENTE DE EXISTENȚĂ A CICLURILOR LIMITĂ

(Rezumat)

Pe baza unor rezultate anterioare ale autorului, obținute prin aplicarea metodei invarianței de flux și a condiției de subtangențialitate aferente acestei metode, se formulează trei noi condiții suficiente de existență a ciclurilor limită. Efectivitatea lor în aplicații presupune utilizarea unei transformări adecvate a variabilei de stare.

BULETINUL INSTITUTULUI POLITEHNIC DIN IAȘI
Tomul XXXVI (XL) Fasc. 1—2, 1990
Secția III
ELECTROTEHNICĂ. ENERGETICĂ. ELECTRONICĂ. AUTOMATIZĂRI

C.D. 538 ; 539.2

SUR LES PERTES D'ÉNERGIE DANS LES NOYAUX MAGNÉTIQUES DE FERRITE DES BOBINES LINÉAIRES EN RÉGIME PERMANENT PÉRIODIQUE NONSINUSOÏDAL

PAR

DANA BALAN et TRAIAN BALAN

1. Introduction

Dans une Note précédente [1] on a proposé, en tant que schéma équivalent pour un noyau de ferrite se comportant d'une façon linéaire dans le champ magnétique, un uniporte linéaire passif. Les paramètres de ce schéma sont indépendants par rapport à la fréquence et on peut les déterminer à l'aide du procédé proposé dans la Note ci-dessus mentionée.

Le but de cette Note est de fournir nombre d'arguments qui renforcent ceux apportés dans [1] pour justifier l'adoption du schéma équivalent proposé et d'étudier certains aspects énergétiques concernant le régime permanent périodique nonsinusoïdal de l'uniporte équivalent à un noyau de ferrite, en considérant les conditions de fonctionement celles précisées dans [1].

Soit une bobine linéaire ayant l'inductance en air L_0, réalisée avec un noyau de ferrite dont les caractéristiques de fréquence sont semblables aux celles de la Fig. 1.

2. Propriétés des noyaux de ferrite magnétique dont le schéma électrique équivalent est un uniporte linéaire passif

On peut caractériser les pertes d'énergie dans le noyau dues à la variation du champ magnétique appliqué, par la dépendance par rapport à la fréquence de certains caractéristiques du matériel (μ'_r, μ''_r et tg δ_m — Fig. 1). Dans une Note antérieure [1] on a proposé un schéma équivalent, ayant les paramètres indépendents de fréquence, pour décrire les propriétés d'un tel noyau de ferrite (Fig. 2).

On peut utiliser, à leur tour, les paramètres établis à partir des caractéristiques de matériel du noyau pour définir ces caractéristiques :

Si

$$L_1 = L_0 \mu'_{r\infty}, \quad L_2 = L_0(\mu'_{rs} - \mu'_{r\infty}), \quad \tau = \frac{L_2}{R_2}, \tag{1}$$

alors

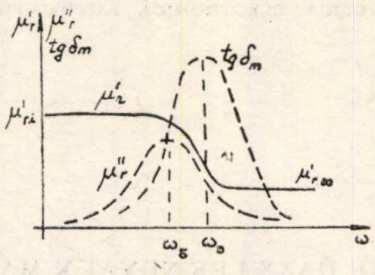

Fig. 1

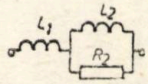

Fig. 2

$$(2)\qquad \mu'_r(\omega)=\frac{L_1}{L_0}+\frac{L_2}{L_0}\cdot\frac{1}{1+\omega^2\tau^2},\quad \mu''_r(\omega)=\frac{L_2}{L_0}\cdot\frac{\omega\tau}{1+\omega^2\tau^2};\quad \operatorname{tg}\delta_m=\frac{\mu''_r}{\mu'_r}.$$

Si l'on analyse les caractéristiques de la Fig. 1, ou celles fournies par le catalogue, on constate que dans le domaine des basses fréquences, $\mu'_r(\omega)=\mu'_{ri}=\mu'_{rs}$, c'est-à-dire l'apport du composant $\mu''_r(\omega)$ est négligeable. Dans ce cas on peut considérer la valeur maximum de la perméabilité visqueuse

$$(3)\qquad \mu''_{r\max}=\mu''_r\left(\frac{1}{\tau}\right)=\frac{\mu'_{rs}-\mu'_{r\infty}}{2},$$

obtenue à une fréquence située au début du domaine de décroissance de la caractéristique, proche à $\mu_{ri}/2$ [4], lorsqu'on néglige le terme $\mu'_{r\infty}$ par rapport à μ'_{rs}.

La pulsation,

$$(4)\qquad \omega_0=\frac{1}{\tau}\sqrt{\frac{\mu'_{rs}}{\mu'_{r\infty}}},$$

qui correspond au maximum du tg δ_m, est supérieure à ω_r, en concordance avec les caractéristiques de la Fig. 1.

La diminution de la fréquence de résonance, ω_r, associée à l'augmentation de la perméabilité magnétique initiale [3], constituent d'autres aspects que résultent de l'analyse des relations (3).

3. Pertes d'énergie en régime permanent périodique nonsinusoïdal (RPPNS) dans les bobines linéaires réalisées sur des noyaux de ferrite

Soit une bobine linéaire à noyau de ferrite ayant la résistance R et l'inductance en air L_0, dont on connaît les paramètres du schéma électrique (uniporte) équivalent (Fig. 3 *a*).

Pour caractériser le comportement du noyau en RPPNS on utilise le schéma série (Fig 3 *b*) ou parallèle en gardant les mêmes signaux pour ces deux schémas.

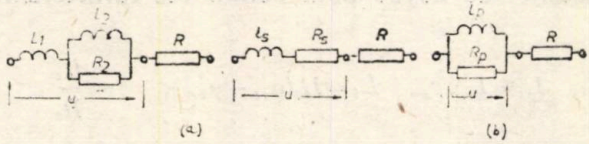

Fig. 3

Les conditions d'équivalence conduisent à :

$$R_s = \frac{\omega^2\tau L_2}{1+\omega^2\tau^2}, \quad L_s = \frac{L_1+L_2+L_1\omega^2\tau^2}{1+\omega^2\tau^2}, \tag{5}$$

respectivement

$$R_p = \frac{(L_1+L_2)^2+L_1^2\omega^2\tau^2}{\tau L_2}, \quad L_p = \frac{(L_1+L_2)^2+L_1^2\omega^2\tau^2}{L_1+L_2+L_1\omega^2\tau^2}. \tag{6}$$

Si les deux signaux sont périodiques, nonsinusoïdaux, de pulsation fondamentale ω_1, alors pour l'harmonique de rang n, $(\omega = n\omega_1)$, les puissances active et réactive deviennent :

$$P_n = \frac{n^2\omega_1^2\tau L_2}{1+n^2\omega_1^2\tau^2} I_n^2 = \frac{\tau L^2}{(L_1+L_2)^2+n^2\omega_1^2\tau^2 L_1^2} U_n^2, \tag{7}$$

respectivement

$$Q_n = \frac{n\omega_1(L_1+L_2+L_1n^2\omega_1^2\tau^2)}{1+n^2\omega_1^2\tau^2} I_n^2 = \frac{L_1+L_2+n^2\omega_1^2\tau^2 L_1}{(L_1+L_2)^2+n^2\omega_1^2\tau^2 L_1^2} U_n^2, \tag{8}$$

tandis que pour les signaux nonsïnusoidaux dont le spectre contient tous les harmoniques on obtient les expressions :

$$P = \tau L_2\omega_1^2 \sum_{n=1}^{\infty} \frac{n^2 I_n^2}{1+n^2\omega_1^2\tau^2} = \tau L_2 \sum_{n=1}^{\infty} \frac{U_n^2}{(L_1+L_2)^2+n^2\omega_1^2\tau^2 L_1^2}, \tag{9}$$

$$Q = \omega_1 \sum_{n=1}^{\infty} \frac{n(L_1+L_2+n^2\omega_1^2\tau^2 L_1)}{1+n^2\omega_1^2\tau^2} I_n^2 = \frac{1}{\omega_1} \sum_{n=1}^{\infty} \frac{L_1+L_2+n^2\omega_1^2\tau^2 L_1}{(L_1+L_2)^2+n^2\omega_1^2\tau^2 L_1^2} \cdot \frac{U_n^2}{n}. \tag{10}$$

Dans le domaine des fréquences basses, si l'on retient seulement les premières 25 harmoniques de telle sorte que $n^2\omega^2\tau^2 \ll 1$, on obtient pour les puissances des expressions simplifiées, avantageuses dans les calculs à caractère techniques. Ainsi pour l'harmonique de rang n il résulte :

$$P_n = \omega_1^2\tau L_2 n^2 I_n^2 = \tau \frac{L_2}{(L_1+L_2)^2} U_n^2, \tag{11}$$

$$Q_n = \omega_1(L_1+L_2) n I_n^2 = \frac{1}{\omega_1(L_1+L_2)} \cdot \frac{U_n^2}{n}. \tag{12}$$

Les puissances active et réactive pour les signaux nonsinusoïdaux dont les spectres contiennent tous les harmoniques jusqu'au rang 25, y compris, deviennent :

$$P = \tau\omega_1^2 L_2 \sum_{n=1}^{25} n^2 I_n^2 = \frac{\tau L_2}{(L_1+L_2)^2} \sum_{n=1}^{25} U_n^2, \tag{13}$$

$$Q = \omega_1(L_1+L_2) \sum_{n=1}^{25} n I_n^2 = \frac{\tau\omega_1 L_2}{L_1+L_2} \sum_{n=1}^{25} \frac{U_n^2}{n}. \tag{14}$$

L'analyse des relations (13), (14) met en évidence le poids du rang de l'harmonique du courant dans l'expression de la puissance qui correspond aux pertes dans le noyau.

Par analogie avec les condensateurs ayant des diélectriques polaires homogènes, étudiés en RPPNS à l'aide d'un schéma dual à celui de la Fig. 2, on retrouve les quotients de surcharge en puissance active :

$$k_p = \frac{P}{P_1} = \frac{\sum_{n=1}^{25} n^2 I_n^2}{I_1^2} = \frac{\sum_{n=1}^{25} U_n^2}{U_1^2} \tag{15}$$

et en puissance réactive :

$$K_Q = \frac{Q}{Q_1} = \frac{\sum_{n=1}^{25} n I_n^2}{I_1^2} = \frac{\sum_{n=1}^{25} U_n^2/n}{U_1^2}, \tag{16}$$

ainsi que le quotient des pertes diélectriques :

$$A = \frac{P}{Q} = \frac{\omega_1 \tau L_2}{L_1 + L_2} \cdot \frac{\sum_{n=1}^{25} n^2 I_n^2}{\sum_{n=1}^{25} n I_n^2} = \frac{\omega_1 \tau L_1}{L_1 + L_2} \cdot \frac{\sum_{n=1}^{25} U_n^2}{\sum_{n=1}^{25} U_n^2/n}. \tag{17}$$

On peut adopter les relations (9), (10) pour le cas du domaine des hautes fréquences à savoir :

$$P = R_s \sum_{n=1}^{\infty} I_n^2, \tag{18}$$

respectivement

$$Q = \omega_1 L_1 \sum_{n=1}^{\infty} n I_n^2. \tag{19}$$

L'analyse des pertes dans le noyau magnétique linéaire de ferrite fonctionnant en RPPNS permet à établir certaines formules utiles dans les calculs utilisés dans les projets. Ces formules soulignent le caractère dual des deux éléments réactifs réels — le condensateur à diélectrique polaire homogène et la bobine à noyau magnétique de ferrite.

4. Conclusions

1. L'uniporte linéaire passif équivalent au noyau magnétique linéaire de ferrite dont les paramètres sont indépendants par rapport à la fréquence est en bon accord avec les caractéristiques de fréquence du noyau.

2. On peut exprimer les pertes d'énergie dans le noyau magnétique de ferrite des bobines fonctionnant en RPPNS par l'intermédiaire des paramètres indépendants de fréquence de l'uniporte équivalent, relevant l'importance du rang de l'harmonique du courant dans l'expression des pertes qui y ont lieu.

3. On obtient des relations qui mettent en évidence le caractère dual de la bobine à noyau magnétique de ferrite et du condensateur au diélectrique polaire homogène.

Reçue le 7 novembre 1989

Institut Polytechnique, Jassy,
Chaire d'Électrotechnique, Mesures
et Machines électriques

BIBLIOGRAPHIE

1. Balan D., Balan T., *Caractéristiques de fréquence pour les bobines à noyau de ferrites du type Ni—Zn.* Bul. Inst. polit., Iaşi, **XXXV (XXXIX)**, *1—2*, s. III, 13—17 (1989).
2. Balan D., Balan T., Ciobanu R., *Some Contributions concerning the Behaviour of Polar Liquid Dielectric in Periodic Non-sinusoidal Electric Fields.* Bul. Inst. polit., Iaşi, **XXXII (XXXVI)**, *1—4*, s. III, 65—69 (1986).
3. Ifrim A., Noţingher P., *Materiale electrotehnice.* EDP, Buc., 1979.
4. Waldron R.A., *Ferrites* (traduit de l'anglais). Dunod, Paris, 1964.

ASUPRA PIERDERILOR DE ENERGIE ÎN MIEZURILE MEGNETICE DIN FERITĂ ALE BOBINELOR LINIARE ÎN REGIM PERIODIC PERMANENT NESINUSOIDAL

(Rezumat)

Se analizează unele aspecte ale pierderilor de energie în miezul de ferită al bobinelor liniare folosind schema echivalentă de tip uniport pasiv cu parametrii independenţi de frecvenţă. Este subliniată importanţa rangului armonicilor de curent în ponderea pierderilor de energie în miez.

BULETINUL INSTITUTULUI POLITEHNIC DIN IAŞI
Tomul XXXVI (XL) Fasc. 1—2, 1990
Secţia III
ELECTROTEHNICĂ. ENERGETICĂ. ELECTRONICĂ. AUTOMATIZĂRI

C.D. 621.3.017.42

L'ÉCHAUFFEMENT EN RÉGIME PERMANENT DE LA PIÈCE EN GRAPHITE D'UN CONTACT ÉLECTRIQUE GLISSANT

PAR

ADRIAN BARABOI et MARICEL ADAM

1. Dans une Note antérieure [1] on a montré que le régime permanent de l'échauffement du contact électrique à point, de type glissant, peut être étudié à l'aide de la théorie du modèle de la sphère de résistivité nulle [2].

Conformément aux hypothèses de calcul se trouvant à la base de cette théorie, le régime permanent de l'échauffement d'une pièce de contact électrique à point, de type glissant, traversé par un courant ayant l'intensité I, est décrit par l'équation différentielle de la forme :

$$\frac{d^2\theta}{dr^2}+\frac{2}{r}\cdot\frac{d\theta}{dr}+\frac{\rho J^2}{\lambda}=0,\quad r\geqslant a, \tag{1}$$

où $\theta(r)$, $J(r)$ représentent la température, respectivement la densité de courant sur la sphère de rayon r et λ, ρ — la conductivité thermique, respectivement la résistivité électrique du matériel.

Par transcription sous forme normée, l'équation différentielle (1) devient :

$$\frac{d^2y}{dx^2}+\frac{2}{x}\cdot\frac{dy}{dx}+\frac{py+q}{x^4}=0,\quad x\geqslant 1, \tag{2}$$

où l'on a utilisé les notations ci-dessous :

$$\begin{cases} x=\dfrac{r}{a},\quad y=\dfrac{\vartheta(r)}{\vartheta_0},\quad p=\dfrac{\rho_0\alpha_R P_c}{\pi(\lambda\rho)_0},\quad q=\dfrac{\rho_p P_e}{2\pi a\vartheta_0(\lambda\rho)_0}, \\ P_e=\dfrac{\rho_p I^2}{2\pi a},\quad \rho_p=\rho_0(1+\alpha_R\theta_p). \end{cases} \tag{3}$$

Les conditions à la limite imposées à la solution de l'équation différentielle (2) sont de la forme :

$$y(1)=\frac{\vartheta_c}{\vartheta_0},\quad \left.\frac{dy}{dx}\right|_{x=1}=-m,\quad \lim_{x\to\infty}y(x)=0,\quad \lim_{x\to\infty}\frac{dy}{dx}=0, \tag{4}$$

où :

$$m=\frac{\mu P_e\rho_0[1+\alpha_R(\theta_p+\vartheta_c)]}{2\pi a\vartheta_0(\lambda\rho)_0},\quad \mu=\frac{P_f}{P_e}. \tag{5}$$

Dans les relations (2) ... (5) on a noté par : ρ_0 — la résistivité du matériel à 0°C, α_R —le coefficient thermique de la résistance, a —le rayon de la surface effective du contact à point, θ_p— la température de régime permanent pour $r\to\infty$, $\vartheta(r)$ — l'échauffement de la zone de contact, y — l'échauffement normé, x — le rayon normé, P_e, ϑ_0 — des valeurs de repère du flux thermique produit par effet J o u l e, respectivement de l'échauffement de la zone de contact, P_f — le flux thermique produit par le frottement des pièces de contact, appliqué sur la surface de rayon a de la pièce étudiée.

Par l'intégration de l'équation différentielle (2), on obtient des solutions de la forme :

$$(6)\qquad y(x)=\begin{cases} A_1\cos(\varphi_1-\sqrt{p}/x)-q/p, \text{ pour } \alpha_R>0, \\ -A_2\,\mathrm{ch}\,(\varphi_2-\sqrt{-p}/x)-q/p, \text{ pour } \alpha_R<0. \end{cases}$$

Dans [1] on étudie le cas $\alpha_R>0$, qui permet le calcul de l'échauffement en régime permanent des contacts glissants établis entre des pièces métalliques.

2. Grâce à ses propriétés lubrifiantes, le graphite est un matériel fréquemment utilisé pour la construction des pièces de contact glissant.

Ayant en vue que le coefficient thermique de la résistance prend, dans ce cas, des valeurs $\alpha_R<0$, on peut étudier la sollicitation thermique d'une pièce de contact en graphite à l'aide de la solution (6_2). Ainsi, compte tenu des conditions à la limite (4), on obtient pour les constantes A_2, φ_2 et pour l'échauffement ϑ_c de la surface de contact les expressions :

$$(7)\qquad \begin{cases} A_2=-\dfrac{\sqrt{m^2\vartheta_0^2p+(p\theta_c+q\vartheta_0)^2}}{p\theta_0}, \quad \varphi_2=\sqrt{-p}+\operatorname{arg\,th}\dfrac{m\vartheta_0\sqrt{-p}}{p\vartheta_c+q\theta_0}, \\ \vartheta_c=\dfrac{\rho_p}{\rho_0\alpha_R}\cdot\dfrac{1-\mathrm{ch}\sqrt{-p}-\mu\sqrt{-p}\,\mathrm{sh}\sqrt{-p}}{2\mathrm{ch}\sqrt{-p}+\mu\sqrt{-p}\,\mathrm{sh}\sqrt{-p}}. \end{cases}$$

Dans le cas d'un contact électrique à point (Fig. 1), réalisé entre les pièces *1*— métallique et *2* — en graphite, la résistance de contact R_c représente la somme des résistances R_1, R_2, introduites séparément par les pièces *1*, *2* à savoir :

$$(8)\qquad R_c=R_1+R_2.$$

On peut calculer la résistance de contact R_2, spécifique à la pièce en graphite, à partir de l'équation connue [2] :

$$(9)\qquad \mathrm{d}R_2=\frac{\rho\,\mathrm{d}r}{2\pi r^2}.$$

Ayant en vue les relations (3), (7), par l'intégration de l'équation (9) on obtient :

$$(10)\qquad R_2=\frac{\rho_p}{4\pi a}+\frac{\rho_0\alpha_R\vartheta_0}{2\pi a\sqrt{-p}}\left[\frac{q}{p}\,\mathrm{th}\sqrt{-p}-\frac{m}{\sqrt{-p}}(\mathrm{sech}\sqrt{-p}-1)\right].$$

La chute de tension sur la résistance totale de contact, R_c, est donnée par la relation :

$$(11)\qquad U_c=R_cI,$$

où I représente l'intensité du courant traversant le contact.

Dans le cas du contact glissant représenté graphiquement dans la Fig. 1 le composant U_2 du chute de tension enregistré sur la pièce en graphite *2*, compte tenu de (8), (11), résulte de la forme :

$$(12)\qquad U_2=R_2I.$$

On peut particulariser les relations (7), (10), (12) pour un contact fix à point en considérant $\mu=0$, $(m=0)$.

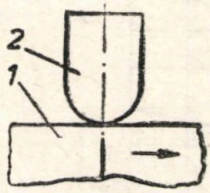

Fig. 1

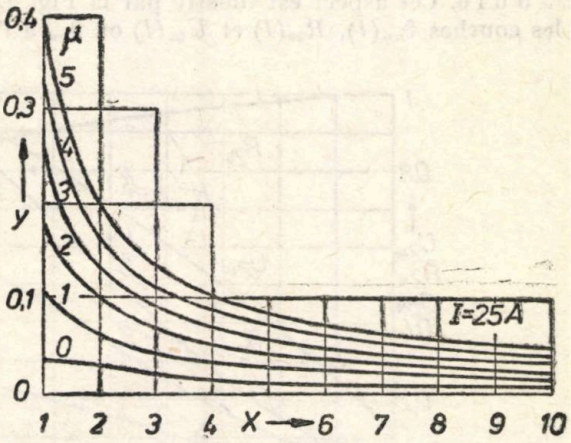

Fig. 2

Les expressions de calcul de la résistance de contact R_1, respectivement du chute de tension U_1, spécifiques aux pièces métalliques d'un contact glissant, sont données dans [1].

3. En utilisant les relations établies par voie théorique on présente un exemple de calcul numérique concernant l'échauffement en régime permanent de la pièce en graphite d'un contact électrique à point de type glissant ; les dimensions et les paramètres thermophysiques de celle-ci ont les valeurs suivantes : $a=4{,}75.10^{-4}$ m, $\rho_0=10^{-5}$ Ωm, $\alpha_R=$ $=-1{,}3.10^{-3}$ $(°C)^{-1}$, $(\lambda\rho)_0=1{,}6.10^{-3}$ ΩW/°C, $\vartheta_0=51{,}55°C$.

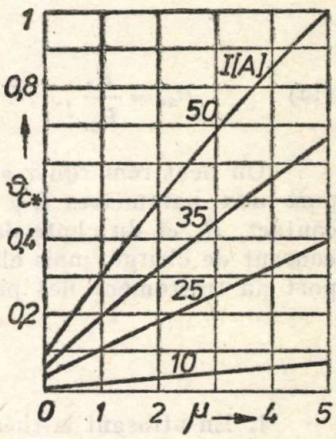

Fig. 3

Dans la Fig. 2 on a représenté sous forme graphique la solution (6_2) de l'équation différentielle (2), qui met en évidence, à l'aide de quelques valeurs imposées au paramètre μ, l'influence du flux thermique P_f sur l'échauffement de la zone de contact.

On a représenté aussi, dans la Fig. 3, les courbes $\vartheta_{c*}(\mu)$, où :

$$\theta_{c*}=\frac{\vartheta_c}{\vartheta_0}. \tag{13}$$

On constate un accroissement marqué de l'échauffement de la surface de contact dû au frottement ; le calcul montre toutefois que cet accroissement influence faiblement les valeurs de la résistance de contact R_2 et du chute de tension U_2 qui, pour $\mu=1 \ldots 5$ et $I=$const., restent environ constantes.

L'échauffement d'un contact électrique glissant fonctionnant en charge est produit simultanément par le frottement des pièces de contact et par l'effet J o u l e. Cet aspect est illustré par la Fig. 4, dans laquelle on a représenté les courbes $\vartheta_{c*}(I)$, $R_{2*}(I)$ et $U_{2*}(I)$ ou ϑ_{c*} a l'expression (13) et :

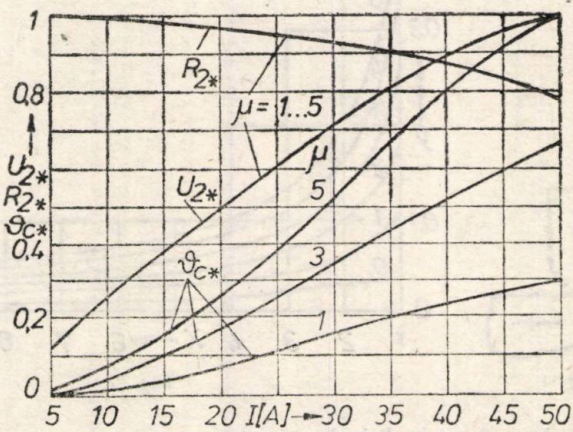

Fig. 4

(14) $$R_{2*}=\frac{R_2}{R_{2r}}, \quad U_{2*}=\frac{U_2}{U_{2r}}, \quad R_{2r}=4{,}89.10^{-3}\ \Omega, \quad U_{2r}=0{,}192\ \text{V}.$$

On peut remarquer ainsi la dépendance de l'échauffement ϑ_{c*} par rapport aux paramètres I, μ et on constate que les valeurs de la résistance de contact, R_2, et du chute de tension, U_2, sont visiblement influencées par le courant de charge, mais elles s'avèrent pratiquement indépendantes par rapport au frottement des pièces de contact.

Conclusions

1. En utilisant la théorie du modèle de la sphère de résistivité nulle on établit des relations nécessaires dans le calcul de l'échauffement en régime permanent de la pièce d'un contact à point de type glissant, caractérisée par des valeurs négatives du coefficient thermique de la résistance.

2. À l'aide des relations déterminées on étudie par voie théorique les influences de divers paramètres sur l'échauffement en régime permanent d'une pièce de contact en graphite.

3. Pour une valeur donnée de l'intensité du courant traversant le contact glissant, on met en évidence que les valeurs de la résistance de contact et du chute de tension sur le contact de la pièce étudiée sont pratiquement indépendantes par rapport au frottement des pièces de contact.

4. À la différence d'un contact fix, dans le cas d'un contact glissant on ne peut pas évaluer l'échauffement de la surface de contact en mesurant seulement le chute de tension, parce-que ce grandeur s'avère pratiquement indépendant

par rapport au frottement des pièces de contact, pendant que l'échauffement de la surface de contact est fortement influencé par celui-ci.

Reçue le 14 novembre 1989

Institut Polytechnique, Jassy,
Chaire d'Énergétique

BIBLIOGRAPHIE

1. Baraboi A., Furnică E., *Le régime permanent de l'échauffement d'un contact électrique à point, de type glissant.* Bul. Inst. polit., Iaşi, **XXXV (XXXIX)**, *1—2*, s. III, 37 (1989).
2. Hortopan Gh., *Aparate electrice.* EDP, Buc., 1980.

ÎNCĂLZIREA ÎN REGIM PERMANENT A PIESEI DE GRAFIT DIN CONSTRUCŢIA UNUI CONTACT ELECTRIC PUNCTIFORM DE TIP ALUNECĂTOR

(Rezumat)

Pe baza modelului sferei de conductivitate infinită se integrează ecuaţia diferenţială de transmisie a căldurii prin conducţie într-o piesă de grafit, din construcţia unui contact electric punctiform, de tip alunecător. Se stabilesc expresii de calcul pentru supratemperatura înregistrată pe suprafaţa de contact, rezistenţa de contact şi căderea de tensiune pe contact, corespunzătoare unei piese de contact caracterizată prin valori negative ale coeficientului de variaţie a rezistivităţii cu temperatura.

BULETINUL INSTITUTULUI POLITEHNIC DIN IAŞI
Tomul XXXVI (XXXX) Fasc. 1—2, 1190
Secţia III
ELECTROTEHNICĂ. ENERGETICĂ. ELECTRONICĂ. AUTOMATIZĂRI

C.D. 538 :539.2

SUR LE FONCTIONNEMENT DES ÉLECTRO-AIMANTS MONOPHASÉS À COURANT ALTERNATIF DE TYPE E—I AYANT DEUX BAGUES DE DÉPHASAGE

PAR

EUGEN HNATIUC

1. Introduction

Afin d'éliminer les vibrations de l'armature mobile des électro-aimants à courant alternatif de type E—I ou E—E on peut se servir seulement d'une bague de déphasage [2] et aussi de deux bagues de déphasage (v. Fig. 1).

Quoiqu'on conserve la validité des relations, des notations et des observations antérieures en ce qui concerne les noyaux magnétiques embrassés par les spires en court-circuit [1], on met en évidence, dans ce qui suit, des relations inédites pour les composants (moyen et oscillant) de la force active d'un tel électro-aimant.

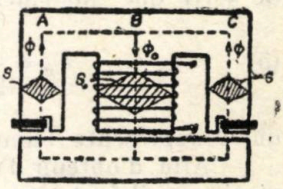

Fig. 1

2. Le calcul des composants et de la pulsation de la force active résultante d'un électro-aimant de type E—I muni avec deux bagues de déphasage

Compte tenu du diagramme des flux magnétiques $\underline{\Phi}_{e1}$ et $\underline{\Phi}_{e2}$ qui apparaissent par suite de la présence des bagues de déphasage, présenté dans la Fig. 2, on peut écrire les relations [1], [2] :

$$(1)\qquad \begin{cases} \cos\theta = \dfrac{1+(m+1)\sin^2\varphi_{sc}}{\sqrt{1+(m+1)(m+3)\sin^2\varphi_{sc}}}, \qquad \cos\alpha = \dfrac{1+\sin^2\varphi_{sc}}{\sqrt{1+3\sin^2\varphi_{sc}}}, \\ \cos\beta = \dfrac{1+(3+2m)\sin^2\varphi_{sc}}{\sqrt{(1+3\sin^2\varphi_{sc})[1+(m+1)(m+3)\sin^2\varphi_{sc}]}}, \end{cases}$$

où m représente la rapport entre l'aire embrassée par la bague en court-circuit, S_1 et l'aire qui n'est pas embrassée par cette bague, S_2 et φ_{sc} — l'angle de déphasage de la spire ayant la résistance électrique R_{sc} et l'inductance L_{sc}.

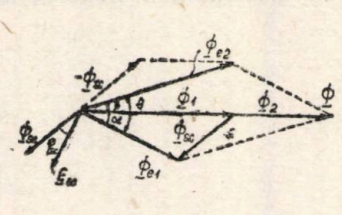

Fig. 2

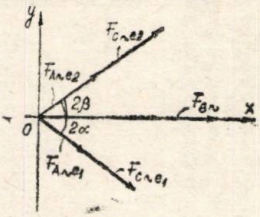

Fig. 3

Les sections transversales des trois colonnes du noyau magnétique (v. Fig. 1) satisfont les relations :

$$S_A = S_C = S, \qquad S_B = S_0 = nS, \qquad S_1 + S_2 = S. \tag{2}$$

Le composant moyen résultant de la force active est la somme des composants moyens : :

$$F_m = F_{Am} + F_{Bm} + F_{Cm}, \tag{3}$$

avec :

$$F_{Am} = F_{Cm} = \frac{\Phi^2}{4\mu_0 S} \cdot \frac{1+(m+1)(m+3)x}{1+3x}, \quad F_{Bm} = F_{B\sim} = \frac{\Phi^2}{\mu_0 Sn}, \quad \sin^2 \varphi_{sc} = x, \tag{4}$$

de sorte que finalement on obtient :

$$F_m = \frac{\Phi^2}{2\mu_0 Sn(1+3x)} [(n+2)(1+3x)+mnx], \tag{5}$$

où Φ représente l'amplitude du flux magnétique.

Afin d'obtenir l'expression du composant oscillant de la force active résultante il faut tenir compte du diagramme de la Fig. 3 et des relations (1), en résultant :

$$\begin{cases} F_{\sim x} = F_{B\sim} + (F_{A\sim e1} + F_{C\sim e1})\cos 2\alpha + (F_{A\sim e2} + F_{C\sim e2})\cos 2\beta, \\ F_{\sim y} = -(F_{A\sim e1} + F_{C\sim e1})\sin 2\alpha + (F_{A\sim e2} + F_{C\sim e2})\sin 2\beta, \\ F_{\sim} = \sqrt{F_{\sim x}^2 + F_{\sim y}^2}. \end{cases} \tag{6}$$

À l'aide des expressions [1] :

$$\begin{cases} F_{A\sim e1} = F_{C\sim e1} = \dfrac{m\Phi^2}{4\mu_0 S(m+1)(1+3x)}, \quad F_{B\sim} = \dfrac{\Phi^2}{\mu_0 Sn}, \\ F_{A\sim e2} = F_{C\sim e2} = \dfrac{[1+(m+1)(m+3)x]\Phi^2}{4\mu_0 S(m+1)(1+3x)}, \end{cases} \tag{7}$$

la relation (6_3) devient :

$$F_{\sim} = \frac{\Phi^2}{2\mu_0 Sn(1+3x)} \sqrt{[(n+2)(1+3x)-mnx]^2 + 16mn(n+2)x^2}, \tag{8}$$

de sorte que pour la valeur minimum de la force d'attraction on obtient :

$$F_{min}=F_m-F_\sim=\frac{\Phi^2}{2\mu_0 Sn(1+3x)}\left\{(n+2)(1+3x)+mnx-\right.$$
$$\left.-\sqrt{[(n+2)(1+3x)-mnx]^2+16mn(n+2)x^2}\right\}. \tag{9}$$

On peut aussi utiliser la relation :

$$p=\frac{F_\sim}{F_m}=\frac{\sqrt{[(n+2)(1+3x)-mnx]^2+16mn(n+2)x^2}}{(n+2)(1+3x)+mnx}, \tag{10}$$

pour évaluer la pulsation de la force active résultante, dont la valeur doit être minimum.

3. Le fonctionnement optimal des bagues de déphasage

Compte tenu des valeurs usuelles ($n=2$), imposées par des critères économiques qui résultent de la technologie de réalisation du noyau magnétique de type E—I, on constate que les relations (5) ,..., (9), (10) deviennent les mêmes que pour les électro-aimants monophasés de type E—I ayant une seule bague de déphasage à savoir :

$$\begin{cases} F_m=\dfrac{\Phi^2}{2\mu_0 S(1+3x)}[2+(m+6)x], \\ F_\sim=\dfrac{\Phi^2}{2\mu_0 S(1+3x)}\sqrt{[2+(6-m)x]^2+32mx^2}, \\ F_{min}=\dfrac{\Phi^2}{2\mu_0 S(1+3x)}\{2+(m+6)x-\sqrt{[2+(6-m)x]^2+32mx^2}\}, \\ p=\dfrac{\sqrt{[2+(6-m)x]^2+32mx^2}}{2+(6+m)x}. \end{cases} \tag{11}$$

On peut donc affirmer que le fonctionnement optimal des bagues de déphasage d'un tel électro-aimant est realisé pour :

$$x=\frac{4}{m+20}, \tag{12}$$

condition d'optimum confirmée par les valeurs maximales de la force F_{min} (v. rel. (9)). On constate aussi que la relation (12) permet d'obtenir des valeurs de la force F_{min} supérieures aux celles qui résultent en utilisant d'autres critères d'optimum [2].

4. Conclusions

On étudie le fonctionnement des électro-aimants monophasés à courant alternativ de type E—I ayant deux bagues de déphasage et on déduit des nouvelles relations qui permettent à évaluer les composants moyen et oscillant de la force active résultante.

L'analyse de ces relations suggère la possibilité de réaliser le fonctionnement optimal des bagues de déphasage par l'accord des paramètres de ces bagues et des valeurs du rapport m, défini par la relation (12).

Reçue le 3 octobre 1989

Institut Polytechnique, Jassy,
Chaire d'Énergétique

BIBLIOGRAPHIE

1. Hnatiuc E., *Sur le fonctionnement des électro-aimants à courant alternatif de type U—I munis avec des bagues de déphasage.* Bul. Inst. polit., Iași, **XXXIV (XXXVIII)**, *1—4*, s. III (1988).
2. Hnatiuc E., *Sur le fonctionnement des électro-aimants monophasés à courant alternatif de type E—I ayant seulement une bague de déphasage.* Bul. Inst. polit., Iași, **XXXV (XXXIX)**, *3—4*, s. III (1989).
3. Rosman H., Savin Gh., *Circuite electrice liniare.* Rotaprint, Inst. polit., Iași, 1974.

CU PRIVIRE LA FUNCȚIONAREA ELECTROMAGNEȚILOR MONOFAZAȚI DE CURENT ALTERNATIV DE TIP E—I PREVĂZUȚI CU DOUĂ SPIRE ÎN SCURTCIRCUIT

(Rezumat)

Prin analiza funcționării electromagneților monofazați de curent alternativ de tip E—I sau E—E prevăzuți cu două spire ecran plasate pe coloanele laterale ale miezului feromagnetic se stabilesc relații inedite ce permit evaluarea componentelor — medie, oscilantă și minimă — ale forței de atracție rezultante.

Ținînd seama de considerente tehnico-economice de realizare tehnologică a unor asemenea miezuri feromagnetice se constată că relațiile obținute devin identice cu cele obținute anterior pentru electromagneții de tip E—I sau E—E prevăzuți cu o singură spiră ecran plasată pe coloana mediană, putîndu-se accepta deci concluziile obținute pentru asemenea electromagneți și în cazul celor considerați în prezenta lucrare, cu privire la funcționarea optimă a spirelor ecran din punct de vedere al obținerii unor valori cît mai mari ale forței minime de atracție.

BULETINUL INSTITUTULUI POLITEHNIC DIN IAŞI
Tomul XXXVI (XL) Fasc. 1—2, 1990
Secţia III
ELECTROTEHNICĂ. ENERGETICĂ. ELECTRONICĂ. AUTOMATIZĂRI

D.C. 621.315.592

GUMMEL-POON PARAMETERS OPTIMAL EXTRACTION FOR COMPUTER-AIDED DESIGN WITH SPICE

BY

I. — C. TEŞU, OCTAV PĂSTRĂVANU, DAN ŞTIURCĂ and TEOHARIE GANCIU

1. Introduction

Circuit simulation program SPICE has been widely used as a tool for the analysis and design of integrated circuits. Although developed in the early seventees it became a standard program due to various types of performed analysis, the implemented algorithms and the predefined models (such as Gummel-Poon for the bipolar transistor or Frohman-Grove for the MOS transistor). Subsequent SPICE versions have input/output graphics, algorithms refinements, preserving practically unchanged the semiconductor device models.

Computer aided solutions for the parameter estimation of MOS models are described by Doganis [1] and Yang [2], while Hewlett-Packard [3] presents an optimal extractor for UCB—SPICE compatible models. For bipolar transistors Sischka presents in [4] a method for SPICE parameter determination without the intrinsic resistors $r_{E'}$, $r_{BB'}$, $r_{C'}$ (s. Fig. 2).

The aim of this paper is to present a computer-aided optimal extraction method for the complete set of dc G—P model parameters (listed in Table 1), starting from sets of μP-acquisitioned experimental data. The extracted parameters validity is tested using model variance and parametric redundancy analysis. A preprocessor (PRAE), including high quality routines of statistics, constrained optimization and eigensystems analysis, implements the main techniques of the methodology we had in view, on a computer compatible with DEC PDP—11/34 running RSX—11M or with PC IBM. The simulated results using SPICE supplied with the extracted parameters by means of the presented methodology are compared with the experimental data, the resulting errors being smaller than the technological spread of the usual devices.

2. Experimental Data Acquisition and Processing

2.1. Parameter Measuring System

The measurement of device characteristics (such as $I_C(U_{BE})$, $U_{BC}=$ $=$const., $I_B(U_{EB})$, $U_{BC}=$const., $I_C(U_{CE})$, $U_{BE}=$const., etc.), may be accomplished with an automatic μP-controlled data acquisition system connected with a host computer, as shown in Fig. 1. The data acquisition unit has an architecture based on the ideas from HP TECAP System [5].

In operation, the device under test is connected to four Stimulus/ Measurement Units (SMUs). The SMUs can be programmed to perform in

one of the two different modes : variable voltage source and current monitor, variable current source and voltage monitor, thus providing the necessary analog voltages (currents) and/or measuring the resulting currents (voltages). This approach offers a great flexibility in performing different measurements (e.g. for bipolar transistors in common emitter, common base, etc.) on the same electronic device without any connection changes. The SMUs are controlled by the Logic Interface Circuit. The A/D system (12 bits, 10 channels) converts the measured quantities for subsequent transmission to the host computer. The μP controls the data flow between the host and data acquisition system, the time sequences of measurements, the SMUs settings and the self calibration. The preprocessor PRAE is implemented on the host computer and delivers the dc G—P parameters for SPICE.

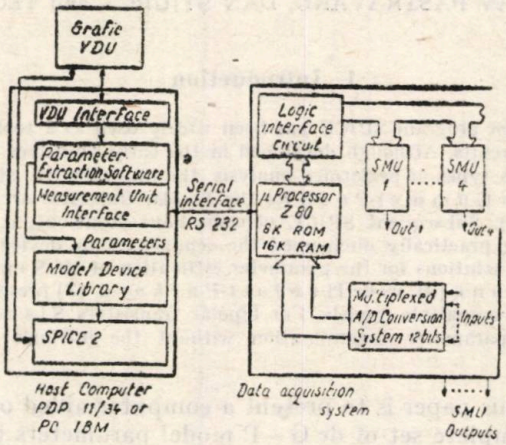

Fig. 1. — Block diagram of the automatic μP-controlled data acquisition system.

2.2. Experimental Data Processing

Suppose that a batch of N devices (volume N assures the determinated estimators consistency) is measured in n distinct points, each measurement being q times repeated, resulting a curve $y(x_j)$, $(j=\overline{1, n})$. Experimental data processing is accomplished in two stages.

In the first stage the erroneous acquisitioned experimental data are isolated. By means of M a s s e y 's test the measurement errors normal distribution is checked for each j (the measurement being q times repeated for each j). Points x_j not passing the test are rejected (or the measurements are repeated), a final new set of points being obtained. The homogeneity of variances :

$$S_i^2 = \sum_{k=1}^{q} \frac{(y_{ik} - \bar{y}_i)^2}{q-1}, \quad (i=\overline{1, N}), \tag{1}$$

where :

$$\bar{y}_i = \sum_{k=1}^{q} \frac{y_{ik}}{q}, \tag{2}$$

is verified for each x_j of the new set. For the subsequent processing only the device measurements coresponding to those x_j where C o c h r a n's test has passed, will be used [6]. Then the hypothesis $\bar{y}_1=\bar{y}_2=\ldots=\bar{y}_N$ is tested by means of the statistic [6] :

$$(3)\qquad \frac{\frac{q}{N-1}\sum_{i=1}^{N}(\bar{y}_i-\bar{y})^2}{\frac{1}{N(q-1)}\sum_{i=1}^{N}\sum_{k=1}^{q}(y_{ik}-\bar{y}_i)^2}\sim F_{N-1;\,N(q-1)},\qquad \left(\bar{y}=\frac{\sum_{i=1}^{N}\sum_{k=1}^{q}y_{ik}}{Nq}\right).$$

The second stage deals with determining a typical device from the experimental data that has passed the above mentioned tests. Its measured mean curve is the nearest in the least squares sens to the N devices mean curve [7]. This device is then completely characterized and its parameters are used as nominal values for the device type.

The measurements performed in order to determine the typical device have to be easy accomplished and must characterize its behaviour well. A good enough compromise is the characteristic $\beta_F(I_C)$, $U_{BC}=0$.

3. DC (forward and reverse) Parameters Optimal Extraction for G—P Model

3.1. The G—P Model Equations

Because the G—P model is widely known we shall present only the dc model equations and the parameters significance. Fig. 2 illustrates the G—P model used in SPICE [8].

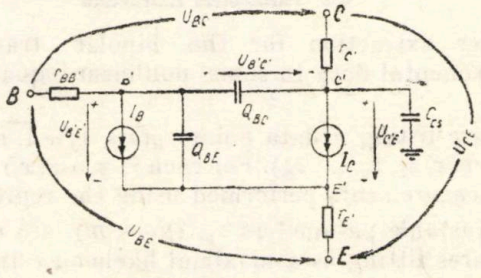

Fig. 2. — The SPICE bipolar transistor model.

The model equations are :

$$(4)\qquad I_C=\frac{I_S}{Q_B}\left[\exp\left(\frac{U_{B'E'}}{U_t}\right)-\exp\left(\frac{U_{B'C'}}{U_t}\right)\right]-$$
$$-\frac{I_S}{BR}\left[\exp\left(\frac{U_{B'C'}}{U_t}\right)-1\right]-C_4I_S\left[\exp\left(\frac{U_{B'C'}}{NC.U_t}\right)-1\right],$$

$$I_B = \frac{I_S}{BF}\left[\exp\left(\frac{U_{B'E'}}{U_t}\right)-1\right]+C_2 I_S\left[\exp\left(\frac{U_{B'E'}}{NE.U_t}\right)-1\right]+ \tag{5}$$

$$+\frac{I_S}{BR}\left[\exp\left(\frac{U_{B'C'}}{U_t}\right)-1\right]+C_4 I_S\left[\exp\left(\frac{U_{B'C'}}{NC.U_t}\right)-1\right],$$

where :

$$Q_B = \frac{Q_1}{2}\left(1+\sqrt{1+4Q_2}\right), \tag{6}$$

with :

$$Q_1 = \frac{1}{1-\dfrac{U_{B'C'}}{V_A}-\dfrac{U_{B'E'}}{V_B}}, \tag{7}$$

$$Q_2 = \frac{I_S}{I_K}\left[\exp\left(\frac{U_{B'E'}}{U_t}\right)-1\right]+\frac{I_S}{I_{KR}}\left[\exp\left(\frac{U_{B'C'}}{U_t}\right)-1\right]. \tag{8}$$

U_t represents the termal voltage ($U_t = kT/q \simeq 25$ mV at room temperature).

The parameters from Eqs. (4) ... (8) and Fig. 2 have the following significance : BF — ideal forward current-gain coefficient, BR — ideal reverse current-gain coefficient, I_S — saturation current, $r_{BB'}$ — base ohmic resistance, $r_{C'}$ — collector ohmic resistance, $r_{E'}$ — emitter ohmic resistance, V_A — forward Early voltage, V_B — reverse Early voltage, I_K — forward knee current, C_2 — forward nonideal base current-coefficient, NE — nonideal b-e emission coefficient, I_{KR} — reverse knee-current, C_4 — reverse nonideal base current-coefficient, NC — nonideal b-c emission coefficient.

3.2. Parameters Extraction

DC parameter extraction for the bipolar transistor means the fitting of the experimental data to some nonlinear equations derived from the G—P model.

Suppose we are fitting n data points $y(x_j)$, $(j=\overline{1, n})$, to a standard or user-defined model $y(x, z_1, z_2, ..., z_m)$. For each j, $y_j = y(x_j)$ represents the mean of the q parallel measurements performed using the representative device in the batch. The adjustable parameters z_p, $(p=\overline{i, m})$, are determined from the weighted least-squares fitting as a maximal likehood estimation [9] :

$$\chi^2(z_1, z_2, ..., z_m) = \sum_{j=1}^{n} \frac{[y_j - y(x_j, z_1, z_2, ..., z_m)]^2}{\sigma_j^2} = \min. \tag{9}$$

The quantities σ_j denote the standard deviation of the measurement errors, coresponding to y_j and have :

$$S_j^2 = \sum_{k=1}^{q} \frac{(y_{jk}-\overline{y}_j)^2}{q-1}; \qquad \overline{y}_j = \frac{1}{q}\sum_{k=1}^{q} y_{jk}, \ (j=\overline{1, n}), \tag{10}$$

as unbiased consistent estimators.

The used equations for the extraction of I_S, $r_{BB'}$, $r_{E'}$, BF, I_K, C_2 and NE are $I_C(U_{BE})$, $U_{BC}=0$ (Eq. (4) with $U_{BC}=0$) and the experimental data set I_C, I_B, U_{BC}, $\beta_F=I_C/I_B$ and the equation $\beta_F(I_C)$, $U_{BC}=0$ (the ratio of Eqs. (5) and (4) for $U_{BC}=0$) with the experimental data set β_F and I_C. Taking into account the intrinsic resistances we can write :

$$I_C=\frac{I_S}{1-\dfrac{U_{BE}-[r_{BB'}+(\beta_F+1)r_{E'}]I_B}{V_B}}\times$$

$$\times\frac{\exp\dfrac{U_{BE}-[r_{BB'}+(\beta_F+1)r_{E'}]I_B}{U_t}-1}{\dfrac{1}{2}\left(1+\sqrt{1+4\dfrac{I_S}{I_K}\exp\left\{\dfrac{U_{BE}-[r_{BB'}+(\beta_F+1)r_{E'})I_B]}{U_t}-1\right\}}\right)} \tag{11}$$

and the well known equation [10], [4] :

$$\frac{1}{\beta_F}=\frac{1}{BF}\left(1+\frac{I_C}{I_K}\right)+\frac{C_2I_S}{I_C}\left[\frac{I_C}{I_S}\left(1+\frac{I_C}{I_K}\right)\right]^{nF/NE} \tag{12}$$

For $I_C\ll I_K$, Eq. (11) can be aproximated by :

$$I_C=I_S\exp\left(\frac{U_{BE}}{U_t}\right). \tag{13}$$

Thus I_S can be determined using (13) and the experimental data corresponding to collector currents 20 ... 50 times less than the I_C value, where $\beta_F(I_C)$ reaches its maximum [4]. In (13) we have assumed an unitary emission coefficient ($nF=1$). But this represents a particular case, being more usefull to determine I_S and nF from (13). If the resulting nF is near unity, we can determine I_S in the hypothesis $nF=1$. If not, both I_S and nF must be included in the SPICE parameters list modifying adequately the program. The employment of equation $I_C=I_S/(1-U_{BE}V_B)\exp(U_{BE}/U_t)$ instead of (13) for I_S determination when $nF\neq1$, does not solve definitively the problem because $1/(1-U_{BE}/V_B)$ leaves practically unchanged the slope of $\ln I_C$ versus U_{BE}.

Eq. (12) (in which no intrinsic resistances are present) is used for the extraction of BF, I_K, C_2 and NE.

With I_S, nF and I_K already determinated we return in Eq. (8) and extract $r_{BB'}$ and $r_{E'}$. The experimental data points used now correspond to high injection levels where the quantities :

$$[r_{BB'}+(\beta_F+1)r_{E'}]I_B \quad\text{and}\quad 4\frac{I_S}{I_K}\left\{\exp\frac{U_{BE}-[r_{BB'}+(\beta_F+1)r_{E'}]I_B}{U_t}-1\right\}$$

can not be any more neglected when we refer to Eq. (8).

Parameters I_{KR}, C_4, BR and NC model β_R variation vs. I_E in reversed region. Their extraction is similar to direct region one because $\beta_R=\beta_R(I_E)$ has approximately the same shape as $\beta_F=(I_C)$.

Intrinsic resistance $r_{C'}$ is determined to fit the experimental data (I_C, U_{CE}, U_{BE}), I_B=const. with (8), in the transistor saturation region. The employed equation for $r_{C'}$ extraction is :

$$I_C = I_S \frac{\exp\frac{A}{U_t} - \exp\frac{B}{U_t}}{\frac{1}{2}\left[1+\sqrt{1+4\frac{I_S}{I_K}\left(\exp\frac{A}{U_t}-1\right)+4\frac{I_S}{I_{KR}}\left(\exp\frac{B}{U_t}-1\right)}\right]} - \frac{I_S}{BR}\left(\exp\frac{B}{U_t}-1\right) - C_4 I_S\left(\exp\frac{A}{U_t}-1\right), \tag{14}$$

where :

$$A = U_{BE} - r_{BB'} I_B - r_{E'}(I_B + I_C), \tag{15}$$

$$B = U_{BE} - r_{BB'} I_B - U_{CE} + r_{C'} I_C. \tag{16}$$

For the determination of the Early voltage V_s, suppose we have acquired the experimental data set $I_{Ci} = I_C(I_{Bi})$, $U_{BC}=0$. For $U_{BC}<0$ ($U_{CE}>U_{BE}$) the equation for I_C is :

$$I_C = \frac{I_{Ci}}{1 - \frac{U_{B'E'i}}{V_B} - \frac{U_{B'C'i}}{V_A}}. \tag{17}$$

For the usual values of V_B we can neglect $U_{B'E'i}/V_B$ at the denominator of (17). Introducing the intrinsic resistances $r_{C'}$ and $r_{BB'}$ we obtain the following expression for V_A :

$$V_A = \frac{I_C}{I_{Ci} - I_C}(I_{Bi} r_{BB'} + U_{CE} - U_{BEi} - r_{C'} I_C). \tag{18}$$

As the Early voltage is not unique for the whole family of output characteristics, in order to benefit of a greater accuracy, V_A will represent the mean of the computed values using only experimental data in the area necessary for transistor modeling. The Early voltage V_B is computed in a similar manner as V_A.

The nonlinear generally speaking optimization problems

$$\chi^2(z_1, z_2, \ldots, z_m) = \min., \tag{19}$$

resulting from the employment of Eqs. (11), (12) and (14), are completed with linear constraints :

$$a_p \leqslant z_p \leqslant b_p, \quad (p = \overline{1, m}), \tag{20}$$

which prevent unexpected deviations of the parameters values.

Two variants of the L e v e n b e r g--M a r q u a r d t algorithm [11], an analytic derivative procedure and a free-derivative one, were implemented in PRAE. So, for numerical ill-conditioned optimization problems (due to an inadvertency between practical data and the model), one can benefit of a higher accuracy by supplying the exact derivatives. For usual cases the Jaco-

bian is calculated numerically and a simple updating procedure is used to reduce computation time.

The minimization algorithm operates in linear constrained domains by introducing suitable variables substitutions [12] :

$$z_p = \frac{a_p + b_p}{2} + \frac{b_p - a_p}{2} \sin V_p, \quad (p = \overline{1, m}), \tag{21}$$

or modifying adequately the objective-function through the penalty method [11] :

$$\chi^2 = \sum_{j=1}^{n} [y_j - y(x_j, z_1, z_2, \ldots, z_m)]^2 + \sum_{p=1}^{m} A_p (a_p - z_p)^2 H(a_p - z_p) + \tag{22}$$
$$+ \sum_{p=1}^{m} B_p (z_p - b_p)^2 H(z_p - b_p).$$

H (....) denotes the H e a v i s i d e function and $A_p > 0$, $B_p > 0$ are weights which have to be assigned to each of the constraints.

The process converges or terminates when any of the following conditions are fullfilled: a) on two succesive iterations, the parameter values agree to a specified number of significant digits ; b) on two succesive iterations the residual sum of squares estimates have relative differences less than a specified small value ; c) the Euclidian norm of the approximate gradient is less than a specified small value which indicates that the solution is close to optimum ; d) the number of function evaluations exceeds a specified number (when convergence is not otherwise achieved) ; e) in exceeding the upper bound of the M a r q u a r d t parameter, the search for a descend direction is abandoned.

None of the model parameters extracted by means of these optimization procedures will be used in numerical simulation without a previous analysis of the model validity.

4. Model Adequacy Test

One can estimate the goodness-of-fit taking into account that the probability distribution for different values of χ at its minimum is a chi-squared distribution with $y - m$ degrees of freedom [9] ; a confidence level greater than 1% for the chi-squared test means the statistical acceptance of the model.

If the uniformity of measurement errors standard deviations is accepted for all data points (x_j, y_j), then the model adequacy may be also tested using the statistic [6] :

$$\frac{S^2_{res}}{s^2} \sim F_{n-m;\, n-1}, \tag{23}$$

in order to compare (with a prescribed confidence level) the residual variance :

$$S^2_{res} = \frac{1}{n-m} \sum_{j=1}^{n} [\bar{y}_j - y(x_j, z_1, z_2, \ldots, z_m)]^2 \tag{24}$$

with the measurement errors variances average s^2.

The preprocessor is also equiped with a redundant parameters analyzer which evaluates the sensitivity of the least-squares function at the extremum z^+, along each eigenvector of the Hessian [1] :

$$S_{z_p}^{\chi^2} = \frac{(J\Delta z_p)^T (J\Delta z_p)}{\chi^2} \cdot \frac{\|z^+\|}{\Delta z_p}, \quad (p = \overline{1, m}) ; \tag{25}$$

J denotes the Jacobian while Δz_p are taken along the eigenvectors. Low sensitivity implies redundant parameters and nonunique parameter values can be obtained for the model to be fitted.

If the Jacobian becomes closed to a rank deficit matrix then the optimization algorithm can not lead to an extremum and the model is independent w.r.t. the corresponding parameter (parameters).

The employed nonlinear optimization procedures return on output good approximations to the Hessian at its minimum point $H(z^+)$ and the square roots of the diagonal elements in the covariance matrix :

$$C = \left(\frac{1}{2} H(z^+)\right)^{-1} \tag{26}$$

represent the confidence limits on estimated model parameters z_p, $(p = \overline{1, m})$ [9].

A parameter can be insignificant for the considered model from the statistical viewpoint, even if it were not found as redundant during the sensitivity analysis. That is why it is neccesary to verify the hypothesis $z_p = \mu_p$, μ_p denoting a value which could simplify the functional relationship between the variables. Since :

$$\frac{1}{\sqrt{C_{pp}}} \sqrt{q}(z_p - \mu_p) \sim tq - 1 \tag{27}$$

we agree to the model simplification when S t u d e n t's test has passed.

5. A General Description of the Preprocessor

PRAE consists of a FORTRAN programs package and its actual version is implemented on a DEC PDP-11/34 computer, using double length floating point representation. A random acces file assures the data transfer between the constitutive programs. The preprocessor architecture is presented in Fig. 3.

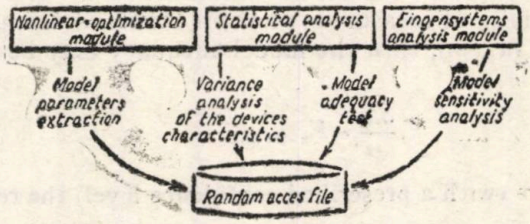

Fig. 3. — The preprocessor architecture.

The statistical analysis module includes the IMSL routines namely : a) MDFI for inverse F probability distribution function calculus ; b) MDCHI

which computes inverse chi-squared probability distribution function; c) MDSTI which computes the inverse of Student's t probability distribution function [13].

Slightly modified versions of the routines ZXSSQ [13], and TJMAR1 [14], constitute the nucleus called to solve the constrained optimization problems. For models linear in parameters, the least-squares fitting is accomplished with the help of the LSEI routine [15]. When there exists no indication in choosing the initial guesses, the procedure ZSRCH [13], allows an automatical generation of start points in the m-dimensional space.

The EISPACK routines TRED 2 and TQL 2 [16] are employed for eigensystems analysis involved in computing (25).

6. Results of Analysis and Simulation

The numerical results we are going to present below point out the previously mentioned steps and are reffering to devices with different technical data: 2N930, BC172, 2N2218, Mo001 Interdesing Ferranti; as an electronic circuit simulator we have used SPICE.

For the chi-squared test we have found the G—P model adequate for 2N930 with a confidence level of 1% in the I_C range 10 μA ... 20 mA, representing almost the whole area recommended for applications; at 23.6°C the estimated parameters are $I_S=3.04\,E-14$,[A], $BF=2\,076$, $I_K=38.2\,E-3$, [A], $C_4=1.104$, $NE=1.333$. On the other hand, for BC 172 the G—P model was accepted only for a smaller I_c range than in the data book ($I_C<40$ mA instead of 100 mA) having the following parameters values: : $I_S=2.34\,E-14$, [A], $BF=252$, $I_K=0.21$,[A], $C_2=0.531$, $NE=1.414$ at 22.5°C. For both devices we have obtained low sensitivity of χ^2_{min} with respect to r_E, and a large technological spread so that the statistical acceptance of a batch was difficult to be realized.

Modifying SPICE for 2N2218 operation simulation and introducing an emmision coefficient $nF=1.07$ in comparison with the default value $nF=1$, our results were considerably improved, as this parameter occurs in an exponent expression.

For the Monochip Mo001 bipolar transistor (standard 20 V bipolar process), β_F standard deviation is reduced; the minimization problem turned out to be numerically well-conditioned. Table 1 presents the extracted parameters values.

Table 1

DC G—P Parameters for the Monochip Mo001 Bipolar Transistor (t_{amb}=17°C)

Parameter	Value	UM	Parameter	Value	UM
BF	279.5		V_B	25.0	V
BR	10.0		I_K	4.95E−3	A
I_S	2.03E−16	A	C_2	72.8	
$r_{BB'}=RB$	203.9	Ω	NE	1.465	
$r_{C'}=RC$	20.0	Ω	IKR	5.81E−3	A
$r_{E'}=RE$	1.4	Ω	C_4	14.8	
V_A	32.0	V	NC	1.123	

Table 2 presents the relative differences between the experimental and simulated values U_{BE}, I_C, β_F for the Monochip transistor. The measurements were performed at 17°C and $U_{BC}=0$.

Table 2

Comparison of Measured and Simulated Data for I_C, U_{BE}, β_F of Monochip Transistors ($t_{amb.}=17°C$, $U_{BC}=0$ V)

I_B μA	U_{BE}, [V] meas.	U_{BE}, [V] comp.	εU_{BE} %	I_C, [μA] meas.	I_C, [μA] comp.	εI_c %	β_F meas.	β_F comp.	$\varepsilon\beta_F$ %
0.1	0.5748	0.5736	0.2	1.9	1.82	3.6	19	18.29	3.7
0.2	0.597	0.5981	−0.16	5.08	4.86	4.3	25.4	24.33	4.2
0.4	0.6228	0.6224	0.06	12.4	12.8	−3.1	31	31.97	−3.1
0.6	0.6363	0.6365	−0.03	23.1	22.3	3.2	38.5	37.25	3.2
0.8	0.6464	0.6464	−0.01	34.6	33.1	4.3	43.25	41.35	4.4
1	0.6543	0.6541	0.03	46.8	44.7	4.4	46.8	44.8	4.3
2	0.6783	0.6778	0.07	117	112	0.9	58.5	56.16	4.0
4	0.702	0.7013	0.1	283	271	4.2	70.75	67.83	4.1
6	0.7155	0.7151	0.05	459	443	3.4	76.5	73.94	3.3
8	0.7252	0.725	0.03	640	620	3.1	80	77.25	3.1
10	0.7326	0.7327	−0.01	818	796	2.5	81.8	79.86	2.5
20	0.7576	0.7576	0	1.68×10^3	1.64×10^3	2.4	84	82.3	2.0
40	0.7854	0.7848	0.07	3.2×10^3	3.11×10^3	2.7	80	77.8	2.8
60	0.8037	0.8028	0.11	4.51×10^3	4.35×10^3	3.6	75.1	72.61	3.3
80	0.818	0.8169	0.13	5.67×10^3	5.45×10^3	3.8	70.78	68.15	3.7
100	0.830	0.8289	0.13	6.7×10^3	6.44×10^3	3.8	67	64.43	3.8

Fig. 4 illustrates a comparison between measured and simulated output characteristics for the Monochip transistor, outside the saturation region. The modelling accuracy is smaller than 3.6%. For the whole working region

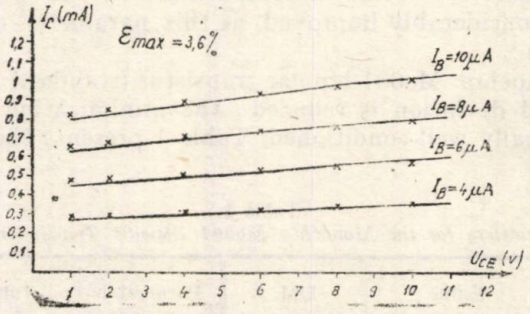

Fig. 4. — Output characteristics for the Monochip transistors; — simulated values; × experimental values.

($I_C=5$ μA ... 10 mA, $U_{CE}=1$ ... 16 V) relative errors less then 6% have been noticed.

For the saturation region, the differences of simulated and experimental data are given in Table 3. The errors exceed 10% in some points showing that further improvements are possible.

Table 3

Simulated and Experimental Data for V—I Characteristics in the Saturation Region (Monochip transistor, $t_{amb.}=17°C$)

I_B, [μA]	100×10^{-3}		1		10		100	
U_{CE}, [mV]	50	100	50	100	50	100	50	100
I_C comp., [μA]	0.163	0.886	2.67	16.2	37.7	220	327	1.770
I_C meas., [μA]	0.173	0.870	3.03	16.0	41.0	235	356	1.680
εI_c, [%]	5.3	−1.8	8.9	−1.25	8.0	6.3	8.1	5.2

For the Monochip transistor, the model validity is verified with a confidence level of 5% and a complex investigation of the G—P model sensitivity points out its notable performances, especially in IC structure simulation.

7. Conclusions

The purpose of this paper was to present a computer-aided optimal extraction method for the complete set of d.c. Gummel—Poon model parameters.

The basic ideas for the development of a fast and accurate μP-controlled acquisition unit for electronic devices measurements were presented. The measurement unit connection to a host computer leads to efficient parameters extraction and statistic model validity performance on larger computers with the dedicated preprocessor PRAE.

The purpose of the experimental data processing was to reject erroneous measurements and to determine the typical device in the batch.

High quality routines of constrained optimization were used to extract the model parameters. Their extraction was performed in the ranges where their sensitivities in the d.c. characteristics were maximum.

Adequacy (essential for modeling purposes) is tested by means of the statistical analysis module and eigensystem analysis module from PRAE.

The presented experimental results agree very closely with the simulations utilising the extracted parameters values.

Acknowledgment. The authors wish to thank Dr. A. Varga for the interesting discussions about nonlinear constrained optimization and to A. Cârstoiu and Al. Ionasek for providing the SPICE versions for both PDP and PC—IBM computers.

Received, June 18, 1989

Polytechnic Institute, Jassy,
Department of Applied Electronics
and
Department of Automations and Electrical Utilizations

REFERENCES

1. Doganis K., Scharfetter D.L., *General Optimization and Extraction of IC Device Model Parameters*, I.E.E.E. Trans. on ED, **30**, *9*, 1 219—1 228 (1983).
2. Yang P., Chatterjee P., *An Optimal Parameter Extraction Program for MOSFET Models*. I.E.E.E. Trans. on ED, **30**, *9*, 1 214—1 219 (1983).
3. * * * *TECAP Software, HP Software Catalog*. Hewlett Packard, 1985.

4. Sischka F., *Eine Methode zur Bestimmung der SPICE Parameter für Bipolare Transistoren*, AEÜ, **39**, 225–232 (1985).
5. Meada K., Ikemoto J., Tsuruda F., Takeda T., *Inteligent Instrument Streamlines dc Semiconductor Parameter Measurements*. HP Journal, **33**, *10*, 3–15 (1982).
6. Sachs L., *Angewandte Statistik — Anwendung Statisticher Methoden*. Springer Verlag, Berlin–Heidelberg, 1985.
7. Herskowitz G.J., Schilling R.B., *Semiconductor Device Modeling for Computer Aided Design*, McGraw-Hill Book Co., NY., 1972
8. Nagel L.W., *SPICE 2–A Computer Program to Simulated Semiconductor Circuits*. Memorandum No. ERL-M 520, Univ. of California, Berkeley, 1975.
9. Press W.H. et al., *Numerical Recipes — The Art of Scientific Computing*. Cambridge University Press, Cambridge, 1986.
10. Getreu J., *Modeling the Bipolar Transistor*. Tektronix Inc., Beaverton, 1976.
11. Jacobs D., (Ed.), *The State of Art in Numerical Analysis*. Academic Press, New York, 1977.
12. Nash J.C., *Compact Numerical Methods for Computers*. Adam Hilger Ltd., Bristol, 1980.
13. * * * *IMSL Library Reference Manual*. 8th edition, IMSL Huston, 1980.
14. Jefferson T.H., *TJMARI — A FORTRAN Subroutine for Nonlinear Least Squares Parameter Estimation*. Sandia Techn. Report SLL 73-0305, Sandia Laboratories, Livermore, 1973.
15. Hanson R.J., Haskell K.H., Sandia Techn. Reports SAND 77-0552, SAND 78-1290, Sandia Laboratories, Albuquerque, 1979.
16. Smith B.T. et al., *Matrix Eigensystems Routines EISPACK Guide*. Lecture Notes in Computer Science, **6**, Springer Verlag, Berlin, Heidelberg and New York, 1976.

EXTRAGEREA PARAMETRILOR GUMMEL–POON PENTRU APLICAŢII ÎN PROIECTAREA ASISTATĂ DE CALCULATOR CU SPICE

(Rezumat)

Se propune o metodă de extragere optimală asistată de calculator a setului complet de parametri Gummel–Poon de curent continuu. Datele experimentale sînt obţinute de către o unitate de achiziţie controlată cu microprocesor conectată la un calculator pe care este implementat un preprocesor care conţine subrutine de calcul statistic şi optimizări cu restricţii. Validitatea parametrilor estimaţi este verificată utilizînd analiza varianţei modelului şi a redundanţei parametrilor. Curbele simulate obţinute cu SPICE cu parametrii extraşi sînt comparate cu datele experimentale, erorile rezultate fiind mai mici decît dispersia tehnologică a dispozitivelor uzuale.

BULETINUL INSTITUTULUI POLITEHNIC DIN IAŞI
Tomul XXXVI (XL) Fasc. 1—2, 1990
Secţia III
ELECTROTEHNICĂ. ENERGETICĂ. ELECTRONICĂ. AUTOMATIZĂRI

D.K. 629.113 ;681.142.671.68

ÜBER SOFTWAREFRAGEN DIE SICH AUF DIE REALISIERUNG EINES BORDRECHNERS ZUR ÜBERWACHUNG EINIGER BEWEGUNGSPARAMETERN DER FAHRZEUGEN UND DEREN MOTOREN BEZIEHEN

VON

M. ANTONESCU, IRINA ANTONESCU, PETRUŢ DUMA und EMILIAN BANU

1. Einleitung

Sowohl die Einfachheit der minimalen Mikrosystemen und die daraus folgenden Vorteile—hohe Zuverlässigkeit, geringe Kosten—als auch die mehrfachen angebotenen Leichtigkeiten veranliessen die Einführung und die schnelle Verbreitung solcher auch in der Fahrzeugentechnik.

Diese Arbeit nimmt sich vor einige Softwarefragen eines Bordrechners zu stellen und Lösungen zu bieten. Betrachtet wird ein Bordrechner zur Überwachung verschiedener Bewegungs- und Motorenparametern.

2. Informationsquellen

Die weiter beschriebenen Gedanken gelten für über Vergaser gespeisten Ottomotoren.

Die Quellen deren Informationen zur Berechnung der in dem dritten Absatz Bestimmten Größen dienen, bestehen aus einen Durchflußgeber (DG) und einen Weggeber (WG). Prinzipiell lassen sich jede Wandler verwenden, die Einschränkungen seiend nur von der Empfindlichkeit und von der Natur der Flüssigkeit bestimmt.

Doch, um die Beziehungen die die überwachten Parametern charakterisieren zu begründen, muß man einige Einzelheiten über die in diesem praktischen Fall verwendeten Wandlern bieten.

Der DG besteht, im Grunde, aus einem Zylinder mit einem Volumen von k mL. Ein von der Kraftstoffpumpe mittels der Flüssigkeit angetriebenen Kolben führt eine hin—zurück Bewegung. In jeder solchen Perioden wird der Motor mit $2k$ mL Treibstoff gespeist. Der elektronische Teil des DG erzeugt eine Reihe von rechteckigen Impulse mit TTL Niveaux. Die Z_{DG} variable Dauer entspricht der Zeit in der $2k$ mL Kraftstoff verbrennt werden. Natürlich sind, im allgemeinen, auch die Impuls und Pausezeit einer Z_{DG} verschieden (s. auch die Abb. 1). Ebenfalls sind die Impuls und Pausezeit einer Z_{DG} auch für mehreren hintereinanderfolgenden Z_{DG} verschieden. Im prakti-

schen versuchten Falle, für $k=5$ mL, Werte der Z_{DG} in der Größenordnung von 100 bis 5 S sind absolut befriedigend für einer breiten Bereich von Lastwagen und Pkws, mit Verbräuchen von 3 bis 35 Liter/100 Km.

Der WG ist ein Photogeber, der die durchgefahrene Strecke in einer proportionaler Zahl von Impulsen mit TTL Niveaux umwandelt. Einer mit l bezeichneten Reifenperipherie entsprechen M Impulse. Für die besprochene Anwendung gelten $M=20$, Impulsdauern von 200 ... 300 μS, bzw. Impulsperioden von wenigstens 1,2 mS. Für einen gewöhnlichen Pkw Reifen entspricht diese Periode einer Spitzengeschwindigkeit von etwa 180 Km/Stunde.

k und M sind festgestellten, vom Aufbau der Wandlern hängenden Parametern, während l vom Reifentypus bestimmt wird (man nimmt natürlich an, daß der Luftdruck den vom Hersteller empfohlenen Wert hat).

3. Überwachten Größen

Unter Anwendung folgender Schreibweisen und Meßeinheiten : Z_{DG} — Signalperiode vom DG, [mS] ; k—der Rauminhalt des DG, [mL] ; N—die Zahl der vom WG in der Z_{DG} Zeit erzeugten Impulse; ΔZ—die in der Berechnung der Geschwindigkeit angenommene Zeitspanne. [mS] ; N_G — die Zahl der vom WG in der ΔZ Zeit erzeugten Impulse ; M — die Zahl der Impulse die der Peripherie des Reifens entspricht ; l — die Kreislinie des Reifens, [zM]; $N_{z_{DG}}$—die gesamte Zahl der Perioden des DG zwischen einem vom Anwender festgestellten Zeitpunkt (Reset) und der Anfang der Bearbeitungen ; N_{WG} — die gesamte Zahl der vom WG erzeugten Impulse in derselben Zeitspanne wie für $N_{z_{DG}}$, die überwachten Größen lassen sich in zwei Klassen erteilen :

1° Augenblicklichen Größen und zwar :

a) der augenblickliche Verbrauch :

$$V_A = \frac{2k}{N \cdot 1/M} \cdot 10^4, \quad [\text{L/100 Km}] ; \tag{1}$$

b) der einheitliche Verbrauch :

$$V_E = \frac{2k}{Z_{DG}} \cdot 60 , \quad [\text{L/Min}] ; \tag{2}$$

c) die Geschwindigkeit :

$$G = \frac{N_G l/M}{\Delta Z} \cdot 36, \ [\text{Km/Stunde}] \tag{3}$$

und :

2°. Angehäuften Größen die der Zeitspanne zwischen dem anfänglichen vom Anwender bestimmten Zeitpunkt (Reset) und dem laufenden Moment entsprechen, nämlich :

a) der gesamte Verbrauch :

$$V_G = 2kN_{z_{DG}} \cdot 10^{-3}, \ [\text{L}] ; \tag{4}$$

b) die gesamte Strecke :

$$S_G = N_{WG} \cdot \frac{l}{M} \cdot 10^{-5}, \quad [\text{Km}]; \tag{5}$$

c) der durchschnittliche Verbrauch :

$$V_D = \frac{V_G}{S_G} \cdot 10^2, \quad [\text{L}/100\ \text{Km}]. \tag{6}$$

B e m e r k u n g. In der Berechnung der Geschwindigkeit (3) wurde $\Delta Z = Z_{DG}$ angenommen, also auch $N_G = N$; natürlich schiebt die als solche die Verwendung der Beziehung (3) keine Schwierigkeiten hervor.

4. Softwarefragen; Lösungen

In der Absicht möglichst viele Fragen über Software zu lösen und damit das Hardware zu vereinfachen, die Zuverlässigkeit zu erhöhen und den Preis des Gerätes herabzusätzen—die Problemen in die man einsteigen muß lassen sich folgendermaßen zerteilen : a) die Informationsanschaffung ; b) die in reeler Zeit Bearbeitung dieser, der Beziehungen (1) ... (6) entsprechend ; c) die in reeler Zeit Anzeige der gewünschten und vom Anwender über eine Tastatur bestimmten Größen.

Für die Geschmeidigkeit und Klarheit des Softwares sind wir der Meinung gewesen, daß die Erteilung der obenerwähnten Aufträge über mehrere, mittels eines in reeler Zeit arbeitenden Bedienungssystem (RZBS) verarbeiteten Prozesse, nützlich wäre.

Auch nur eine prinzipielle Beschreibung des RZBS kann unmöglich Raum im Rahmen dieser Arbeit finden. Es reicht aus zu sagen, daß das RZBS das Beleben und Aufheben der Prozesse vom Vorrang und von den im System auftretenden Ereignissen abhengend ermöglicht. Das Beleben und Aufheben erfolgen Gleichzeitig mit den Speichern bzw. Wiederherstellung der Prozessenzustände in eigene Stapeln. Das Beleben eines vorher aufgehobenen Prozesses einbezieht offenbar seine Wiederaufnahme vom Aufhebungspunkt an.

Im realisierten System führten wir zwei Vorgänge ein, deren Aufträge jenen am Anfang dieses Absatzes entsprechen und zwar :

1° *Der Anzeigevorgang* (AV) entspricht dem c) Punkt und bezieht sich auf : α) Tastaturabfrage und Identifizierung der gedrückten Taste (falls nötig) ; β) dynamische Anzeige der über die Taste bestimmte Größe. Die Anzeige erfolgt über 6 Stellen (daraus 3 für den Bruchteil) die Anzeigezellen mit 7 Segmenten verwenden. Jede Zelle ist 1,5 mS aktiv. Es sind also etwa 10 hintereinanderfolgenden mS dieser Tätigkeit erteilt. Die 6 Stellen schreiben eine Rechengenauigkeit in der Größenordnung von mL für Verbräuche, M/S für Geschwindigkeit und M für gefahrene Strecke ; γ) vom Anwender angeforderte Initialisierungen (Reset) für V_G, S_G, V_D ; δ) Feststellung des unmittelbar nach einem aus der Unterbrechung Rückehr Zeitpunktes und das Lancieren des BV mittels RZBS.

2° *Dem Bearbeitungsvorgang* (BV), der dem b) Punkt entspricht kommen zu : α) die Berechnung der Beziehungen (1) ... (6) unter Zerteilung der Rechenzeit in Zeitabständen von je 15 mS ; β) die Vergegenwärtigung des Anzeigespeichers ; γ) das Rückehr in AV mittels RZBS (und zwar aus einer Unterbrechung).

Das Mikrosystem arbeitet in periodischen Unterbrechungen mit einer Periode von 1 mS (die ausreichend ist um die in einem Latch gespeicherten Information des WG zu erfassen).

3° *Der Bedienungsabschnitt* der Unterbrechungen (BAU) muß folgende, dem a) Punkt entsprechende Problemen lösen : α) die Datenanschaffung vom DG und WG was die Messung der Z_{DG} mit einer Genauigkeit von 1 mS und die Zählung der Impulse vom WG in derselben Zeitspanne bedeutet ; β) die Erfassung der aufsteigenden Flanken des Signals vom DG (alle Bearbeitungen erfolgen in reeler Zeit und zwar in eine kürzere Zeit als Z_{DG}) ; γ) das Erkennen der Notwendigkeit des Bearbeitungsvorgangs (mittels Erfassung zwei hintereinenderfolgenden aufsteigenden Flanken des Signals vom DG) ; δ) falls nötig, die Messung einer Tastebetätigungszeit ; ε) die Messung von Zeitspannen von 15 mS, die dem BV zukommen ; ζ) unter der Annahme, daß die Bearbeitungen am Ende sind, oder eine Zeitspanne von 15 mS vorbei ist, das Rückehr in BV mittels RZBS.

Eine qualitative Darstellung der Tätigkeitenreihenfolge erscheint in der Abb. 1.

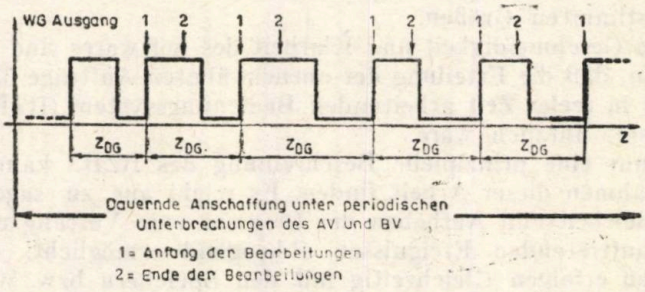

Abb. 1

In den Zeitintervallen 1→2 schieben sich die Anzeigen und die Bearbeitungen ein (in einem Rhytmus von 10 mS Anzeige, 15 mS Bearbeitungen) während in 2→1 nur Anzeigen erfolgen. Eine dauernde Anschaffung (in Zeitabständen von 1 mS) unterbricht periodisch beide Vorgänge.

Ein prinzipielles Flußdiagramm der Softwarestruktur die der vorher beschriebenen Gedanken entspricht ist in der Abb. 2 dargestellt.

Der Sprung von einem Vorgang in den anderen mittels RZBS benötigt etwa 350 μS während die Unterbrechungen nicht akzeptiert sind. Um keine Informationen die in dieser Zeit erscheinen können zu verlieren, das Lancieren des BV vom AV erfolgt unmittelbar nach dem Rückehr aus einer Unterbrechung. Ebenfalls, weil die Zeitabstände von 15 mS die dem BV zukommen im BAU erfaßt sind, das Aufheben des BV und das Lancieren des AV müßen im BAU stattfinden. Weil der Endezeitpunkt der Bearbeitungen unabhängig von der Unterbrechungserscheinung ist und der AV nur aus dem

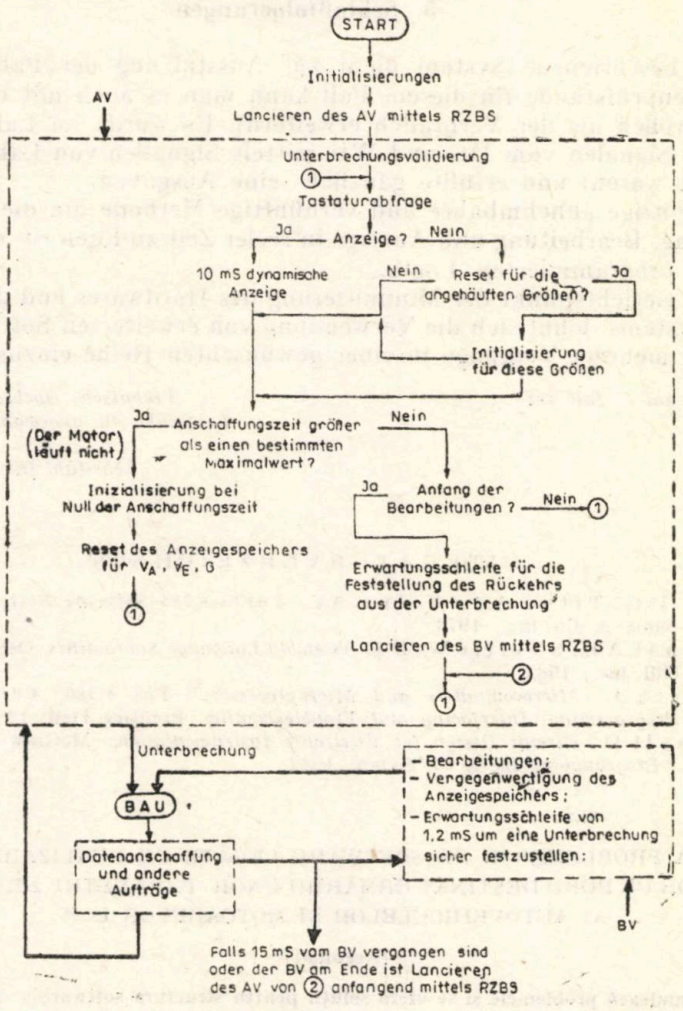

Abb. 2

BAU lanciert werden kann, der BV endet mit einer Warteschleife von etwa 1,2 mS während mit Sicherheit eine Unterbrechung erscheint.

Für die Bearbeitungen verwendet man hauptsächlich Unterroutinen für Multiplikation und Division von ganzen Binarzahlen von 8; 16; 24 Bits. Die Bruchteile gewinnt man auch unter Berechnungen mit Ganzzahlen.

Das System Hardware ist standard, minimal und basiert auf ein Z 80 Mikroprozessor. Es benötigt eine periodische Unterbrechungsquelle (z.B. ein CTC Kreis) sowie ein oder zwei (vom Typus abhängend) PIO. Sie sind der Tastaturabfrage, dem Steuer der Anzeigesegmenten, der Datenanschaffung sowie für das Reset des Latches (das die Information vom WG speichert) bestimmt.

5. Schlußfolgerungen

Das beschriebene System dient zur Ausstattung der Fahrzeuge und der Motorenprüfstände (in diesem Fall kann man es auch mit der Messung anderer Größen als der Verbrauch erweitern). Es wurde im Labor getestet (wobei die Signalen vom DG und WG mittels Signallen von Laborgeneratoren ersetzt waren) und erfüllte gänzlich seine Ausgaben.

Die einzige annehmbahre und vernünftige Methode um die Fragen der Anschaffung, Bearbeitung und Anzeige in reeler Zeit zu lösen ist die Verwendung der programmierten Logik.

Vom Gesichtspunkt der Minimisierung des Hardwares und der Biegsamkeit des Systems, lohnt sich die Verwendung von erweiterten Softwaremitteln im Stande mehrere Vorgänge in einer gewünschten Reihe einzuschieben.

Eingegangen am 1. Juli 1989

Technische Hochschule, Jassy,
Lehrstuhl für angewandte Elektronik
und
Lehrstuhl für Physik

LITERATURVERZEICHNIS

1 Larsen D.G., Titus A.J., Titus A.C., *8 080—8 085 Software Design*. Howard W. Sams & Co Inc., 1978.
2. Leventhal A.L., Saville W., *Z 80 Assembly Language Subroutines*. Osborne/McGraw-Hill Inc., 1983.
3. Uffenbeck J., *Microcomputers and Microprocessors: The 8 080, 8 085 and Z 80. Programming, Interfacing and Troubleshouting*. Prentice Hall, 1985.
4. Wobschall D., *Circuit Design for Electronic Instrumentation*. McGraw-Hill, 1987.
5. Zaks R., *Programming the Z 80*. Sybex, 1982.

ASUPRA PROBLEMELOR DE SOFTWARE LEGATE DE REALIZAREA UNUI CALCULATOR DE BORD DESTINAT URMĂRIRI UNOR PARAMETRI DE DEPLASARE AI AUTOVEHICULELOR ȘI MOTOARELOR LOR

(Rezumat)

Se formulează problemele și se oferă soluții pentru structura software a unui calculator de bord pentru autovehicule (sau standuri de probă) implementat prin folosirea unui microsistem organizat în jurul microprocesorului Z 80. Se au în vedere posibile surse de informații, relații de calcul pentru mărimile urmărite, sarcinile software și repartizarea lor pe procese, intercalarea proceselor printr-un sistem de operare în timp real.

BULETINUL INSTITUTULUI POLITEHNIC DIN IAȘI
Tomul XXXVI (XL) Fasc. 1—2, 1990
Secția III
ELECTROTEHNICĂ. ENERGETICĂ. ELECTRONICĂ. AUTOMATIZĂRI

C.D. 621.314

CONVERTISSEUR ANALOGIQUE – DIGITAL AVEC RÉSOLUTION EN PROGRAMME

PAR

LIVIU BRENIUC, M. CREȚU et C. SĂRMĂȘANU

1. Introduction

Dans les systèmes d'aquisition des dates analogiques, les convertisseurs les plus utilisés sont ceux à approximations successives [1], [2]. En principe, les parties composantes d'un tel convertisseur sont: le régistre d'approximations successives, le bloc de conversion D/A et le comparateur.

Dans ce qui suit on présente un convertisseur A/D dont le régistre d'approximations successives est contenu dans une mémoire, en présentant ainsi l'avantage de selectionner la résolution et d'augmenter la vitesse de conversion.

2. Le principe de la méthode

Le schéma bloc du convertisseur proposé, ayant le même mode de fonctionnement que celui présenté dans [3], est representé dans la Fig. 1. Le registre d'approximations (SAR) est réalisé avec une mémoire PROM. Ils sont necessaires 2^{n+1} états différents, donc $n+1$ bits d'adresses $(A_0, \ldots, A_n)$, pour une résolution de n bits du convertisseur. Avec les bits d'adresse $A_{n+1}, \ldots,$

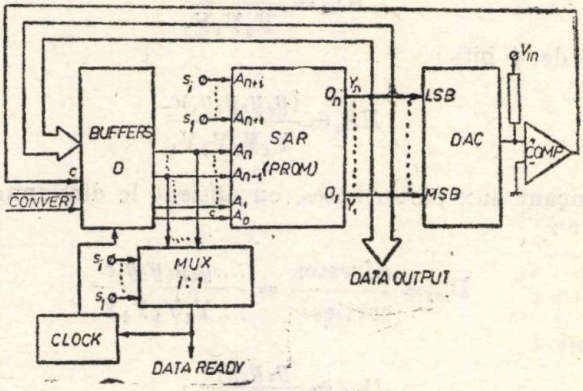

Fig, 1

A_{n+i}, la mémoire se divise en 2^i segments, ayant la capacité 2^{n+1}, dans laquelle l'algorithme, pour la conversion de résolution n, $n-1$, ..., $n-2^i$, est enregistré. La sélection de la résolution du convertisseur est réalisee par l'intermédiaire des entrées S_1, ..., S_i qui sont liées aussi aux entrées d'adresse du multiplexeur MUX i : 1. En fonction de la résolution choisie on sélectionne, à l'aide du multiplexeur, le dernier bit testé, qui aura la valeur logique 1 avant la fin de la conversion. Ce signal est accessible à la sortie, DATA READY, il indique la fin de la conversion et il arrête en même temps le générateur de tact CLOCK. Une nouvelle série de conversions sera réalisée par le signal $\overline{\text{CONVERT}}$ qui annule le régistre BUFFERS.

Pour programmer la mémoire afin de fonctionner comme régistre d'approximations successives on emploie le rapport d'état :

$$RS = \frac{(y_n y_{n-1} \cdots y_2 y_1)c}{Y_n Y_{n-1} \ldots Y_2 Y_1},$$

où Y_1 ,..., Y_n sont les sorties de la mémoire, y_1, ..., y_n — les entrées d'adresse et c — la sortie de comparation.

En utilisant ce rapport d'état, on élimine la nécessité de préciser la résolution du convertisseur [3], et par suite, le nombre des sorties/entrées de la mémoire, ce qui représente un avantage. Les sorties Y_1, Y_2, Y_3, ..., dans l'ordre donné, sont connectées aux entrées numériques du convertisseur D/A, DAC, en commençant avec le bit le plus significatif, MSB. Après la comparation, en courant, du signal d'entrée V_{in} et de celui produit par DAC, le comparateur COMP fournit le signal de commande c, le schéma étant synchronisé par le signal de tact émis par le CLOCK.

3. La programmation de la mémoire

Afin d'illustrer par des exemples l'algorithme de programmation de la mémoire ayant une résolution de n bits, dans la Fig. 2 on représente l'organigramme d'un convertisseur avec une resolution de 3, respectivement 4 bits.

Le rapport d'état pour le convertisseur de 3 bits est :

$$RS_3 = \frac{(y_3 y_2 y_1)c}{Y_3 Y_2 Y_1}$$

et pour celui de 4 bits :

$$RS_4 = \frac{(y_4 y_3 y_2 y_1)c}{Y_4 Y_3 Y_2 Y_1}$$

d'où, en renonçant aux paranthèses, on obtient le dictionnaire d'inscription de la mémoire :

$$D_{\text{ins}} = \frac{\text{adresses}}{\text{sorties}} = \frac{\ldots. y_4 y_3 y_2 y_1 c}{\ldots. Y_4 Y_3 Y_2 Y_1},$$

Par conséquent

$$D_{\text{ins}_3} = \frac{y_3 y_2 y_1 c}{Y_3 Y_2 Y_1},$$

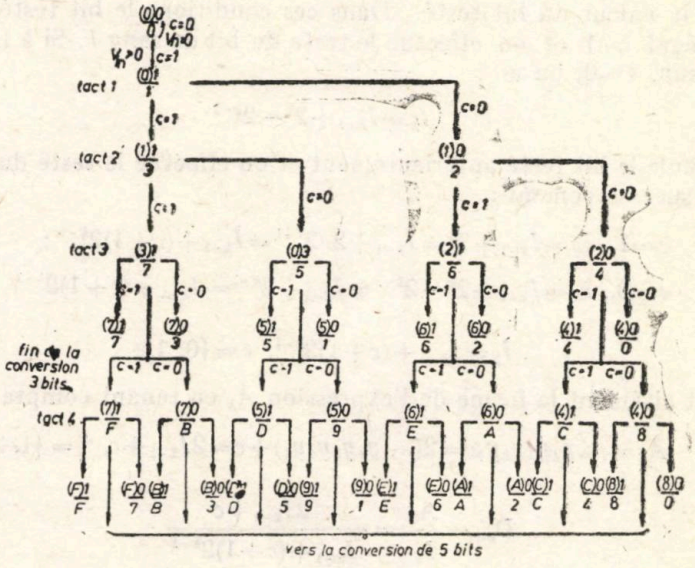

Fig. 2

en résultant les états :

$$\frac{0}{0},\ \frac{1}{1},\ \frac{2}{2},\ \frac{3}{3},\ \frac{4}{4},\ \frac{5}{6},\ \frac{6}{5},\ \frac{7}{7},\ \frac{8}{0},\ \frac{9}{4},\ \frac{A}{1},\ \frac{B}{5},\ \frac{C}{2},\ \frac{D}{6},\ \frac{E}{3},\ \frac{F}{7}$$

et

$$D_{\text{ins}_4} = \frac{y_4 y_3 y_2 y_1 c}{Y_4 Y_3 Y_2 Y_1}$$

en résultant les états :

$$\frac{0}{0},\ \frac{1}{1},\ \frac{2}{2},\ \frac{3}{3},\ \frac{4}{4},\ \frac{5}{6},\ \frac{6}{5},\ \frac{7}{7},\ \frac{8}{8},\ \frac{9}{C},\ \frac{A}{9},\ \frac{B}{D},\ \frac{C}{A},\ \frac{D}{E},\ \frac{E}{B},\ \frac{F}{F},\ \frac{10}{0},$$

$$\frac{11}{8},\ \frac{12}{1},\ \frac{13}{9},\ \frac{14}{2},\ \frac{15}{A},\ \frac{16}{3},\ \frac{17}{B},\ \frac{18}{4},\ \frac{19}{C},\ \frac{1A}{5},\ \frac{1B}{D},\ \frac{1C}{6},\ \frac{1D}{E},\ \frac{1E}{7},\ \frac{1E}{F}.$$

Pour un convertisseur à grande résolution on se propose de trouver une formule de récurrence qui puisse être utilisée dans la programation sur calculateur.

Soit le dictionnaire d'inscription ayant la forme :

$$D_{\text{ins}} = \frac{\ldots. y_4 y_3 y_2 y_1 c}{Y_4 Y_3 Y_2 Y_1} = \frac{\text{adresses}}{\text{sorties}} = \frac{A_k}{I_k},$$

où : A_k — adresses, représente l'état antérieur, et I_k — sorties, représente l'état présent du convertisseur. Si après la comparaison il résulte $c=1$, on a :

$$I_k = I_{k-1} + 2^k,$$

où k est la valeur du bit testé. Dans ces conditions le bit testé antérieurement est égal à 1 et on effectue le teste du bit de rang k. Si à la suite de la comparaison, $c=0$, on a :

$$I_k = I_{k-1} + 2^k - 2^{k-1}$$

ce qui annule le bit testé antérieurement et on effectue le teste du bit de rang k. On a successivement :

$$c=1,\ I_k = I_{k-1} + 2^k = I_{k-1} + 2\cdot 2^{k-1} = I_{k-1} + (c+1)2^{k-1};$$

$$c=0,\ I_k = I_{k-1} + 2^k - 2^{k-1} = I_{k-1} + 2^{k-1} = I_{k-1} + (c+1)2^{k-1}$$

et donc

$$I_k = I_{k-1} + (c+1)2^{k-1},\ c=\{0, 1\}.$$

On déduit aisément la forme de l'expression A_k en tenant compte que :

$$A_k = \ldots y_4 y_3 y_2 y_1 c = 2(\ldots y_4 y_3 y_2 y_1) + c = 2I_{k-1} + c,\ c=\{1, 2\}$$

et donc :

$$D_{ins} = \frac{A_k}{I_k} = \frac{2I_{k-1}+c}{I_{k-1}+(c+1)2^{k-1}}.$$

Ayant en vue que A_k est un nombre quelconque, $N \in [0\ ;\ 2^{n+1}]$, on peut écrire $N = 2I_{k-1} + c$, d'où $I_{k-1} = (N-c)/2$. Dans ce cas il résulte

$$D_{ins} = \frac{A_k}{I_k} = \frac{N}{(N-c)_0/2 + (c+1)2^{k-1}}.$$

Cet algorithme reste valable pour $N \in [0\ ;\ 2^n]$, mais la dernière comparaison change l'algorithme ; si $c=1$ les sorties I_k restent les mêmes; si $c=0$ on rend égal avec zéro le dernier bit testé. On a ainsi :

$$c=1,\ D_{ins} = \frac{A_k}{I_k} = \frac{N}{(N-1)/2};\qquad c=0,\quad D_{ins} = \frac{A_k}{I_k} = \frac{N}{N/2 - 2^{k-1}}.$$

Dans les relations ci-dessus n répresente la résolution du convertisseur et k, la valeur du bit testé. En considérant que :

$$N = \ldots a_5 a_4 a_3 a_2 a_0 = \ldots + a_5 2^5 + a_4 2^4 + a_3 2^3 + a_2 2^2 + a_1 2^1 + a_0 2^0$$

on peut déduire la valeur de k à savoir

$$\begin{aligned} &N = \{0, 1\},\ k=0,\\ &N = \{2, 3\},\ k=1,\\ &N = \{4, \ldots, 7\},\ k=2,\\ &\quad\vdots\\ &N = \{100, \ldots, 1FF\},\ k=8,\\ &\quad\vdots \end{aligned}$$

Dans le but d'écrire le programme de la mémoire pour une résolution n du convertisseur, on donne à N toutes les valeurs de l'intervalle $[0, 2^{n+1}]$, on choisit le facteur k d'une façon adéquate et on calcule la valeur de la sortie à l'aide des relations antérieures.

4. Les caractéristiques du convertisseur réalisé

On a expérimenté un convertisseur à approximations successives réalisé avec une résolution par programmation de 8; 7; 6 et 5 bits. Son schéma est représenté dans la Fig. 3.

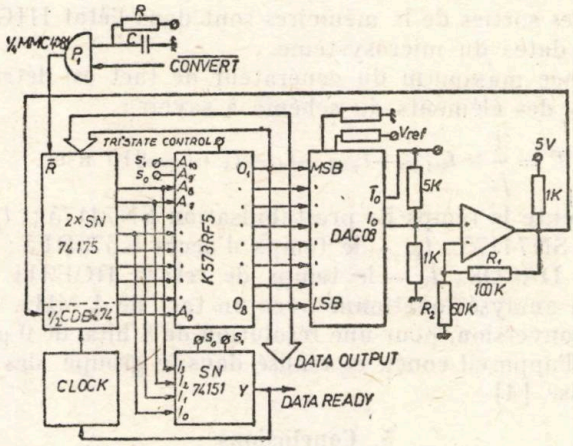

Fig. 3

La mémoire utilisée pour la synthèse du régistre d'approximations successives (SAR) est du type K573RF5, avec une capacité de $2k \times 8$. Les sorties de la mémoire, O_1, ..., O_8, sont appliquées à l'entrée par un régistre BUFFERS (qui a son tour est realisé avec $2 \times$ SN74175 et 1/2 CDB474) et aux entrées numériques (en ordre MSB ... LSB) du convertisseur D/A du type DACO8. Les sorties de la mémoire sont connectées à DACO8 par l'intérmédiaire de huit coupleurs optiques pour obtenir une bonne atténuation du bruit des circuites intégrés digitals. Pour augmenter la vitesse de travail le circuit ROB311 réalise la comparaison en courant, le résultat c en l'appliquant à l'entrée.

L'hystérésis du comparateur, introduit pour éviter les commutations parasites, est :

$$V_H = \frac{R_2}{R_1 + R_2} (V_{OH} - V_{OL}) \simeq 2{,}5 \text{ mV},$$

où V_{OH}, V_{OL} sont les tensions correspondantes des niveaux logiques 1 et 0. La synchronisation du schéma est assurée par le générateur de tacte CLOCK, le transfert des dates de l'entrée du régistre BUFFERS étant réalisé au front positif du tact.

Compte tenu qu'une résolution de 8 bits réclame une mémoire de $2^{8+1} = 512$ bits $= 1/2$ K, par les entrées S_0, S_1 la mémoire a été divisée en quatre segments, en inscrivant le programme pour une résolution de 8; 7; 6; 5 bits dans un segment. Les entrées S_0, S_1 de la mémoire et du multiplexeur sont interconnectées pour détecter la fin de la conversion. Ainsi, pour une résolution de 7 bits, par exemple, au septième tact la sortie Y_7 se trouve en 1 logique,

et au tact suivant $y_7=1$, DATA READY=1 et le générateur de tact s'arrête. C'est dans ce moment que le système d'acquisition est informé qu'on peut prendre les dates. Le groupe R, C fournit la temporisation nécessaire au ressetage du régistre BUFFERS et le signal $\overline{\text{CONVERT}}$ annonce une nouvelle conversion. Puisque ce convertisseur appartient à un microsystème on introduit aussi le signal TRISTATE CONTROL, actif sur 1 logique. Quand ce signal est 1, les sorties de la mémoires sont dans l'état HIGH Z, éliberant les régistres de dates du microsystème.

La fréquence maximum du générateur de tact est déterminée compte tenu des retards des éléments du schéma à savoir :

$$T=\frac{1}{f}\geqslant t_{\text{set-up}}+t_{p\text{HL}}+t_{ac}+t_S+t_r=810 \text{ nsec},$$

où : $t_{\text{set-up}}$ represente le temps de prestabilisation SN74175 ; $t_{p\text{HL}}$ — le temps de propagation SN74175 ; t_{ac} — le temps d'accès K573RF5 ; t_S — le temps de stabilisation DACO8 ; t_r — le temps de retard ROB311.

Le schéma analysé fonctionne avec un tact de 1 MHz, ce qui conduit à un temps de conversion, pour une résolution de 8 bits, de 9 μsec, ce qui permet d'encadrer l'appareil conçu et réalisé dans le groupe des convertisseurs à grande vitesse [4].

5. Conclusions

1. Le convertisseur à approximations successives réalisé présente la nouveauté d'une résolution par programmation, qui assure l'augmentation de la vitesse de conversion lorsqu'on reçoit des signals analogiques de natures différentes.

2. On a expérimenté un convertisseur à résolution de 8; 7; 6; 5 bits qui fonctionne avec un tact de 1 MHz. En ce cas, à une résolution de 8 bits correspond un temps de conversion de 9 μsec, mieux celui du AD570 (25 μsec) [1], [2].

3. Pour inscrire la mémoire on a réalisé un programme en FORTRAN-77 qui vérifie l'exactitude des formules utilisées.

Reçue le 30 octobre 1989

Institut Polytechnique, Jassy,
Chaire d'Électrotechnique, Mesures
et Machines électriques

BIBLIOGRAPHIE

1. * * * *Analog Device Short From Guide.* Norwood, Massachusetts, U.S.A., 1980.
2. * * * *Data Acquisition Handbook, National Semiconductor.* Santa Clara, California, U.S.A., 1978.
3. Reus N., Lazăr C., Lazăr A., *Sinteza convertoarelor analog-numerice folosind metoda simbolică.* Sess. jubil. de commun. scient., Inst. Polyt., Iaşi, 10—12 nov. 1988, IV, 98—101.
4. Săm păleanu M., *Circuite pentru conversia datelor.* Ed. Tehn., Buc, 1980.

CONVERTOR ANALOG — NUMERIC CU REZOLUŢIE PROGRAMABILĂ

(Rezumat)

Se propune un convertor analog — numeric la care registrul de aproximaţii succesive, spre deosebire de modelele clasice, este implementat într-o memorie, cu avantajul selectării rezoluţiei şi al creşterii vitezei de conversie. Modelul experimental, realizat pe baza schemei electrice prezentate, la un tact de 1 MHz, realizează un timp de conversie de 9 μsec., memoria fiind înscrisă pe baza unui program în Fortran-77 care verifică valabilitatea formulelor din lucrare.

BULETINUL INSTITUTULUI POLITEHNIC DIN IAȘI
Tomul XXXVI (XL) Fasc. 1—2, 1990
Secția III
ELECTROTEHNICĂ. ENERGETICĂ. ELECTRONICĂ. AUTOMATIZĂRI

D.C. 621.316.543

CONSIDERATIONS CONCERNING A TRANSISTORISED MONOPHASE INVERTER CHARACTERISED BY LOW VOLTAGE POWER SUPPLY AND A WAVE WITH HIGH CONTENT IN FUNDAMENTAL

BY

M. FLOREA, AL. LAZĂR and C. POȘA

1. Introduction

Today there is an increased interest in low dc voltage inverters. In most cases inverters must have the same parameters of output voltage like the ordinary mains. For this fact the output wave must have a high content in fundamental.

The low dc voltage makes unsatisfactory the use of thyristors, that is why power transistors will be prefered. There is the problem of the losses efficiency which appears in this case, because of the saturation collector — emitter voltage increasing along with the collector current rise.

The paper presents an inverter with a three steps synthesized wave, together with harmonic analysis of several waveforms which can be obtained with this configuration. At the same time a distortion analysis in connection with the voltage control possibilities is presented.

2. The Basic Configuration

To achieve a three steps synthesized wave, three monophase bridges parallely coupled on the side of dc current and in line on the side of ac current are used [1]. The schematic circuit of the inverter is presented in Fig. 1.

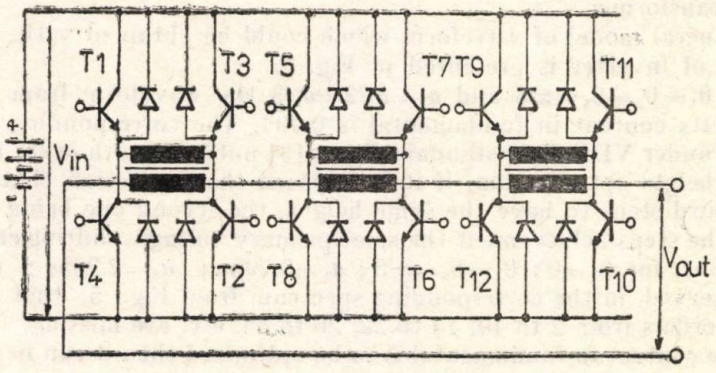

Fig. 1. — The schematic circuit of the inverter.

If the waveforms of the primary voltages are properly shifted the added secondary voltages will form a stepped waveform like in Fig. 2 which shows a waveform defined on 16 intervals.

This configuration have the following advantages :

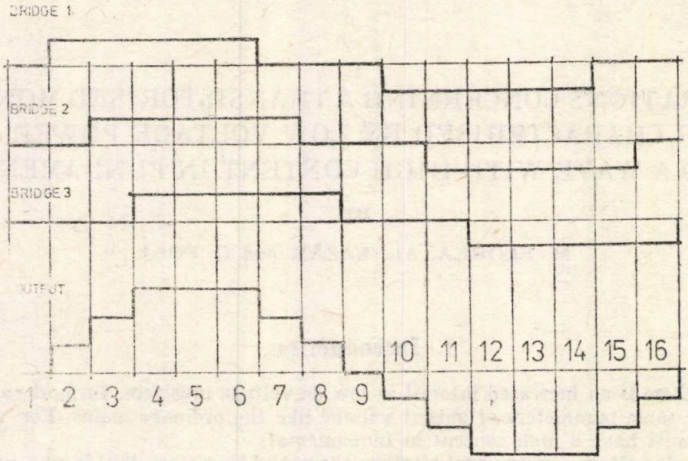

Fig. 2. — The steps achievement.

a) The output power is equally divided among those three bridges resulting lower intensities of collector current and consequently lower collector — emitter saturation voltages and thus a better efficiency.

b) The waveform has a high content in fundamental.

It is possible to optimize the waveform in order to reduce the low order harmonics. Generally we can use three methods of optimization [2] : a) at equally spaced steps there are the heights of steps which are optimized ; b) at equal heights the pulses spacing may be optimized ; c) it is possible to optimize both the heights of steps and their spacing.

There is the method from b) variant which is in keeping with our configuration.

It can be used also a variant by changing the ratio of transformation of each transformer.

A general model of waveform which could be obtained with this configuration of inverter is presented in Fig. 3.

For $\theta_1=\theta_2=\theta_3=\pi/8$ and $a_1=a_2/2=a_3/3$ the waveform from Fig. 2 is obtained. Its content in fundamental is 0.991. The corresponding spectrum (Fig. 4) is under VDE 0160 standard limits [3] until the 15th order harmonic.

For heigts optimization, if it is imposed the restriction that the first and the third steps to have the same height, the second one being different, then, for the steps achievement the same primary voltages shifting can be preserved. Thus, for $\theta_1=0$; $\theta_2=\theta_3=\pi/6$; $a_1=0.795a$; $a_2=2.205a$; $a_3=3a$, it can be observed, in the corresponding spectrum from Fig. 5, that the harmonics of orders from 2 to 10, 14 to 22, 26 to 34, etc. are missing.

If the content in fundamental is to be optimized then it can be generally written :

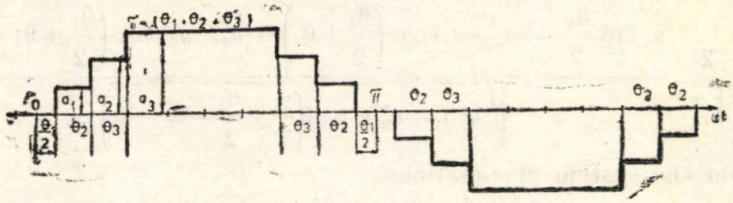

Fig. 3. — General 3 steps waveform.

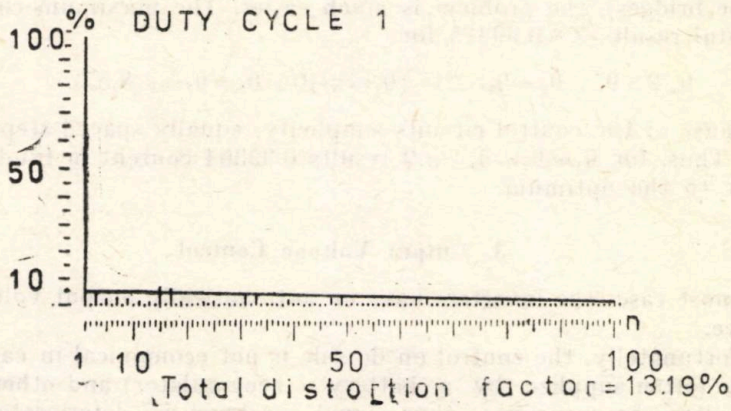

Fig. 4. — Corresponding spectrum of the waveform having $\theta_1 = \theta_2 = \theta_3 = \pi/8$; $a_1 = a$; $a_2 = 2a$; $a_3 = 3a$.

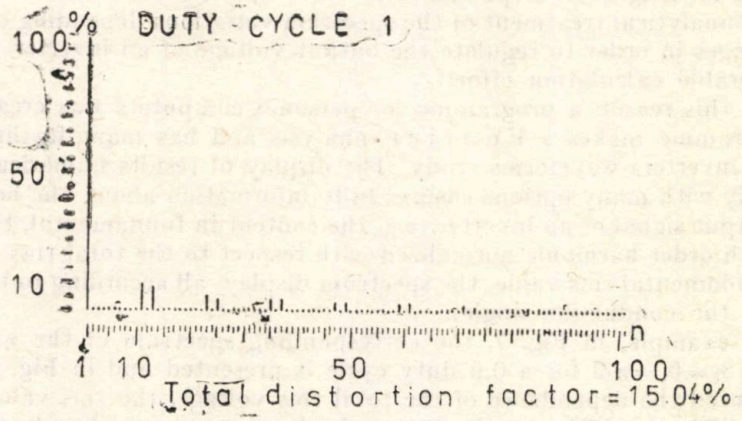

Fig. 5. — Corresponding spectrum of the waveform having $\theta_1 = 0$; $\theta_2 = \theta_3 = \pi/6$; $a_1 = 0.795\ a$; $a_2 = 2.205a$; $a_3 = 3a$.

$$Z=\frac{2}{\sqrt{\pi}}\cdot\frac{a_1\cos\frac{\theta_1}{2}+(a_2-a_1)\cos\left(\frac{\theta_1}{2}+\theta_2\right)+(a_3-a_2)\cos\left(\frac{\theta_1}{2}+\theta_2+\theta_3\right)}{\sqrt{a_1^2\theta_2+a_2^2\theta_3+a_3^2\left(\frac{\pi}{2}-\frac{\theta_1}{2}-\theta_2-\theta_3\right)}}.$$

From the system of equations :

$$\frac{\partial Z}{\partial\theta_1}=0,\quad \frac{\partial Z}{\partial\theta_2}=0,\quad \frac{\partial Z}{\partial\theta_3}=0,\quad \frac{\partial Z}{\partial a_1}=0,\quad \frac{\partial Z}{\partial a_2}=0,\quad \frac{\partial Z}{\partial a_3}=0,$$

eventually numerically solved, the optimum heights and steps spacing will be found.

If equally heights are adopted (resulting equally distribution of power among the bridges), the problem is much easier. The maximum content in fundamental results $Z=0.99315$ for :

$$\theta_1/2\simeq 9^\circ\ ;\ \theta_2=\theta_3=21^\circ\ (\theta_1=\pi/10\ ;\ \theta_2=\theta_3=\pi/8.57).$$

Because of the control circuits simplicity, equally spaced steps will be prefered. Thus, for $\theta_1=\theta_2=\theta_3=\pi/9$ results 0.99304 content in fundamental, very near to the optimum.

3. Output Voltage Control

In most cases the inverters have an automatically output voltage control device.

Unfortunatelly, the control on dc side is not economical in case of low dc voltage (often supplied by a battery – accumulator) and other control methods alter the waveform, thus signal spectrum is deteriorated.

We analysed the method of output voltage control based on the pulses width control on each step. The method is presented in Fig. 6.

The problem of certain waveform optimization can certainly be analytically treated. If there are imposed restrictions for certain harmonics, conditions for heights of steps and/or for their spacing will result.

The analytical treatment of the spectrum variations depending on waveform changes in order to regulate the output voltage of an inverter requires a considerable calculation effort.

For this reason a programme for personal computers was created [4]. The programme makes a Fourier analysis and has many facilities suitable for inverters waveforms study. The display of results numerically and graphically with many options ensures fully information about the behaviour of the output signal of an inverter (e.g. the content in fundamental, the value of the n-th order harmonic normalized with respect to the total rms value or to the fundamental rms value, the spectrum display, all according to the pulse width or the conduction angle).

For example, in Fig. 7, the corresponding spectrum of the waveform with $\theta_1=\theta_2=\theta_3=\pi/9$ for a 0.9 duty cycle is presented and in Fig. 8 there are presented the dependence of the total rms voltage, the rms value of the first, the fifth, the 17th and the 19th order harmonics according to the duty cycle.

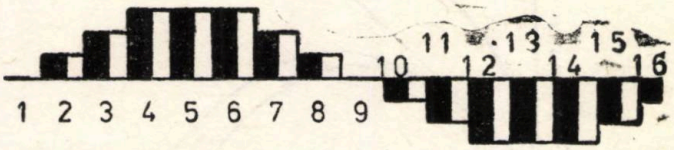

Fig. 6. — Output voltage regulation by pulse width control.

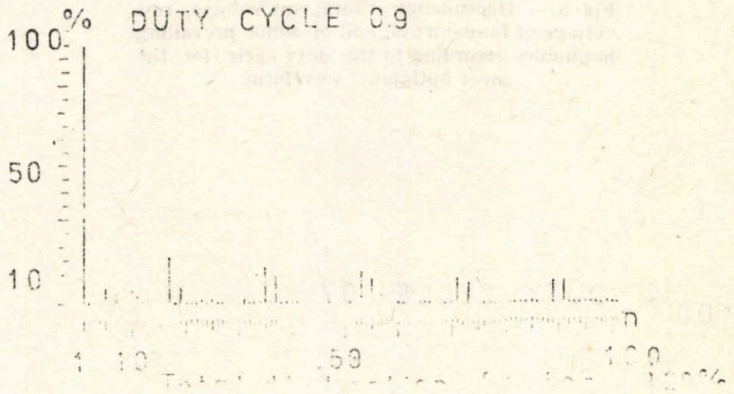

Fig. 7. — Corresponding spectrum of the waveform having $\theta_1=\theta_2=\theta_3=\pi/9$; $a_1=a$; $a_2=2a$; $a_3=3a$; (near optimum), for a duty cycle of 0.9.

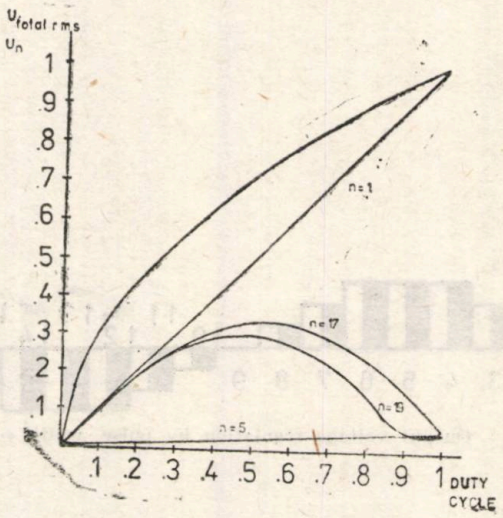

Fig. 8. — Dependence of total rms voltage, rms voltage of fundamental and of some prevailing harmonics according to the duty cycle for the „near optimum" waveform.

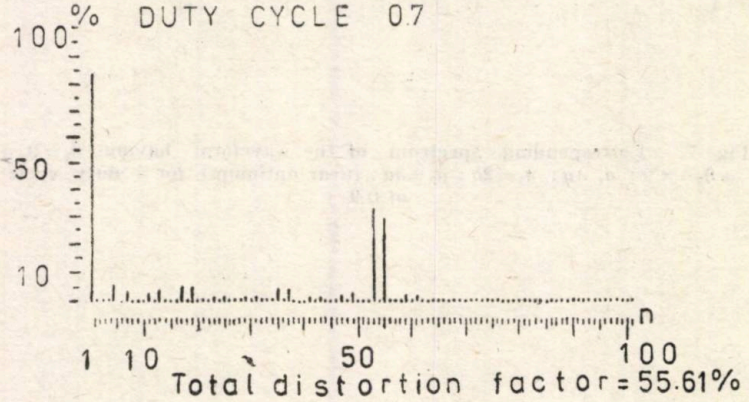

Fig. 9. — Corresponding spectrum of the near optimum waveform, for a duty cycle of 0.7, having 3 pulses per interval.

It can be observed that starting with a waveform which at a duty cycle of 1 has low order harmonics with reduced values, these are keeping low during regulating the output voltage, prevailing the harmaonics with frequency as a linear combination of choping frequency and fundamental one :

$$f=kf_c\pm f_1,$$

where : f — prevailing frequency, f_c — chopping frequency, f_1 — fundamental frequency, (k=0, 1, 2, ...).

For the up mentioned waveform (the near optimum one), for f_1=50 Hz and for 18 intervals (therefore f_c=900 Hz), the 17th and the 19th harmonics prevail, that means harmonics frequency are 850 Hz respectively 950 Hz.

Moreover, it is known that, [2], [4], if we increase chopping frequency, the frequency of the prevailing harmonic will be much increased. For example, in Fig. 9, the spectrum corresponding to the same waveform with 18 intervals and 3 steps, for a 0.7 duty cycle is presented.

Filtration in this case is much easier resulting net advantages as for as volume, weight and price of filter are considered. As a disadvantage, a slight reduction of efficiency appear due to the supplementary losses appeared in switching process.

4. Experimental Results

Taking into account the above mentioned observations, we have achieved an inverter based on the functional scheme from Fig. 1. The output voltage is like in Fig. 2, with 16 equally intervals and three equally steps. Output voltage regulation is made by pulses width control variant.

Other parameters : a) input voltage range : 20 to 30 V_{dc} ; b) output voltage : 220 V rms $\pm$5% ; c) output power : 1 KVA. The efficiency measured when supplying at minimum voltage of 20 V is 56%. A good agreement with theoretical results was obtained from the output voltage spectrum point of view. Using a filter with 40 dB attenuation at a frequency of 750 Hz, the total distortion factor remains less then 10% while both input voltage varies between 20 and 30 V and the load current between 0.1 and 5 A.

5. Conclusions

It can be said that the proposed scheme is well keeping with the inverters supplied from low dc voltages.

The programme for spectrum variations study represents an useful tool because it offers fully information concerning the output signal behaviour during voltage regulation for a given configuration of inverter, and it allows an easy comparison with other solutions.

By the help of this programme some of the performances which can be obtained with the mentioned configuration were underlined resulting that these can be adapted to many applications in different variants.

Received, April 6, 1989

Polytechnic Institute, Jassy,
Department of Applied Electronics

REFERENCES

1. Alexa D., Micu D., *Invertoare şi redresoare cu parametri energetici ridicaţi*. Ed. Tehn., Buc., 1986.
2. Bhagwat P.M., Stefanovic V.R., *Generalized Structure of Multilevel PWM Inverter*. I.E.E.E. Trans., **IA-19**, *6* (1983).
3. Heumann K., *Basic Principle of Power Electronics*. Springer Verlag, Berlin, 1986.
4. Florea M., Lazăr A., Poşa C., *Influenţa reglării tensiunii asupra spectrelor unor forme de undă specifice invertoarelor*. Jubil. Scient. Sess., Polyt. Inst., Jassy, 1988.

CONSIDERAŢII PRIVIND UN INVERTOR TRANZISTORIZAT MONOFAZAT CARACTERIZAT PRINTR-O TENSIUNE JOASĂ DE ALIMENTARE ŞI DE O UNDĂ CU UN CONŢINUT BOGAT ÎN FUNDAMENTALĂ

(Rezumat)

Se prezintă o configuraţie de invertor formată din trei punţi monofazate conectate în paralel pe partea de curent continuu şi în serie pe partea de curent alternativ.

Se arată avantajele acestei structuri privind posibilitatea obţinerii unui randament ridicat chiar şi la alimentarea la tensiuni reduse, atunci cînd pierderile în conducţie devin o problemă. Aceasta deoarece puterea se distribuie pe trei punţi, fiecare funcţionînd la curenţi mai mici, deci cu pierderi mai mici pe tranzistoarele în conducţie. Se obţin avantaje şi în ceea ce priveşte formele de undă ce se pot realiza din punctul de vedere al distorsiunilor, existînd posibilitatea optimizării formelor de undă în scopul reducerii armonicilor de ordin coborît.

Se prezintă şi aspecte privind reglarea tensiunii de ieşire şi influenţa acesteia asupra spectrului tensiunii de ieşire. S-a studiat, cu ajutorul unui program conceput special în acest scop, o metodă de reglare larg folosită, prin controlul lăţimii pulsurilor.

BULETINUL INSTITUTULUI POLITEHNIC DIN IAŞI
Tomul XXXVI (XL) Fasc. 1—2, 1990
Secţia III
ELECTROTEHNICĂ. ENERGETICĂ. ELECTRONICĂ. AUTOMATIZĂRI

D.C. 621.3.014; 621.33

HARMONIC RESONANCE EFFECTS ON ELECTRIC NETWORKS SUPPLYING ELECTRICAL TRACTION STATIONS

BY

ILIE POPESCU, IUSTINA ZAHARIA and CAMELIA PETRESCU

1. Introduction

The electric railway traction is supplied by electric networks having a non-sinusoidal steady-state mode. Driven rectifiers, that produce the special trapezoidal voltage waveform for electric traction, insert higher order harmonics in the electric motor circuit and, more evidently, in the supply network. As a result, current harmonics produce increased power losses in the feeders and electric motors, and may also give dangerous interferences with the railway signal system (circuit), especially if resonances occur at harmonic frequencies. The currents/voltages resonance overload the electric equipment (transformers, capacitor banks, etc.).

The current wave-form in the secondary winding of the traction transformer have a pronounced non-sinusoidal character and may be approximated by a trapezoidal wave-form ; its amplitude is roughly 60 ... 70 % refered to the equivalent sinusoidal current. All odd and even harmonics are present in the spectrum of the one-phase transformer current. The odd harmonics amplitudes decrease with frequency and the even harmonics have amplitudes much smaller than the odd ones, if no resonance occurs at harmonic frequencies.

The aim of this paper is to study the influence of the capacitor bank value and that of the filters on the resonance modes produced in the network.

2. The Equivalent Harmonic Electric Circuit

Let us consider an electric network which supply electric railway traction stations as well as transformer stations supplying linear, balanced consumers. The equivalent electric circuit for the k th harmonic is represented in Fig. 1. All elements in the circuit may be considered linear for all industrial harmonics, except the electric locomotive which is a harmonic generator.

The parameters R_3', kX_3' are negligible when compared to those of the linear consumer (R_1', kX_1').

The study of the resonance modes may be effectuated for different loads, using the computer, where the worst cases are considered. The equivalent electric circuit at the harmonic generator terminals is represented in Fig. 2. The following relations are fullfiled :

$$R_1'=2R_1',\ R_L=2R_L',\ X_{T1}=2X_{T1}',\ X_L=2X_L';\ X_0=2X_0'.$$

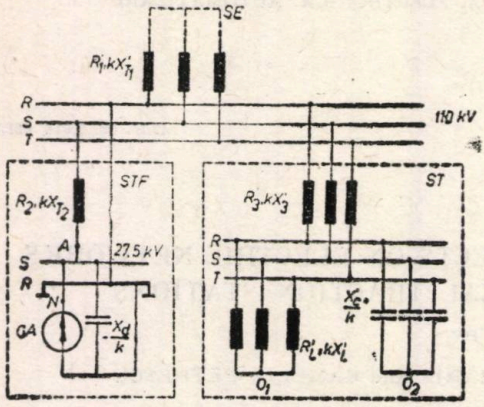

Fig. 1. — The equivalent electric circuit for the kth harmonic of an electric network that supplies electric railway traction and linear, balanced consumers.

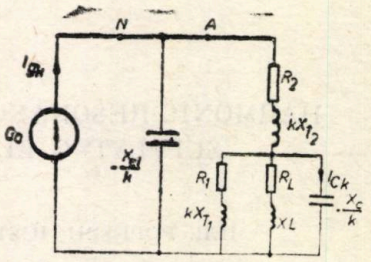

Fig. 2. — The equivalent electric circuit for the kth harmonic at harmonic generator terminals.

The case of a small linear load is further considered ($R_L \ll R_1$, $X_L \ll X_{T1}$). The complex impedance for the kth harmonic is :

$$(1)\qquad \underline{Z}_k = \frac{\underline{Z}_{C1k}\underline{Z}_{Ak}}{\underline{Z}_{C1k}+\underline{Z}_{Ak}} = \frac{\underline{Z}_{C1k}\left(\underline{Z}_{T2k}+\dfrac{\underline{Z}_{sk}\underline{Z}_{Ck}}{\underline{Z}_{sk}+\underline{Z}_{Ck}}\right)}{\underline{Z}_{C1k}+\underline{Z}_{T2k}+\dfrac{\underline{Z}_{sk}\underline{Z}_{Ck}}{\underline{Z}_{sk}+\underline{Z}_{Ck}}},$$

where

$$(2)\qquad \underline{Z}_{C1k}=-\mathrm{j}\frac{X_{C1}}{k},\quad \underline{Z}_{T2}=R_2+\mathrm{j}kX_{T2},\quad \underline{Z}_{sk}=R_1+\mathrm{j}kX_{T1},\quad \underline{Z}_{Ck}=-\mathrm{j}\frac{X_C}{k}.$$

The real and imaginary part of $\underline{Z}_k$ are respectively

$$(3)\ \mathcal{R}e(\underline{Z}_k)=\frac{(X_{C1}^2/k^2)\,M_k}{M_k^2+k^2(N_k-X_{C1}/k^2)^2},\quad (4)\ \mathcal{I}m(\underline{Z}_k)=-\frac{X_{C1}}{k}\cdot\frac{M_k^2+k^2N_k^2-X_{C1}N_k}{M_k^2+k^2(N_k-X_{C1}/k^2)^2},$$

where t he following notations are used :

$$(5)\qquad M_k=R_2+\frac{R_1X_C^2}{k^2R_1^2+(k^2X_{T1}-X_C)},$$

$$(6)\qquad N_k=X_{T2}-X_C\frac{R_1^2+X_{T1}(k^2X_{T1}-X_C)}{k^2R_1^2+(k^2X_{T1}-X_C)^2}.$$

The expression of $\underline{Z}_k$ modulus as, well as the Nyquist diagram of $\underline{Z}_k$, points out the existence of three resonant frequencies : two current resonances and a voltage one.

When resistances are small compared to reactances the rangs of resonant harmonics are :

$$k_s = \sqrt{\frac{X_C(X_{T1}+X_{T2})}{X_{T1}X_{T2}}}, \tag{7}$$

respectively

$$k_{p1,2} = \tag{8}$$

$$= \sqrt{\frac{X_{Cl}X_{T1}+X_C(X_{T1}+X_{T2}) \pm \sqrt{X_{Cl}^2X_{T1}^2+X_C^2(X_{T1}+X_{T2})^2+2X_{Cl}X_cX_{T1}(X_{T1}-X_{T2})}}{2X_{T1}X_{T2}}}.$$

The resistance of a network that supplies an electric traction station does not change in practice with harmonic frequency and it is much smaller than the fundamental reactance. The exact expressions of k_s and k_p also give three resonance frequencies which are the roots of the equation $\mathcal{I}m(\underline{Z}_k)=0$. These values are close to those performed with the relations (7) and (8). The modulus of the impedance at the resonance frequencies is highly influenced by the resistance values (Fig. 3) ; the Nyquist diagram of the complex impedance is also influenced by these resistances (Fig. 4).

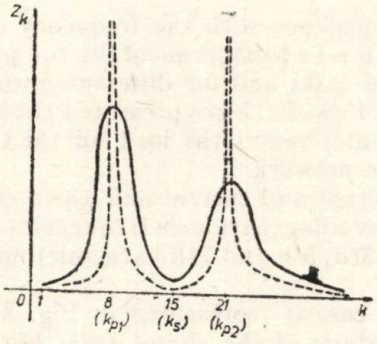

Fig. 3.— Dependence of Z modulus vs. frequency.

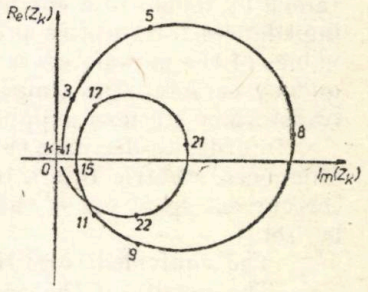

Fig. 4. — $\underline{Z}$ Nyquist diagram.

The resonance curves obtained analitically (Fig. 3) are in good agreement with the values measured in the traction stations as well as with the published ones in the field [5].

The equivalent circuit of a network that supplies both the traction station and transformer one is represented in Fig. 2, where $\underline{Z}_k$, the complex impedance at the harmonics generator terminals, is given by :

$$\underline{Z}_k = \frac{\underline{Z}_{clk}\underline{Z}'_{Ak}}{\underline{Z}_{clk}+\underline{Z}'_{A_k}} = \frac{\underline{Z}_{clk}\left(\underline{Z}_{T2k}+\dfrac{\underline{Z}'_{sk}\underline{Z}_{Ck}}{\underline{Z}'_{sk}+\underline{Z}_{Ck}}\right)}{\underline{Z}_{clk}+\underline{Z}_{T2k}+\dfrac{\underline{Z}'_{sk}\underline{Z}_{Ck}}{\underline{Z}'_{sk}+\underline{Z}_{Ck}}}, \tag{9}$$

with

$$(10)\qquad \underline{Z}'_{sk}=\frac{\underline{Z}_{sk}\underline{Z}_{Lk}}{\underline{Z}_{sk}+\underline{Z}_{Lk}}=\frac{(R_1+\mathrm{j}kX_{T1})(R_L+\mathrm{j}kX_L)}{R_1+R_4+\mathrm{j}k(X_{T1}+X_L)}=$$

$$=\frac{R_1R_L(R_1+R_L)+k^2(R_1X_L^2+R_LX_{T1}^2)}{(R_1+R_L)^2+k^2(X_{T1}+X_L)^2}-\mathrm{j}k\frac{R_1^2X_L+R_L^2X_{T1}+k^2X_{T1}X_L(X_{T1}+X_L)}{(R_1+R_L)^2+k^2(X_{T1}+X_L)^2}.$$

If the resistances are small when compared to reactances at fundamental frequency, then Z'_{sk} is an inductivity, namely :

$$(11)\qquad \underline{Z}'_{sk}=\mathrm{j}k\frac{X_{T1}X_L}{X_{T1}+X_L},\quad X_L>X_{T1},$$

and $\mathcal{I}m(\underline{Z}'_{sk})=0$ gives the same number of resonance frequencies for this circuit which contain four reactif elements. The order of the resonance harmonics are practically the same as in the previous case (Table 1.) If resistances are taken into account, then three resonance frequencies occur ; for X_2 of the same order of magnitude as X_{T1} partial cycles may appear in the N y q u i s t diagram.

3. The Obtained Results

In what follows the dependence of impedance with the frequency obtained by means of a computer and the N y q u i s t diagrams of the complex impedances for the two previously discussed cases and for different normal values of the parameters is presented. In the Figs. 5 ... 7 are presented the frequency caracteristics (impedances and currents) versus the load for the two transformer stations supplied by the electric network.

In order to decrease the distorsion of voltage and current and their consequences, electric filters tunned at the prevailing harmonic frequencies in the current spectrum of the locomotive (the 3rd, 5th and 7th harmonic) must be set.

The equivalent electric circuit in this case is represented in Fig. 8.

The results of the computer-aided analysis of the circuit from Fig. 8 are presented in the Table 1. These results point out the existence of a current resonance, followed by a voltage one ; then the sequence is respected.

The first three voltage resonances are given by the tunned filters ($k=3, 5, 7$). The amplitudes of the signals are much smaller near the resonance frequencies of the filters; the resonance frequencies of the equivalent station circuit increases ($k=16$) and the resonance signal amplitude decreases. The resonance modes depend on the load of the two electric stations (the transformer station and the railway transformer one). Changes in the load of the railway traction determine changes in the amplitudes of the current harmonics as well as changes in the value of the capacitor bank X_{C_1} (if possible). The amplitude and order of the resonance harmonics depend to a great extend on the presence and the value of the capacitor bank X_{C_1}, for a nominal value of the inear load (R_L, kX_L). The increase of the electric traction load doesn't modify the order of the voltage resonance ($k=18$) but the order of the parallel resonances decreases (s. Table 1). At the same time the increase of the traction

Table 1

	Equivalent circuit without filters (Fig. 2)						Equivalent circuit with filters (Fig. 5)	
	Without linear load			With linear load				
Circuit parameters Ω	$R_1=28\times10^{-4}$ $R_2=15\times10^{-3}$ $X_{L1}=0.314$ $X_{L2}=0.471$ $X_C=60$ $X_{Cl}=\infty$	$R_1=28\times10^{-4}$ $R_2=15\times10^{-3}$ $X_{L1}=0.314$ $X_{L2}=0.471$ $X_C=60$ $X_{Cl}=120$	$R_1=734\times10^{-4}$ $R_2=45\times10^{-3}$ $X_{L1}=0.263$ $X_{L2}=0.3$ $X_C=60$ $X_{Cl}=120$	$R_1=28\times10^{-4}$ $R_2=15\times10^{-3}$ $X_{L1}=0.314$ $X_{L2}=0.471$ $X_C=60$ $X_{Cl}=\infty$ $R_L=10.5$ $X_L=24$	$R_1=28\times10^{-4}$ $R_2=15\times10^{-3}$ $X_{L1}=0.314$ $X_{L2}=0.471$ $X_C=60$ $X_{Cl}=120$ $R_L=10.5$ $X_L=24$	$R_1=734\times10^{4}$ $R_2=45\times10^{-3}$ $X_{L1}=0.263$ $X_{L2}=0.3$ $X_C=60$ $X_{Cl}=120$ $R_L=10.5$ $X_L=24$	$R_1=28\times10^{-4}$ $X_{L1}=0.314$ $X_C=60$ $R_L=10.5$ $R_3=0.6$ $R_5=0.9$ $R_7=1.28$ $X_C=15$ $X_{C7}=84$	$R_2=15\times10^{3}$ $X_{L2}=0.471$ $X_{Cl}=\infty$ $X_L=24$ $X_{L3}=16.39$ $X_{L5}=16.73$ $X_{L7}=17$ $X_{C5}=42$
Normal harmonic orders								
k_1	13	11	11	14	10	11	16	
k_2	18	18	21	18	18	21	18	
k_3	—	22	26	—	22	26	—	
I_{Ck1}/I_{gk1}	7.6	8.9	8	8.1	4.3	14	2.75	
I_{Ck2}/I_{gk2}	2.4	2.6	2.2	0.07	0.07	1.96	0.005	
I_{Ck3}/I_{gk3}	—	22	6.9	—	11.2	13	—	

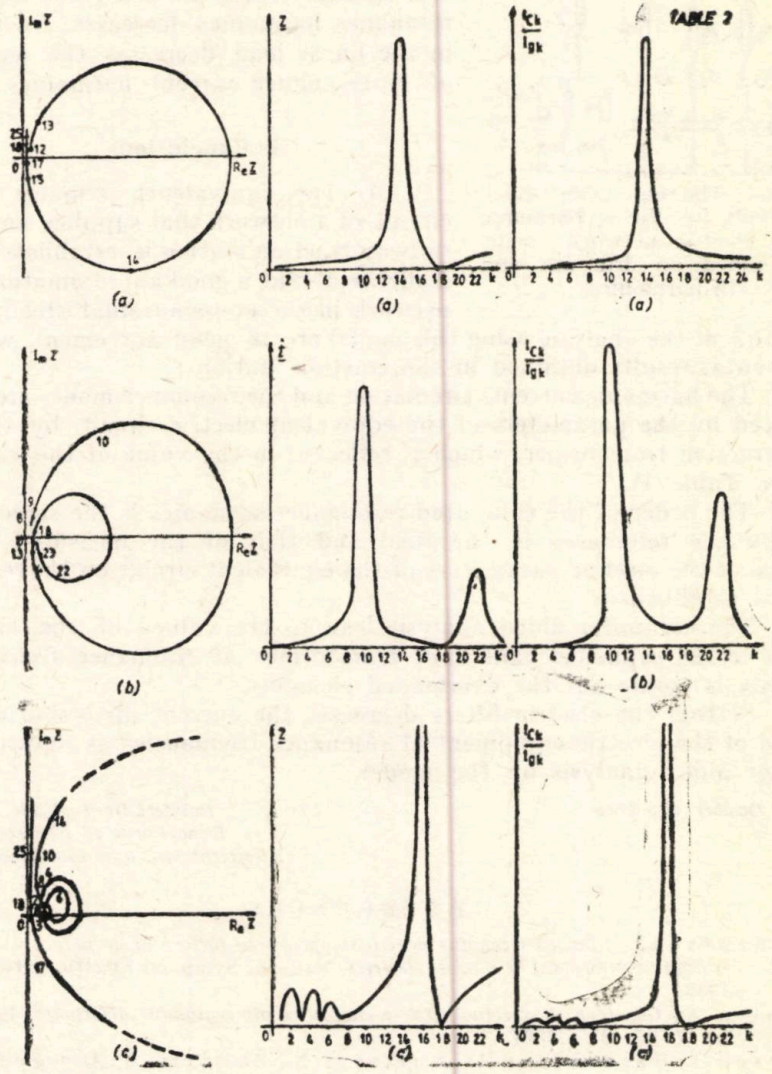

Fig. 5. — $\underline{Z}$ Nyquist diagrams: *a* — without C_1 and without filters; *b* — with C_1 and without filters; *c* — with C_1 and filters.

Fig. 6. — Dependence of $\underline{Z}$ modulus vs. frequency (cases *a*, *b*, *c*).

Fig. 7. — Dependence of $\underline{I}_{Ck}/\underline{I}_{gk}$ modulus vs. frequency in cases *a*, *b*, *c*.

load increases also the current harmonics which are amplified at parallel resonance frequencies both in the transformer station (T_1) and in its capacitor bank (X_C). Changes in the load of the transformer station (T_1) modify the resonance modes (the amplitude and order of the resonance harmonics). As

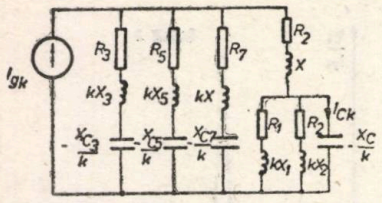

Fig. 8. — The equivalent electric circuit for the k harmonic of an electric network with filters tuned on 3rd, 5th and 7th harmonics.

this load increases, the order of the voltage resonance harmonics decreases. An increase in the linear load decreases the amplitude of the resonance current harmonics.

4. Conclusions

1. The equivalenth armonic electric circuit of a network that supplies an electric railway traction station is established. This model represent a good approximation of the network in the non-sinusoidal steady-state; the results of the analysis using this model are in good agreement with the experimental results obtained in the traction stations.

2. The harmonic currents circulation and the resonance modes are highly influenced by the parameters of the equivalent electric circuit, by the load of the traction transformer, which is reflected in the value of the capacitor bank (s. Table 1).

3. The order of the computed resonance harmonics is the same as that given by the references in the field and that of the measured values. influence of the electric parameters of the equivalent circuit on the resonance modes is established.

4. The computer aided analysis lead to the values of the harmonic currents in the capacitor bank and transformer at resonance frequencies; this analysis points out the overloaded elements.

5. Setting the electric filters decreases the current distorsion and the overload of the electric equipment at resonance frequencies as shown by the computer aided analysis on the model.

Received, October 20, 1989

Polytechnic Institute, Jassy,
Department of Electrotechnics,
Electrical Machines and Measurements

REFERENCES

1. Iordăchescu I., *Măsurări comune pentru compensarea factorului de putere şi atenuarea regimului deformant în reţelele electrice.* National Symp. on Electric Network, Cluj, 1988.
2. Ţugulea A., *Consideraţii privind efectele energetice ale regimului deformant.* Energetica, **34**, *1*, 27–31 (1986).
3. Popescu I., Bărbulescu D., Sufleţel N., Zaharia I., *Asupra determinării puterii şi energiei active disipată în reţelele electrice neramificate care alimentează receptoare neliniare.* Energetica, **36**, *2*, 81–84 (1988).
4. Dan A.M., Kisvolcsey J., Varju G. *Filtering of Harmonics Generated by Thyristor Controlled A.C. Traction System.* ICHPS II, Manitoba, 1986, 404–413.
5. Christl N., Koelseh H., *Comparison of Digital Calculation and Field Measurements of the Harmonic Distorsion at the A.C. Side of the Durnrohr HVDC Converter Station.* ICHPS II, Manitoba, 1986, 73–76.

REGIMURI DE REZONANŢĂ PE ARMONICI ÎN REŢELE CARE ALIMENTEAZĂ STAŢII DE TRACŢIUNE ELECTRICĂ FEROVIARĂ

(Rezumat)

Se modelează o reţea electrică care alimentează atît staţii de transformare cu receptoare neliniare (tracţiune electrică feroviară) cît şi receptoare liniare. Cu ajutorul schemelor echivalente stabilite se determină suprasolicitările ce apar pe bateria de codensatoare şi transformator în regimuri de rezonanţă pe armonici.

BULETINUL INSTITUTULUI POLITEHNIC DIN IAŞI
Tomul XXXVI (XL) Fasc. 1—2, 1990
Secţia III
ELECTROTEHNICĂ. ENERGETICĂ. ELECTRONICĂ. AUTOMATIZĂRI

C.D. 621.316.052

L'INFLUENCE DES ERREURS DE L'INFORMATION SUR LES CALCULS DES RÉGIMES DES SY STÈMES ÉLECTROÉNERGÉTIQUES

PAR

GH. CÂRŢINĂ

1. Introduction

Parmi des diverses problèmes du dialogue dispatching—ordinateur dans la conduite des systèmes électroénergétiques, le travail ci-contre s'arrête sur ceux concernant l'exactitude de l'information et l'influence de celle-ci sur le calcul des régimes, sur les régimes optimaux. Vraiement, dans l'analyse des régimes des systèmes électroénergétiques, pour l'évaluation de leur économicité, à partir des informations disponibles (les puissances injectées aux noeuds, les paramètres du schéma équivalent), on calcule les grandeurs d'état des régimes respectives (les valeurs des tensions aux noeuds, leurs déphasages), les pertes de puissance, etc. À partir des mêmes informations, dans certaines conditions, on détermine par calcul les régimes optimals de fonctionnement. Les décisions dans la conduite des systèmes électroénergétiques, ayant à la base les calculs mentionnés ci-dessus, dépendent des valeurs des données d'entrée, des erreurs qui les touchent. Dans ce sens le travail s'occupe de l'influence des erreurs de l'information (les données d'entrée) sur les calculs et sur les décisions concernant la conduite des systèmes respectifs.

2. Les erreurs qui concernent les données d'entrée

Les erreurs qui peuvent affecter les données d'entrée sont systématiques ou aléatoires. Dans le cas des premières, la valeur de l'erreur est déterminée chaque fois à partir d'une loi connue. Dans le cas des erreurs aléatoires la grandeur et le signe des ceux-ci sont des variables aléatoires. Les erreurs des données d'entrée et leurs influence présentent un grand interêt dans l'analyse de l'économicité des régimes, dans l'efficacité des régimes optimals, dans le calcul des régimes planifiés, etc.

Dans le Tableau 1 sont présentées les limites possibles des erreurs systématiques et aléatoires en fonction des facteurs qui conduisent à leurs apparition [1]. Il faut souligner que la probabilité des erreurs extrêmes est au dessous de 1%. On peut constater, par exemple, que la valeur déterminée par calcul de la résistance peut être assez différente par rapport à la valeur réelle si on ignore l'influence de la température de l'air, l'influence du courant I, de la vitesse du vent v, etc. Parmi les erreurs les plus importantes par leurs consé-

quences sont celles liées à la mesure des puissances actives et réactives. Pour mettre en évidence l'influence des erreurs sur les régimes calculés il a été nécessaire le calcul d'un grand nombre de régimes utilisant les programmes FAST et NEWOPT de la bibliothèque ELECTRA. Le nombre des régimes calculés est assez grand dans le cas des erreurs aléatoires, où il faut utiliser des modèles probabilistes.

Tableau 1

Erreurs possibles des données concernant les charges aux noeuds et les paramètres du schéma électrique

Les facteurs qui provoquent l'erreur	La grandeur	L'erreur possible %
Erreurs systématiques		
Mesure des charges avec mégawattmètres	P	$-3{,}6 \ldots -7$
	Q	$1 \ldots 2$
Ignoration de la dépendence $R(I, v, t)$	R_L	$-18 \ldots +22$
Ignoration des fils de garde	X_L	$1 \ldots 3$
Ignoration de l'influence du circuit parallèle	X_L	$-4 \ldots -8$
Ignoration du dispositif de réglage en charge	R_T	$-16 \ldots +16$
	X_T	$-13 \ldots +13$
Erreurs aléatoires		
Erreurs de mesure	P	$-15 \ldots +15$
	Q	$-10 \ldots +10$
Ignoration des modifications des valeurs I, v, t	R_L	$-16 \ldots +16$
Ignoration des modification de la température des enroulements du transformateur	R_T	$-12 \ldots +12$
Erreurs dans la détermination de ΔP_{cc}, ΔU_{cc}	R_T, X_T	$-10 \ldots +10$

En tant que référence on a considéré le régime qui tient compte de l'influence des erreurs respectives. Les autres régimes on été comparés avec le régime de référence suivant la relation

$$\Delta Y = \frac{Y_{réf} - Y_{err}}{Y_{réf}}, \ [\%]. \tag{1}$$

3. Résultats expérimentaux

Afin de tester l'influence de différentes erreurs sur les grandeurs d'état calculés et sur les pertes de puissance on a considéré le réseau de 220 KV dont le schéma est présenté dans la Fig. 1. Dans le Tableau 2 est présentée l'influence des erreurs systématiques sur la valeur des pertes de puissance, pour le réseau représenté dans la Fig. 1. La variation des pertes de puissance pour le même réseau, dans le cas des erreurs aléatoires, est donnée dans le Tableau 3.

Si l'influence des erreurs des données d'entrée sur les valeurs des tensions aux noeuds est relativement faible on ne peut pas dire la même chose quant à l'influence sur les pertes de puissance, tant pour le régime pleine charge que pour celui de charge réduite (30%). L'influence sur les pertes de

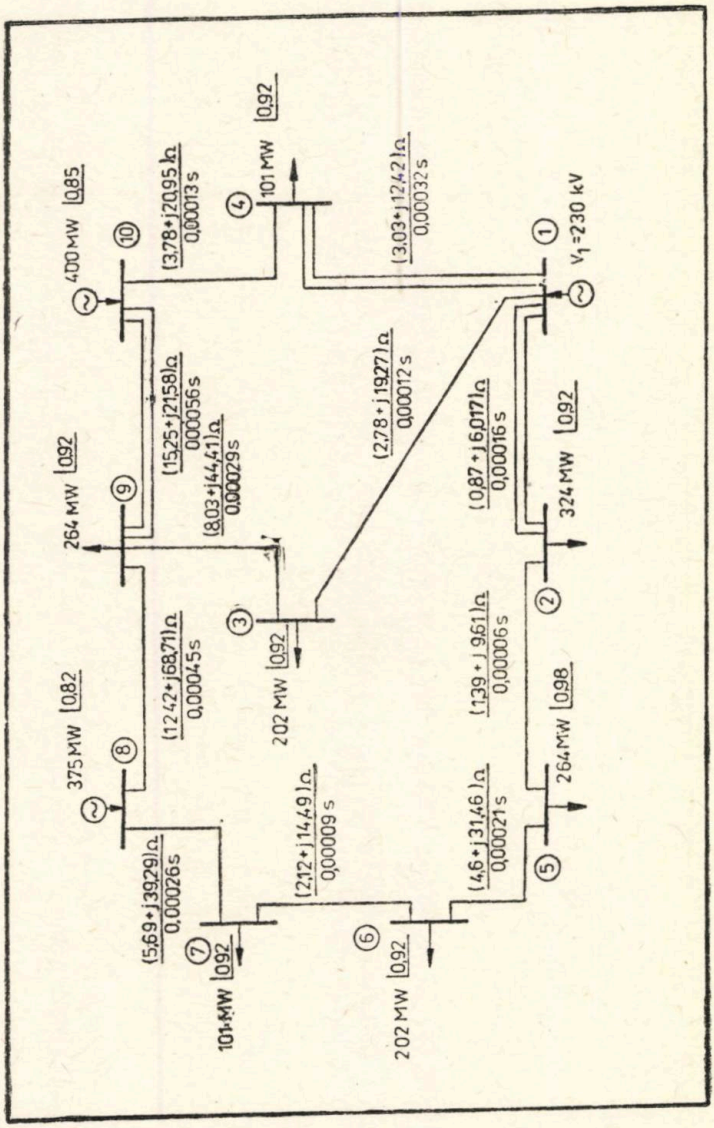

Fig. 1. — Le schéma du réseau de 220 KV.

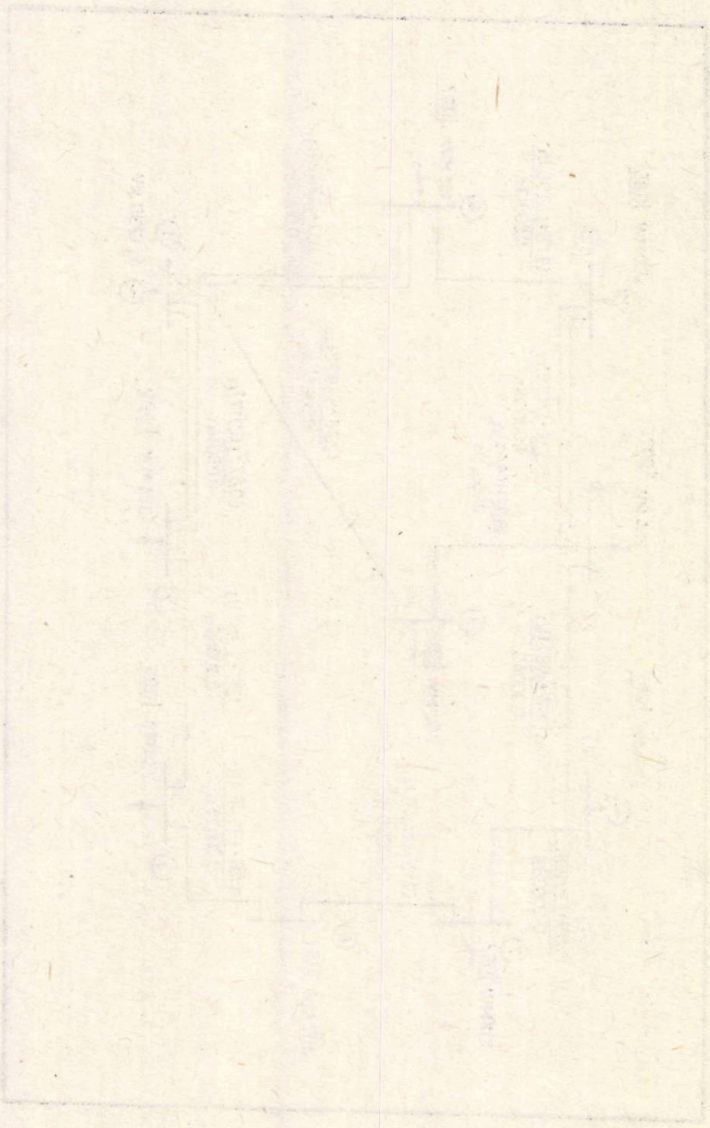

Tableau 2

La variation des pertes de puissance dans le cas des erreurs systématiques

	L'hypothèse de calcul	ΔP en pleine charge (100 %)	ΔP en régime de charge réduite (30 %)
a	Le régime de réference (sans erreurs)	34,057 MW	4,338 MW
b	L'ignoration du réglage en charge	+ 0,061 %	− 0,115 %
c	L'ignoration de l'influence du circuit parallèle	− 0,032 %	+ 0,023 %
d	L'ignoration de la modification de la température de l'air (−20°C)	−10,59 %	−10,25 %
e	Erreurs cumulées (*b*+*c*+*d*)	−10,63 %	−10,32 %
f	L'ignoration de la modification de la température de l'air (−10°C)	− 8,078 %	− 8,041 %
g	Erreurs cumulées (*b*+*c*+*f*)	− 8,764 %	− 8,713 %

Tableau 3

La variation des pertes de puissance dans le cas des erreurs aléatoires

	L'hypothèse de calcul	ΔP en pleine charge (100 %)	ΔP en régime de charge réduite (30 %)
a	Régime de référence (sans erreurs)	34,057 MW	4,338 MW
h	Régime P+3,3 %, Q+7,5 %	+ 8,52 %	6,98 %
i	Régime *h*+l'ignoration de la température (−20°C)	− 2,97 %	−13,39 %
j	Régime P−10 %, Q−8,6 %	−17,54 %	− 3,98 %
k	Régime *j*+l'ignoration de la température (−20°C)	−26,27 %	−22,15 %
l	Régime P−3,35 %, Q−0,55 %	− 5,021 %	− 4,013 %
m	Régime *l*+l'ignoration de la température (−10°C)	−13,29 %	−12,014 %

puissance reste importante même dans le régime où les erreurs ont de valeurs moyennes (les hypothèses *f* et *g* — Tableau 2 et les hypothèses *l* et *m* — Tableau 3).

Une grande influence ont les erreurs des données d'entrée sur l'évolution du processus d'optimisation de la repartition des sources réactives, calculé avec le programme NEWOPT. Suivant l'hypothèse admise on arrive à des résultats différents concernant les puissances de compensation aux noeuds, les pertes de puissances dans le régime optimal, etc. Le régime optimal est différent selon l'hypothèse de calcul adoptée (Tableaux 4, 5 et 6).

Tableau 4

L'évolution du processus d'optimisation dans le cas de l'hypothèse a

L'itération	La puissance de compensation, [MVar], dans le noeud :				ΔP, [MW]
	2	*3*	*6*	*12*	
0	—	—	—	—	33,78
1	22,73	—	18,26	8,96	33,16
2	58,16	6,75	26,08	8,96	32,71
3	97,58	14,57	26,84	8,96	32,34
4	135,53	26,58	28,84	8,96	32

Tableau 5

L'évolution du processus d'optimisation dans le cas de l'hypothèse e

L'itération	La puissance de compensation, [MVar], dans le noeud:				ΔP, [MW]
	2	*3*	*6*	*12*	
0	—	—	—	—	24,91
1	32,46	0,14	13,91	3,46	24,50
2	71,98	6,55	18,89	3,46	24,18
3	112,51	15,07	18,94	3,46	23,93

Tableau 6

L'évolution du processus d'optimisation dans le cas de l'hypothèse k

L'itération	La puissance de compensation, [MVar], dans le noeud :				ΔP, [MW]
	2	*3*	*6*	*12*	
0	—	—	—	—	30,20
1	22,11	—	18,40	9,45	29,65
2	57,33	6,84	26,31	9,45	29,25
3	96,70	14,61	29,18	9,45	28,92
4	134,90	26,31	29,18	9,45	28,65

4. Conclusions

Les erreurs qui affectent les données d'entrée peuvent atteindre des valeurs importantes et l'influence des ces erreurs, surtout sur les pertes de puissance, est assez grande, généralement au dessus de 10%. L'ignoration de cette influence peut conduire à des régimes très différents par rapport aux ceux réels. Dans le calcul des régimes optimals il est nécessaire que les données d'entrée soient les plus exactes que possible.

Reçue le 24 octobre 1989

Institut Polytechnique, Jassy,
Chaire d'Énergétique

BIBLIOGRAPHIE

1. Идельчик В.И., Новиков А. С., Палмерчук С. И., *Влияние погрешностей информации на расчету оптимальных режимов.* Энергетика и транспорт, *2*, 22—29 (1982)
2. Koglin A.J., Oeding D., Schmidt K.D., *Identification of Topological Errors in State Estimation.* Second Intern. Conference of Power System Monitoring and Control, Conference Publication No. *266*, Institution of Electrical Engineers, London, 1986, 140—145.

INFLUENŢA ERORILOR INFORMAŢIEI ASUPRA CALCULULUI REGIMURILOR SISTEMELOR ELECTROENERGETICE

(Rezumat)

Erorile care afectează datele de intrare pot avea valori importante, iar influenţa acestor erori, mai ales asupra pierderilor de putere, este destul de mare, în general peste 10%. În cazul regimurilor optimale este necesar ca datele de intrare să fie cît mai exacte cu putinţă.

BULETINUL INSTITUTULUI POLITEHNIC DIN IAŞI
Tomul XXXVI (XL) Fasc. 1—2, 1990
Secţia III
ELECTROTEHNICĂ. ENERGETICĂ. ELECTRONICĂ. AUTOMATIZĂRI

GHEORGHE VASILIU

1903—1989

L'enseignement supérieur électrotehnique a subi une perte irréparable par la mort, après une longue maladie, du professeur docteur ès sciences, Gheorghe Vasiliu, survenue le 8 novembre 1989.

Nè à Jassy, le 17 février 1903, dans une famille de modestes employés, Gheorghe Vasiliu a reçu son instruction scolaire et universitaire dans cette même ville, vieille capitale de la Moldavie et centre de culture bien connu. Il a obtenu le titre d'ingénieur électricien en 1927, après avoir suivi les cours de l'Institut d'Electrotehnique auprès de la Faculté des Sciences de l'Université de Jassy. Remarqué, pendant ses études, par le professeur Ştefan Procopiu, il a été retenu dans l'enseignement supérieur, dans la même année, comme assistant à la chaire d'Électricité et Magnétisme. Promu chef de travaux an 1934 il prépare, sous la surveillance du professeur Procopiu, une thèse de doctorat avec une thème concernant la suppression des harmoniques dans les machines de courant continuu, qu'il a soutenue brillament en 1936.

Dès la création de l'École Polytechnique á Jassy, en 1937, Gheorghe Vasiliu devient le titulaire de la chaire d'Électrotechnique, d'abord en

qualité de maître de conférences (1938) et puis promu professeur (1940).

La carière didactique du professeur Gheorghe V a s i l i u, qui s'étend le long d'un demi siècle, est fermement entrecroisée avec le destin, parfois hostile, de l'enseignement supérieur technique de Jassy.

Depuis sa jeunesse il s'est rallié aux cercles d'intellectuels qui ont milité avec énergie et conviction pour l'idée de la création de l'École Polytechnique de Jassy, en étant d'un des promoteurs de ce mouvement constitué par des hommes conscients de l'importance nationale de ce desidérata ardent.

Dans l'histoire de l'Institut Polytechnique de Jassy et en même temps de l'enseignement supérieur technique roumain, le nom du professeur Gheorghe V a s i l i u est considéré comme un digne successeur de ces illustres prédécesseurs — Dragomir H u r m u z e s c u et Ştefan P r o c o p i u. Il a apporté une contribution essentielle à l'instruction de plus de 40 générations d'ingénieurs et a dirigé, avec compétence et bienveillance, de nombreuses thèses de doctorat. En même temps le professeur Gheorghe V a s i l i u a soutenu une vaste activité scientifique orientée en divers domaines allant de l'autoexcitation des machines synchrones jusqu'à la création de nouveaux types de magnetomètres de haute sensibilité, de la mesure de la radioactivité des sols jusqu'à l'étude de l'effet P r o c o p i u. Dans toutes ses recherches il a réussi à mettre en valeur son esprit inventif de pair avec des remarquables qualités d'expérimentateur de talent.

Maintenant, quand le professeur Gheorghe V a s i l i u a quitté ce monde, ceux qui l'ont connu en tant qu'étudiants ou collaborateurs, expriment leur profonde conviction que avant tout il a laissé le souvenir d'un homme tout à fait supérieur sur le plan moral, dans son caractère s'alliant la modestie avec la générosité, la correctitude avec l'indulgence, la noblesse d'âme avec l'absence totale des ambitions mesquines, en soutenant toujours sa position avec discrétion et même une certaine dose de pudeur mais incapable d'accepter les compromis.

Ses anciens collaborateurs sont profondément persuadés que la semence plantée le long des années dans les esprits et les âmes de ceux qui ont été ses élèves et collaborateurs va produire les fruits attendus par celui qui a été le professeur Gheorghe V a s i l i u. C'est le plus sincère hommage qu'on peut apporter à sa mémoire.

Hugo Rosman

BULETINUL INSTITUTULUI POLITEHNIC DIN IAŞI
Tomul XXXVI (XL) Fasc. 1—2, 1990
Secţia III
ELECTROTEHNICĂ. ENERGETICĂ. ELECTRONICĂ. AUTOMATIZĂRI

RECENZII

BOOK REVIEWS РЕЦЕНЗИЙ

WERNSTEDT J., *Experimentelle Prozessanalyse*. VEB Verlag Technik, Berlin, 1989, 391 S., ISBN 3-341-00676-1.

Mit dem gegenwärtig hohen Niveau des Einsatzes des Meß-, Steuer-, Regelungs- und Rechentechnik in technologischen Prozeßen ist auch eine ständige Anpassung und Weiterentwicklung von mathematisch-statistischen Methoden zur Prozeßanalyse und -modellierung verbunden. Die Sygnal- und Systemmodelle finden ihre Anwendung bei der Analyse, dem Entwurf und dem Betrieb automatischer und Automatisierter Steureungssysteme. Der gegenwärtige Stand auf dem Gebiet der experimentellen Prozeßanalyse ist durch eine ausserordentlich große Mannigfaltigkeit von verschiedenen Verfahren gekennzeichnet. Anwender und Studierende stehen deshalb vor der schwierigen Aufgabe, eine Übersicht zu bekommen und eine geeignete Auswahl der Verfahren zu treffen.

Das vorliegende Buch stellt eine vom praktischen Aspekt ausgegangene Einführung in die Grundlagen des Wissenschaftsgebiets der experimentellen Prozeßanalyse für Ingenieure und Studierende der Ingenieurwissenschaften dar, besonders der Fachrichtungen Technische Kybernetik und Automatisierungstechnik. Diesem Ziel folgend, kann man die Breite des dargestellten Gebiets den Kapitelüberschrift leicht entnehmen : 1. Einführung (Stellung des Modells, Praktische Beispiele, Gesamtkonzeption, Klassifikation) ; 2. Beschreibung des Amplitudenverhaltens von Signalen (Zielstellung, Grundlagen der Wahrscheinlichkeitsrechnung und der Statistik) ; 3. Beschreibung des dynamischen Verhaltens von Signalen (Grundlagen der Beschreibung deterministischer und stochastischer Signale, Signalmodelle, Methoden der Signalaufbereitung) ; 4. Bestimmung des dynamischen Verhaltens ungestörter Systeme (Systemmodelle und Testsignale, Ein-/Ausgangs-Modelle im Zeitbereich, Ein-/Aussgangs-Modelle im Frequenzbereich, Ermittlung des Zustands/Beobachter) ; 5. Bestimmung des statischen Verhaltens von gestörten Systemen (Grundlagen der Schätztheorie, Schätzverfahren, Methoden der optimalen Versuchsplanung) ; 6. Bestimmung der dynamischen Verhaltens gestörter Systeme (Zielstellung, Schätzung der Stützbstellen der Kerne der Volterra-Reihe und der Koeffizienten der Differenzengleichung, Entwurf von Testsignalfolgen, Schätzung des Zustands/Zustandsfilter, Ausgewählte Probleme der Schätzung dynamischer Systems).

Der Inhalt des Buches und die Art der Behandlung spiegeln die lange Hochshul- und Forschungserfahrung des Authors wieder, der um Anschaulichkeit bemüht ist und durch Querverbindungen, zahlreiche und sorgfältig ausgewählte textbegleitende Übungen und treffende Illustrationen fördert.

M. Voicu

ISIDORI A. (Ed.), *Nonlinear Control Systems Design*. Preprints of the IFAC Symposium, Capri, Italy, June 14—16, 1980, XIV + 491 pp.[1])

In the preface of his book : *Methods of Nonlinear Analysis*, 1969 (vol. I), Richard Bellman said : „The demands of modern science inexorably force

---

[1]) The IFAC Proceedings of NOLCOS '89 are going to appear during 1990 by Pergamon Press.

the mathematician to explore the nonlinear world. That is a difficult and often humbling journey with painfully crude maps and rather primitive direction-finders cannot be gainsaid, but in return it can be asserted that it is richly rewarding." What can be said two decades after? Concerning the control of systems described by nonlinear mathematical models, „a major breackthrough occured at the beginning of this decade, primarily due to the application of mathematical concepts derived from the field of differential geometry. ... Around the mid of the decade, a further thrust was added by the appearance of new methods for the analysis of nonlinear input—output differential relations, and by the efforts to combine the results of the geometric analysis with the methods of the asymptotic analysis, primarily singular perturbations and center manifold theory". (From the preface, signed by the Preprints' editor). In this respect the NOLCOS '89 Symposium and the 99 papers presented at this event reflect the state of the art and the development tendencies in nonlinear control theory. The topics approached by researches of more than 20 countries are very significant, and they may be transparently identified following the session titles: Stability and Regulation I, Optimal Control of Nonlinear Systems, Discrete Time Systems I, Input—Output Methods of Analysis and Design, Variable Structure Systems, Nonlinear Control of Mechanical Systems, Algebraic Methods in Nonlinear Control Theory I, Adaptive Control of Continuous-Time Nonlinear Systems, Stability and Regulation II, Geometric Methods in Nonlinear Control Theory I, Adaptive Control of Discrete-Time Nonlinear Systems, Nonlinear Control of Electrical Systems, Geometric Methods in Nonlinear Control Theory II, Discrete Time Systems II, Stability and Regulation III, Nonsmooth Analysis and Differential Inclusion, Stability and Regulation IV, Algebraic Methods in Nonlinear Control Theory II, Nonlinear Control of Chemical System.

The volume is highly recommended to applied mathematicians, physicists, control/systems engineers and it is a valuable stepping stone towards further study and research in nonlinear control systems design.

M. Voicu

CONRAD W., *Technische Kuriositäten*. Urania-Verlag, Leipzig, Jena, Berlin, 3. Aufl., 1989, 216 S., ISBN 3-332-00124-8.

Eine Auswahl der „Gutenacht-Geschichten" ist in diesem Lesebuch anthalten. Es sind 15 zeitlose „Lesebuchgeschichten" aus der Technik — spannend, witzig, informativ und immer anregend, Jeder Beitrag ist so geschrieben und reich illustriert, daß er seine Aktualität nicht verliert, obwohl es um historischen Begebenheiten aus der Technik geht. Er ist für den Techniker und den Wissenschaftler ebenso exakt und informativ wie für den „normalen" Zeitungsleser interessant und verständlich. Die Breite des dargestellten Gebiets kann mann leicht den Titeln der Geschichten entnehmen: Die treibende Kraft; Das ewig Bewegliche; Altes Thema Sonnenenergie; Rund um den heimischen Herd; Rette sich, wer kann; Schreiben und Lesen, Hören und Sehen; „Automobil" auf mannigfache Weise; Volldampf auf Straßen und Schienen; Altes, junges Fahrrad; Navigare necesse est; Stelzen, Segel und Rotoren; Galerie der Luftschiffe; Die Erben des Ikarus; Informationen unterwegs; Kleines Automatentheater. Hier findet jeder Leser, selbst wenn ihn das Thema Technik nicht interessiert, bestimmt immer wieder eine oder zwei Geschichten für das „berühmte Viertelstündchen".

M. Voicu

MIEL G., FIEBICH R., *Steuern und Regeln, selbst erlebt*. Urania-Verlag, Leipzig, Jena, Berlin, 2. Aufl., 1989, 223 S., ISBN 3-332-00125-6.

Das Buch stellt die vom praktischen Aspekt ausgegangenen wichtigsten Schaltungen der Steuerungs- und Regelungstechnik dar. Es konzentriert sich auf elektronischen Schaltungen und Einrichtungen, was die Anwendungen in Verbin-

dung mit der Schlüsseltechnologie Mikroelektronik in der Automatisierungstechnik ermöglichen. Das Ziel dieses Buches ist das eigene Experiment, das eigene Erkennen und Erleben von physikalisch—technischen Zusammenhängen, und natürlich als Ergebnis davon das fertige Gerät. Inhatllich wird stufenweise vorgegangen. Die Kapitel des Buches haben die folgenden Titel : 1. Grundlagen (Gleichrichter, Z-Dioden, stabilisiertes Netzteil) ; 2. Elektronisches Meßen nichtelektrischer Größen (Meßen zweks Steuern und Regeln, Meßverstärker, elektronischer Belichtungsmeßer, elektronische Waage) ; 3. Digitales Meßen (digitale Grundschaltungen, integrierte Digitalschaltungen, elektronischer Zähler, Zählerstand Dekodierung, Digitalzähler, Digitaluhr, Drehzahlmeßer) ; 4. Steuerungstechnik (Thyristor und Triacsteller, Belichtungszeitsteuerung, Steuerung mit Schall, Drehzahlsteller, programmierte Ablaufsteuerung) ; 5. Fernsteueretchnik (Fernsteuersignale, Sender- und Empfängeranlagen) ; 6. Regeltechnik (von der Steuerung zur Regelung, Spannungsregler, Analogregler, Nachlaufregler).

Das Buch wendet sich an Oberschulabsolventen und Studenten aller technischen Fachrichtungen, die in kurzgefasster Form die Automatisierungstechnik durch Anwendungsbeispiele kennenlernen wollen.

M. Voicu

HRONICEK J., KRIZ E., WEBER J., *Steuer- und Regeltechnik.* Bohmann Verlag, Wien, 1986, 209 S., ISBN 3-7002-0591-0.

Das ist ein Buch für den Unterrichtsgebrauch an Beruffschulen für Lehrberufe Elektromechaniker und -maschinenbauer, Electromechaniker für Starkstrom, Elektroinstallateur, Betriebselektriker, Starkstrommonteur, Elektromechaniker für Schwachstrom, Meß- und Regelmechaniker. Die Breite des dargestellten Gebiets kann man gut den Kapitel und Unterkapitelüberschrift entnehmen : A. Bauelemente der Steuer- und Regeltechnik (Grundbegriffe der Halbleitertechnik, Dioden, Transistor, Mehrschichtdioden, Mechanische Schaltelemente (Relais, Schütz) ; B. Elektrisches Meßen nichtelektrischer Größen (Allgemeines, Begriffsbestimmung, Einteilung der Meßwertaufnehmer) ; C. Stellglieder (Allgemeines, Einteilung der Stellgeräte, Stellantriebe, Stellglieder für elektrische Energie, Stellglieder für Flüssigkeiten und Gase, Stellglieder für feste Stoffe, Praktisch ausgeführte Anlagenbeipiele mit Stellgliedern) ; D. Verstärker (Allgemeines, Verstärkungsfaktoren, Eingangs- und Ausgangswiderstand, Frequenzverhalten eines Verstärkers, Belastbarkeit, Außteuerbereich, Idealer Verstärker, Einteilung der praktischen Verstärker, Verstärker mit Rückkopplung, Differenzverstärker (Operationsverstärker, Verstärkerarten, Bauformen) ; E. Einführung in die Digitaltechnik (Begriffsbestimmungen, Binäre Grundschaltungen bzw. Grundverknüpfungen, Wahrheitstabellen und Arbeitstabellen, Logische Verknüpfungen, Funktionen, Gatter-Grundschaltungen, Schaltungen mit Speicherverhalten (Informationsspeicher), Zählschaltungen, Duale Zahlen Digitale Meßungen) ; F. Steuerungen (Begriffe und Definitionen, Unterscheidungsmarkmale von Steuerungen, Sicherheit, Prüfung und Fehlersuche, Wartung, Schaltungsunterlagen, Entwicklung und Aufbau von Grundschaltungen, Ausführungsbeispiele steurungstechnischer Schaltungen) ; G. Regelung (Grundbegriffe, Beispiele von praktischen Regelsystemen, Unstetige Regeleinrichtungen, Stetige Regeleinrichtungen, Regelkreis, Glieder in Steuerketten und Regelkreisen, Zeitverhalten von Strecken in Steuerungen und Regelungen, Regelgüte, Aus der Praxis der Regelgungstechnik) ; H. Stromrichter (Gleichrichter, Wechselrichter, Einrichtungs- und Zweirichtungsstromrichter, Umkehr-Stromrichter, Umrichter, Wechselstromsteller, Gleichstromsteller) ; I. Oszilloskop und schreibende Meßgeräte (Aufbau und Wirkungsweise des Oszilloskops, Meßungen mit dem Oszilloskop, Schreibende Meßgeräte).

Selbstverständlich ist das Buch praxisorientiert. Daher haben sich die Autoren besonders um eine verständliche Darstellung bemüht. Treffende Illustrationen fördern die Anschauung des Lesers. Ansonsten sind text, schematische Darstellung und Gleichungen kurz, sauber und übersichtlich angeordnet.

Das Buch ist für einen breiten Leserkreis von Interesse, da die ausgegriffenen Probleme in technischen Einrichtungen auftreten und gelöst werden müßen.

M. Voicu

* * * *Technik automatisierter Führungssysteme*. Militärverlarg der DDR, Berlin, 1990, 236 S., ISBN 3-327-00758-6.

Automatisierte Führungssysteme werden gegenwärtig in alles Teilstreitkräften eingeführt bzw. vervollkomment. Das vorliegende Fachbuch soll einem breiten Leserkreis einen Überblick über vorhandene und in absehbarer Zeit zu erwartende Technik geben. Inhaltlich wird stufenweise vorgegangen. Die Kapitel des Buches haben die folgenden Titel : 1. Grundlagen automatisierter Führungssysteme ; 2. Technologie der Informationsbearbeitung in automatisierten Führungssystemen der Luftverteidigung ; 3 .Datenerfassungs-, Speicher- und Übertragungstechnik ; 4. Rechentechnik ; 5. Prozeß- und Universalrechentechnik ; 6. Informationsdarstellungstechnik ; 7. Prinzipien perspektivischer Technik. Selbstverständlich kann dieses Buch die vorhandene Spezialliteratur zum Aufbau der verschiedenen Systeme und Geräte einschließlich ihrer Nutzungstechnologie nich ersetzen.

Das Buch wendet sich an Fachleute die eine Übersicht über wichtige Fachbegriffe (und ihre englischen und russischen Entsprechungen) und Fragen der Automatisierung in allen Bereichen des Militärwesens haben sollen.

M. Voicu

BOMZE I. M., POTSCHER B. M., *Game Theoretical Foundations of Evolutionary Stability*. Springer Verlag, Berlin, Heidelberg, New York, VI + 145 pp., ISBN 3-540-50766-3.

This volume is the 324th published in the Lecture Notes in Economics and Mathematical Systems Series of Springer Verlag.

As stated by the authors in the Introduction, the purpose of this book is to provide an unifying theoretical framework for the (mathematical) theory of evolutionary stability. Further on, the authors intend to introduce some basical results in this theory.

Briefly, the problem of evolutionary stability is as follows. Let $\mathcal{P}$ be the set of possible states and, $f(Q, P)$, P, $Q \in \mathcal{P}$, the real-valued „payoff" function describing the system. Let P be the initial state, and let $P_\varepsilon(Q) := (1-\varepsilon)P + \varepsilon Q$, $0 < \varepsilon < 1$, be another state. The state P is an „evolutionary stable state" if for all $Q \in \mathcal{P}$, $Q \neq P$, there is an $\varepsilon(Q)$, $0 < \varepsilon(Q) < 1$ such that :

$$f(Q, P_\varepsilon(Q)) - f(P, P_\varepsilon(Q)) < 0,$$

whenever $0 < \varepsilon < \varepsilon(Q)$. This definition — not from the reviewed volume — is easily interpreted in terms of game theory and for systems considered as populations. Indeed, one sub-population can be considered to remain in the initial state, P, while a little part of population is subject to a mutation to the state Q. The strategy concerns the contest of the two sub-populations. The model can ben applied to biological populations and to economic processes. In the opinion of the present reviewer, the model could also be applied in modelling the cultural evolution in society, as well as science evolution (stability of paradigms).

The content of the book is organised on 8 chapters. The first one, although titled *Introduction*, is in fact a preface. The second chapter is devoted to the basical presentation of the (evolutionary) game theory However, I doubt the newcomer in the field find this introduction on any help, although some aspects are nicely systematised for the use of teachers.

It is in the third chapter the authors define the evolutionary stability and present some basical results related to stability and present some basical results related to stability conditions.

The fourth chapter deals with „uninvadability", i.e. uniform evolutionary stability. This concept is related to the existence of a protective global invasion barrier. (The terms are borrowed from biology). The authors prove the possibility of existing infinitely many uninvadable states, and provide conditions the state is uninvadable.

The topic of the fifth chapter is *Games with Bilinear Average Mean Payoff*. In chapter six, evolutionary stability is analysed for games with mixed strategies, relating this stability to extremality properties. It is also proved that under some

natural conditions, the number of evolutionarily stable states is finite.

In chapter seven, population games (mixed strategy games of particular kind) are analysed, related to evolutionary stability and uninvadability.

The last chapter is devoted to the time evolution of systems characterised by evolutionary stability. It is proved that uninvadability implies dynamical stability, while evolutionary stability does not.

An Appendix giving some proofs, the References list, and the List of Symbols end the volume.

This monograph is an interesting reading for those involved in biomathematics. It is a significant contribution in this field, although it is only a preliminary draft for a more complete and clearer monograph.

H. N. Teodorescu

ASTROM K. J., WITTENMARK B., *Adaptive Control.* Addison-Wesley, Reading Mass., New York, Amsterdam, Bonn, 1989, 526 pp., ISBN 0-201-09720-6.

In spite of the fact that there are still many unsolved theoretical and practical issues, adaptive control proves to be a very promissing solution for industrial applications.

The knowledge about adaptive techniques is widely scattered in the literature. So, this book has evolved from many years of research and teaching in adaptive control and it can serve as an introduction for the newcomer to get a good grasp of the field.

The contents of the book are organized into 13 chapters and two appendixes. Illustrating the aim of the book, their titles are very significant and transparent: 1. What Is Adaptive Control ?; 2. Why Adaptive Control ?; 3. Real-time Parameter Estimation; 4. Model-reference Adaptive Systems; 5. Self-tuning Regulators; 6. Stability, Convergence, and Robustness; 7. Stochastic Adaptive Control; 8. Auto-tuning; 9. Gain Scheduling; 10. Alternatives to Adaptive Control; 11. Practical Aspects and Implementation; 12. Applications; 13. Perspectives on Adaptive Control; A. Regulator Design; B. Positive Real Transfer Functions.

The book is certainly of interest to a large community of readers. It contains many examples, applications and discussions. It reflects a long experience of the two very renowed authors and can be useful to anyone looking for an accessible insight and presentation of adaptive control.

M. Voicu

BUDIG P.-K. (Hg.), *Technik-Wörterbuch: Elektrotechnik, Elektronik; English — Deutsch.* 4. unveränd. Aufl., VEB Verlag Technik, Berlin, 1989, 800 S., ISBN 3-341-00880-2.

Electrotechnics and electronics in the large have contributed and continue to play an important role in the contemporary scientific and technical revolution. They have opened numerous possibilities towards mechanization and automation of industrial processes, in which the modern microelectronics nowaday brings genuine solutions for new and various application domanis.

In this respect the dictionary presents the state of the art and development tendencies in the terminology in two languages whose qualified speakers have substantially contributed to the development of electrotechnics and electronics. By studying text books, monographs and journals in German and English the editor and its co-workers have collected about 60,000 terms covering the following topics: electrophysics, electrotechnical measurements, electrochemistry, materials, electrical machines and drives, apparatus, high-voltage technique, power generation, transmission and distribution, power electronics, insulators and insulation, electric heat, electric lighting, information theory, electroacoustics, electromedicine, semiconductors, electronic components and devices, optoelectronics, superconductors, laser technique, information technique, communication engineering, radio engineering, automatic control, remote control technique, data processing, computers and computing, microprocessors and microcomputers. Directions for use and lists of

symbols and abbreviations facilitate to understand the pertinent comments which accompany frequently the English—German equivalences. The quality of printing is excellent ensuring a very good survery to the user.

The book constitutes a necessary and useful tool for German speaking students, engineers and scientists who are interested to read in English the numerous and of good quality publications in electrotechnics and electronics in the large published in England, USA, Canada, and elsewhere.

M. Voicu

OWENS D. H. (Ed.), *Adaptive Systems in Control and Signal Processing.* Vol. **I** and **II,** Preprints of the IFAC Simposium, Glasgow, UK, April 19—21, 1989 [1]), 685 pp.

Nowaday the adaptive control theory can offer many implementable solution, which are starting to have some industrial impact. A rough estimate is that approaches in this field, and to offer many implementable solutions to the of this IFAC Symposium was to bring to light the latest points of view and approaches in this field, and to offer many implementable solutions to the practitioners. In this respect the topics of the Symposium are very significant, and they may be transparently identified following the titles of the papers : *Adaptive Control — a Perspective* (K. J. Astrom), *Self-adaptive Algorithms for Two -dimensional Signal Sources* (P. E. Wellsted), *Adaptive Control-Robustness and Performance Enhancement* (I. D. Landau), *Optimal Off-line Signal Processing* (Y. Z. Tsypkin and E. D. Aved'yan), *System Identification in a Noise Free Environment* (L. Ljung), *Uncertaintly Information and Estimation* (G. C. Goodwin, D. Q. Mayne and M. E. Saldago), *Recursive Estimation and Modelling of Non-stationary and Non-linear Time Series* (P. C. Young), *Stochastic Dynamics of Blind Decision Feedback Equalizer Adaptation* (R. A. Kennedy, B. D. O. Anderson and R. R. Bitmead), *Adaptive Control within the Class of Stabilizing Controllers for a Time-varying Nominal Plant* (J. B. Moore and T. T. Tay), *A Direct Adaptive Controller for a Class of Stable and Time-varying Plant* (F. Giri, M. M'Saad, L. Dugard and J. M. Dion), *Adaptive Control Applied to the Disturbance Accommodation Problem* (B. A. Brandin), *Internal Model Adaptive Control Systems* (J. Guan, L. Wang and D. H. Owens), *Tracking of Multiple Targets* (C. A. Deacon and D. P. Atherton), *Feedforward Adapted Position Controller* (R. Strietzel and Y. Kaddaha), *Expression of Generalized Adaptive Law using Delta Operator* (T. Suzuki and K. Tanaka), *Improvement of the Tracking Property for the Linear Quadratic Adaptive Controller* (T. Yamamoto, S. Omatu and H. Ishihara), *Discrete-time Iterative Learning Controller using Approximate Inverse-model* (T. Ishihara, K. Abe and H. Takeda), *Continuous-time Generalised Predictive Control* (P. J. Gawthrop and H. Demircioglu), *Optimal Control Redesign of Generalised Predictive Control* (R. R. Bitmead, M. Gevers and V. Wertz), *Input—output-representation of Predictive Control-algorithms* (A. Schumann), *Co-ordinated Decentralized Adaptive Control Large-scale Dynamical Systems* (B. M. Mirkin, M. H. Gandelman and T. Man-Su), *Adaptive Pole Placement for System with Abnormal Measurement Data* (P. Xialong), *Adaptive Pole-placement Algorithm Based on Common Factor Elimination* (K. Konishi and T. Yoshimura), *H^{∞} Robust Linear Estimator* (M. J. Grimble, D. Ho and A. Elsayed), *Learning in a Noisy Domain* (T. C. Fogarty), *Decoupling-adaptive Control of a Class of Multivariable Systems* (Zhang Weiying, Wang Zhou-jun and Zhang Xiao-hua), *Direct Adaptive Control with the Robust Least Squares Method* (V. Z. Filipovič and B. D. Kovacevič), *Adaptive Control with Linear Non-parametric Models* (M. Jordan and R. Isermann), *The Convergence of a Modifield ELS Algorithm* (A. S. Bozin and M. B. Zarrop), *Design of Adaptive Digital Set-point Tracking Controllers*

[1]) The IFAC Proceedings are going to appear during 1990 by Pergamon Press, Headington Hill Hall, Oxford OX 30 MW, United Kingdom.

Incorporating Recursive Impulse-response Matrix Identifiers for Type-one Multivariable Plants (B. Porter and A. Khaki-Sedigh), *A New Direct Adaptive Control Algorithm for Multivariable Systems with the Arbitrary and Unkown Interactor Matrix and Global Convergence Analysis* (Chai Tian You), *Adaptive Dead-beat Control with Innovation Representations* (I. Bencsik and G. Michaletzky), *Adaptive Control of Dynamic Tracking Measurable State Variable System* (Liu Changli, Li Xueping and Nie Weiqing), *Application of Adaptive Control on a Simple Arm* (I. Moscovitz and A. Feuer), *Identification and Adaptive Control of Mechanical Systems with Friction* (J. C. Maron), *On-line Simulation for Control of British Gas Transmission Network* (T. Newport, J. J. Piggott, S. G. Williams and S. M. Henderson), *Discrete-time Adaptive Control for Continuous-time Systems using Limiting-zero Model and its Application* (N. Mizumo and D. Fujii), *The Adaptive Deadbeat Controller* (A. Walsh), *Multivariable Adaptive Control of an Environmental Test Chamber* (J. M. Dion, L. Dugard, Nguyen Minh Tri, G. Sanchez, A. Franco and D. Rey), *Implementation of an Adaptive Autopilot Unit* (X. L. Xia, D. Q. Leng, C. E. Yang, J. M. Hou and Q. Song), *Optimal Adaptive Robust Controller for Hydroturbine Regulation* (Wang Hong), *Mean Exit Times and Rates of Convergence for Stochastic Systems with Applications and Adaptive Control* (S. P. Meyn and P. E. Caines), *Fault Detection and Diagnosis in a Chemical Plant using Sequential Hypothesis Testing* (X. J. Zhand and M. B. Zarrop), *Robust Identification Scheme in an Adaptive Track-controller for Ships* (T. Holzhuter), *Adaptive Grasping Force Control for Manipulator Hand using Fuzzy Set Theory* (Y. Dote, N. Odagiri and F. Konno), *Self-adaptive Automotive Engine Management* (P. E. Wellstead and P. G. Scotson), *An Industrial Adaptive PID Controller* (T. Hagglund and K. J. Astrom), *Multivariable Adaptive Control: an Industrial Drying Process Application* (F. De Sario, M. Ricci and A. Visioli), *An Adaptive Autopilot for Inland Ships* (H. Duetz), *Adaptive Robotic Deburring* (G. M. Bone, M. A. Elbestawi, L. Liu and K. Sinha), *A Microcontroller-based Real-time Control System for ac Drives* (M. S. Khanniche and M. Belaroussi), *Application of Multilayer Perceptions as Adaptive Channel Equaliser* (G. J. Gibson, S. Siu and C. F. N. Howard), *Input-constrained Self-tuning Control of a Robot Link* (P. Lohnberg and J. van Amerongen), *Self-tuning PI Control of a Solar Power Plant* (F. R. Rubio, F. M. Hughes and E. F. Camacho), *Self-tuning Control of Blood Pressure: Single Variable and Multivariable Studies* (D. A. Linkens and N. E. Monsour), *A Semi-infinite Horizon LQ Self-tuning Regulator for ARMAX Plants Based on RLS* (E. Mosca and J. M. Lemos), *The Use of Disturbances Measurement Feedforward in LQG Self-tuners* (M. Sternad), *Multivariable LQJ Self-tuning Control with Disturbances Measurement Feedforward* (K. J. Hunt and M. Sebek), *Multirate Self-tuning Control of Multivariable Systems* (R. Scattolini), *Optimal Approaches to Self-tuning PID Control* (P. Vega and M. B. Zarrop), *An Extended Self-tuning Multivariable PI Controller* (T. T. Jussila, J. T. Tanttu, M. Piirto and H. N. Koivo), *Self-tuning PID Control of Muscle-relaxant Drug Administration in Operating Theatres* (D. A. Linkens, M. Denai, A. J. Asbury, A. D. MacLeod and W. M. Gray), *Filtered and Predicted States for Discrete-time Adaptive Control* (K. Warwick and K. J. Burnham), *Computationally Efficient Self-tuning Algorithms* (M. S. Ahmed and I. A. Haseeb), *Adaptive Temperature Control of a Water Bath by using Multivariable Self-tuning Control* (S. Omatu, T. Yamamoto and M. Hotta), *Self-tuning Control with Alternative Sets of Uncertain Process Models* (V. Peterka), *Robust Adaptive LQ Control Scheme* (J. Suh and P. Ioannou), *Robust Stability Conditions for Adaptive Control Systems* (L. Wang and D. H. Owens), *The F-iteration Approach to H^{∞} Control* (M. J. Grimble and N. A. Fairbairn), *Robustness in Adaptive Control from a Frequency Domain System Identification Perspective* (S. Gunnarsson), *Robust Adaptive Redesign without Persistent Excitation* (A. A. Bahnasawi and M. S. Mahmoud), *Adaptive Control for Partial Model Matching in Frequency Domain for Non-minimum Phase Systems* (K. Ohkubo and A. Sano), *A Robust Controller in the Presence of Unmodelled Dynamics* (Gu Zingyuan and Wang

Wei), *A U-D Fixed Interval Smoother in Backward Pass Realization* (K. Watanabe and S. G. Tzafestas), *The Adaptive Method for Filtering the Reflection Waves in Parameter Identifications of Non-uniform Distributed Systems* (Z. Trzaska), *Lattice Algorithms with Variable Forgetting Factors Detecting Interventions and Parametric Changes* (D. De la Fuente and D. F. Garcia), *Least Square Type of Adaptive Filter with Optimally Stabilized Convergency Based on Eigen-structure Approach* (A. Sano, H. Ohmori and M. Furuya), *A Maximum Likelihood Algorithm for Estimating Damped Sinusoids* (D. R. Farrier and A. R. Prior-Wandesforde), *Applications of Entropy of Patterns and Forms to Signal Processing* (G. Jumarie), *The Positive-real and Strictly Positive-real Property of Sampled System* (Zhihua Qu), *Parameter-adaptive PID-control Based on Continuous-time Process Models* (K. Peter and R. Isermann), *Implicit Modelling of Noise versus the Use of a Fixed Noise Model* (A. R. M. Soeterhoek, H. B. Verbruggen and P. P. J. van den Bosch), *Model-referenced Adaptive Control of Manipulation Robots: a Simplified Approach* (S. P. Patarinski), *Application of Microcomputer-based Model Reference Adaptive Control to a Hydraulic Positioning System* (H. Unbehauen, P. Du and U. Keuchel), *Adaptive Control Based on Exact Model Matching* (K. Ichikawa), *A Design of Non-linear MRACS and the Proof of Stability* (S. Okubo), *Model Reference Control for Discrete-time Non-linear System* (S. Shin and T. Kitamori), *Unification of Continuous and Discrete Model Reference Adaptive Control* (Zhang Qiren and Qu Zhihua), *Adaptation of the Switching Hyperplanes in Cautious Sliding Control with Application to Mechanical Systems* (M. Partovi and R. Longchamp), *Discrete Variable Structure Control for an Active Anti-vibration* (A. Parvinmehr, R. D. Greenough, A. J. Wilkinson and A. Jenner), *An Expert Adaptive PID Controller* (S. Thompson and E. G. McCluskey), *Concurrent Array Processing for Linear Multivariable Feedback Control Systems* (E. Rogers and Yun Li), *Convergence Properties of Associate Memory Storage for Learning Control Systems* (P. C. Parks and J. Militzer), *A Real Time Supervision System for Adaptive Control* (M. Samaan, M. Duque and M. M'Saad), *Design of Adaptive Digital Set-point Tracking PI Controllers Incorporating Expert Tuners for Multivariable Plants* (A. H. Jones), *Recursive Identification of Overparametrized Systems* (L. Xia, V. Krishnamurthy and J. B. Moore), *Grey-box Modelling & Identification, using Physical Knowledge and Bayesian Techniques* (H. J. A. F. Tulleken), *On Stability Analysis of Equilibrium Points of Variational Adaptive Control Schemes* (G. Casalino, A. Ferrara and R. Minciardi), *An Improved Identification Algorithm of Stochastic Time-delay Systems* (Wei-Xing Zheng and Chun-Bo Feng), *Bayesian Filtering for Discrete-time Systems with Random Structure* (E. Kliokys and R. Kulhavy), *On a Higher Order Recursive Technique for Frequency Estimation* (M. P. Spathopoulos), *Bayesian Approach to Optimal Input Design for Failure Detection* (F. Keresteciogl u and M. B. Zarrop), *Adaptive Input Estimation* (A. Ahlen and M. Sternad), *Robust Parameter Estimation Procedure for ε-Contamined Probability Distribution Models with Uncertain Gross-error* (K. Uosaki and K. Saito), *Parameter Estimation of a Class of Discrete Time Varying Systems* (D. Juricic), *Real-time Estimation of Parameter Bounds for Linear Plants with Bounded Disturbance* (A. L. Bunich), *An Adaptive Controller for Non-linear Systems* (K. Warwick, Q. M. Zhu and J. L. Douce), *Indirect Adaptive Control of Linearly Parametrized Non-linear Systems* (G. Bastin and G. Campion), *A Non-linear Adaptive LIA Stateggy to Control some Thermal Processes* (M. Lakrori, A. Montano and M. Duque), *Self-tuning Control of Block-orientated Non-linear Systems* (J. Voros), *Long-range Predictive Control of Non-linear Systems on the Basis of the Hammerstein Model* (R. Bars and R. Haber), *Self-tuning Control of a Stochastic Non-linear Object* (V. Kaminskas, D. Janickiene and D. Vitkute).

The volumes are highly recommended to applied mathematicians, physicists, control/systems students and engineers, and is a very valuable source for further study and research in adaptive control systems design.

M. Voicu

CASTI J. L., *Alternate Realities, Mathematical Models of Nature and Man.* John Wiley & Sons, New York, 1989, 493 pp., ISBN 0-471-61842-x.

In experimental science, the principal focus regards the development of new instruments and techniques for measuring various aspects of natural phenomena, with all other considerations subservient to this primary task. So it is also in theoretical science, where the overarching problem is how to capture the processes of Nature and Man in formal mathematical representations, with all matters of technique and choice of methods being of secondary consideration.

This book addresses the interface between these complementary aspects of scientific practice. In this respect the titles of the chapters are very transparent and significant : 1. The ways of model-making : natural systems and formal mathematical representations ; 2. Pattern and the emergence of living forms : cellular automata and discrete dynamics ; 3. The analytical engine : a Newtonian view of brain, minds and mechanisms ; 4. Catastrophes and life : the singularities of ecological and natural resource systems ; 5. Order in chaos : turbulence and pattern in the flow of fluids, populations and money ; 6. Strategies for survival ; competition, games and the theory of evolution ; 8. The geometry of human affairs : connective structure in art, literature and games of chance ; 9. How do we know ? Myths, models and paradigms in the creation of beliefs. Discussion, questions, problems, and exercises follow each chapter, reinforcing and amplifying the concepts considered. Extensive notes and references are also included for every chapter.

For teachers, students, and researchers in mathematical modeling and/or general applied mathematics, the book presents an exciting and refreshing approach to capturing the processes of nature and man in formal mathematical terms.

M. Voicu

BERMAN A., NEUMAN M., STERN R. J., *Non-negative Matrices in Dynamic Systems.* John Wiley & Sons, New York, 1989, 167 pp., ISBN 0-471-62074-2.

This book concerns the application of the theory of nonnegative matrices to certain problems arising in positive linear differential and control systems. As such, the book will be used as a graduate level course or seminar text in applied mathematics. Furthermore, since nonnegative matrices and positive linear dynamic systems are relevant in economics, engineering, numerical analysis, operations research, as well as various life and social sciences, it is to expect that it will also be of interest to workers in these fields.

In order to point out the reader feeling for the content of the book we give in the sequel the titles of the chapters : 1. Convex Sets ; 2. Matrix Theory Backround ; 3. Differential and Control System Preliminaries ; 4. Exponentially Nonnegative Matrices ; 5. Extended *M*-matrices ; 6. Cone Reachability ; 7. Applications to Feedback Control ; 8. Controllability, Observability, and Realizability of Positive Control Systems.

The book may be useful to researchers and students in engineering, economics, numerical analysis, and operations research, as well as in the life and social sciences.

M. Voicu

DORF R. C., *Modern Control Systems.* Addison-Wesley, Reading Mass., New York, Amsterdam, Bonn, 1989, 603 pp., ISBN 0-201-14278-3.

„Man cannot inherit the past, he has to recreate it". Through this motto preceding the dedication of the book to his students, R. C. Dorf expresses lapidarly the aim of one of the fundamental inventions of humankind : the education.

The purpose of the book is to present the structure of feedback control theory and to provide a sequence of exciting discoveries as the reader proceeds through the text and problems.

Having in mind that the most important and productive approach to learning is for the reader to rediscover and recreate anew the answers and methods of the past, the author has organised the book in the following 12 chapters and four appendixes : 1. Introduction to Control Systems ; 2. Mathematical Models of Systems ; 3. Feedback Control System Characteristics ; 4. The Performances of Feedback Control Systems ; 5. The Stability of Linear Feedback Systems ; 6. The Root Locus Method ; 7. Frequency Response Methods ; 8. Stability in the Frequency Domain ; 9. Time-Domain Analysis of Control Systems ; 10. The Design and Compensation of Feedback Control Systems ; 12. Design Case Studies ; A. Laplace Transform Pairs ; B. Symbols and Units, Conversion Factors ; C. An Introduction to Matrix Algebra ; D. Decibel Conversion.

The book is written in a very clear and rigorous style, the author, well known specialist in automatic control systems, presenting the material with pedagogical skill. Using numerous worked examples and problems the book is of interest to students and lecturers involved with courses on control engineering and represents a valuable documentary source for scientists and engineers involved in automatic control systems design and practice.

M. Voicu

ZWART H. J., *Geometric Theory for Infinite Dimensional Systems.* Lecture Notes in Control and Information Sciences No. *115*, Springer Verlag, Berlin, Heidelberg, 1989, 156 pp., ISBN 3-540-50512-1.

This book provides a systematic treatment of the geometrical aspects involved by the extensive development of the infinite dimensional systems theory. The analogies with the final dimensional case are pointed out in order te ensure a better understanding of the text.

Making a valuable contribution to the litterature devoted to infinite dimensional systems, the significance of this monograph follows from the covered topics : Invariance concepts ; System invariance concepts ; Disturbance decoupling problem ; Controlled invariance for discrete spectral system ; The disturbance decoupling problem with measurement feedback ; The disturbance decoupling problem with measurement feedback and stability. Several examples given in an appendix illustrate the basic concepts presented in this work.

The boock is recommended to researchers and post-graduate students interested in the field of system geometric theory.

Oct. Păstrăvanu

EICHENAUER C., *Transient System Analysis on a Personal Computer.* J. Wiley & Sons Inc., New York, 1988, 392 pp., ISBN 0-471-61209-x.

This book lays a systematic mathematical foundation for the computer assisted analysis of transient systems, based on a systems analysis course given at General Electric.

The first part reviews the mathematical techniques, the electrical and mechanical network elements to be used.

After consolidating the individual steps to be assimilated, several practical problems of transient systems analysis are presented.

The following chapters stress the numerical analysis principles for numerical approximation, numerical integration, matrix computation as essential tools to exploit the computer capabilities.

Exercises and a number of 28 appendices containing complete BASIC program listings for all the numerical examples in the text accompany the theoretical considerations.

The book is highly recommended to practicing engineers, senior technicians and students.

Adriana Păstrăvanu

LEWIS R. W., MORGAN K. (Ed.), *Numerical Methods in Thermal Problems.* Vol. VI, Part 1 & Part 2, Pineridge Press Ltd., Swansea, 1989, ISBN 0-906674-69-7.

These two volumes contain the papers presented at the Sixth International Conference on Numerical Methods in Thermal Problems held in Swansea during the period July 3rd — 7th, 1989. There are 169 contributions separated into the following eleven sections : Phase change problems ; Heat conduction ; Solidification and casting processes ; Natural and/or forced convection ; Radiative heat transfer ; Thermal and/or mechanical loads ; Heat and mass transfer ; Novel computational techniques ; Parallel processing ; Fire and/or combustion simulation ; Industrial and scientific applications.

This collection of carefully selected papers gives an overview of new trends in research all over the world and is addressed to engineers, mathematicians, physicists interested in applying computational techniques for the study of thermal problems.

Oct. Păstrăvanu

LEREDDE H., BIGOT H., *Normes de programmation FORTRAN 77.* INRIA Diffusion, Inst. Nat. de Recherche en Informat. et en Automat., 50 pp., ISBN 2-7261-0594-7.

Le livre présente la définition d'un sousensemble de règles pour la réalisation d'un logiciel portable en FORTRAN, norme 77.

Lorsque l'on parle de normes de programmation, elles peuvent être de différents niveaux à savoir : a) liste des instructions n'étant pas universelles ; b) normes de programmation ; c) normes de la bibliothèque MODULAD.

Ce livre se trouve à mi-chemin entre les niveaux a) et b) et malgré ses imperfections constitue une bonne base pour le programmeur.

On présente des règles concernant les éléments utilisés en FORTRAN 77, des règles directement liées aux instructions FORTRAN 77 et un détail de certains règles et compléments sur les règles.

On présente des règles qui se réfèrent aux éléments utilisés et qui interviennent dans les instructions ; les conventions d'écriture de ces instructions sont précisées.

Dans un deuxième paragraphe les différentes instructions FORTRAN 77 sont présentées. De plus, il est bien précisé lesquelles sont autorisées dans le cadre de MODULAD.

Dans le troisième paragraphe on précise les règles d'utilisation de certaines instructions.

Cristea Pal

WIESNER P., *Technologie des Elektronenstrahlschweissens.* VEB Verlag Technik, Berlin, 1989, 100 S., ISBN 3-341-00640-0.

This book deals with the possibilities of welding large workpieses by electron beams.

The first part refers shortly on the constructive principle of the electronic guns, the domain in which this method is used, the welding process. The variation of the material temperature, in depth and along the joint, is analysed.

The computation of the electron beam power takes into account the thickness of the joint and the welded materials. The optimal focussing of the beam and the influence of its transversal or longitudinal swinging for different materials in discussed. The weldability of the non- and low-alloyed steels, of the chromium-toothed rims, duplex gears is shown. The constructive solutions used for such nickel austenitic steels and of other metals is presented.

The joining technology of the complet shaped pieces, namely shafts, gears, joints, are given. The choosing method of the welding parameters for different aluminium alloys is analysed.

The last part gives examples of electron beams industrial welding, the equipment accomplished with this end in view, and the problems raised by their operation ; the working life of the solid cathods, the control of the equipments, the positioning of the pieces and the automatic supply as well as the ensuring of the joint quality.

The bibliography lists 118 titles.

M. Oprişor

BIERNSON G., *Principles of Feedback Control.* A Wiley-Interscience Publication, New York, Chichester, Brisbane, Toronto, Singapore, 1988, vol. 1, 497 pp. ; vol. 2 637 pp. ; ISBN 0-471-82167-5 (vol. 1), ISBN 0-471-50120-4 (vol. 2).

The book deals with general concepts of feedback control and related theory. The examples used in presenting this book pertain to systems controlling mechanical elements (servo-mechanisms), but the concepts are much more general and apply to all systems where the feedback-control principle is implemented.

Volume 1, entitled *Feedback System Design*, contains 7 chapters, which present theoretical and practical principles for designing feedback control systems. Volume 2, named *Advanced Control Topics*, repeats chapter 1 (Introduction) and contains chapters 8 to 15 which include digital computer simulation and studies of sample-data control sytems, AC control systems, mechanical structural dynamics, statistical analysis of random signals, radar tracking, nonlinear control and advanced feedback analysis techniques.

The first volume builds on classical frequency-response analysis techniques to develop general practical methods for designing complex multiloop control systems which are applied to DC electric-motor servos. There are also described the general time behaviour of feedback control loops, analyzed the effects of load disturbances and finally presented a detailed study of the design of a control system for positioning an optical instrument stage.

To supply a broad basis for developing control systems, the first volume is increased by the second one which covers advanced control topics. Primarily, we are given the analyses of AC-modulated signals in feedback-control systems and of sampled-data systems used in digital data processing. Because mechanical structural resonance is the primary limitation on the dynamic performance of systems that control mechanical elements, the issue of structural dynamics is introduced. Then, it is analyzed the response of a control system to a random input that is statistically characterized and its application to radar tracking. There are also investigated the effects of nonlinearities in feedback-control systems and presented advanced techniques for the analysis of stability and transient response.

The book ends with the description of a unique control system developed by the author wich represents the basis for the GCA wafer-stepping photolithography equipment for fabricating integrated circuits.

The combination of these two volumes gives a broad engineering foundation for developing feedback control systems.

Corneliu Lazăr

Tipărit la Întreprinderea Poligrafică Iaşi
sub comanda nr. 18/1990

1991 APR 17

40822

F 1503/3

BULETINUL INSTITUTULUI POLITEHNIC DIN IAŞI

Tomul XXXVI (XL)

Fasc. 3–4

Secţia III

ELECTROTEHNICĂ
ENERGETICĂ
ELECTRONICĂ
AUTOMATIZĂRI

1990

BULETINUL INSTITUTULUI POLITEHNIC DIN IAŞI

Tomul XXXVI (XL)

Fasc. 3–4

Secţia III

ELECTROTEHNICĂ
ENERGETICĂ
ELECTRONICĂ
AUTOMATIZĂRI

1990

EDITORIAL STAFF

Prof dr. ing. **VITALIE BELOUSOV** (President)

Prof. dr. doc. **D. I. MANGERON** (Honorary President)

Conf. dr. ing. **MIRCEA MANOLOVICI** (Secretary)

Conf. dr. ing. **MATEI MACOVEANU**

Prof. dr. doc. ing. **ALFRED BRAIER** (Editor)

Prof. dr. ing. **HUGO ROSMAN** (Editor)

Prof. dr. ing. **MIHAIL VOICU** (Head of the Exchange Service)

Prof. dr. **AUREL BEJANCU**

Prof. dr. ing. **VICTOR BULACOVSCHI**

Prof. dr. ing. **MIHAI LUCANU**

Prof. dr. ing. **SPIRIDON CREȚU**

Prof. dr. ing. **ADRIAN RADU**

Conf. dr. ing. **AURELIA GRIGORIU**

BULETINUL INSTITUTULUI POLITEHNIC DIN IAŞI
BULLETIN OF THE POLYTECHNIC INSTITUTE OF JASSY
ИЗВЕСТИЯ ЯССКОГО ПОЛИТЕХНИЧЕСКОГО ИНСТИТУТА
Tomul XXXVI (XL), Fasc. 3–4 1990

Secţia III

ELECTROTEHNICĂ. ENERGETICĂ. ELECTRONICĂ. AUTOMATIZĂRI

S U M A R

Pag.

C. PETRESCU, Studiul cîmpului magnetic creat de un tub dielectric avînd o mişcare de rotaţie uniformă într-un cîmp electric transversal şi omogen (engl., rez. rom.) 1
H. ROSMAN, Rezonanţa globală la porţile de acces ale unui cuadripol general, liniar, neautonom, în regim permanent armonic (franc., rez. rom.) 7
EM.-CR. SAVIN, Unele observaţii privind teorema compensaţiei (engl., rez. rom.) 15
T. MARCU şi O. PĂSTRĂVANU, Diagnoza sistemelor automate prin clasificarea liniară a estimaţiilor modelelor (engl., rez. rom.) 21
C. MĂRCUŢĂ şi L. GORAŞ, Traductor numeric de deplasare bazat pe un nou tip de convertor inductanţă—perioadă de timp (engl., rez. rom.) 27
A. CREŢU, R. COCIU, E. CREŢU şi L. COCIU, Metodă de zero pentru măsurarea parametrilor bobinelor şi condensatoarelor cu pierderi (franc., rez. rom.) . . 33
D. BELAUS şi D. ZAMFIR, Metodă şi relaţie de calcul pentru măsurarea puterii active, cu wattmetru cu bobină amper şuntată (franc., rez. rom.) 39
M. CREŢU, L. BRENIUC şi C. SĂRMĂŞANU, Asupra măsurării numerice a razei macaralelor cu braţ orizontal (franc., rez. rom.) 47
L. BRENIUC, M. CREŢU şi C. SĂRMĂŞANU, Asupra estimării sarcinii admisibile la cîrlig pentru macaralele cu braţ orizontal (franc., rez. rom.) 53
I. ANDRONE şi V. BAHRIN, Posibilitatea de funcţionare în autocascadă a motorului asincron cu rotorul în colivie (engl., rez. rom.) 57
N. D. ALEXANDRU şi I. F. MASHEH, Sinteza circuitului codor CMI (engl., rez. rom.) 65
C. GÎŢLAN şi D. ALEXA, Circuit de comandă pentru motorul de circuit continuu cu conţinut redus în armonici superioare la intrare (engl., rez. rom.) 69
C. PAL şi D. ZAMFIR, Asupra unei metode de generare a graficelor de viteză pentru motoarele pas cu pas din cadrul sistemelor de acţionare (germ., rez. rom.) 73
R. OLÁH, Contribuţii la studiul comportării la impuls a prizelor de pămînt în soluri cu rezistivitate de valoare ridicată (germ., rez. rom.) 81
V. ALEXANDRESCU, R. SFICHI, GH. CÂRŢINĂ, E. VOINEA şi V. ŢĂRANU, Un algoritm pentru calculul regimului permanent al generatorului asincron (franc., rez. rom.) 87
GH. CÂRŢINĂ, V. ALEXANDRESCU şi E. VOINEA, Problema energiei reactive în reţelele electrice cu microhidrocentrale (franc., rez. rom.) 93
RECENZII 97

BULETINUL INSTITUTULUI POLITEHNIC DIN IAŞI
BULLETIN OF THE POLYTECHNIC INSTITUTE OF JASSY
ИЗВЕСТИЯ ЯССКОГО ПОЛИТЕХНИЧЕСКОГО ИНСТИТУТА
Tome XXXVI (XL), Fasc. 3–4 1990

Section III

ELECTROTECHNICS. ENERGETICS. ELECTRONICS. AUTOMATION

CONTENTS

Pp.

C. PETRESCU, Study of the Magnetic Fields Created by a Dielectric Tube Rotating Uniformly in a Transversal Homogeneous Electric Field (English, Romanian summary) 1

H. ROSMAN, La résonance globale aux portes d'accès d'un quadripôle général, linéaire, nonautonome, en régime permanent harmonique (Freanch, Romanian summary) 7

EM.-CR. SAVIN, Some Observations concerning the Compensation Theorem (English, Romanian Summary) 15

T. MARCU and O. PĂSTRĂVANU, Control Systems Diagnosis Via Linear Classification of Model Estimations (English, Romanian summary) 21

C. MĂRCUŢĂ and. L. GORAŞ, Numeric Displacement Transducer Using a New Type Inductance-to-Time-Period Converter (English, Romanian summary) 27

A. CREŢU, R. COCIU, E. CREŢU et L. COCIU, Méthode de zéro pour la mesure des paramètres des bobines et des condensateurs linéaires à pertes (French, Romanian summary) 33

D. BELAUS et D. ZAMFIR, Méthode et relation de calcul pour mesurer la puissance active avec un wattmètre à bobine de courant shuntée (French, Romanian summary) 39

M. CREŢU, L. BRENIUC et C. SĂRMĂŞANU, Sur la mesure numérique du rayon des grues à volée horizontale (French, Romanian summary) 47

L. BRENIUC, M. CREŢU et C. SĂRMĂŞANU, Sur l'estimation de la charge admissible au crochet de la grue à volée horizontale (French, Romanian summary) 53

I. ANDRONE and V. BAHRIN, The Possibility of the Self-Cascaded Machine Running of a Squirrel-Cage Induction Motor (English, Romanian summary) 57

N.D. ALEXANDRU and I. F. MASHEH, Synthesis of a CMI Coder (English, Romanian summary) 65

C. GÎTLAN and D. ALEXA, Three-Phase Fully Controlled Bridge Circuit with Low Content of Higher Harmonics at the Input, for D.C. Motor Drive (English, Romanian summary) 69

C. PAL und D. ZAMFIR, Über eine Methode der Entwerfung der Geschwindigkeitsdiagramme für Schrittmotoren im Rahmen eines Antriebssystems (German, Romanian summary) 73

R. OLÁH, Beiträge zum Studium des Verhaltens der Erdungen in Böden mit erhöhtem Widerstand bei Impulsen (German, Romanian summary) 81

V. ALEXANDRESCU, R. SFICHI, GH. CÂRŢINĂ, E. VOINEA et V. ŢĂRANU, Un algorithme de calcul du régime permanent du générateur asynchrone (French, Romanian summary) 87

GH. CÂRŢINĂ, V. ALEXANDRESCU et E. VOINEA, Le problème de l'énergie réactive dans les réseaux électriques avec des microhydrocentrales (French, Romanian summary) 93

BOOK REVIEWS 97

BULETINUL INSTITUTULUI POLITEHNIC DIN IAŞI
Tomul XXXVI (XL), Fasc. 3—4, 1990
Secţia III
ELECTROTEHNICĂ. ENERGETICĂ. ELECTRONICĂ. AUTOMATIZĂRI

D.C. 538.12 ; 537.226

STUDY OF THE MAGNETIC FIELD CREATED BY A DIELECTRIC TUBE ROTATING UNIFORMLY IN A TRANSVERSAL HOMOGENEOUS ELECTRIC FIELD

BY

CAMELIA PETRESCU

1. Introduction

In a previous paper [1], the magnetic field created by a dielectric tube moving uniformly in axial direction in a transversal homogeneous electric field was studied. In what follows the study of the magnetic field produced by the tube rotating in the same electric field is effectuated. The length of the tube being large with respect to its radius, the problem has a translational symmetry.

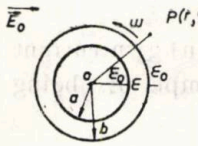

Fig. 1

In the Fig. 1 is represented a cross-section in the dielectric tube. The electric field $\bar{E}_0$ is homogeneous and stationary before the tube is placed in this one and is still homogeneous at infinity in the presence of the tube.

The dielectric tube is rotating uniformly, with constant angular velocity ω around the axis of the tube.

2. Mathematical Description of the Problem

Presence of moving bodies generally modifies the Maxwell-Hertz equations, so that the electric and magnetic field intensities and flux densities in a reference system S, expressed as functions of the same vectors in another reference system S_0, which has velocity $\bar{v}$ with respect to S, are given by the following relations [2] :

$$
\left\{
\begin{aligned}
&\bar{E} = \gamma_{HC}(\bar{E}_0 - \bar{v} \times \bar{B}_0) - \frac{\gamma_{HC}-1}{v^2}\,\bar{v}(\bar{E}_0\bar{v}),\\
&\bar{H} = \gamma_{HC}(H_0 + \bar{v} \times \bar{D}_0) - \frac{\gamma_{HC}-1}{v^2}\,\bar{v}(\bar{H}_0\bar{v}),\\
&\bar{D} = \gamma_{HC}\left(\bar{D}_0 - \frac{1}{c^2}\,\bar{v} \times \bar{H}_0\right) - \frac{\gamma_{HC}-1}{v^2}\,\bar{v}(\bar{D}_0\bar{v}),\\
&\bar{B} = \gamma_{HC}\left(\bar{B}_0 + \frac{1}{c^2}\,\bar{v} \times \bar{E}_0\right) - \frac{\gamma_{HC}-1}{v^2}\,(\bar{B}_0\bar{v})\bar{v},
\end{aligned}
\right. \tag{1}
$$

where

$$\gamma_{HC}=1+\frac{v^2}{c^2}+\frac{v^4}{c^4}+\ldots+\frac{v^{2k}}{c^{2k}}, \qquad k>0, \qquad c=\frac{1}{\sqrt{\mu\varepsilon}}.$$

In this exemple the moving system has a velocity $v=\omega r$ less than 1 m/s so that $v^2/c^2 \ll 1$ (ex: for $\varepsilon_r=4$, $c=150\,000$) Km/s, and relations (1) become:

$$(2) \qquad \begin{cases} \bar{E}=\bar{E}_0-\bar{v}\times\bar{B}_0, & \bar{H}=\bar{H}_0+\bar{v}\times\bar{D}_0, \\ \bar{D}=\bar{D}_0-\dfrac{1}{c^2}\,\bar{v}\times\bar{H}_0, & \bar{B}=\bar{B}_0+\dfrac{1}{c^2}\,\bar{v}\times\bar{E}_0, \end{cases}$$

which means the Maxwell—Hertz equations hold. It follows that the electromagnetic field is quasi-stationary and rot $\bar{E}=0$; potential V satisfies Laplace's equation, $\Delta V=0$.

The solution of this equation, determined in [1], is:

$$V_2=\left(A_2 r+\frac{B_2}{r}\right)\cos\varphi.$$

According to the local form of the magnetic circuit law:

$$(3) \qquad \operatorname{rot}\bar{H}=\varepsilon\frac{\partial\bar{E}}{\partial t}+\operatorname{rot}(\bar{D}\times\bar{v});$$

the only source for the existence of the magnetic field is the Röntgen current with the experimental density $J_R^{(ex)}$ (in the considered example $\bar{E}_0$ being stationary):

$$(4) \qquad \begin{aligned} \bar{J}_R^{(ex)}&=\operatorname{rot}(\bar{P}\times\bar{v})=\operatorname{rot}[(P_r\bar{e}_r+P_\varphi\bar{e}_\varphi)\times v\bar{e}_\varphi]=\operatorname{rot}(P_r\omega r\bar{k})= \\ &=\omega\frac{\partial P_r}{\partial\varphi}\,\bar{e}_r-\omega\frac{\partial(rP_r)}{\partial r}\,\bar{e}_\varphi, \end{aligned}$$

where $\bar{J}_R^{(ex)}\neq 0$ only for $r\in[a, b]$, in the dielectric material.

The radial component of polarization $\bar{P}$ is:

$$(5) \qquad P_r=(\varepsilon-\varepsilon_0)E_r=-(\varepsilon-\varepsilon_0)\left(A_2-\frac{B_2}{r^2}\right)\cos\varphi,$$

where A_2 and B_2 are given by the following expressions [1]:

$$(6) \qquad A_2=\frac{2E_0b^2(\varepsilon_r+1)}{a^2(1-\varepsilon_r)^2-b^2(1+\varepsilon_r)^2}, \qquad B_2=\frac{2E_0a^2b^2(\varepsilon_r-1)}{a^2(1-\varepsilon_r)^2-b^2(1+\varepsilon_r)^2}.$$

The Röntgen current density is then:

$$(7) \qquad \bar{J}_R^{(ex)}=\omega(\varepsilon-\varepsilon_0)\left[\left(A_2-\frac{B_2}{r^2}\right)\sin\varphi\cdot\bar{e}_r+\left(A_2+\frac{B^2}{r^2}\right)\cos\varphi\cdot\bar{e}_\varphi\right].$$

The sudden variation of the polarization on the surfaces $r=a$ and $r=b$ determines two surface Röntgen currents having the following densities:

$$(8)\quad \begin{cases} \bar{J}_{lR_a}^{(ex)} = \mathrm{rot}_s(\bar{P}\times\bar{v}) = \bar{e}_r \times [(P_r\bar{e}_r + P_\varphi \bar{e}_\varphi)\times \omega a \bar{e}_\varphi] = -\omega a P_r(a)\bar{e}_\varphi, \\ \bar{J}_{lR_b}^{(ex)} = -\bar{e}_r \times [(P_r\bar{e}_r + P_\varphi \bar{e}_\varphi)\times \omega b \bar{e}_\varphi] = \omega b P_r(b)\bar{e}_\varphi . \end{cases}$$

Using (5), the expressions for the Röntgen surface current densities become:

$$(9)\quad \begin{cases} \bar{J}_{lR_a}^{(ex)} = \omega a(\varepsilon-\varepsilon_0)\left(A_2 - \dfrac{B_2}{a^2}\right)\cos\varphi\cdot\bar{e}_\varphi , \\ \bar{J}_{lR_b}^{(ex)} = \omega b(\varepsilon_0-\varepsilon)\left(A_2 - \dfrac{B_2}{b^2}\right)\cos\varphi\cdot\bar{e}_\varphi . \end{cases}$$

In order to compute the magnetic field created by the rotating tube, the magnetic vector potential $\bar{A}$ is used. In this exemple $\bar{A}$ satisfies Poisson's equation:

$$\Delta\bar{A} = -\mu_0 \bar{J}_R^{(ex)},$$

or:

$$(10)\quad \Delta A_H = -\bar{J}_R^{(ex)},$$

where $A_H = A/\mu_0$.

In infinite space the solution for (10) in a problem with translational symmetry, is [3]:

$$(11)\quad \bar{A}_H = \frac{1}{2\pi}\left[\int_{\mathcal{T}_\infty} \bar{J}_R \ln\frac{1}{R}\,dA' + \int_C \bar{J}_{lR}\ln\frac{1}{R}\,ds\right],$$

where $\bar{J}_R$ is the volume Röntgen current density, $\bar{J}_{lR}$ — thesurface Röntgen current density, and R — the distance from element dA' or ds to the point where A_H is computed.

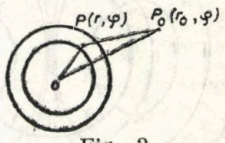

Fig. 2

Following the notations from Fig. 2:

$$R = \sqrt{r^2 + r_0^2 - 2rr_0\cos(\varphi-\varphi_0)}\,.$$

Using expressions (4) and (9) for the current densities $\bar{J}_R^{(ex)}$ and $\bar{J}_{lR}^{(ex)}$ relation (11) lead to:

$$\begin{aligned} \bar{A}_H = \frac{1}{2\pi}\Bigg\{ & \int_a^b dr\int_0^{2\pi}\omega(\varepsilon-\varepsilon_0)\left(A_2 - \frac{B_2}{r^2}\right)\sin\varphi\,.\ln\frac{1}{\sqrt{r^2+r_0^2-2rr_0\cos(\varphi-\varphi_0)}}\,r\,d\varphi\cdot\bar{e}_r + \\ & + \int_a^b dr\int_0^{2\pi}\omega(\varepsilon-\varepsilon_0)\left(A_2 + \frac{B_2}{r^2}\right)\cos\varphi\,.\ln\frac{1}{\sqrt{r^2+r_0^2-2rr_0\cos(\varphi-\varphi_0)}}\,r\,d\varphi\cdot\bar{e}_\varphi + \\ & + \omega a(\varepsilon-\varepsilon_0)\int_0^{2\pi}\left(A_2 - \frac{B_2}{a^2}\right)\cos\varphi\,.\ln\frac{1}{\sqrt{a^2+r_0^2-2ar_0\cos(\varphi-\varphi_0)}}\,a\,d\varphi.\bar{e}_\varphi + \\ & + \omega b(\varepsilon_0-\varepsilon)\left(A_2 - \frac{B_2}{b^2}\right)\int_0^{2\pi}\cos\varphi\,.\ln\frac{1}{\sqrt{b^2+r_0^2-2br_0\cos(\varphi-\varphi_0)}}\,b\,d\varphi\cdot\bar{e}_\varphi\Bigg\}. \end{aligned} \quad (12)$$

Once the magnetic vector potential $\bar{A}$ is known, the magnetic field intensity is computed using relation :

$$\bar{H}=\text{rot}\ \bar{A}_H , \tag{13}$$

which means, in polar coordinates,

$$\bar{H}=\text{rot}\ \bar{A}_H=\left[\frac{1}{r}\cdot\frac{\partial}{\partial r}\ (rA_{H\varphi})-\frac{1}{r}\cdot\frac{\partial A_{Hr}}{\partial\varphi}\right]\bar{k}. \tag{14}$$

3. Results and Numerical Calculations

Direct integration of relation (12) is difficult so that a numerical integration method will be used. The Simpson method is adapted in order to process a double numerical integration. This algoritm gives acceptable precission when the BASIC mathematical library is used giving aprox. 6 precise digits when the intervals $[a, b]$ and $[0, 2\pi]$ are divided in 20 subintervals.

Potential vector $\bar{A}_H$ is computed in the nodes of a net having the step $h_r=1$ cm in the direction $\bar{e}_r$ and $h_\varphi=\pi/6$ in direction $\bar{e}_\varphi$.

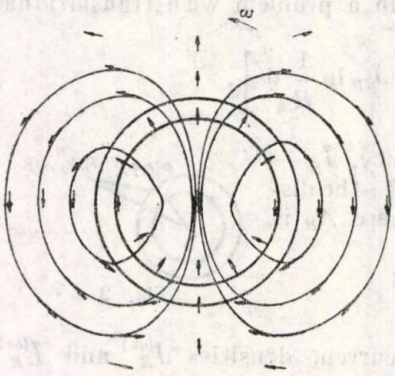

Fig. 3

The numerical values used in computations were :

$$E_0=20\,000\ \text{V/cm}\ ;\quad a=2.25\ \text{cm}\ ;$$

$$b=2.75\ \text{cm}\ ;\quad \varepsilon_r=4\ ;\quad \omega=5\ \text{rad/s}.$$

The results of the computation were used in order to draw the spectrum of the field $\bar{A}_H=A_{Hr}\bar{e}_r+A_{H\varphi}\bar{e}_\varphi$ (Fig. 3).

The numerical results show that :

a) The magnetic vector potential field lines follow the Röntgen current density ones.

b) The spectrum for $\bar{A}_H$ in this problem is similar to that of $\bar{H}$ in the exemple presented in [1].

c) A_H modulus varies periodicaly with respect to φ, the period being π ; A_H has maximum values for $\varphi=0$ and $\varphi=\pi$ and minimum values for $\varphi=\pi/2$ and $\varphi=3\pi/2$ (for $r=r_0>b$). If $r=r_0<a$ then the maximum values are attained for $\varphi=\pi/2$ and $\varphi=3\pi/2$ and the minimum ones for $\varphi=0$ and $\varphi=\pi$ (Fig. 4 *a*).

d) A_H modulus has a maximum value for $r=b$ (when $\varphi=\varphi_0=$const.) and decreases for $r>b$ (Fig. 4 *b*).

In order to compute the magnetic field intensity a numerical derivation is used. The derivatives in relation (14) are expressed by means of regressive finite differences which give the following expression for $\bar{H}$:

$$\bar{H}(r_0, \varphi_0) = \frac{1}{r_0}\left[\frac{(r_0+\Delta r)A_{H\varphi}(r_0+\Delta r, \varphi_0) - r_0 A_{H\varphi}(r_0, \varphi_0)}{\Delta r} - \right.$$

$$\left. - \frac{A_{H\varphi}(r_0, \varphi_0+\Delta\varphi) - A_{Hr}(r_0, \varphi_0)}{\Delta\varphi}\right]\bar{k}. \tag{15}$$

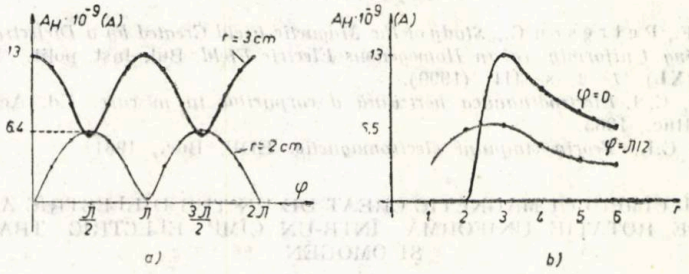

Fig. 4

Fig. 5 *a* represents the magnetic field intensity H versus φ for $r=2$ cm and $r=3$ cm respectively ; Fig. 5 *b* represents H versus r for $\varphi=0$. This figure shows that H is periodical with respect to $\varphi(T=2\pi)$ having maximum values for $\varphi=0$ and $\varphi=\pi$, minimum values for $\varphi=\pi/2$ and $3\pi/2$. A rapid decrease of H with respect to r is observed for $r>b$ (Fig. 5 *a*).

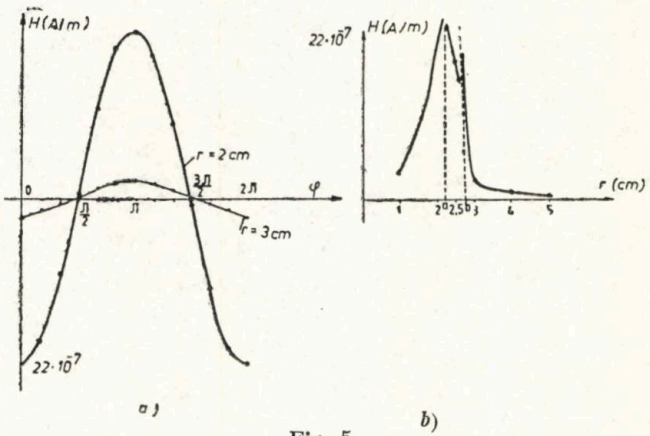

Fig. 5

4. Conclusions

If the results obtained in this paper are compared with those from [1] may be drawn the conclusion that the magnetic field intensity produced by a dielectric tube rotating with angular velocity $\omega=5$ rad/s is more than 280 times greater than that produced by same tube moving in axial direction with the velocity $v=2$ m/s (inside the tube), all the other conditions being unchanged. However in the exemple presented in this paper, $\bar{H}$ has only the axial component, while in [1] $\bar{H}$ has only the transversal ones.

Besides, the magnetic field is concentrated inside the tube in the rotating problem and outside the tube ($r \in [b, 2b]$) in the translating tube problem.

Received, April 3, 1990

Polytechnic Institute, Jassy,
Department of Electrotechnics

REFERENCES

1. Trifan F., Petrescu C., *Study of the Magnetic Field Created by a Dielectric Tube Moving Uniformly in an Homogenous Electric Field.* Bul. Inst. polit., Iaşi, **XXXVI (XL)**, *1—2*, s. III (1990).
2. Mocanu, C. I. *Electrodinamica hertziană a corpurilor în mişcare.* Ed. Acad., R.S.R., Buc., 1985.
3. Mocanu C.I., *Teoria cîmpului electromagnetic.* EDP, Buc., 1981.

STUDIUL CÎMPULUI MAGNETIC CREAT DE UN TUB DIELECTRIC AVÎND O MIŞCARE DE ROTAŢIE UNIFORMĂ ÎNTR-UN CÎMP ELECTRIC TRANSVERSAL ŞI OMOGEN

(Rezumat)

Se determină expresia densităţii curentului Röntgen creat de un tub dielectric ce se roteşte uniform într-un cîmp electric transversal şi omogen şi prin integrare numerică se determină potenţialul vector al cîmpului magnetic şi apoi prin derivare numerică se determină intensitatea cîmpului magnetic şi spectrul său.

BULETINUL INSTITUTULUI POLITEHNIC DIN IAŞI
Tomul XXXVI (XL), Fasc. 3—4, 1990
Secţia III
ELECTROTEHNICĂ. ENERGETICĂ. ELECTRONICĂ. AUTOMATIZĂRI

C.D. 621.392.5

LA RÉSONANCE GLOBALE AUX PORTES D'ACCÈS D'UN QUADRIPÔLE GÉNÉRAL, LINÉAIRE, NONAUTONOME, EN RÉGIME PERMANENT HARMONIQUE

PAR

HUGO ROSMAN

1. Introduction

On a denommé, dans une Note précédente [1], par *résonance multipolaire globale*, un nouveau concept qui caractérise les régimes permanents harmoniques de fonctionnement d'un multipôle linéaire, nonautonome, dans lesquels la relation

$$\sum_{k=1}^{n} Q_k = 0, \tag{1}$$

est satisfaite, où Q_k représente la puissance réactive échangée par le multipôle avec l'extérieur à la porte k et n — le nombre des portes. Dans la Note ci-dessus mentionnée on a étudié en détail *la résonance quadripôlaire globale*, en considérant le cas des biportes linéaires nonautonomes.

Le but de cette Note est d'élargir les résultats de cette étude en considérant le cas de quadripôles généraux linéaires nonautonomes (QGLN) qui fonctionnent également en régime permanent harmonique.

Les équations d'un tel quadripôle ont la forme connue [2], [3] :

$$\begin{bmatrix} \underline{U}_1 \\ \underline{I}_1 \\ \underline{U}_3 \end{bmatrix} = \begin{bmatrix} \underline{A}_{11} & \underline{A}_{12} & \underline{A}_{13} \\ \underline{A}_{21} & \underline{A}_{22} & \underline{A}_{23} \\ \underline{A}_{31} & \underline{A}_{32} & \underline{A}_{33} \end{bmatrix} \begin{bmatrix} \underline{U}_2 \\ \underline{I}_2 \\ \underline{I}_3 \end{bmatrix}, \tag{2}$$

où $\underline{A}_{ij}$, $(i, j = 1, 2, 3)$, sont les paramètres fondamentaux du QGLN (Fig. 1).

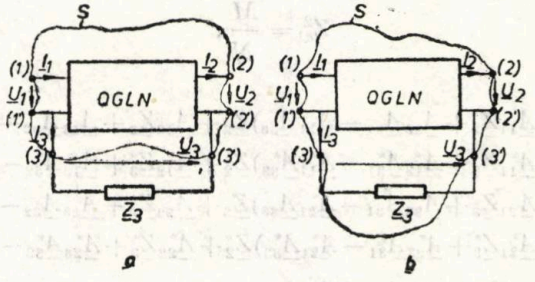

Fig. 1

2. La résonance globale des quadripôles généraux (RGQG)

On peut concevoir l'existence de deux types différents de tels régimes selon que la surface fermée dont on applique le théorème de l'énergie électromagnétique renferme, à l'intérieur de celle-ci, où ne renferme pas l'impédance $\underline{Z}_3$. En régime permanent harmonique ce théorème permet à évaluer les puissances active et réactive échangées par le quadripôle avec l'extérieur à l'aide de la relation :

$$\iint_{S'} \underline{\mathbf{S}}\, \mathbf{dA}_{\text{int}} = P + \mathrm{j}Q, \tag{3}$$

où $\underline{\mathbf{S}} = \underline{\mathbf{E}} \times \underline{\mathbf{H}}^*$ représente l'expression en complexe du vecteur de P o y n t i n g et $\mathbf{dA}_{\text{int}}$ — l'élément vectoriel d'aire ayant le sens positif de la normale orienté vers l'intérieur de la surface S'.

Dans ce qui suit on va denommer avec RGQG de type *a* la résonance globale qui correspond au cas représenté dans la Fig. 1 *a* et avec RGQG de type *b* celle se référant à la situation considérée dans la Fig. 1 *b*.

3. Le diagramme de l'impédance du récepteur dans les regimes RGQG

On peut déterminer la puissance reactive échangée avec l'extérieur à la porte d'entrée à l'aide de la relation :

$$Q_1 = \frac{X_{e1}}{Z_{e1}^2}\, U_1^2, \tag{4}$$

où

$$\underline{Z}_{e1} \triangleq \frac{\underline{U}_1}{\underline{I}_1} = R_{e1i} + \mathrm{j}X_{e1} = \frac{(\underline{A}_{11}\underline{Z}_3 + \underline{A}_{13}\underline{A}_{31} - \underline{A}_{11}\underline{A}_{33})\underline{Z}_2 + \underline{A}_{12}\underline{Z}_3 + \underline{A}_{13}\underline{A}_{32} - \underline{A}_{12}\underline{A}_{33}}{(\underline{A}_{21}\underline{Z}_3 + \underline{A}_{23}\underline{A}_{31} - \underline{A}_{21}\underline{A}_{33})\underline{Z}_2 + \underline{A}_{22}\underline{Z}_3 + \underline{A}_{23}\underline{Z}_{32} - \underline{A}_{22}\underline{A}_{33}} \tag{5}$$

représente l'impédance équivalente du QGLN à la porte d'entrée et

$$\underline{Z}_2 \triangleq \frac{\underline{U}_2}{\underline{I}_2} = R_2 + \mathrm{j}X_2, \quad \underline{Z}_3 \triangleq \frac{\underline{U}_3}{\underline{I}_3} = R_3 + \mathrm{j}X_3. \tag{6}$$

Évidemment afin d'établir l'expression (5) on a tenu compte des équations (2) du QGLN.

Vu la relation (5) il s'ensuit que

$$Z_{e1}^2 = \frac{M}{N}, \tag{7}$$

où

$$\begin{aligned} M &= [(\underline{A}_{11}\underline{Z}_3 + \underline{A}_{13}\underline{A}_{31} - \underline{A}_{11}\underline{A}_{33})\underline{Z}_2 + \underline{A}_{12}\underline{Z}_3 + \underline{A}_{13}\underline{A}_{32} - \underline{A}_{12}\underline{A}_{33}] \times \\ &\times [(\underline{A}_{11}^*\underline{Z}_3^* + \underline{A}_{13}^*\underline{A}_{31}^* - \underline{A}_{11}^*\underline{A}_{33}^*)\underline{Z}_2^* + \underline{A}_{12}^*\underline{Z}_3^* + \underline{A}_{13}^*\underline{A}_{32}^* - \underline{A}_{12}^*\underline{A}_{33}^*], \\ N &= [(\underline{A}_{21}\underline{Z}_3 + \underline{A}_{23}\underline{A}_{31} - \underline{A}_{21}\underline{A}_{33})\underline{Z}_2 + \underline{A}_{22}\underline{Z}_3 + \underline{A}_{23}\underline{A}_{32} - \underline{A}_{22}\underline{A}_{33}] \times \\ &\times [(\underline{A}_{21}^*\underline{Z}_3^* + \underline{A}_{23}^*\underline{A}_{31}^* - \underline{A}_{21}^*\underline{A}_{33}^*)\underline{Z}_2^* + \underline{A}_{22}^*\underline{Z}_3^* + \underline{A}_{23}^*\underline{A}_{32}^* - \underline{A}_{22}^*\underline{A}_{33}^*]. \end{aligned} \tag{8}$$

Tous calculs effectués (v. l'Annexe) on obtient :

$$(9)\qquad M=a_1(R_3, X_3)(R_2^2+X_2^2)+a_2(R_3, X_3)R_2+a_3(R_3, X_3)X_2+a_4(R_3, X_3),$$

avec

$$a_1(R_3, X_3)=A_{11}^2\left\{\left[R_3-\mathcal{R}e\left(\frac{\underline{A}_{11}\underline{A}_{33}-\underline{A}_{13}\underline{A}_{31}}{\underline{A}_{11}}\right)\right]^2+\right.$$
$$\left.+\left[X_3+\mathcal{I}m\left(\frac{\underline{A}_{11}\underline{A}_{33}-\underline{A}_{13}\underline{A}_{31}}{\underline{A}_{11}}\right)\right]^2\right\}\geqslant 0,$$

$$a_2(R_3, X_3)=2\mathcal{R}e(\underline{A}_{11}^*\underline{A}_{12})(R_3^2+X_3^2)+2\{-2\mathcal{R}e(\underline{A}_{33})\mathcal{R}e(\underline{A}_{11}^*\underline{A}_{12})+$$
$$+\mathcal{R}e[\underline{A}_{13}(\underline{A}_{11}^*\underline{A}_{32}+\underline{A}_{12}^*\underline{A}_{31})]\}R_3+2\{-2\mathcal{I}m(\underline{A}_{33})\mathcal{R}e(\underline{A}_{11}^*\underline{A}_{12})+$$
$$+\mathcal{I}m[\underline{A}_{13}(\underline{A}_{11}^*\underline{A}_{32}+\underline{A}_{12}^*\underline{A}_{31})]\}X_3+2\mathcal{R}e(\underline{A}_{13}\underline{A}_{32}-\underline{A}_{12}\underline{A}_{33})\times$$
$$\times(\underline{A}_{13}^*\underline{A}_{31}^*-\underline{A}_{11}^*\underline{A}_{33}^*),\qquad(10)$$

$$a_3(R_3, X_3)=2\mathcal{I}m(\underline{A}_{11}^*\underline{A}_{12})(R_3^2+X_3^2)+2\{2\mathcal{R}e(\underline{A}_{33})\mathcal{I}m(\underline{A}_{11}^*\underline{A}_{12})+$$
$$+\mathcal{I}m[\underline{A}_{13}(\underline{A}_{11}^*\underline{A}_{32}-\underline{A}_{12}^*\underline{A}_{31})]\}R_3+2\{2\mathcal{I}m(\underline{A}_{33})\mathcal{I}m(\underline{A}_{11}^*\underline{A}_{12})+$$
$$+\mathcal{R}e[\underline{A}_{13}(\underline{A}_{11}^*\underline{A}_{32}-\underline{A}_{12}^*\underline{A}_{31})]\}X_3+2\mathcal{I}m(\underline{A}_{13}\underline{A}_{32}-\underline{A}_{12}\underline{A}_{33})\times$$
$$\times(\underline{A}_{13}^*\underline{A}_{31}^*-\underline{A}_{11}^*\underline{A}_{33}^*),$$

$$a_4(R_3, X_3)=A_{12}^2\left\{\left[R_3-\mathcal{R}e\left(\frac{\underline{A}_{12}\underline{A}_{33}-\underline{A}_{13}\underline{A}_{31}}{\underline{A}_{12}}\right)\right]^2+\right.$$
$$\left.+\left[X_3+\mathcal{I}m\left(\frac{\underline{A}_{12}\underline{A}_{33}-\underline{A}_{13}\underline{A}_{31}}{\underline{A}_{12}}\right)\right]^2\right\}\geqslant 0.$$

Quant à X_{e1}, sa expression a été obtenue dans une Note précédente [5] à savoir :

$$(11)\qquad X_{e1}=\frac{L}{N},$$

où

$$(12)\qquad L=b_1(R_3, X_3)(R_2^2+X_2^2)+b_2(R_3, X_3)R_2+b_3(R_3, X_3)X_2+b_4(R_3, X_3),$$

avec

$$b_1(R_3, X_3)=\mathcal{I}m(\underline{A}_{11}\underline{A}_{21}^*)(R_3^2+X_3^2)+\{\mathcal{I}m[\underline{A}_{31}(\underline{A}_{13}\underline{A}_{21}^*-\underline{A}_{11}^*\underline{A}_{23})]-$$
$$-2\mathcal{R}e(\underline{A}_{33})\mathcal{I}m(\underline{A}_{11}\underline{A}_{21}^*)\}R_3-\{\mathcal{R}e[\underline{A}_{31}(\underline{A}_{13}\underline{A}_{21}^*-\underline{A}_{11}^*\underline{A}_{23})]+$$
$$+2\mathcal{I}m(\underline{A}_{33})\mathcal{I}m(\underline{A}_{11}\underline{A}_{21}^*)\}X_3+\mathcal{I}m(\underline{A}_{13}\underline{A}_{31}-\underline{A}_{11}\underline{A}_{23})\times$$
$$\times(\underline{A}_{23}^*\underline{A}_{31}^*-\underline{A}_{21}^*\underline{A}_{33}^*),$$

$$b_2(R_3, X_3)=\mathcal{I}m(\underline{A}_{11}\underline{A}_{22}^*+\underline{A}_{12}\underline{A}_{21}^*)(R_3^2+X_3^2)+\{-2\mathcal{R}e(\underline{A}_{33})\mathcal{I}m(\underline{A}_{11}\underline{A}_{22}^*+$$
$$+\underline{A}_{12}\underline{A}_{21}^*)+\mathcal{I}m[\underline{A}_{13}(\underline{A}_{21}^*\underline{A}_{32}+\underline{A}_{22}^*\underline{A}_{31})-\underline{A}_{23}(\underline{A}_{11}^*\underline{A}_{32}+\underline{A}_{12}^*\underline{A}_{31})]\}R_3-$$
$$-\{2\mathcal{I}m(\underline{A}_{33})\mathcal{I}m(\underline{A}_{11}\underline{A}_{22}^*+\underline{A}_{12}\underline{A}_{21}^*)+\mathcal{R}e[\underline{A}_{13}(\underline{A}_{21}^*\underline{A}_{32}+\underline{A}_{22}^*\underline{A}_{31})-$$

$$-\underline{A}_{23}(\underline{A}^*_{11}\underline{A}_{32}+\underline{A}^*_{12}\underline{A}_{31})]\}X_3+2\mathcal{R}e(\underline{A}_{31}\underline{A}^*_{32})\mathcal{I}m(\underline{A}_{13}\underline{A}^*_{23})-$$

$$-\mathcal{I}m[\underline{A}_{23}\underline{A}^*_{31}(\underline{A}_{12}\underline{A}^*_{23}-\underline{A}^*_{13}\underline{A}_{22})-\underline{A}_{32}\underline{A}^*_{33}(\underline{A}^*_{11}A_{23}-\underline{A}_{13}\underline{A}^*_{21})]+$$

$$+A^2_{33}\mathcal{I}m(\underline{A}_{11}\underline{A}^*_{22}+\underline{A}_{12}\underline{A}^*_{21}),$$

(13)
$$b_3(R_3, X_3)=\mathcal{R}e(\underline{A}_{11}\underline{A}^*_{22}-\underline{A}_{12}\underline{A}^*_{21})(R^2_3+X^2_3)+\{2\mathcal{R}e(\underline{A}_{33})\mathcal{R}e(\underline{A}_{11}\underline{A}^*_{22}-$$

$$-\underline{A}_{12}\underline{A}^*_{21})+\mathcal{R}e[\underline{A}_{13}(\underline{A}^*_{21}\underline{A}_{32}-\underline{A}^*_{22}\underline{A}_{31})-\underline{A}_{23}(\underline{A}^*_{11}\underline{A}_{32}-\underline{A}^*_{12}\underline{A}_{31})]\}R_3-$$

$$-\{2\mathcal{R}e(\underline{A}_{33})\mathcal{I}m(\underline{A}_{11}\underline{A}^*_{22}-\underline{A}_{12}\underline{A}^*_{21})+\mathcal{I}m[\underline{A}_{13}(\underline{A}^*_{21}\underline{A}_{32}-\underline{A}^*_{22}\underline{A}_{31})-$$

$$-\underline{A}_{23}(\underline{A}^*_{11}\underline{A}_{32}-\underline{A}^*_{12}\underline{A}_{31})]\}X_3+2\mathcal{I}m(\underline{A}_{13}\underline{A}^*_{23})\mathcal{I}m(\underline{A}_{31}\underline{A}^*_{32})+$$

$$+\mathcal{R}e[\underline{A}^*_{31}\underline{A}_{33}(\underline{A}_{12}\underline{A}^*_{23}-\underline{A}^*_{13}\underline{A}_{22})-\underline{A}_{32}\underline{A}^*_{33}(\underline{A}^*_{11}\underline{A}_{23}-\underline{A}_{13}\underline{A}^*_{21})]-$$

$$-A^2_{33}\mathcal{R}e(\underline{A}_{11}\underline{A}^*_{22}-\underline{A}_{12}\underline{A}^*_{21}),$$

$$b_4(R_3, X_3)=\mathcal{I}m(\underline{A}_{12}\underline{A}^*_{22})(R^2_3+X^2_3)+\{\mathcal{I}m[\underline{A}_{32}(\underline{A}_{13}\underline{A}^*_{22}-\underline{A}^*_{12}\underline{A}_{23})]-$$

$$-2\mathcal{R}e(\underline{A}_{33})\mathcal{I}m(\underline{A}_{12}\underline{A}^*_{22})\}R_3-\{\mathcal{R}e[\underline{A}_{32}(\underline{A}_{13}\underline{A}^*_{22}-\underline{A}^*_{12}\underline{A}_{23})]-$$

$$-2\mathcal{I}m(\underline{A}_{33})\mathcal{I}m(\underline{A}_{12}\underline{A}^*_{22})\}X_3+\mathcal{I}m(\underline{A}_{13}\underline{A}_{32}-\underline{A}_{12}\underline{A}_{33})\times$$

$$\times(\underline{A}^*_{23}\underline{A}^*_{32}-\underline{A}^*_{22}\underline{A}^*_{33}).$$

Si on substitue les expression (11) et (7) dans (4) et on tient compte de (9) et (12) il résulte :

(14)
$$Q_1=\frac{L}{M}U^2_1=$$

$$=\frac{b_1(R_3, X_3)(R^2_2+X^2_2)+b_2(R_3, X_3)R_2+b_3(R_3, X_3)X_2+b_4(R_3, X_3)}{a_1(R_3, X_3)(R^2_2+X^2_2)+a_2(R_3, X_3)R_2+a_3(R_3, X_3)X_2+a_4(R_3, X_3)}.$$

En ce qui concerne la puissance réactive échangée par le QGLN considéré, à la porte de sortie, avec le récepteur, on peut la déterminer à l'aide de la relation :

(15)
$$Q_2=X_2I^2_2$$

où [6][1])

(16)
$$I^2_2=\frac{\alpha(R_3, X_3)U^2_1}{a_1(R_3, X_3)(R^2_2+X^2_2)+a_2(R_3, X_3)R_2+a_3(R_3, X_3)X_2+a_4(R_3, X_3)},$$

avec

(17)
$$\alpha(R_3, X_3)=|\underline{Z}_3-\underline{A}_{33}|^2=[R_3-\mathcal{R}e(\underline{A}_{33})]^2+[X_3-\mathcal{I}m(\underline{A}_{33})]^2>0,\ (\underline{Z}_3\neq\underline{A}_{33}).$$

En même temps on peut obtenir la puissance réactive echangée par le QGLN avec l'impédance $\underline{Z}_3$, à la porte *3*, *3'*, à l'aide de la relation

(18)
$$Q_3=X_3I^2_3.$$

---

[1]) Dans la relation (9) de [6] se sont frayées quelques erreurs, facilement à rectifier et qui ne'influencent pas le fond des résultats.

Si on utilise la dernière équation (2) ainsi que les relations (6) résulte :

$$\underline{I}_3 = \frac{\underline{A}_{21}\underline{Z}_2 + \underline{A}_{32}}{\underline{Z}_3 - \underline{A}_{33}} \underline{I}_2, \tag{19}$$

de sorte que

$$I_3^2 = \frac{\beta(R_3, X_3) U_1^2}{a_1(R_3, X_3)(R_2^2 + X_2^2) + a_2(R_3, X_3) R_2 + a_3(R_3, X_3) X_2 + a_4(R_3, X_3)}, \tag{20}$$

où

$$\beta(R_3, X_3) = |\underline{A}_{21}\underline{Z}_2 + \underline{A}_{32}|^2 = A_{21}^2 \left\{ \left[R_2 + \mathcal{R}e\left(\frac{\underline{A}_{32}}{\underline{A}_{21}}\right)\right]^2 + \left[X_2 + \mathcal{I}m\left(\frac{\underline{A}_{32}}{\underline{A}_{21}}\right)\right]^2 \right\} > 0, \tag{21}$$

3.1. RGQG de type *a*

Dans ce cas les régimes de résonance globale sont réalisés si, compte tenu de la condition (1), la relation

$$Q_1 + Q_2 = 0 \tag{22}$$

est vérifiée.

Si l'on substitue, en (22), les expressions (14) et (15) des puissances réactives Q_1, Q_2 et compte tenu de (16), (17), résulte l'équation :

$$b_1(R_3, X_3)(R_2^2 + X_2^2) + b_2(R_3, X_3) R_2 + [b_3(R_3, X_3) - \alpha(R_3, X_3)] X_2 + b_4(R_3, X_3) = 0. \tag{23}$$

On a considéré que

$$a_1(R_3, X_3)(R_2^2 + X_2^2) + a_2(R_3, X_3) R_2 + a_3(R_3, X_3) X_2 + a_4(R_3, X_3) > 0 \tag{24}$$

vu que le QG LN, en alimentant, par hypothèse, un récepteur passif, la puissance active fournie au récepteur est, nécessairement, positive ($P_2 > 0$, v. [6]).

L'expression (23), qui représente l'équation d'un cercle, constitue *le diagramme de l'impédance du récepteur dans les régimes RGQG de type a d'un QGLN, en régime permanent harmonique, alimenté en sens directe.* Évidement, compte tenu que le récepteur est considéré passif, il faut retenir seulement l'arc de cercle situé dans le demi-plan $R_2 \geqslant 0$.

Par une voie tout à fait analogue il est possible à determiner le diagramme de l'impédance du récepteur dans les régimes RGQG de type *a* du QGLN alimenté en sens inverse, le régime en étant, également, permanent harmonique.

Si on compare l'équation (23) avec celle du diagramme de l'impédance du récepteur dans les régimes qui réalisent la résonance à la porte d'entrée d'un QGLN (v. [5], rel. (18)) on constate aisément que les deux diagrammes sont des arcs de cercle dont les centres ont la même abscisse la différence des ordonnées en étant $\alpha(R_3, X_3)/2b_1(R_3, X_3)$.

Dans les cas ou l'afixe de l'impédance $\underline{Z}_3$ décrit le cercle $b_1(R_3, X_3) = 0$, c'est-à-dire si

$$\mathcal{I}m(\underline{A}_{11}\underline{A}^*_{22}+\underline{A}_{12}\underline{A}^*_{21})(R_3^2+X_3^2)+\{\mathcal{I}m[\underline{A}_{31}(\underline{A}_{13}\underline{A}^*_{21}-\underline{A}^*_{11}\underline{A}_{23})]-$$

$$-2\mathcal{R}e(\underline{A}_{33})\mathcal{I}m(\underline{A}_{11}\underline{A}^*_{21})\}R_3-\{\mathcal{R}e[\underline{A}_{31}(\underline{A}_{13}\underline{A}^*_{21}-\underline{A}^*_{11}\underline{A}_{23})]+ \tag{25}$$

$$+2\mathcal{I}m(\underline{A}_{33})\mathcal{I}m(\underline{A}_{11}\underline{A}^*_{21})\}X_3+\mathcal{I}m(\underline{A}_{13}\underline{A}_{31}-\underline{A}_{11}\underline{A}_{23})(\underline{A}^*_{23}\underline{A}^*_{31}-\underline{A}^*_{21}\underline{A}^*_{33})=0,$$

le diagramme de l'impédance du récepteur, dans les régimes RGQG de type *a* d'un QGLN, alimenté en sens directe, devient un segment de droite.

3.2. RGQG de type *b*

Tels régimes sont caractérisés par la relation :

$$Q_1+Q_2+Q_3=0. \tag{26}$$

Compte tenu des expressions (14), (15) et (18) des puissances réactives Q_1, Q_2, Q_3, ainsi que de (16) et (20), on obtient l'équation :

$$b_1(R_3, X_3)(R_2^2+X_2^2)+b_2(R_3, X_3)R_2+[b_3(R_3, X_3)-\alpha(R_3, X_3)]X_2+ \tag{27}$$

$$+b_4(R_3, X_3)-\beta(R_3, X_3)=0.$$

Cette expression représente l'équation d'un cercle en constituant *le diagramme de l'impédance du récepteur dans les régimes RGQG de type b d'un QGLN, en régime permanent harmonique, alimenté en sens directe.* Si le récepteur est passif alors seulement l'arc de cercle situé dans le demi-plan $R_2 \geqslant 0$ a un sens physique.

Par une voie similaire on peut aussi déterminer le diagramme de l'impédance du récepteur dans les régimes RGQG de type *b* d'un QGLN alimenté en sens inverse.

Si on compare les équations (23) et (27) on observe que celles-ci représentent deux cercles concentriques. Toutefois on peut constater que si la condition (25) est vérifiée alors les deux diagrammes ci-dessus deviennent des droites parallèles.

Il est possible à déterminer, dans les même régimes (RGQG), les diagrammes de l'impédance équivalente à la porte d'entrée d'un QGLN en régime permanent harmonique, tant à l'alimentation en sens directe qu'à celle en sens inverse du quadripôle. Dans ce but on tient compte que pour des valeurs données de l'impédance $\underline{Z}_3$, invariables pour une structure donnée du QGLN, la relation (5) représente une transformation *linéaire* (7) qui réalise la transformation conforme des cercles situés dans le plan $\underline{Z}_2$ en cercles se trouvant dans le plan $\underline{Z}_{e1}$, de sorte que ces diagrammes sont également des cercles.

4. Conclusions

On definit, en utilisant le concept de résonance multipolaire globale introduit dans [1], les régimes de résonance globale des quadripôles généralis linéaires, nonautonomes, en régime permanent harmonique.

Il est possible à distinguer deux types de tels régimes selon que la surface S', dont on applique le théorème de l'énergie électromagnétique, contient (type *a*) ou ne contient pas (type *b*) à son intérieur l'impédance $\underline{Z}_3$ du quadripôle.

On détermine les équations des diagrammes de l'impédance du récepteur dans les régimes de résonance globale (de type *a* ou *b*) d'un quadripôle général linéaire nonautonome.

Annexe

Compte tenu de (8) et tous calculs effectués on obtient

$$M=\{A_{11}^2(R_3^2+X_3^2)+2\mathcal{R}_e[\underline{A}_{11}^*(\underline{A}_{13}\underline{A}_{31}-\underline{A}_{11}\underline{A}_{33})]R_3+2\mathcal{I}_m[\underline{A}_{11}^*(\underline{A}_{13}\underline{A}_{31}-\underline{A}_{11}\underline{A}_{33})]X_3+$$
$$+|\underline{A}_{13}\underline{A}_{31}-\underline{A}_{11}\underline{A}_{33}|^2\}(R_2^2+X_2^2)+\{2\mathcal{R}_e(\underline{A}_{11}^*\underline{A}_{12})(R_3^2+X_3^2)+$$
$$+2\mathcal{R}_e[\underline{A}_{11}^*(\underline{A}_{13}\underline{A}_{32}-\underline{A}_{12}\underline{A}_{33})+\underline{A}_{12}(\underline{A}_{13}^*\underline{A}_{31}^*-\underline{A}_{11}^*\underline{A}_{33}^*)]X_3+$$
(A.1)
$$+2\mathcal{R}_e(\underline{A}_{13}\underline{A}_{32}-\underline{A}_{12}\underline{A}_{33})(\underline{A}_{13}^*\underline{A}_{31}^*-\underline{A}_{11}^*\underline{A}_{33}^*)\}R_2+\{2\mathcal{I}_m(\underline{A}_{11}^*\underline{A}_{12})(R_3^2+X_3^2)+$$
$$+2\mathcal{I}_m[\underline{A}_{11}^*(\underline{A}_{13}\underline{A}_{32}-\underline{A}_{12}\underline{A}_{33})+\underline{A}_{12}(\underline{A}_{13}^*\underline{A}_{31}^*-\underline{A}_{11}^*\underline{A}_{33}^*)]X_3+$$
$$+2\mathcal{I}_m(\underline{A}_{13}\underline{A}_{32}-\underline{A}_{12}\underline{A}_{31})(\underline{A}_{13}^*\underline{A}_{33}^*-\underline{A}_{11}^*\underline{A}_{33}^*)\}X_2+A_{12}^2(R_3^2+X_3^2)+$$
$$+2\mathcal{R}_e[\underline{A}_{12}^*(\underline{A}_{13}\underline{A}_{32}-\underline{A}_{12}\underline{A}_{33})]R_3+2\mathcal{I}_m[\underline{A}_{12}^*(\underline{A}_{13}\underline{A}_{32}-\underline{A}_{12}\underline{A}_{33})]X_3+|\underline{A}_{13}\underline{A}_{32}-\underline{A}_{12}\underline{A}_{33}|^2.$$

Or

$$\mathcal{R}_e[\underline{A}_{11}^*(\underline{A}_{13}\underline{A}_{32}-\underline{A}_{12}\underline{A}_{33})+\underline{A}_{12}(\underline{A}_{13}^*\underline{A}_{31}^*-\underline{A}_{11}^*\underline{A}_{33}^*)]=-2\mathcal{R}_e(\underline{A}_{33})\mathcal{R}_e(\underline{A}_{11}^*\underline{A}_{12})+$$
$$+\mathcal{R}_e[\underline{A}_{13}(\underline{A}_{11}^*\underline{A}_{32}+\underline{A}_{12}^*\underline{A}_{31})],$$
$$\mathcal{I}_m[\underline{A}_{11}^*(\underline{A}_{13}\underline{A}_{32}-\underline{A}_{12}\underline{A}_{33})-\underline{A}_{12}(\underline{A}_{13}^*\underline{A}_{31}^*-\underline{A}_{11}^*\underline{A}_{33}^*)]=-2\mathcal{I}_m(\underline{A}_{33})\mathcal{R}_e(\underline{A}_{11}^*\underline{A}_{12})+$$
(A.2)
$$+\mathcal{I}_m[\underline{A}_{13}(\underline{A}_{11}^*\underline{A}_{32}+\underline{A}_{12}^*\underline{A}_{31})],$$
$$\mathcal{I}_m[\underline{A}_{11}^*(\underline{A}_{13}\underline{A}_{32}-\underline{A}_{12}\underline{A}_{33})+\underline{A}_{12}(\underline{A}_{13}^*\underline{A}_{31}^*-\underline{A}_{11}^*\underline{A}_{33}^*)]=2\mathcal{R}_e(\underline{A}_{33})\mathcal{I}_m(\underline{A}_{11}^*\underline{A}_{12})+$$
$$+\mathcal{I}_m[\underline{A}_{13}(\underline{A}_{11}^*\underline{A}_{32}-\underline{A}_{12}^*\underline{A}_{31})],$$
$$\mathcal{R}_e[\underline{A}_{11}^*(\underline{A}_{13}\underline{A}_{32}-\underline{A}_{12}\underline{A}_{33})-\underline{A}_{12}(\underline{A}_{13}^*\underline{A}_{31}^*-\underline{A}_{11}^*\underline{A}_{33}^*)]=2\mathcal{I}_m(\underline{A}_{33})\mathcal{I}_m(\underline{A}_{11}^*\underline{A}_{12})+$$
$$+\mathcal{R}_e[\underline{A}_{13}(\underline{A}_{13}^*\underline{A}_{32}-\underline{A}_{12}^*\underline{A}_{31})]$$

et

$$A_{11}^2(R_3^2+X_3^2+2\mathcal{R}_e[\underline{A}_{11}^*(\underline{A}_{13}\underline{A}_{31}-\underline{A}_{11}\underline{A}_{33})]R_3+2\mathcal{I}_m[\underline{A}_{11}^*(\underline{A}_{13}\underline{A}_{31}-\underline{A}_{11}\underline{A}_{33})]X_3+$$
$$+|\underline{A}_{13}\underline{A}_{31}-\underline{A}_{11}\underline{A}_{33}|^2=A_{11}^2\left\{\left[R_3-\mathcal{R}_e\left(\frac{\underline{A}_{11}\underline{A}_{33}-\underline{A}_{13}\underline{A}_{31}}{\underline{A}_{11}}\right)\right]^2+\left[X_3+\mathcal{I}_m\left(\frac{\underline{A}_{11}\underline{A}_{33}-\underline{A}_{13}\underline{A}_{31}}{\underline{A}_{11}}\right)\right]^2\right\},$$
(A.3)
$$A_{12}^2(R_3^2+X_3^2)-2\mathcal{R}_e[\underline{A}_{12}(\underline{A}_{12}^*\underline{A}_{33}^*-\underline{A}_{13}^*\underline{A}_{32}^*)]R_2+2\mathcal{I}_m[\underline{A}_{12}(\underline{A}_{12}^*\underline{A}_{33}^*-\underline{A}_{13}^*\underline{A}_{32}^*)]X_3+$$
$$+|\underline{A}_{13}\underline{A}_{32}-\underline{A}_{12}\underline{A}_{33}|^2=A_{12}^2\left\{\left[R_3-\mathcal{R}_e\left(\frac{\underline{A}_{12}\underline{A}_{33}-\underline{A}_{13}\underline{A}_{31}}{\underline{A}_{12}}\right)\right]^2+\left[X_3+\mathcal{I}_m\left(\frac{\underline{A}_{12}\underline{A}_{33}-\underline{A}_{13}\underline{A}_{31}}{\underline{A}_{12}}\right)\right]^2\right\},$$

de sorte que l'expression (A.1) devient :

$$\left(A_{11}^2\left\{\left[R_3-\mathcal{R}_e\left(\frac{\underline{A}_{11}\underline{A}_{33}-\underline{A}_{13}\underline{A}_{31}}{\underline{A}_{11}}\right)\right]^2+\left[X_3+\mathcal{I}_m\left(\frac{\underline{A}_{11}\underline{A}_{33}-\underline{A}_{13}\underline{A}_{31}}{\underline{A}_{11}}\right)\right]^2\right\}\right)(R_2^2+X_2^2)+$$
(A.4)
$$+(2\mathcal{R}_e(\underline{A}_{11}\underline{A}_{12}^*)(R_3^2+X_3^2)+2\{-2\mathcal{R}_e(\underline{A}_{33})\mathcal{R}_e(\underline{A}_{11}^*\underline{A}_{12})+\mathcal{R}_e[\underline{A}_{13}(\underline{A}_{11}^*\underline{A}_{32}+\underline{A}_{12}^*\underline{A}_{31})]\}R_3+$$
$$+2\{-2\mathcal{I}_m(\underline{A}_{33})\mathcal{R}_e(\underline{A}_{11}^*\underline{A}_{12})+\mathcal{I}_m[\underline{A}_{13}(\underline{A}_{11}^*\underline{A}_{32}+\underline{A}_{12}^*\underline{A}_{31})]\}X_3+$$
$$+2\mathcal{R}_e(\underline{A}_{13}\underline{A}_{32}-\underline{A}_{12}\underline{A}_{33})(\underline{A}_{13}^*\underline{A}_{31}^*-\underline{A}_{11}^*\underline{A}_{33}^*))R_2+(2\mathcal{I}_m(\underline{A}_{11}^*\underline{A}_{12})(R_3^2+X_3^2)+$$

$$+2\{2\mathcal{R}_e(\underline{A}_{33})\mathcal{I}_m(\underline{A}^*_{11}\underline{A}_{12})+\mathcal{I}_m[\underline{A}_{13}(\underline{A}^*_{11}\underline{A}_{32}-\underline{A}^*_{12}\underline{A}_{31})]\}R_3+$$

$$+2\{2\mathcal{I}_m(\underline{A}_{33})\mathcal{I}_m(\underline{A}^*_{11}\underline{A}_{12})+\mathcal{R}_e[\underline{A}_{13}(\underline{A}^*_{11}\underline{A}_{32}-\underline{A}^*_{12}\underline{A}_{31})]\}X_3+$$

$$+2\{2\mathcal{I}_m(\underline{A}_{33})\mathcal{I}_m(\underline{A}^*_{11}\underline{A}_{12})+\mathcal{R}_e[\underline{A}_{13}(\underline{A}^*_{11}\underline{A}_{32}-\underline{A}^*_{12}\underline{A}_{31})]\}\ X_3+2\mathcal{I}_m(\underline{A}_{13}\underline{A}_{32}-\underline{A}_{12}\underline{A}_{33})\times$$

$$\times(\underline{A}^*_{13}\underline{A}^*_{31}-\underline{A}^*_{11}\underline{A}^*_{33}))X_2+A^2_{12}\left\{\left[R_3-\mathcal{R}_e\left(\frac{\underline{A}_{12}\underline{A}_{33}+\underline{A}_{13}\underline{A}_{31}}{\underline{A}_{12}}\right)\right]^2+\right.$$

$$\left.+\left[X_3+\mathcal{I}_m\left(\frac{\underline{A}_{12}\underline{A}_{33}-\underline{A}_{13}\underline{A}_{31}}{\underline{A}_{12}}\right)\right]^2\right.$$

Reçue le 3 août 1989

Institut Polytechnique, Jassy,
Chaire d'Électrotechnique, Mesures
et Machines électriques

BIBLIOGRAPHIE

1. Rosman H., *Rezonanța globală la porțile de acces ale unui cuadripol diport liniar, pasiv și reciproc, în regim permanent sinusoidal.* Bul. Inst. polit., Iași, **XV (XIX)**, *1—2*, s. III, 19—24 (1969).
2. Сигорский В. П., *Общая теория четырехполюсника.* Изд. АН УССР, Киев, 1955.
3. Șora C., *Cuadripolul electric.* Ed. Tehn., Buc., 1964.
4. Mocanu C.I., *Teoria cimpului electromagnetic.* EDP, Buc., 1981.
5. Rosman H., *La résonance à la porte d'entrée d'un quadripôle général, linéaire et passif, en régime permanent harmonique.* Bul. Inst. polit., Iași, **XXXV (XXXIX)**, *3—4*, s. III, 1—11 (1989).
6. Rosman H., *Sur le théorème du transfert de la puissance active maximum par un quadripôle général, en régime permanent harmonique.* Bul. Inst. polit., Iași, **XXXIV (XXXVIII)**, *1—4*, s. III, 7—16 (1988).

REZONANȚA GLOBALĂ LA PORȚILE DE ACCES ALE UNUI CUADRIPOL GENERAL, LINIAR, NEAUTONOM, ÎN REGIM PERMANENT ARMONIC

(Rezumat)

Se definesc, pe baza conceptului de rezonanță multipolară globală introdus în [1], regimurile de rezonanță ale cuadripolilor generali, liniari, neautonomi.

Se disting două tipuri de astfel de regimuri, după cum suprafața S', căreia i se aplică teorema energiei electromagnetice, conține (tip *a*) sau nu (tip *b*) în interiorul său impedanța $\underline{Z}_3$ a cuadripolului.

Se determină ecuațiile diagramelor-loc geometric ale impedanței receptorului în regimurile de rezonanță globală (de tip *a* sau *b*) ale unui cuadripol general, liniar, neautonom.

BULETINUL INSTITUTULUI POLITEHNIC DIN IAȘI
Tomul XXXVI (XL), Fasc. 3—4, 1990
Secția III
ELECTROTEHNICĂ. ENERGETICĂ. ELECTRONICĂ. AUTOMATIZĂRI

D.C. 621.311

SOME OBSERVATIONS CONCERNING THE COMPENSATION THEOREM

BY

EMANUEL-CRISTIAN SAVIN

1. Introduction

In this paper, a general matrix formulation is introduced, based on a numerical analysis method usually referred to as *Kron's (or Woodbury's) matrix inversion by modification method*, from which the compensation theorem (known also as variation theorem) results by replacing the general algebraic notations with those corresponding to the loop analysis method.

The first to outline the deep significance of matrix inversion by modification methods for the analysis of linear and linearized systems were S.B. Haley and K.W. Current. In [1], they have used a multiparameter change formula derived by S.B. Haley in [2], to develop a theoretical foundation for designing general representation—independent and computationally efficient algorithms, to treat system response change.

In what follows it is stressed that the extremely simple Kron's formula, which corresponds to a single-parameter change, may permit to introduce a unifying formal approach in network sensitivity analysis theory. In a subsequent paper, it will be shown how several sensitivity analysis methods derive directly from the matrix formulation developed here. Consequently, it is conjectured that the matrix modification technics could also constitute very well suited fundamentals to derive useful didactical methods for teaching circuits and systems.

The compensation theorem [3] and Kron's method [4] are shortly reviewed in §§ **2** and **3**, respectively. In § **4**, it is demonstrated that the compensation theorem is a consequence of the matrix inversion by modification formula. As the compensation theorem is stated in terms of branch (or loop) currents, in order to construct a concise demonstration, the matrix framework is developed by using the loop analysis notations.

Based on the matrix formulation introduced in § **4**, in § **5**, some interesting remarks relating the compensation theorem with network sensitivity analysis are considered. For instance, in terms of loop analysis notations, an explicit formula for the sensitivites of loop currents with respect to the impedances placed on the links is derived. The formula reveals that each of these sensitivites is directly related to an element of the inverse of the loop impedance matrix. Although this result is remarkable simple, we did not found it to be explicitly mentioned in the literature.

Despite the framework is developed in terms of loop analysis notations, it involves only purely algebraic operations, so that it might have used the nodal or even the hybrid notations as well, with corresponding similar results. However, we will no longer insist on these analogies here.

2. The Compensation Theorem

We consider a well-defined, linear time-invariant and uniquely solvable network, $\mathcal{N}$, and assume that by extracting an impedance which can vary, Z_j, as shown in Fig. 1 [3], the remaining one-port, N, is well-defined too. As it is known [5], a network $\mathcal{N}$ is said to be well-defined if it does not contain any circuit element which is coupled, electrically or nonelectrically, to some physical variable outside it. Assuming that a single element Z_j of $\mathcal{N}$ has changed its value, the compensation theorem provides a simplified procedure to calculate the effect of this change on the currents and voltages of the network, as compared with solving again for the fundamental responses.

As we will discuss in terms of loop analysis method, we also assume that all circuit elements of $\mathcal{N}$ are current-controlled.

We are interested in the effect of the change ΔZ_j on some current I_k in the network. When the impedance Z_j changes, the currents change to $I_j+\Delta I_j$, $I_k+\Delta I_k$, etc. The compensation theorem states that the changes ΔI_j, ΔI_k, etc. may be calculated by considering the network $\tilde{\mathcal{N}}$ represented in Fig. 2, which we will call the large change sensitivity network of network $\mathcal{N}$. The corresponding one-port $\tilde{N}$ is obtained from N after replacing all the independent generators by their internal impedances, and the voltage ΔV_{I_j} denotes :

$$\Delta V_{I_j} \triangleq \frac{\Delta Z_j (Z_{in}^j + Z_j)}{Z_{in}^j + Z_j + \Delta Z_j} I_j. \tag{1}$$

We remark that ΔI_j may be expressed directly as follows :

$$\Delta I_j = -\frac{\Delta Z_j I_j}{Z_{in}^j + Z_j + \Delta Z_j}. \tag{2}$$

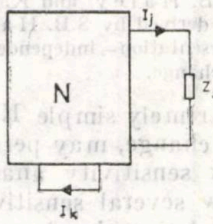

Fig. 1

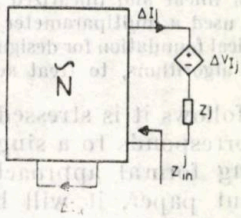

Fig. 2

The significant advantage of the compensation theorem is that the loop impedance matrix $\mathbf{Z}_L$ of $\tilde{N}$ remains the same as that of the unperturbed network. Thus, we can calculate ΔI_i, ΔI_k, etc. by using the elements of the matrix $\mathbf{Z}_L^{-1}$ which is assumed to be evaluated in an earrlier stage of the analysis.

3. The Matrix Inversion by Modification Formula

Let us consider two $n \times n$ matrices $\mathbf{Z}_L$ and $\mathbf{Z}_\Delta$ which differ from each other by only one diagonal element, say the jjth, as follows :

$$z_{jk}^{\Delta} = z_{jk},\ j \neq k, \quad \text{and} \tag{3}$$

$$z_{jj}^{\Delta} = z_{jj} + \Delta z_{jj}, \tag{4}$$

where z_{jk} and z_{jk}^{Δ} represent the jkth element of the matrices $\mathbf{Z}_L$ and $\mathbf{Z}_\Delta$, respectively. Supposing that $\mathbf{Z}_L^{-1}$ has been computed, let y_{jk} be its jkth element. The K r o n's matrix inversion by modification method [4], [6] provides us with the following formula :

$$\mathbf{Z}_{\Delta}^{-1}=\mathbf{Z}_{L}^{-1}-\left(\frac{\Delta z_{jj}}{1+y_{jj}\Delta z_{jj}}\right)\mathbf{M}_{j}, \tag{5}$$

where $\mathbf{M}_j$ is an $n\times n$ matrix defined by

$$\mathbf{M}_{j}\overset{\Delta}{=}[y_{1j}\ y_{2j}\ \cdots\ y_{nj}]^{T}[y_{j1}\ y_{j2}\ \cdots\ y_{jn}]. \tag{6}$$

The relation (5) shows that the inverse of $\mathbf{Z}_\Delta$ can be found by modifying the inverse of $\mathbf{Z}_L$, which is already known.

4. The Compensation Theorem—a Consequence of Kron's Formula

Let us write the loop equation system for the network $\mathcal{N}$ considered in § 2, as follows :

$$\mathbf{Z}_{L}\mathbf{I}_{L}=\mathbf{E}_{L}, \tag{7}$$

with

$$I_{L_j}=I_{j}\ \text{and}\ I_{L_k}=I_{k}, \tag{8}$$

where $\mathbf{I}_L$ represents the loop current vector and $\mathbf{E}_L$ the vector of the loop voltage sources ; I_{L_j} denotes the jth element of $\mathbf{I}_L$.

Solving Eq. (7) for the loop currents, we obtain

$$\mathbf{I}_{L}=\mathbf{Z}_{L}^{-1}\mathbf{E}_{L}. \tag{9}$$

A change ΔZ_j of the impedance Z_j determines a diagonal change

$$\Delta z_{jj}=\Delta Z_{j} \tag{10}$$

of matrix $\mathbf{Z}_L$ that is transformed in the matrix $\mathbf{Z}_\Delta$ (s. the notations in § 3) for which relation (4) is valid. The change ΔZ_j leads to a change $\Delta\mathbf{I}_L$ of the loop current vector and Eq. (9) becomes

$$\mathbf{I}_{L}+\Delta\mathbf{I}_{L}=\mathbf{Z}_{\Delta}^{-1}\mathbf{E}_{L}. \tag{11}$$

Using the matrix inversion by modification formula (5), Eq. (11) may be written as follows :

$$\mathbf{I}_{L}+\Delta\mathbf{I}_{L}=\left\{\mathbf{Z}_{L}^{-1}-\left(\frac{\Delta Z_{j}}{1+y_{jj}\Delta Z_{j}}\right)\mathbf{M}_{j}\right\}\mathbf{E}_{L}. \tag{12}$$

Substituting the loop current vector $\mathbf{I}_L$ given by (9) in Eq. (12) we obtain

$$\Delta\mathbf{I}_{L}=-\left(\frac{\Delta Z_{j}}{1+y_{jj}\Delta Z_{j}}\right)\mathbf{M}_{j}\mathbf{E}_{L}. \tag{13}$$

Let us observe that from Eq. (9) we can also derive the following relation :

$$[y_{j1}\ y_{j2}\ \cdots\ y_{jn}]\,\mathbf{E}_{L}=I_{L_j}. \tag{14}$$

Then, considering the definition (6) of matrix $\mathbf{M}_j$ and using the hypothesis (8), Eq. (13) may be written as follows :

$$\Delta\mathbf{I}_{L}=[y_{1j}\ y_{2j}\ \cdots\ y_{nj}]^{T}\left(-\frac{\Delta Z_{j}}{1+y_{jj}\Delta Z_{j}}I_{j}\right). \tag{15}$$

We remark that, by definition,

$$y_{jj} \triangleq \frac{E'_{L_j}}{I'_{L_j}}, \quad (E_{L_k}=0, \quad k\neq j). \tag{16}$$

Thus, as shown in Fig. 3, we can express y_{jj}, defined by (16), in the following form :

$$y_{jj}=(Z^j_{in}+Z_j)^{-1}. \tag{17}$$

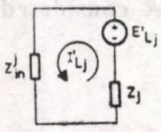

Fig. 3

We observe that replacing $Z^j_{in}+Z_j$, given by (17), in the definition of ΔV_{I_j} (s. (1)), we have

$$\Delta V_{I_j}=\frac{\Delta Z_j}{1+y_{jj}\Delta Z_j} I_j, \tag{18}$$

and consequently, ΔI_j expressed by Eq. (2) may also be written as

$$\Delta I_j=-\frac{y_{jj}\Delta Z_j}{1+y_{jj}\Delta Z_j} I_j. \tag{19}$$

Let us now denote by $[(-\Delta V_{I_j})]$ a column vector that has all elements zero except the jth element, which is $(-\Delta V_{I_j})$. Using this notation, Eq. (15) may be written as follows :

$$\Delta \mathbf{I}_L=\mathbf{Z}_L^{-1}[(-V_{I_j})], \tag{20}$$

with ΔI_j given by (19) and

$$\Delta I_k=-\frac{y_{kj}\Delta Z_j}{1+y_{jj}\Delta Z_j} I_j. \tag{21}$$

Obviously, Eq. (20) represents precisely the expression of the compensation theorem.

We stress that the demonstration given above involves only purely algebraic operations, independently of any physical argument, so that, instead of using peculiar notations, we can consider the following general matrix formulation for Eq. (20) :

$$\Delta \mathbf{x}=\mathbf{A}^{-1}[(-b_{x_j})]. \tag{22}$$

Eq. (22) expresses the fact that the changes in the responses of a linear time-invariant network due to a single diagonal change ΔA_j of its interaction matrix, may be interpreted as representing the responses of the corresponding large change sensitivity network (s. § **2**).

5. Some Remarks Relating the Compensation Theorem with Network Sensitivity Analysis

Let us consider some interesting remarks concerning the sensitivities of loop currents with respect to the impedances placed on the links, that

result imediately from Eq. (15). As it may be seen, we can directly write (consider Eqs. (19) and (21) too):

$$(23)\qquad \frac{\partial I_j}{\partial Z_j} = -\,y_{jj}\,I_j, \qquad \text{and} \qquad (24)\qquad \frac{\partial I_k}{\partial Z_j} = -\,y_{kj}I_j.$$

So, we have

$$(25)\qquad S^{I_j}_{Z_j} = -\,y_{jj}Z_j \text{ and, respectively,} \qquad (26)\qquad S^{I_k}_{Z_j} = -\,y_{kj}Z_j(I_j/I_k).$$

We denote by $\mathcal{Z}_{\mathcal{L}}$ the set of the link impedances:

$$(27)\qquad \mathcal{Z}_{\mathcal{L}} = \{Z_1, Z_2, \ldots, Z_j, \ldots, Z_n\},$$

and, based on (23) and (24), we remark that the Jacobian matrix of $\mathbf{I}_L$ at $\mathcal{Z}_{\mathcal{L}}$ is given by

$$(28)\qquad \mathbf{J} = -\,\mathbf{Z}_L^{-1}\mathbf{I}_D,$$

where $\mathbf{I}_D$ is a $n \times n$ diagonal matrix with

$$(29)\qquad I^D_{jk} = 0 \text{ for } j \neq k, \qquad \text{and} \qquad (30)\qquad I^D_{jj} = I_{L_j}.$$

In a corresponding manner we can write in the general case

$$(31)\qquad \mathbf{J} = -\,\mathbf{A}^{-1}\mathbf{x}_D.$$

As a final remark, we note that from Eq. (15) we can also write:

$$(32)\qquad \frac{\partial \mathbf{I}_L}{\partial \mathbf{Z}_j} = \mathbf{Z}_L^{-1}[(-I_j)].$$

So, $\partial \mathbf{I}_L/\partial \mathbf{Z}_j$ represent the loop current vector of the sensitivity network $\tilde{\mathcal{N}}^*$ shown in Fig. 4. We stress that once the large change sensitivity network $\tilde{\mathcal{N}}$ obtained, the sensitivity network $\tilde{\mathcal{N}}^*$ results immediately.

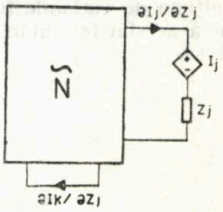

Fig. 4

6. Conclusions

It is demonstrated that the compensation theorem is a consequence of K r o n s matrix inversion by modification method. As the compensation theorem is stated in terms of branch or loop currents, in order to be concise, the demonstration is formulated by using the loop analysis notations. However, as it is pointed out, the operations involved are purely algebraic, so that the considered formulation constitutes in fact a general matrix framework. For a given network, based on this matrix formulation, one may directly construct the corresponding sensitivity and large change sensitivity networks in terms of the set of fundamental responses considered. When the loop analysis notation is used, the particular large change sensitivity network is precisely the same as that one considered by the compensation theorem.

An explicit formula for the sensitivities of the loop currents with respect to the impedances placed on the links is also derived.

Although developed for linear time-invariant networks in order to clearly state the problems, the results obtained are valid for linear time-varying networks as well.

Received, May 25, 1990

Polytechnic Institute, Jassy,
Department of Fundamentals of Electrotechnics

REFERENCES

1. Haley S.B., Current K.W., *Response Change in Linearized Circuits and Systems: Computational Algorithms and Applications.* Proc. I.E.E.E, **73**, 5—24 (1985).
2. Haley S.B., *Large Change Response Sensitivity of Linear Networks.* I.E.E.E. Trans., **CAS-27**, 305—310 (1980).
3. Chirlian P.M., *Basic Network Theory.* McGraw-Hill, New York, 1969.
4. Chua L.O., Lin P.M., *Computer-Aided Analysis of Electronic Circuits.* Prentice-Hall, Englewood Cliffs, New Jersey, 1975.
5. Chua L.O., Desoer C.A., Kuh E.S., *Linear and Nonlinear Circuits.* McGraw-Hill., New York, 1987.
6. Householder A.S., *A Survey of Some Closed Methods for Inverting Matrices.* J. Soc. Industr. Appl. Math., **5**, 155—169 (1957).

UNELE OBSERVAŢII PRIVIND TEOREMA COMPENSAŢIEI

(Rezumat)

Se demonstrează că teorema compensaţiei este o consecinţă a formulei lui Kron pentru inversarea matricilor prin modificări. Se construieşte un cadru matriceal general, independent de orice considerent fizic, bazat pe formula lui Kron, care se poate particulariza pentru orice mulţime de variabile fundamentale considerată. Teorema compensaţiei constituie particularizarea acestei formulări matriceale pentru cazul notaţiilor corespunzătoare metodei curenţilor ciclici.

BULETINUL INSTITUTULUI POLITEHNIC DIN IAŞI
Tomul XXXVI (XL), Fasc. 3—4, 1990
Secţia III
ELECTROTEHNICĂ. ENERGETICĂ. ELECTRONICĂ. AUTOMATIZĂRI

D.C. 621-501.1

CONTROL SYSTEMS DIAGNOSIS VIA LINEAR CLASSIFICATION OF MODEL ESTIMATIONS

BY

TEODOR MARCU and OCTAVIAN PĂSTRĂVANU

1. Introduction

The operating ranges of control systems are characterized by the evolution of the output variables registered for standard input signals. These values can be the input of a data compression process which eliminates the redundant information from the experimental results and gives a parameters set. From the classification theory standpoint, these parameters mean the extracted features representing a pattern vector [1]. The classifiers enable the mapping from the features space to the decisions one. Each working characteristic corresponds to a point in the decision space, considered as a class.

Our aim being an on-line diagnosis of control systems [2]...[4], we propose to use, for linear separable classes, linear and quadric least-squares minimum distance classifiers [1], based on the models estimations classification. The data compression is done by means of the continuous/discrete-time process models identification.

In the case of the failure in recognizing the model as one of the training set of the classifier, we propose the application of gnostical methods for fault diagnosis [5], through the estimated parameters robust filtering, which leads to the indication of the fault source.

2. Features Selection

The control systems are described by a continuous/discrete-time model [6]. These can be the subject of an identification process of this model, after the application of one of the standard inputs. The estimated parameters of the model can be used for the classification of the type of the system evolution [2].

One of the frequently used identification methods is the recursive least-squares algorithm. This determines, from the input-output data, the parameters of the discrete-time model:

(1) $$A(q^{-1})y(t)=B(q^{-1})u(t)+v(t),$$

where:

(2) $A(q^{-1})=1+a_1q^{-1}+ \dots +a_Lq^{-L}$, (3) $B(q^{-1})=b_1q^{-1}+ \dots +b_Pq^{-P}$

and t is the normalized time, $u(t)$ — the input at the moment t, $y(t)$ — the output at the moment t, q^{-1} — the one step time delay operator, $v(t)$ — the residuum of the model.

By using the notations:

$$\theta=[a_1 \dots a_L \; b_1 \dots b_P], \tag{4}$$

$$\varphi(t)=[-y(t-1) \dots -y(t-L) \; u(t-1) \dots u(t-P)]^T, \tag{5}$$

where T denotes the transposed matrix, the model (1) can be written as:

$$y(t)=\varphi^T(t)\theta+v(t). \tag{6}$$

For the one-line determination of the parameters one minimizes the criterion:

$$V(\theta)=\sum_{s=1}^{t}\lambda^{t-s}\, v^2(s), \qquad \lambda\in(0,\,1], \tag{7}$$

obtaining the following recursive algorithm, which is robust to the rounding errors [6]:

$$\hat{\theta}(t)=\hat{\theta}(t-1)+K(t)v(t); \tag{8}$$

here

$$v(t)=y(t)-\varphi^T(t)\hat{\theta}(t-1), \quad K(t)=\frac{P(t-1)\varphi(t)}{\lambda+\varphi^T(t)\,P(t-1)\varphi(t)}$$

$$P(t)=K(t)K^T(t)+\frac{1}{\lambda}[I-K(t)\varphi^T(t)]\,P(t-1)[I-\varphi(t)K^T(t)].$$

With this method we select $M=P+L$ parameters at each iteration.

If a continuous-time model is utilized, characterized by the transfer function, we can use this procedure to which we add the discrete — continuous conversion on the basis of the bilinear z-transform.

3. Least-squares Minimum Distance Classifiers

The classifier represents a device which is trained to assign a features set to one of the learned classes:

$$C_1,\; C_2,\; \dots,\; C_K. \tag{9}$$

The linear least-squares minimum distance classifier is characterized by a linear operator that maps the patterns which belong to the M-dimensional feature space into the K-dimensional decision space, wherein the patterns belonging to C_i are made to cluster around a preselected point V_i, $(i=\overline{1,\,K})$. The matrix of the classifier is determined so that the overall mean-square error incurried in the mapping is minimized [1].

Let us consider a set of M-dimensional patterns, Z_{ij}, $(i=\overline{1,\,K};\, j=1,\, N_i)$, where N_i — the number of evolutions that belong to the same class C_i. These are to be mapped into a specified point in the decision space, by the operator:

$$F=S_{vz}S_{zz}^{+}, \tag{10}$$

with

$$S_{vz}=\sum_{i=1}^{K}\sum_{j=1}^{N_i}\frac{P_i}{N_i}V_iZ_{ij}^T, \quad (11) \qquad S_{zz}=\sum_{i=1}^{K}\sum_{j=1}^{N_i}\frac{P_i}{N_i}Z_{ij}Z_{ij}^T, \quad (12)$$

where P_i is the *a priori* probability of the appereance of C_i, $(i=\overline{1, K})$, S_{zz}^+ denotes the generalized inverse of the matrix S_{zz}, determined through the analysis of their singular values [7].

We choose V_i to be the vertices of the K-unit vectors:

$$V_i=[0 \dots 0 \underset{i}{1} 0 \dots 0]^T, \quad \|V_i\|^2=1. \quad (13)$$

To classify a given pattern that characterizes the evolution of a system

$$Z=\hat{\theta}=[z_1 \dots z_M]^T \quad (14)$$

means to mapp it into the decision space $L=FZ$ and then characterize it as belonging to C_{i_0} if it is mapped closest to V_{i_0}, according to the criterion:

$$D_{i_0}^2=\min_i\{D_i^2\}, \quad D_{i_0}^2\leqslant T_h, \quad D_i^2=\|L-V_i\|^2, \quad (i=\overline{1, K}), \quad (15)$$

where T_h denotes a threshold caracterizing the separability of a class. For example $T_h=0.5$, knowing that the distance between V_i's is equal to $\sqrt{2}$ and $T_h=(\sqrt{2}/2)^2$.

The quadric least-squares minimum distance classifiers are found using the same procedure, considering as features z_j^2, z_jz_k, z_j, resulting from the vector Z (14), their total number of these being $M(M+3)/2$.

In the case when we augment the training set of features obtained in new conditions, caracterizing one of the same classes or we introduce new classes, we avoid a new synthesis by means of an adaptive one [8]. So, if we add a new vector of features $Z_{i\alpha}$ to the class i_α, we must adapt the matrix of the classifier according to:

$$F^\alpha=S_{vz}^\alpha S_{zz}^{\alpha+}, \quad (16)$$

where:

$$S_{vz}^\alpha=S_{vz}+V_{i\alpha}Z_{i\alpha}^T, \quad (17)$$

$$S_{zz}^{\alpha+}=S_{zz}^+-\frac{(S_{zz}^+Z_{i\alpha})(Z_{i\alpha}^TS_{zz}^+)}{(1+Z_{i\alpha}^TS_{zz}^+Z_{i\alpha})}. \quad (18)$$

If we add a new class we must reconsider the vectors V_i defined by (13) and we recalculate F given by (10), according to the new dimension of the decision space that grows to $K+1$. We avoid the recomputation of F by means of (16) ... (18) augmenting only the new terms that appear in the matrices S_{vz} and S_{zz} respectively.

4. Procedure of the Control Systems Diagnosis

The diagnosis procedure involves the following steps:

S1. The determination of a continuous/discrete-time model and the choice of an on-line identification method of this model.

S2. The off-line synthesis of the control system classifier.

S3. The on-line diagnosis :

S3.1. The features selection by means of the on-line model parameters identification.

S3.2. The classification of the current system evolution.

S3.3. In the case when current the system does not belong to the class that describes the correct system evolution, the determining of those parameters which deviate from the normal values by means of the robust filtering [5].

5. Experimental Results

In order to validate the proposed diagnosis via linear classification of model estimations, the entire methodology was implemented and tested by means of an IBM PC compatible computer. To implement the different steps routines from the IMSL and SIPAC computer libraries [9], [10] were adapted, modified and used.

We have studied through simulation the d.c. electric motor diagnosis with separate excitation at constant flow, with the following characteristics : 3.5 KW, 20 A, 220 V, 1 000 rot./min. Assuming the quasi-linear behaviour of the motor arround a point of work, we have used a two-order linear model described by the following transfer function :

$$G(s)=\frac{a}{b+cs+s^2}, \qquad a=362, \quad b=34.5, \quad c=1.32. \tag{19}$$

Using the bilinear z-transform (BZT) the system was stimulated with a pseudorandom binary signal. Additively, we have stimulated the process with a gaussian noise with zero mean and variance that provides a certain signal to noise ratio (SNR). The sample period $T=0.08$ s was used. The recursive least-squares algorithm, the recursive instrumental variable algorithm, the recursive prediction error minimization combined with the extended recursive least-squares algorithm [6] were applied for selecting at each 8 s (100 iterations) the continuous-time model parameters, using BZT. The first enumerated algorithm gives for this example, the best results.

For the identification procedure the least-squares recursion was initialized by : $\hat{\theta}(0)=0$, $P(0)=\alpha I$, $\alpha=10^7$, I denoting the unity matrix of order $M=3$ and using for, the ponderation factor the variation law :

$$\lambda(t)=\lambda(t-1)\lambda_0+[1-\lambda_0], \quad t\geqslant 1, \quad \lambda(0)=0.97, \quad \lambda_0=0.99. \tag{20}$$

The parameters $\{\hat{a}, \hat{b}, \hat{c}\}$ were used for the synthesis of a linear and a quadric classifier, with one class : those for which the motor works correctly.

Knowing the following dependences :

$$a=f_1(1/L); \quad b=f_2(R_r, 1/L, R_r/L); \quad c=f_3(R_r/L), \tag{21}$$

where L is the rotor inductance and R_r the rotor resistance, we have simulated the faults by reducing the physical parameters L and R_r according to :

$$R_{r_1}=\frac{R_r}{K_d}, \qquad L_1=\frac{L}{K_d}, \qquad K_d>1, \tag{22}$$

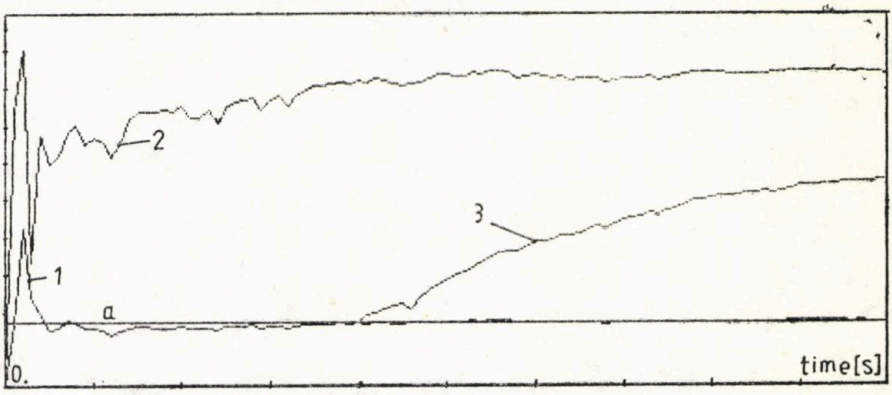

Fig. 4 *a*. — The identified parameter *a*: *1* — case *1*; *2* — case *2*; *3*— case *3*.

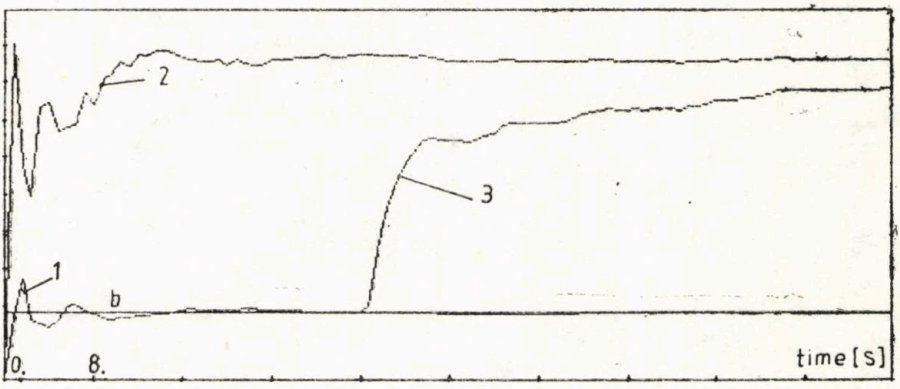

Fig. 4 *b*. — The identified parameter *b*: *1* — case *1*; *2* — case *2*; *3* — case *3*.

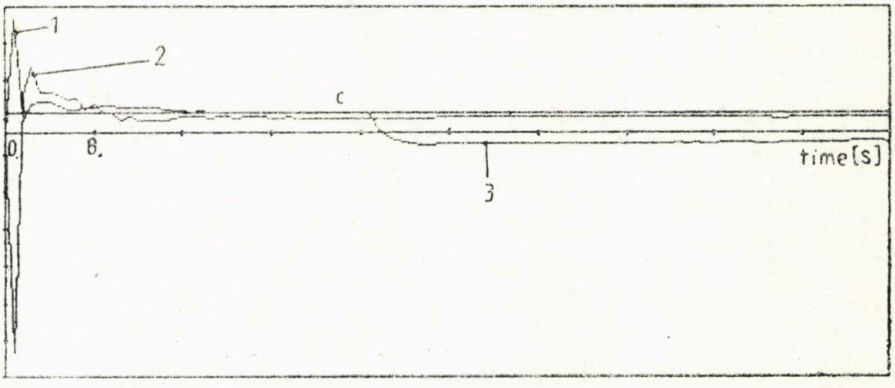

Fig. 4 *c*. — The identified parameter *c*: *1* — case *1*; *2* — case *2*; *3* — case *3*.

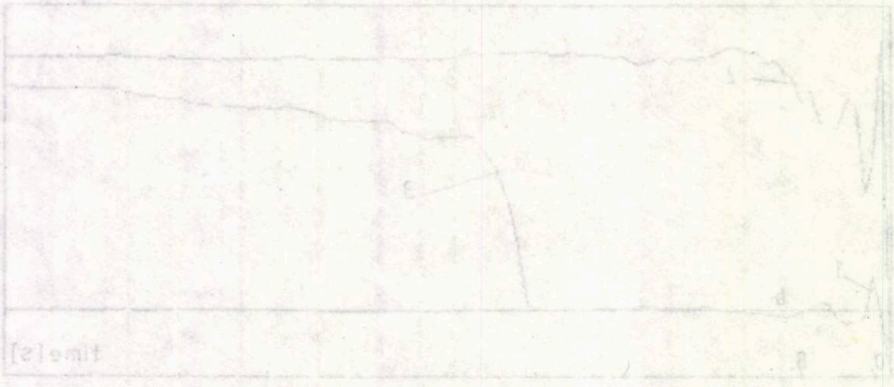

this situation corresponding to a short circuit of a part of the rotor winding.

We present some variation curves of the system output after 24 s (300 points) in the case of correct work $K_d=1$ (Fig. 1) and respectively of a short circuit ($K_d=5$ from the begining (Fig. 2) and $K_d=5$ after 32 s of simulation from the begining (Fig. 3)). Also, we present in Fig. 4 *a*, *b*, *c* the variation curves of the parameters resulted from the identification procedure, corresponding to each of the respectively situations mentionated above.

We have obtained the following diagnosis results:

a) For $K_d=1$, we have modified the SNR. The classification has indicated the correct work for SNR ≥ 4 (liniar classifier) and SNR ≥ 3 (quadric classifier).

b) For SNR $=10$, we have modified the factor K_d. We have obtained good results by the faults detection for $K_d \geq 3$ (linear classifier) and $K_d \geq 2$ (quadric classifier).

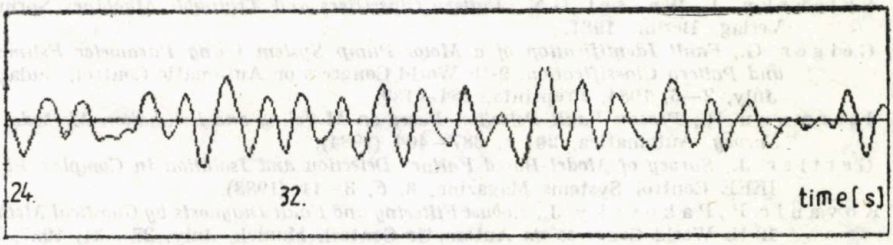

Fig. 1. — System output, normal work ($K_d=1$) — case *1*.

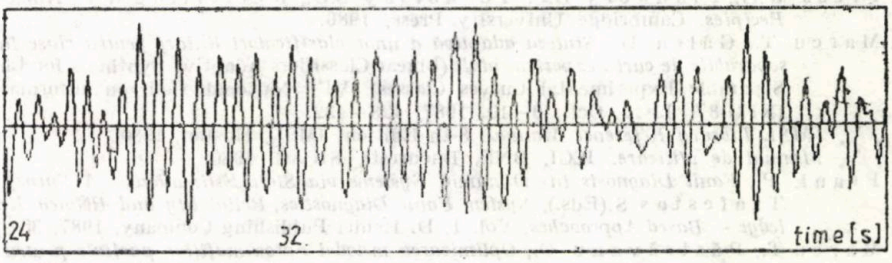

Fig. 2. — System output, abnormal work ($K_d=5$ from the begining) — case *2*.

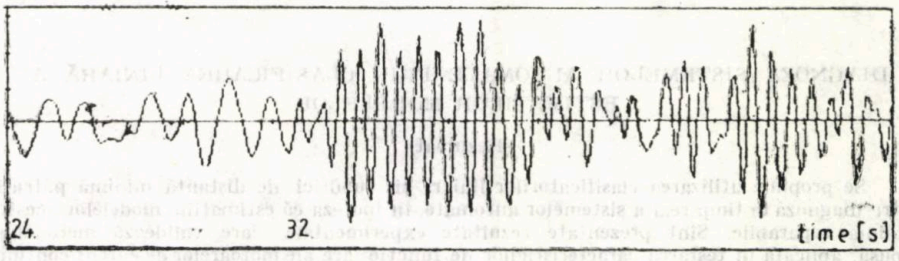

Fig. 3. — System output, abnormal work ($K_d=5$, after 32 s — case *3*.

6. Conclusions

The obtained results in the diagnosis by using the quadric classifiers may be considered as useful and interesting. The disadvantage of their use is the greater number of operations involved in classification.

Our approach can be applied to the control systems for which the features are the state variables and to the variable parameters systems [11]. In these cases it is necessary a supplementary step of segmentation]12], for the distinct stages identification of the system evolution. The extention of the presented results in these underlined cases will be the aim of our further studies.

Received, December 5, 1989

Polytechnic Institute, Jassy,
Department of Automation,

REFERENCES

1. Sklansky J., Wassel G.N., *Pattern Classifiers and Trainable Machines.* Springer-Verlag, Berlin, 1981.
2. Geiger G., *Fault Identification of a Motor-Pump System Using Parameter Estimation and Pattern Classification.* 9-th World Congress on Automatic Control, Budapest, July, 2—6, 1984, Preprints, 184—189.
3. Isermann R., *Process Fault Detection Based on Modeling and Estimation Methods — A Survey.* Automatica, **20**, *4*, 387—404 (1984).
4. Gertler J., *Survey of Model-Based Failure Detection and Isolation in Complex Plants.* IEEE Control Systems Magazine, **8**, *6*, 3—11 (1988).
5. Kovanic P., Pakovsky J., *Robust Filtering and Fault Diagnosis by Gnostical Methods.* 10-th World Congress on Automatic Control, Munich, July, 27— 31, 1987, Preprints, 86—90.
6. Tertişco M., Stoica P., Popescu Th., *Identificarea asistată de calculator a sistemelor.* Ed. Tehn., Buc., 1987.
7. Press W.H., Flannery B.P., Teukolsky S.D., Wetterling W.T., *Numerical Recipies.* Cambridge University Press, 1986.
8. Marcu T., Gâlea D., *Sinteza adaptivă a unor clasificatori liniari pentru clase liniar separabile de curbe experiementale* (Linear Classifiers Adaptive Synthesis for Linear Separable Experimental Curves Classes), VI[th] National Coll. on Informatics; INFO-87, Jassy, Oct., 9—10, 1987, 428—432.
9. *** *IMSL Library Reference Manual.* 8-th Edition, IMSL, Huston, 1980.
10. *** *Manual de utilizare.* ICCI, BNP, București, SIPAC, 1980.
11. Frank P., *Fault Diagnosis in Dynamic Systems via State Estimation — A Survey.* In Tzafestas S.(Eds.), *System Fault Diagnostics, Reliability and Related Knowledge — Based Approaches,* Vol. **1**, D. Reidel Publishing Company, 1987, 35— 98.
12. Marcu T., Păstrăvanu O., *Optimizarea metodei aproximațiilor parțiale pentru segmentarea curbelor experimentale* (Partial Approximation Method Optimization for Experimental Curves Segmentation). VI[th] National Coll. on Informatics, INFO-87, Jassy, Oct. 9—10, 1987, 433—439.

DIAGNOZA SISTEMELOR AUTOMATE PRIN CLASIFICAREA LINIARĂ A ESTIMAȚILOR MODELELOR

(Rezumat)

Se propune utilizarea clasificatorilor liniari și cuadrici de distanță minimă pătratică pentru diagnoza în timp real a sistemelor automate, în ipoteza că estimațiile modelelor acestora sînt liniar separabile. Sînt prezentate rezultate experimentale care validează metodologia propusă, aplicată în testarea caracteristicilor de funcționare ale motoarelor de curent continuu. Pentru clasificare s-au folosit rezultatele identificării parametrice *on-line*.

BULETINUL INSTITUTULUI POLITEHNIC DIN IAȘI
Tomul XXXVI (XL), Fasc. 3—4, 1990
Secția III
ELECTROTEHNICĂ. ENERGETICĂ. ELECTRONICĂ. AUTOMATIZĂRI

C.D. 621.382.383

NUMERIC DISPLACEMENT TRANSDUCER USING A NEW TYPE INDUCTANCE-TO-TIME-PERIOD CONVERTER

BY

CORNELIA MĂRCUȚĂ and LIVIU GORAȘ

1. Introduction

The use of process computers and numeric equipments for automatic control required transducers with numerical output. A solution for realization of such transducer consists in a configuration containing a sensor (S), an adapter (A) and an analog-to-digital converter (ADC) (Fig. 1).

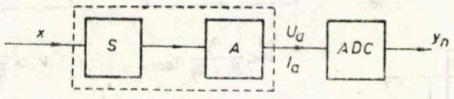

Fig. 1

The analog-to-digital conversion of the adapter output signal (bridge, amplifier, compensator) is economically justified only when one ADC is used to convert the output of more adapters. In other cases, solution with the sensor and the adapter contained in the same functional block are prefered. A solution of this kind consist in the introduction of inductive or capacitive sensors in oscillators, in this way a direct conversion of nonelectrical quantities into frequency or into time-period being obtained. Further, their conversion into code is easily realized.

Frequently, mechanical displacements are sensed using inductive sensors. In recent years, there have been some preoccupations, concerning the inductance-to-time-period conversion [1]...[4].

In this paper a possibility to realize a digital transducer for mechanical displacement measurements using a simple inductance-to-time-period ($L-T$) converter is presented.

2. Transducer Description

The schematic circuit of the transducer is shown in Fig. 2.

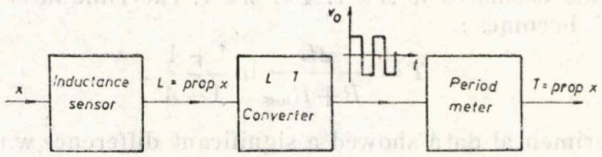

Fig. 2

Assuming ideal behaviour for the elements of the measuring chain we can consider that :

a) the sensor inductivity depends linearly vs. the mechanical displacement and

b) the $L-T$ converter [3] built with inductive sensor produces a square wave output having the time period T proportional to the displacement x.

The circuit which realizes the displacement-to-time-period conversion is presented in Fig. 3 *a*, where $L(x)$ is the displacement inductive sensor imbedded into a single OA astable multivibrator.

3. Analysis of the $L-T$ converter

In the hypothesis of an ideal OA, the results of a transient analysis on the models presented in Figs. 3 *b* and 3 *c* with initial conditions :

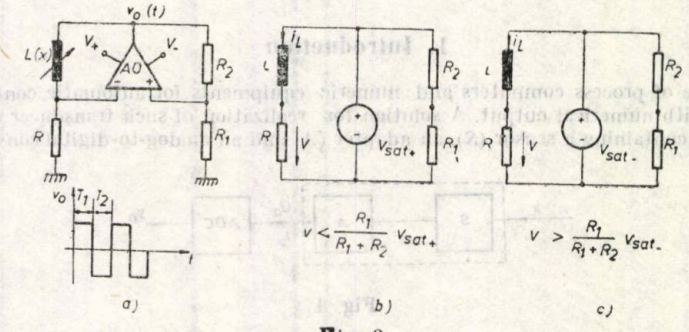

Fig. 3

$$i_{L0-} = V_{sat-} \frac{R_1}{R(R_1+R_2)}, \quad i_{L0+} = V_{sat+} \frac{R_1}{R(R_1+R_2)}$$

respectively, led to the following expression of the time period T :

$$T = T_1 + T_2 = \frac{L}{R+R_{loss}} \left(\ln \frac{1+kA}{1-A} + \ln \frac{1+A/k}{1-A} \right) \tag{1}$$

where :

$$A = \frac{R_1(R+R_{loss})}{R(R_1+R_2)}, \quad k = \left| \frac{V_{sat-}}{V_{sat+}} \right| ;$$

here R_{loss} is the series resistance equivalent to the inductor losses, V_{sat-} and V_{sat+} — the negative and positive saturation voltages of the OA.

The circuit oscillates if $A<1$. For $k=1$, the time-interval T_1 is equal to T_2 and T becomes :

$$T = \frac{2L}{R+R_{loss}} \ln \frac{1+A}{1-A} . \tag{2}$$

The experimental data showed a significant difference w.r.t. the theoretical ones. The model has been further improved by introducing a constant

linear resistance [1]) at the output of the OA (output resistance). In this new conditions, the time period T becomes:

$$T = T_1 + T_2 = \frac{L}{R_e}\left(\ln\frac{1+kA'}{1-A'} + \ln\frac{1+A'/k}{1-A'}\right), \tag{3}$$

with $A'<1$, where:

$$A' = \frac{R_1[(R+R_{loss})(R_1+R_2+r_0)+r_0(R_1+R_2)]}{(R_1+R_2)[R(R_1+R_2+r_0)+R_1r_0]},$$

$$R_e = \frac{(R+R_{loss})(R_1+R_2+r_0)+r_0(R_1+R_2)}{R_1+R_2+r_0}.$$

The theoretical results obtained with these relations were in a very good agreement with the experimental ones.

4. Experimental Results Concerning the $L-T$ Converter

In order to verify the validity of the improved model adopted an $L-T$ converter was constructed using a ROB 115 operational amplifier type, using precision resistances boxes (accuracy class=0.02) for R_1, R_2, R and a precision, inductance box (a.c.=0.2) with R_{loss} =29.3 Ω, measured in d.c.

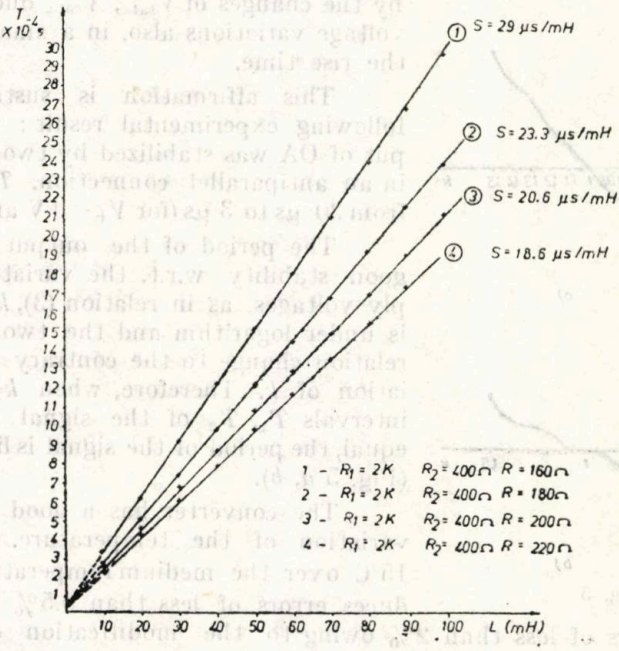

Fig. 4

[1]) In fact, the output resistance of the AO corresponding to V_{sat_-} and V_{sat_+} are neither identical nor linear.

The values of the converter components were adopted not only to satisfy the oscillation condition, but also to provide an as great as possible period in order to have a good sensitivity.

The purposes of the experiments were the following: a) the plot of the dependence $T(L)$ for different values of the resistance R; b) the determination of the nonlinearity error of the converter; c) the determination of the degree of accuracy for the adopted model and of the eventual supplementary error sources due to supply voltages and temperature variations.

In Fig. 4, the experimental dependence $T(L)$ for different values of the resistances and for L between 10 and 100 mH is shown.

Relation (3) shows that the $T(L)$ plot depends essentially of the value of R, i.e. reducing R, enhances T and the absolute sensitivity of the converter (practically, between 18.6 and 29 μs/mH).

The nonlinearity error of the converter determined from the experimental tabulated data is less than 0.5%.

The relative deviation between $T(L)$ obtained experimentally an dthe values obtained by relation (3) is less than 2%. This shows that the relation (3), determined by taking into consideration an output resistance of the saturated AO, r_0 ($r_0 \simeq 200\ \Omega$), represents a good approximation of the real dependence $T(L)$.

Computing by extrapolation of the experimental data the period corresponding to zero inductivity a residual time period of about 30 μs was found. This value depends on the nonideal character of the OA. It is influenced by the changes of V_{sat-}, V_{sat+} due to the supply voltage variations also, in a small measure by the rise time.

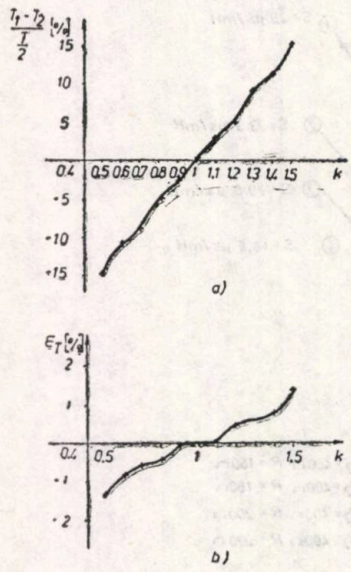

Fig. 5

This affirmation is sustained by the following experimental result: when the output of OA was stabilized by two Zener diodes in an antiparallel connection, T_r is reduced from 30 μs to 3 μs (for $V_+ = 9$ V and $V_- = 12$ V).

The period of the output signal has a good stability w.r.t. the variation of the supply voltages, as in relation (3), $k = |V_{sat-}/V_{sat+}|$ is under logarithm and the two terms of the relation change to the contrary with the variation of k. Therefore, when $k \neq 1$, even the intervals T_1, T_2 of the signal becomes nonequal, the period of the signal is little influenced (Fig. 5 *a*, *b*).

The converter has a good behaviour at variation of the temperature. A change of 15°C over the medium temperature (23°C) produces errors of less than 0.5% and a change of 25°C, errors of less than 2% owing to the modification of V_{sat+}, V_{sat-} and of the output resistances of the OA.

The temperature error can be reduced still more, by adding a supplementary resistance at the output of the OA, but at the price of the sensitivity reduction.

Practically, for the reduction of the error from 2% to 1% it was necessary to supplement the output resistance of OA with 1.2 k and consequently the sensitivity was reduced to a half.

5. Experimental Results Concerning the Numerical Displacement Inductive Transducer

The dependence $T(x)$ for an inductive transducer with a mobile coil with a 50 cm stroke was investigated for displacements between 5 and 25 cm, for which the relation $L(x)$ is approximatively linear.

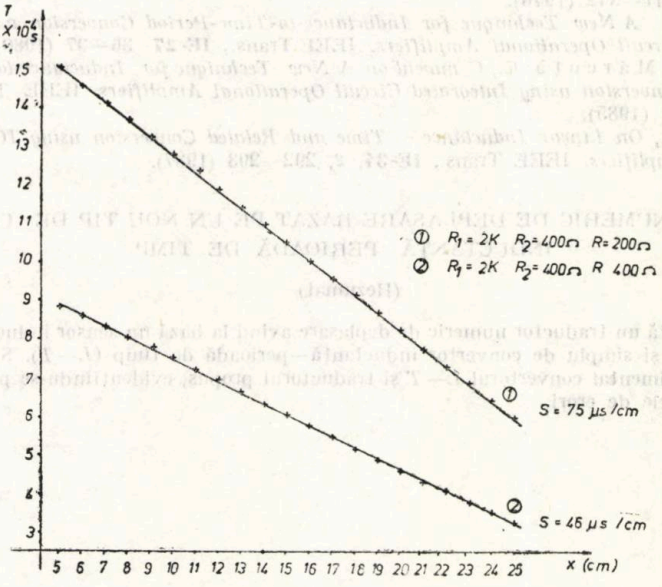

Fig. 6

The experimental $T(x)$ is presented in Fig. 6 for two values of R of the $L-T$ converter ($R=200\ \Omega$, $400\ \Omega$). The absolute transducer sensitivity was found 75 μs/cm and 46 μs/cm, respectively. The error of nonlinearity resulted from the experimental tabulated date was less than 0.5%.

6. Conclusions

The method proposed in this paper concerning the realization of the numerical displacement inductive transducer is simple and allows the direct conversion of the displacement into time-period.

It can be used for measuring medium and large displacement from 0 ... 100 mm to 0 ... 2 000 mm.

The theoretical analysis of the $L-T$ led to the relation (3) for the time period output which was in a good agreement with the experimental data.

The numeric displacement transducer proposed exhibits a good linearity, sensitivity and a good behaviour at variations of supply voltages and temperature.

Received, March 10, 1990

Polytechnic Institute, Jassy,
Department of Electrical Measurements
and
Department of Electronics

REFERENCES

1. A h m a d W., I a n i M.A., *Inductance-to-Time-Period Conversion*. IEEE Trans., **IECI-23**, 341—342 (1976).
2. S e n a n i R., *A New Technique for Inductance-to-Time-Period Conversion using Integrated Circuit Operational Amplifiers*. IEEE Trans., **IE-27**, 36—37 (1980).
3. G o r a ş L., M ă r c u ţ ă C., *Comment on A New Technique for Inductance-to-Time-Period Conversion using Integrated Circuit Operational Amplifiers*. IEEE Trans., **IE-32**, 35 (1985).
4. S e n a n i R., *On Linear Inductance — Time and Related Conversion using IC Operational Amplifiers*. IEEE Trans., **IE-34**, *2*, 292—293 (1987).

TRADUCTOR NUMERIC DE DEPLASARE BAZAT PE UN NOU TIP DE CONVERTOR INDUCTANŢĂ—PERIOADĂ DE TIMP

(Rezumat)

Se prezintă un traductor numeric de deplasare având la bază un senzor inductiv introdus într-un tip nou şi simplu de convertor inductanţă—perioadă de timp ($L-T$). Se analizează teoretic şi experimental convertorul $L-T$ şi traductorul propus, evidenţiindu-se performanţele acestora şi sursele de erori.

BULETINUL INSTITUTULUI POLITEHNIC DIN IAȘI
Tomul XXXVI (XL), Fasc. 3—4, 1990
Secția III
ELECTROTEHNICĂ. ENERGETICĂ. ELECTRONICĂ. AUTOMATIZĂRI

C.D. 621.317.083.2

MÉTHODE DE ZÉRO POUR LA MESURE DES PARAMÈTRES DES BOBINES ET DES CONDENSATEURS LINÉAIRES À PERTES

PAR

ADRIAN CREȚU, RADU COCIU, ELENA CREȚU et LIVIA COCIU

1. Introduction

En continuant les recherches antérieures en ce qui concerne la mesure des paramètres R, L, C des circuits de c.a. [1] ... [6] on propose une méthode de zéro, de haute sensibilité, qui permet la mesure des paramètres des bobines et des condensateurs linéaires, à un facteur de qualité réduit.

2. Le schéma structural de mesure

Le schéma électrique de principe, qui correspond à la méthode de zéro pour la mesure des paramètres des bobines, est indiqué dans la Fig. 1.

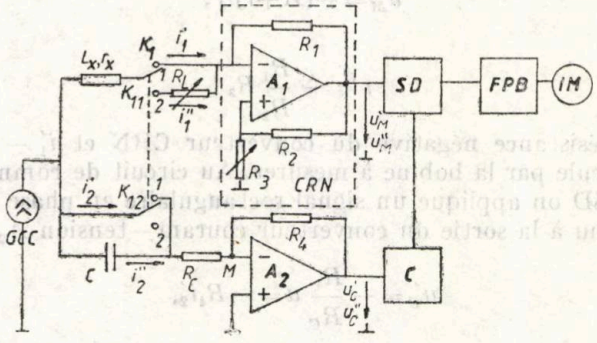

Fig. 1

La première branche du schéma de mesure contient l'élément du circuit à mesurer, la bobine d'inductivité L_x et la résistance r_x, que l'on peut connecter par la section K_{11} du commutateur K_1, soit directement (K_{11} en position *1*), soit par l'intermédiaire d'une résistance réglable R_L (K_{11} en position *2*) au convertisseur de résistance négative CRN [10], réalisé à l'aide de l'amplificateur opérationnel A_1 et les résistances R_1, R_2, R_3.

La deuxième branche a un caractère actif (K_{12} en position *1*) ou bien capacitif—actif (K_{12} en position *2*) et contient une résistance fixe R_C, un

condensateur C considéré sans pertes et un converteur courant—tension, réalisé à l'aide de l'amplificateur opérationnel A_2 et la résistance R_4.

L'indicateur de zéro (de quadrature) utilisé est constitué par un instrument magnéto-électrique IM, connecté avec le filtre passe-bas FPB, dans le circuit de sortie d'un synchrodétecteur SD à une borne commune entre ses circuits de mesure et de commande [9].

Les deux branches du schéma de mesure, connectées pratiquement en dérivation (le point M est un point virtuel de masse et l'impédance du circuit de mesure du synchrodétecteur SD est pratiquement infinie, $i_M \approx 0$) sont alimentées avec un signal sinusoïdal, de pulsation ω, par le générateur de courant constant GCC. Pour le circuit de mesure du synchrodétecteur SD, ayant l'impédance d'entrée pratiquement infinie ($i_M \approx 0$), on applique le signal sinusoïdal u_M, proportionnel et en opposition de phase avec le courant i_1, de la première branche du schéma (par la bobine à mesurer) et pour son circuit de commande un signal rectangulaire, en phase avec le signal sinusoïdal u_C, proportionnel et en opposition de phase avec le courant i_2 qui passe par la deuxième branche de mesure. La conversion du signal sinusoïdal u_C en signal rectangulaire se réalise par l'intermédiaire d'un circuit formateur d'impulsions (comparateur) CFI.

La mesure des paramètres de la bobine L_x, r_x comporte deux étapes :

a) La première, pour la mesure de la résistance de pertes r_x, le commutateur K_1 bipositionnel, à deux sections K_{11} et K_{12}, est branché en position *1*, en shuntant ainsi le condensateur C.

Au circuit de mesure du synchrodétecteur SD on applique le signal sinusoïdal obtenu à la sortie d'lamplificateur opérationnel A_1, ayant l'expression :

$$u'_M = -(R+r)i'_1, \tag{1}$$

où [10] :

$$r = -\frac{R_1}{R_2}R_3 \tag{2}$$

représente la résistance négative du converteur CRN et i'_1 — l'intensité du courant qui circule par la bobine à mesurer. Au circuit de commande du synchrodétecteur SD on applique un signal rectangulaire en phase avec le signal sinusoïdal obtenu à la sortie du converteur courant—tension A_2, c'est-à-dire :

$$u'_C = -\frac{R_4}{R_C}u = -R_4 i'_2, \tag{3}$$

où : i'_2 est l'intensité du courant qui circule par la résistance R_2 et u — la tension appliquée aux bornes des deux branches du schéma de mesure connectées en parallèle.

La déviation α de l'instrument magnéto-électrique IM a, dans cette première étape, l'expression [9] :

$$\alpha = S_{SD}U'_M \cos(\widehat{\underline{U}'_M, \underline{U}'_C}) \tag{4}$$

qui, tenant compte de (1) et (3), devient

$$\alpha = S_{SD}U'_M \cos(\widehat{\underline{I}'_1, \underline{U}}), \tag{5}$$

où S_{SD} représente la sensibilité globale du synchrodétecteur utilisé.

On règle la résistance r du converteur CRN (par l'intermédiaire de la résistance R_3, le rapport R_1/R_2=const.) jusqu'à ce que la déviation α de l'instrument IM, donnée par la relation (5), devient égale à zéro. En ce moment la tension u aux bornes de la branche inductive et le courant i_1' sont en quadrature et la résistance totale de cette branche devient égale à zéro, respectivement :

$$r-r_x=0. \tag{6}$$

Tenant compte de (2) et de (6) il résulte :

$$r_x=R_3\frac{R_1}{R_2}. \tag{7}$$

En adoptant pour le rapport des résistances R_1/R_2 des valeurs adéquates, en fonction des gammes de mesure imposées au début, on peut étalonner la résistance R_3 directement en valeurs de la résistance de pertes r_x de l'élément appartenant au circuit mesuré (bobine linéaire ou condensateur linéaire à schéma équivalent en série).

b) Dans la deuxième étape, en gardant la résistance négative du converteur CRN à la valeur (7), résultée de la première étape, on passe le commutateur K_1 en position *2*. En conséquence, dans la première branche, en série avec la bobine de mesure et le converteur CRN, on introduit la résistance réglable connue R_L et dans l'autre branche, en série avec la résistance R_C, on introduit le condensateur C, supposé sans pertes.

Au circuit de mesure du synchrodétecteur SD on applique, dans ce cas, le signal sinusoïdal :

$$u_M''=-(R_1+r)i_1'', \tag{8}$$

en opposition de phase avec le courant i_2'' de la branche inductive—active L_x, R_L et au circuit de commande un signal rectangulaire, en phase avec le signal sinusoïdal :

$$u_C''=-R_4i_2'', \tag{9}$$

en opposition de phase avec le courant i_2'' de la branche capacitive—active C, R_C.

En tenant compte de (8) et (9), de l'équation (4) résulte l'expression de la déviation α de l'instrument magnéto-électrique IM dans la nouvelle situation à savoir :

$$\alpha=S_{SD}U_M''\cos(\underline{\underline{U}}_M'', \underline{\underline{U}}_C'')=S_{SD}U_M''\cos(\underline{\underline{I}}_1'', \underline{\underline{I}}_2''). \tag{10}$$

On règle la résistance R_L jusqu'à ce que la déviation α devient de nouveau égale à zéro, moment qui coïncide à celui de la réalisation de la quadrature des courants i_1'' et i_2'' qui circulent par les deux branches du schéma de mesure. Dans ce moment, entre les paramètres L_x, R_L, C, R_C, appartenant aux deux branches connectées en parallèle, est vérifiée la condition connue [7], [8] :

$$L_x=R_LR_CC. \tag{11}$$

Pour des valeurs adéquates (en fonction de la sensibilité et la précision à réaliser) du produit $R_C C = \text{const.}$, qui correspondent à chaque gamme de mesure imposée initialement, on peut étalonner la résistance R_L directement par rapport aux valeurs de l'inductivité propre L_x à mesurer.

La méthode proposée peut être utilisée aussi pour la mesure des paramètres C_x, r_x des condensateurs à pertes, ayant le schéma équivalent série. Dans ce but le condensateur à mesurer doit être connecté à la première branche (au lieu de la bobine L_x) et au lieu du condensateur étalon C doit être introduite une bobine à paramètres L, r_L, connus (la résistance R_C renferme aussi r_L).

La sensibilité de mesure du schéma proposé dans le cas de la mesure d'inductivité propre L_x, possible à calculer par une méthodologie similaire à celle utilisée dans [7], a l'expression :

$$(12) \qquad S_\alpha = \frac{\mathrm{d}\alpha}{\mathrm{d}R_L}\Big|_{U_M=\text{ct.}} = S_{SD} U_M \frac{L_x(R_L + L_x R_C C\omega^2)}{\sqrt{R_\delta^2\omega^2C^2+1}\,(R_L^2+\omega^2L_x^2)^{3/2}},$$

où ω est la pulsation du signal d'alimentation du générateur GCC.

Dans le moment de la quadrature des courants appartenant aux deux branches, compte tenu de la condition (11), l'expression (12) devient :

$$(13) \qquad S_{\alpha_0} = S_{SD} U_M \frac{R_C C\omega}{R_L(1+\omega^2C^2R_\delta^2)}.$$

Étant donné que la sensibilité globale du synchrodétecteur dépend, surtout, de la sensibilité de mesure de l'instrument magnéto-électrique utilisé (microampèremètre ou galvanomètre), de (13) il résulte que les erreurs de sensibilité dans la détermination de la quadrature des courants sont pratiquement négligeables pour un intervalle étendu des valeurs du paramètre à mesurer.

D'ailleurs, l'expression (13) permet la détermination, par des calculs assez simples, pour chaque gamme de mesure de l'inductivité L_x, des valeurs de travail optima des paramètres de circuit C, R_C et de la pulsation ω, de sorte qu'on assure la sensibilité de mesure maxima pour tout le domaine de mesure (on obtient $S_{\alpha_0 \max} = S_{SD} U_M / 2R_L$ pour $Q = L_x/R_L = CR_C = 1$).

Les erreurs introduites à la mesure des résistances de pertes r_x sont déterminées, généralement (v. (7)), par celles du convertisseur de résistance négative CRN (qui augmentent avec la fréquence), les erreurs de mesure de l'inductivité L_x (la capacité C_x), comme il résulte de (11) et par les erreurs de construction des éléments du circuit étalon utilisé.

3. Conclusions

On propose une méthode de zéro destinée à la mesure des paramètres des circuits de c.a. linéaires qui permet la mesure simple, par un double processus de zéro, tant pour l'inductivité propre et pour la capacité que pour la résistance de pertes des bobines, respectivement des condensateurs linéaires caractérisés par des facteurs de qualité réduits (≈ 1). Le schéma proposé est caracterisé par une sensibilité de mesure élevée, l'indicateur de zéro utilisé en étant un instrument magnéto-électrique de grande sensibilité.

L'annulation de la déviation de l'instrument (la quadrature) en chaque des deux étapes de mesure (l'augmentation de la résistance r_x, respectivement de l'inductivité L_x) est réalisée par le réglage d'une seule résistance de précision (R_3, respectivement R_L) en existant la possibilité d'automatisation, relativement simple, de ce processus.

On peut obtenir les valeurs des paramètres à mesurer directement par l'étalonnage des deux résistances réglables (R_3, respectivement R_L) par rapport aux valeurs de r_x, respectivement L_x (ou C_x), selon la relation (7), respectivement (11).

La fréquence du signal d'alimentation affecte seulement la sensibilité de mesure du schéma (v. 13)).

En partant du schéma proposé on peut construire des appareils pour la mesure des paramètres R, L, C caractérisés par un rapport performance/prix supérieur à celui réalisé par les appareils actuels (ponts, Q-mètres, etc.).

Reçue le 19 mars 1990

Institut Polytechnique, Jassy,
Chaire d'Électrotechnique et Machines électriques

BIBLIOGRAPHIE

1. Creţu A., *Metodă şi aparat pentru detectarea rezonanţei în circuitele electrice.* Patent R.S.R. *94 218* (1987).
2. Creţu A., *Aparat pentru măsurarea parametrilor bobinelor şi condensatoarelor liniare.* Bul. Inst. polit., Iaşi, **XXVII (XXXI)**, *1—2*, s. III, 43—52 (1981).
3. Creţu A., *Aparat penru măsurarea paratmetrilor RLC ai circuitelor de curent alternativ liniare.* Patent R.S.R. *97 826* (1989).
4. Creţu A., *Metodă de zero şi aparat pentru indicarea rezonanţei în circuitele derivaţie complet-aperiodice.* Patent R.S.R., *94 116* (1987).
5. Creţu A., Creţu E., *About Resonance Indication in Complete-Aperiodic Parallel Circuits.* Bul. Inst. polit., Iaşi, **XXXIII (XXXVII)**, *1—4*, s. III, 25—31 (1987).
6. Creţu A., Creţu E., Cociu R., *The Aperiodic Q-metter.* Bul. Inst. polit., Iaşi, **XXXIV (XXXVIII)**, *1—4*, s. III, 27—32 (1988).
7. Savin G., *Metodă pentru măsurarea inductanţelor şi capacităţilor în regim permanent armonic şi nearmonic, prin defazarea curenţilor la 90°.* Thèse de doctorat, Inst. polit., Iaşi, 1961.
8. Creţu A., *About the Coils and Condensers Parameters Measurement for 90° Phase Angle,* Bul. Inst. polit., Iaşi, **XXXV (XXXIX)**, *1—2*, s. III, 25—29 (1989).
9. Creţu A., *Detector—amplificator sensibil la fază.* Patent R.S.R., *83 632* (1983).
10. Bulucea C., *Circuite integrate liniare.* Ed. Tehn., Buc., 1976.

METODĂ DE ZERO PENTRU MĂSURAREA PARAMETRILOR BOBINELOR ŞI CONDENSATOARELOR CU PIERDERI

(Rezumat)

Se propune şi se studiază o metodă de zero pentru măsurarea parametrilor bobinelor şi condensatoarelor liniare cu pierderi, care, printr-un dublu procedeu de zero, simplu şi rapid, permite determinarea atît a rezistenţei de pierderi cît şi a inductivităţii, respectiv capacităţii elementelor de circuit liniare avînd schema echivalentă serie.

Se prezintă şi se studiază schema de principiu a unui aparat destinat măsurării parametrilor R, L, C ai circuitelor liniare de c.a., la frecvenţe joase, cu factor de calitate redus ($Q<1$). Se stabilesc ecuaţiile de funcţionare şi se calculează sensibilitatea de măsură.

Se evidenţiază faptul că rezultatele experimentale, în concordanţă cu cele teoretice, obţinute pe baza acestei metode, permit realizarea unor aparate cu performanţe ridicate, superioare celor existente în stadiul actual.

BULETINUL INSTITUTULUI POLITEHNIC DIN IAȘI
Tomul XXXVI (XL), Fasc. 3—4, 1990
Secția III
ELECTROTEHNICĂ. ENERGETICĂ. ELECTRONICĂ. AUTOMATIZĂRI

C.D. 621.317.383

MÉTHODE ET RELATION DE CALCUL POUR MESURER LA PUISSANCE ACTIVE AVEC UN WATTMÈTRE À BOBINE DE COURANT SHUNTÉE

PAR

DORIN BELAUS et DOINA ZAMFIR

1. Introduction

Les derniers années, les entreprises industrielles sont de plus en plus intéressées à étudier les caractéristiques de fonctionnement en charge de chaque moteur électrique afin de trouver les moyens à économiser la consommation d'energie électrique.

Si la machine n'est pas équipée d'un appareillage de mesure adéquat (comptoir, wattmètre), il faut couper le courant et monter les appareils dont on dispose. Cette opération est difficile à réaliser si le processus technologique ne permet pas l'arrêt de la machine.

Nous proposons dans ce qui suit une solution convenable concernant la mesure de la puissance active absorbée (ou de l'énergie) par chaque moteur électrique en charge si le réseau d'alimentation ne permet pas d'installer des transformateurs de courant, ou bien s'il faut effectuer la mesure en courant continu.

2. La méthode proposée

On doit disposer d'un wattmètre à bobine de courant divisée en deux demi-bobines qui peuvent être connectées par un commutateur, d'abord en série et puis en parallèle. La bobine de tension du wattmètre ne pose pas de problèmes quant à son branchement au réseau.

Les bornes d'accès de la bobine de courant peuvent être branchées à n'importe quelle résistance qui se trouve en série au consommateur d'énergie électrique, de façon que la bobine de courant soit shuntée. Le schéma de mesure proposé est présenté dans la Fig. 1 *a*, *b*.

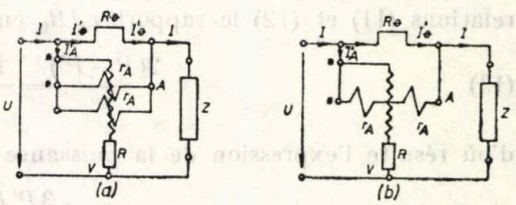

Fig. 1

Dans ce que suit on va prouver que la valeur de la résistance shuntée n'influence pas le calcul de la puissance et par conséquent il n'est pas nécessaire de la connaître. Cette résistance peut être celle d'échauffement du bimétal d'un relais thermique ou bien les contacts d'un contacteur, etc.

Notons par I'_A et I''_A les intensités des courants qui circulent par les demibobines ampère connectées en parallèle et respectivement en série ; par r_A — la résistance d'une demibobine et par R_θ —la résistance du shunt.

Dans le calcul on admet que $z_A = r_A$ et que le courant absorbé par le recepteur reste constant au cours des mesures effectuées. On néglige aussi le courant qui circule par la bobine de tension du wattmètre.

Les puissances indiquées par l'aiguille du wattmètre dans ces deux cas seront :

$$(1) \qquad P' = UI'_A \cos\varphi = K_1\alpha_1, \qquad (2) \qquad P'' = UI''_A \cos\varphi = K_2\alpha_2,$$

ou l'on a noté par α_1 et α_2 la déviation de l'aiguille pour le cas a et respectivement b, K_1, K_2 — constantes du wattmètre pour ces deux échelles, pour la bobine de courant ($K = U_n I_n / N_{div}$, [W/div.]).

Les théorèmes de Kirchoff fournissent pour le cas a :

$$(3) \qquad I = I'_A + I'_\theta, \qquad (4) \qquad I'_A \frac{r_A}{2} = I'_\theta R_\theta,$$

et pour le cas b :

$$(5) \qquad I = I''_A + I''_\theta, \qquad (6) \qquad 2I''_A r_A = I''_\theta R_\theta.$$

Compte tenu de (5) et (6) il résulte :

$$(7) \qquad I = I'_A\left(1 + \frac{r_A}{2R_\theta}\right), \qquad (8) \qquad I = I''_A\left(1 + \frac{2r_A}{R_\theta}\right).$$

En introduisant les relations (7) et (8) dans les expressions des puissances (1) et (2), on obtient :

$$(9) \quad P' = U\frac{I}{1 + r_A/2R_\theta}\cos\varphi = K_1\alpha_1, \quad (10) \quad P'' = U\frac{I}{1 + 2r_A/R_\theta}\cos\varphi = K_2\alpha_2.$$

Mais le terme $UI\cos\varphi = P$ représente la puissance active absorbée par le récepteur, donc :

$$(11) \quad P' = \frac{P}{1 + r_A/2R_\theta} = K_1\alpha_1, \quad (12) \quad P'' = \frac{P}{1 + 2r_A/R_\theta} = K_2\alpha_2.$$

Pour éliminer les résistances inconnues r_A et R_θ on élimine entre les relations (11) et (12) le rapport r_a/R_θ en obtenant

$$(13) \qquad \frac{2(P - P')}{P'} = \frac{P - P''}{2P''},$$

d'où résulte l'expression de la puissance P, absorbée par le récepteur :

$$(14) \qquad P = \frac{3P'P''}{4P'' - P'},$$

soit :

$$(14') \qquad P = \frac{3K_1K_2\alpha_1\alpha_2}{4K_2\alpha_2 - K_1\alpha_1},$$

où :

$$(15) \qquad K_1 = \frac{U_n I_{np}}{N_{div}} \quad \text{et} \quad K_2 = \frac{U_n I_{ns}}{N_{div}},$$

avec: U_n — la tension nominale de la bobine volt, qui reste invariable pendant les mesures; I_{np} — le courant nominal de la bobine ampère dans les demibobines liées en paralléle; I_{ns} — le courant nominal de la bobine ampère dans les demibobines liées en série; N_{div} — le nombre des divisions du cadrane de l'appareil.

On recommande d'effectuer d'abord la mesure avec les demibobines en parallèle, parce que:

$$I_{np}=2I_{ns}. \tag{16}$$

En vertu de cette relation on observe que:

$$K_1=2K_2 \tag{17}$$

de sorte que la relation (14′) devient:

$$P=\frac{3}{2}K_1\frac{\alpha_1\alpha_2}{2\alpha_2-\alpha_1} \quad \text{ou} \quad (18') \qquad P=3K_2\frac{\alpha_1\alpha_2}{2\alpha_2-\alpha_1}. \tag{18}$$

Les formules (18) et (18′) fournissent la valeur de la puissance active cherchée, en fonction des déviations α_1 et α_2 de l'aiguille de l'appareil et des constantes K_1 ou K_2.

3. Le calcul des erreurs

Afin de calculer les erreurs on tient compte du fait que le résultat est obtenu à la suite de deux mesures et d'un calcul algébrique. On devra appliquer la manière de calcul des erreurs recommandée aux mesures indirectes en développant la fonction $P(\alpha_1, \alpha_2)$ en série de Taylor, où on neglige les termes d'ordre supérieur. Ainsi, pour l'erreur relative on applique la relation:

$$\varepsilon_r=\frac{\Delta P}{P}=\frac{\partial P}{\partial\alpha_1}\cdot\frac{\Delta\alpha_1}{P}+\frac{\partial P}{\partial\alpha_2}\cdot\frac{\Delta\alpha_2}{P} \tag{19}$$

qui, tous calculs effectués, conduit à:

$$\varepsilon_r=\frac{1}{2\alpha_2-\alpha_1}\left(2\alpha_2\frac{\Delta\alpha_1}{\alpha_1}-\alpha_1\frac{\Delta\alpha_2}{\alpha_2}\right); \tag{20}$$

elle reste valable pour la formule (18′) aussi.

Les rapports $\Delta\alpha_1/\alpha_1$ et $\Delta\alpha_2/\alpha_2$ sont calculés à l'aide de la relation:

$$\frac{\Delta\alpha}{\alpha}=\frac{c}{100}\cdot\frac{\alpha_{max}}{\alpha_x}, \tag{21}$$

où: c répresente la classe de précision de l'appareil; α_{max} — l'angle maximum de déviation de l'aiguille de l'appareil; α_x — l'angle de déviation lu sur l'échelle pendant la mesure.

En considérant les termes de la relation (20) en valeurs absolus, l'erreur relative maximum sera:

$$|\varepsilon_r|_{max}=\frac{1}{2\alpha_2-\alpha_1}\left(2\alpha_2\frac{\Delta\alpha_1}{\alpha_1}+\alpha_1\frac{\Delta\alpha_2}{\alpha_2}\right). \tag{22}$$

Pour analyser la variation de l'erreur en fonction de la puissance et des paramètres du circuit on va modifier la rélation (22) en la multipliant et divisant par $\frac{3}{2}K_1\alpha_1\alpha_2$; on obtient :

$$|\varepsilon_r|_{max}=\frac{2}{3}\cdot\frac{P}{K_1}\left(\frac{2}{\alpha_1}\cdot\frac{\Delta\alpha_1}{\alpha_1}+\frac{1}{\alpha_2}\cdot\frac{\Delta\alpha_2}{\alpha_2}\right). \tag{22'}$$

À l'aide des expressions (11) et (12) on détermine α_1 et α_2 en fonction de P, r_A et R_θ :

$$\alpha_1=\frac{2R_\theta P}{K_1(r_A+2R_\theta)}, \tag{23}$$

$$\alpha_2=\frac{R_\theta P}{K_2(2r_A+R_\theta)}, \tag{24}$$

de sorte que la relation (22') devient, tout en gardant les variations relatives α_1 et α_2, de la forme :

$$|\varepsilon_r|_{max}=\frac{2}{3}\left[\left(\frac{r_A}{R_\theta}+2\right)\frac{\Delta\alpha_1}{\alpha_1}+\frac{K_2}{K_1}\left(\frac{2r_A}{R_\theta}+1\right)\frac{\Delta\alpha_2}{\alpha_2}\right]. \tag{25}$$

En tenant compte de (17) la relation (25) devient

$$|\varepsilon_r|_{max}=\frac{2}{3}\left[\left(\frac{r_A}{R_\theta}+2\right)\frac{\Delta\alpha_1}{\alpha_1}+\frac{1}{2}\left(\frac{2r_A}{R_\theta}+1\right)\frac{\Delta\alpha_2}{\alpha_2}\right]. \tag{26}$$

Si on remplace $\Delta\alpha_1/\alpha_1$ et $\Delta\alpha_2/\alpha_2$ par (21) on obtient l'expression:

$$|\varepsilon_r|_{max}=\frac{1}{3}\frac{c\alpha_{max}}{100}\left[2\left(\frac{r_A}{R_\theta}+2\right)\frac{1}{\alpha_1}+\left(\frac{2r_A}{R_\theta}+1\right)\frac{1}{\alpha_2}\right]. \tag{27}$$

On introduit le notation $r_A/R_\theta=m$ et la valeur maximum de l'erreur sera alors :

$$|\varepsilon_r|_{max}=\frac{1}{3}\cdot\frac{c}{100}\alpha_{max}\left[2(m+2)\frac{1}{\alpha_1}+(2m+1)\frac{1}{\alpha_2}\right]. \tag{27'}$$

On observe que l'erreur maximum dépend de la somme de deux termes, chacun variant en raison inverse par rapport à l'angle α, comme dans le cas de tout appareil à aiguillle indicatrice, mais affectée par un paramètre m, positif, qui doit être étudié séparément compte tenu que $\alpha_1\neq\alpha_2$. Afin d'apprecier plus exactement la valeur réelle de l'erreur on va étudier ci-dessous la contribution de chaque terme de la relation (27') séparément. On utilise la notation :

$$|\varepsilon_r|_{max}=|\varepsilon_r|_{m_1}+|\varepsilon_r|_{m_2},$$

où :

$$|\varepsilon_r|_{m_1}=\frac{2}{3}\cdot\frac{c}{100}\cdot\frac{\alpha_{max}}{\alpha_1}(m+2)=\frac{2}{3}A_1(m+2) \tag{28}$$

et :

$$|\varepsilon_r|_{m_2}=\frac{1}{3}\cdot\frac{c}{100}\cdot\frac{\alpha_{max}}{\alpha_2}(2m+1)=\frac{1}{3}A_2(2m+2), \tag{29}$$

où l'on a noté par $A_1=\frac{c}{100}\cdot\frac{\alpha_{max}}{\alpha_1}$ et respectivement, $A_2=\frac{c}{100}\cdot\frac{\alpha_{max}}{\alpha_2}$ les erreurs relatives de l'appareil aux mesures de α_1 et α_2, c'est-à-dire aux

mesures directes, en absence de R_0, ($R_0=\infty$, $m=0$), pour le cas des demibobines connectées en parallèle (A_1) ou en série (A_2).

On peut analyser la contribution du facteur m en considérant A_1 et A_2 constants pour certaines valeurs de α_1 et α_2.

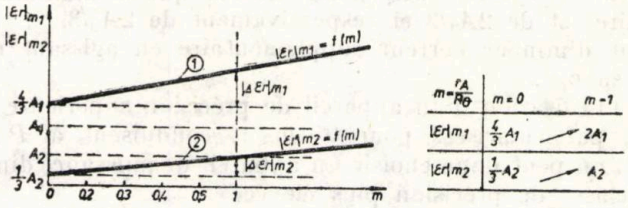

Fig. 2

Le diagramme de la Fig. 2 présente la variation de $|\varepsilon_r|_{m_1}$ et $|\varepsilon_r|_{m_2}$ en fonction de m.

Le rapport des relations (23) et (24) conduit à

$$\frac{\alpha_1}{\alpha_2}=\frac{2K_2}{K_1}\cdot\frac{2r_A+R_0}{r_A+2R_0}, \tag{30}$$

ou, en introduisant m:

$$\frac{\alpha_1}{\alpha_2}=\frac{2K_2}{K_1}\cdot\frac{2m+1}{m+2}=\frac{2m+1}{m+1}, \tag{31}$$

où l'on a tenu compte de (17).

Pour $m=0$ résulte

$$\alpha_2=2\alpha_1 \tag{32}$$

ce qui conduit à $A_1=2A_2$.

On observe du diagramme ci-dessus que les erreurs augmentent d'une façon linéaire en fonction du paramètre m, l'erreur étant double pour $m=1$ à la première mesure, pendant que pour la deuxième, l'erreur atteint la même valeur que celle obtenue pour la mesure directe (A_2). Cela signifie que dans l'intervale $m\in[0, 1]$ la deuxième mesure conduit à une erreur variant de $A_2/3$ jusqu'à A_2, donc diminuée par rapport à celle de la mesure directe ($R_0=\infty$).

En effectuant la moyenne arithmétrique des erreurs aux limites de l'intervalle ($m=0$, $m=1$) on observe un nivellement des erreurs de $3A_1/4$ jusqu'à $5A_1/8$.

Les relations (28) et (29), conduisent, pour $m=0$, à :

$$|\varepsilon_r|_{m_{10}}=\frac{4}{3}\cdot\frac{c}{100}\cdot\frac{\alpha_{\max}}{\alpha_1}=\frac{4}{3}A_1 \tag{33}$$

et

$$|\varepsilon_r|_{m_{20}}=\frac{1}{3}\cdot\frac{c}{100}\cdot\frac{\alpha_{\max}}{\alpha_2}=\frac{1}{3}A_2. \tag{34}$$

Par opposition à la mesure directe, celle à l'aide du shunt introduit une erreur supplémentaire :

$$|\Delta\varepsilon_r|_{m1}=|\varepsilon_r|_{m1}-|\varepsilon_r|_{m10}=\frac{2}{3}\cdot\frac{c}{100}\cdot\frac{\alpha_{\max}}{\alpha_1}m \tag{35}$$

et

$$(35) \qquad |\Delta\varepsilon_r|_{m2} = |\varepsilon_r|_{m2} - |\varepsilon_r|_{m20} = \frac{2}{3} \cdot \frac{c}{100} \cdot \frac{\alpha_{max}}{\alpha_2} m,$$

donc un accroissement proportionnel à m.

Si on choisit $r_A \leqslant R_\theta$, $(m \leqslant 1)$, on observe que le maximum de l'erreur supplémentaire est de $2A_1/3$ et respectivement de $2A_2/3$.

On peut diminuer l'erreur supplémentaire en agissant d'une manière adéquate à savoir :

1. Par l'utilisation d'un appareil de précision supérieure. Les relations (11) et (12), particularisées pour $0 < m \leqslant 1$, conduisent à $P > P' > 2P/3$ et $P > P'' > P/3$; on peut donc choisir un appareil de puissance diminuée jusqu'à $2P/3$ et de classe de précision plus élevée.

2. En choisissant un appareil convenable de façon que la déviation de l'aiguille soit plus proche du dernier tiers du cadran. Les mêmes relations (11) et(12) donnent pour $m=1$:

$$\alpha_1 = \frac{2}{3} \cdot \frac{P}{K_1} \quad \text{et} \quad \alpha_2 = \frac{1}{3} \cdot \frac{P}{K_2},$$

donc les déviations de l'aiguille ne dépassent pas 2/3 de l'échelle et on peut choisir un appareil plus sensible dont l'aiguille peut dévier jusqu'à la fin de l'échelle.

3. Par le choix d'un rapport $m = r_A/R_\theta$, afin que l'erreur soit minimum. On observe, si l'on analyse les courbes *1* et *2* de la Fig. 2, que la valeur moyenne des erreurs est située entre $3A_1/4$ et $5A_1/8$. En imposant la condition que la moyenne arithmétique ne dépasse pas l'erreur de la mesure directe aux demibobines couplées en parallèle (A_1), il en résulte :

$$\frac{|\varepsilon_r|_{m1} + |\varepsilon_r|_{m2}}{2} = \frac{2A_1(m+2) + A_2(2m+1)}{6} = A_1.$$

Compte tenu de l'égalite $A_1 = 2A_2$, le calcul fournit pour m la valeur $m=0{,}5$, c'est-à-dire :

$$(37) \qquad r_A = \frac{R_\theta}{2}.$$

On peut, donc, limiter l'intervalle des valeurs pour m de zero à 0,5.

4. Conclusions

La méthode proposée est simple et capable à être appliquée aux installations électriques qui ne disposent pas d'un appareillage specialisé pour les mesures d'énergie ou de la puissance, sans interrompre l'alimentation du récepteur. Ils s'avèrent nécesaires quatre conducteurs à fil isolé aux pinces à attacher, deux pour la bobine volt, aux bornes du récepteur et deux pour la bobine ampère, qui peuvent être branchés sur n'importe quelle résistance qui se trouve dans le trajet du courant (relais thermique, contacts, etc.), de preférence plus grande que $2r_A$.

Il est nécessaire à effectuer deux mesures; une fois avec les demibobines ampère disposées en parallèle et puis avec les demibobines en série

ce qu'on réalise à l'aide du commutateur de courant du watt mètre. On calcule ensuite la puissance à l'aide des relations (18) ou (18').

Si l'on respecte la condition $R_0 \geqslant 2r_A$ la méthode est tout aussi précise que celle directe. Il n'est pas nécessaire à connaître la valeur de la résistance R_0.

Les installations peuvent être munies d'abord avec des shunts afin de mesurer les courants, shunts qui peuvent servir également pour mesurer la puissance par la méthode proposée ci-dessus. On peut utiliser cette méthode pour la mesure de la puissance dans les installations à courant continu.

Reçue le 15 mars 1990

. *Institut Polytechnique, Jassy,*
Chaire de Machines électriques
et Électrotechnique générale
et
Chaire d'Automations

METODĂ ŞI RELAŢIE DE CALCUL PENTRU MĂSURAREA PUTERII ACTIVE, CU WATTMETRU CU BOBINĂ AMPER ŞUNTATĂ

(Rezumat)

În scopul urmăririi consumului de energie al motoarelor electrice la anumite intervale de timp este necesară introducerea unui wattmetru în schema de alimentare a motorului, fie în mod permanent, fie ori de cîte ori este nevoie. Pentru a nu întrerupe, în scopul măsurării, circuitul electric, se propune folosirea unui wattmetru cu două semibobine amper cu comutator serie—paralel. Legînd semibobinele în paralel cu un rezistor oarecare de pe traseul de alimentare al motorului (rezistenţa unui releu termic) şi efectuînd două măsurători succesive, se stabileşte relaţia de calcul cu ajutorul căreia se poate aprecia în mod corect valoarea puterii măsurate.

BULETINUL INSTITUTULUI POLITEHNIC DIN IAŞI
Tomul XXXVI (XL), Fasc. 3—4, 1990
Secţia III
ELECTROTEHNICĂ. ENERGETICĂ. ELECTRONICĂ. AUTOMATIZĂRI

C.D. 621.317 ; 621.34 ; 621.87

SUR LA MESURE NUMÉRIQUE DU RAYON DES GRUES À VOLÉE HORIZONTALE

PAR

M. CREŢU, LIVIU BRENIUC et C. SĂRMĂŞANU

1. Introduction

Il est obligatoire à connaître, en n'importe quell moment, la position du chariot porte-crochet sur la volée horizontale pour déterminer le couple de renversement et pour augmenter la fiabilité et le degré de sécurité en exploitation des grues [3].

La Fig. 1 représente le schéma d'enroulement du câble va-et-vient du chariot de charge. Le chariot *4* est équipé avec un tambour à cliquet pour fixer et étendre le câble *6* et un ressort *3* pour atténuer les chocs mécaniques.

Le câble *6*, étendu sur les roulettes *1*, est tiré par le tambour *2* mis en fonction par un moteur électrique par l'intermédiaire du réducteur mécanique. Des jalons sont fixés sur la volée horizontale *7* de la grue, à des distances de 10 m, sur toute sa longueur, de tel façon qu'on puisse estimer approximativement, de la cabine de commande, la position du chariot de charge par rapport à l'axe de la tour.

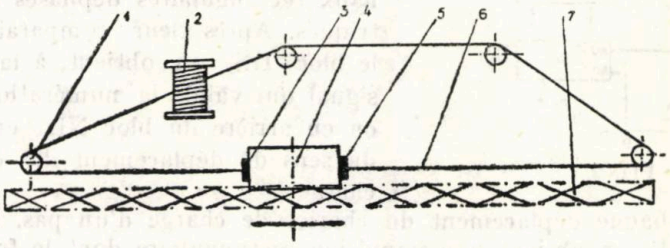

Fig. 1

Les câbles va-et-vient sont moulés dans une couche sur le tambour et déroulés selon le sens du mouvement du chariot porte-crochet.

2. Possibilités de mesurer le rayon à élément sensible numérique

Pour déterminer, en n'importe quel moment, la distance axe chariot mobile — axe tour, on peut utiliser des éléments sensibles de déplacement connus, mais leur nombre est limité par les conditions de travail et la gamme des déplacement à mesurer (0...45 m) [1], [2].

Les câbles va-et-vient étant actionnés par le tambour on dispose de la possibilité de coupler, sur son axe, l'élément sensible. Ainsi, par l'intermédiaire d'un réducteur mécanique ayant une démultiplication adéquate, on peut coupler une règle incrémentale. Même si elle donne des dates très précises (règle incrémentale optique), elle ne peut pas être utilisée en air libre et est aussi fortement influencée négativement par l'effet des jeux mécaniques.

Les disques optiques incrémentals ou absolus sont plus résistants et plus fiables. Mais ils soulèvent de nombreux problèmes d'optique et de mécanique concernant surtout la précision. Le traitement des signals afin d'afficher par voie numérique les valeurs des déplacements et le sens du mouvement est classique et ne pose pas de problèmes.

Bien que les règles à frappe électromagnétique utilisées pour mesurer les déplacements donnent des précisions inférieures à celles obtenues par les règles optiques [1], [2], leur fiabilité et résistance mécanique les recommande en tant qu'éléments sensibles dans les schémas de mesure numérique du rayon des grues.

3. Schéma de mesure utilisé

Les éléments de base de ce schéma sont : la règle incrémentale circulaire RC, les éléments sensibles de déplacement ES_1, ES_2, le discriminateur de sens DS, le générateur de tacts GT, le numérateur pour établir le pas NP, le sélecteur de pas SP, le numérateur de longueur NS, le décodeur D et le circuit pour l'affichage numérique de la longueur ANL (Fig. 2).

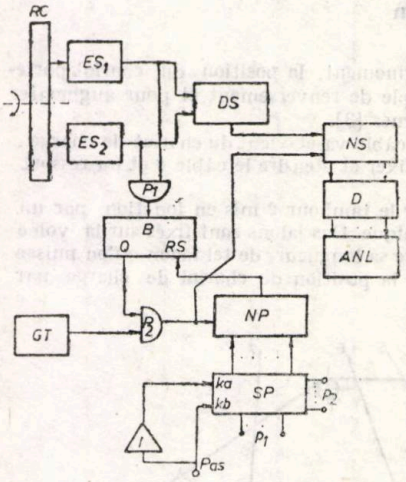

Fig. 2

3.1. Le fonctionnement du schéma

Les éléments sensibles de proximité ES_1, ES_2, situés devant la règle à frappée de réluctance, émettent d'une façon synchrone avec les pas, deux signaux rectangulaires déphasés à 90° électriques. Après leur comparaison, **dans** le bloc DS, on obtient, à la sortie, un signal qui valide la numération, devant ou en arrière du bloc NL, en fonction du sens de déplacement du chariot de charge.

Pour chaque déplacement du chariot de charge d'un pas, à la sortie de la porte P_1 on obtient une impulsion rectangulaire dont le front positif détermine le passage du flip-flop B dans l'état $Q=1$. De ce moment-ci les impulsions du GT vont vers le numérateur de longueur NL et le numérateur qui établit le pas, NP.

Puisque le règle à frappée de réluctance RC (Fig. 3) est divisée en n zones ferromagnétiques et D est le diamètre du tambour d'entrainement du câble du chariot, le déplacement minimum enregistré par l'installation de mesure devient égal au pas p de la règle:

$$P = \frac{\pi D}{n}, \quad [\text{mm}].$$

La valeur (en mm) du pas p est chargée par le NP en utilisant ses entrées de chargement parallèles. Les impulsions du GT provoquent la décrémenta-

tion du numérateur NP qui, après p impulsions revient à l'état zéro ; à ce point le numérateur commande l'effacement du bistable B et, par conséquent, le bloquage de la porte P_2 et aussi un nouveau chargement parallèle avec le pas p. De la sorte, pour chaque déplacement d'un pas du chariot, des impulsions se dirigent vers NL ; selon le sens du déplacement ils s'accumulent ou sont réduits dans le numérateur où, donc, est inscrite, en n'importe quel moment, la valeur mesurée du rayon de la grue. En employant l'information trouvée en NL et par l'intermédiaire des blocs D et ANL, on réalise l'indication numérique du rayon. Le schéma permet aussi la sélection de la valeur du pas, en utilisant le bloc de sélection SP, en fonction de la valeur du signal „pas".

3.2. Le sensor de déplacement

Le déplacement est saisi à l'aide d'une règle circulaire RC à frappée de réductance (Fig. 3) dont les zones ferromagnétiques (hachurées) alternent avec celles qui ne sont pas ferromagnétiques. La règle est fixée directement, sous le réducteur mécanique, comme intermédiaire à l'axe du tambour qui actionne les câbles. Devant la règle se trouvent les éléments sensibles de proximite ES_1 et ES_2 du type IPO51PO24 qui génèrent une impulsion négative en présence des secteurs métalliques ferromagnétiques (réluctance minimum), de sorte qu'à une rotation complète de la règle correspond un nombre d'impulsions égal avec celui des pas de la circonférence de la règle.

Si p est le pas de la règle, les éléments de proximité ES_1, ES_2 sont situés à un intervalle de $kp+3p/4$, $(k=0, 1, ..., n)$, de sorte que les signals générés par celui-ci soient dephasés de 90° électriques, déphasage nécessaire pour le discriminateur de sens DS (Fig. 2).

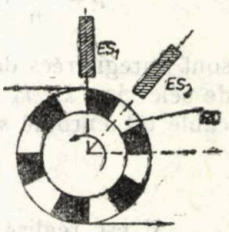

Fig. 3

3.3. Le circuit discriminateur de sens (DS)

Il est réalisé à l'aide de deux bistables du type D (MMC4013) commandés en anti-phase par les éléments sensibles de proximité ES_1, ES_2, en obtenant pour les sorties Q_1, Q_2 les valeurs $Q_1=1$, $Q_2=0$ quand le chariot se déplace en avant et $Q_1=0$, $Q_2=1$ quand le chariot se déplace en arrière.

Dans la Fig. 4 on indique les formes d'ondes des signals aux sorties des éléments sensibles et du signal de numération des pas pour le déplacement en avant (*b*), (*c*), (*d*), et respectivement, pour le déplacement en arrière (*e*), (*f*), (*g*).

Dans le montage, les sorties $Q_1=1$, $Q_2=1$ valident les entrées de numération en avant et respectivement en arrière, du numérateur de longueur NL.

3.4. Bloc numérateur pour établir le pas (NP)

Il est réalisé avec trois circuits décimals du type MMC4092 ; le schéma permet la modification de la valeur du pas quand, sur le tambour le câble est enroulé, au maximum, deux couches.

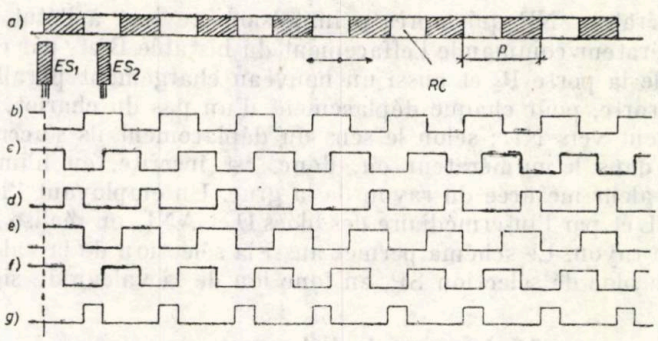

Fig. 4

Si D et D_1 sont les diamètres moyens des enroulements sur la I-ère et, respectivement, la II-ième couche et la règle circulaire à frappée de réluctance est munie avec n zones ferromagnétiques, les valeurs des pas (en binaire) :

$$p=\frac{\pi D}{n},\ [\text{mm}],\qquad \text{respectivement,}\qquad p_1=\frac{\pi D_1}{n},\ [\text{mm}],$$

sont enregistrées dans le bloc sélecteur de pas SP (3 X MMC4019) ; ses entrées de sélection k_a, k_b sont commandées par le signal „pas", 0 ou 1, selon que le câble est enroulé sur la I-ère ou sur la II-ième couche.

3.5. Le générateur de tacts (GT)

Il est réalisé avec βE555 et fonctionne à une fréquence de 100 KHz. Le schéma de mesure n'exige pas une stabilité différente pour la fréquence des tacts si celle des pas qui dépendent de la vitesse du tambour d'entraînement des câbles lui en est inférieure. Tout comme sur la grue, le tambour qui actionne les câbles va-et-vient du chariot de charge est entraîné par un moteur électrique de 1 500 tours/min. avec un réducteur mécanique ayant le rapport de 31,5, et compte tenu [3] que sur la surface de la règle RC à frapée de réluctance il y a q pas, la fréquence maximum des pas est :

$$f_p=9\,\frac{1\,500}{60\cdot 31,5}=7,1\ \text{Hz},$$

d'où il résulte que la période des pas est $T_p=0,14$ s, tandis que la période du signal de tact est $T=1/10^5=10$ μs.

Pour un diamètre du tambour $D=400$ mm la longueur du câble enroulée à une rotation du tambour, égale à un pas, est :

$$p=\frac{\pi D}{n}=139,55\ \text{mm}.$$

On choisit $p=140$ mm et par conséquent pendant une moitié de période ($0,5T_p=70$ ms) il faut passer vers la numération p impulsions, ou 140 impulsions d'une fréquence $f=100$ KHz. La durée nécessaire pour leur passage

est $\Delta t = 140.10 = 1{,}4$ ms (Fig. 5), inférieure à une moitié de période des pas (70 ms) et en conséquence la fréquence du générateur de tacts GT peut varier entre des limites larges sans affecter la précision.

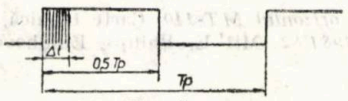

Fig. 5

3.6. Le bloc numérateur de longueur (NL)

Il est réalisé avec 5 circuits décimals (MMC40192) et en fonction de l'état du discriminateur de sens DS (Fig. 2), p ou p_1, les impulsions sont comptées directement ou inversement par NL. C'est ainsi que dans le NL on effectue l'addition ou la soustraction des paquets de p ou p_1 impulsions et par cette voie, en n'importe quel moment, la valeur en mm du déplacement du chariot de charge de la grue est enregistrée dans le numérateur.

Quand le chariot revient dans la position initiale, qui correspond à la valeur „zéro" du déplacement, l'effacement du NL devient possible par l'intermédiaire d'un contact actionné directement par l'opérateur ou par un limiteur de course.

L'indication numérique de la valeur obtenue à la suite de la mesure est réalisée par 3 affichages à 7 ségments avec cathode commun MDE2111, commandés par 3 décodeurs MMC4511 [4].

4. Résultats expérimentaux et conclusions

Cette installation de mesure a été testée en laboratoire sur un poste d'essai où le déplacement du chariot a été simulé par le déplacement du curseur d'une règle incrémentale optique equipée avec un instrument de sortie du type Numerom 301, avec une résolution de 0,1 mm. Dans le Tableau 1 on présente, par comparaison, les valeurs des déplacements indiquées par l'installation réalisée, en simulant aussi sur la règle optique (R_1, [mm], respectivement R_2, [mm]) et les erreurs rélatives, [%].

Tableau 1

R_1, [mm]	0,00	980	10 080	20 160	35 280	41 580	45 360
R_2, [mm]	0,00	976	10 064	20 138	35 180	41 430	45 195
%		0,4	0,15	0,10	0,28	0,36	0,36

Il est à remarquer le fait que sur le poste d'essai l'installation ne réalise pas des erreurs qui dépassent 0,4%.

On peut adapter l'installation réalisée à n'importe quel type de grue a volée horizontale.

Le schéma utilisé peut être élargi pour pouvoir indiquer le couple et la charge maximum actionnée par le crochet.

Reçue le 7 avril 1990

Institut Polytechnique, Jassy,
Chaire de Mesures Electriques

BIBLIOGRAPHIE

1. Götte K., *Taschenbuch Betriebsmesstechnik*. VEB Verlag Technik, Berlin, 1974.
2. Micu C. et al., *Aparate şi sisteme de măsurare în construcţia de maşini*. Ed. Tehn., Bucureşti, 1980.
3. . . . *Macara turn cu braţ orizontal MT-140*. Carte tehnică, Bucureşti, 1986.
4. . . . *General Catalogue 1981/82*. MBLE, Philips, Eindhoven, 1981.

ASUPRA MĂSURĂRII NUMERICE A RAZEI MACARALELOR CU BRAŢ ORIZONTAL

(Rezumat)

Plecînd de la necesitatea creşterii gradului de siguranţă în exploatare a macaralelor cu braţ orizontal, se prezintă schema unei instalaţii de măsurare numerică a razei, care utilizează ca element sensibil o riglă incrementală circulară cu tastare de reluctanţă, cuplată pe axul tobei de antrenare a cablului căruciorului de sarcină. Instalaţia verificată în laborator poate fi utilizată şi la înfăşurarea cablului în două straturi.

BULETINUL INSTITUTULUI POLITEHNIC DIN IAŞI
Tomul XXXVI (XL), Fasc. 3—4, 1990
Secţia III
ELECTROTEHNICĂ. ENERGETICĂ. ELECTRONICĂ. AUTOMATIZĂRI

C.D. 621.34 : 621.87

SUR L'ESTIMATION DE LA CHARGE ADMISSIBLE AU CROCHET DE LA GRUE À VOLÉE HORIZONTALE

PAR

LIVIU BRENIUC, M. CREŢU et C. SĂRMĂŞANU

1. Introduction

Il est absolument nécessaire de connaître dans n'importe quel moment la position du chariot de la grue (le rayon de la grue) et d'estimer la charge admissible au crochet pour augmenter la sécurité pendant le fonctionnement des grues à volée horizontale [2], [4].

Les procédés de mesure et d'estimation ont comme point de départ la supposition qu'on connaît la caractéristique charge admissible — rayon.

Dans ce qui suit on présente une nouvelle possibilité d'estimation de la charge admissible.

2. Le principe de la méthode

Dans la Fig. 1 on représente les caractéristiques charge admissible—rayon pour la grue de type MT-140, munie avec deux chariots, l'un de 6 t, l'autre de 12 t. On peut remarquer que ces caractéristiques s'éloignent de la forme hyperbolique idéale sous l'influence d'autres facteurs à savoir : le contrepoids de la grue, le poids du chariot, la vitesse du vent, etc. [4].

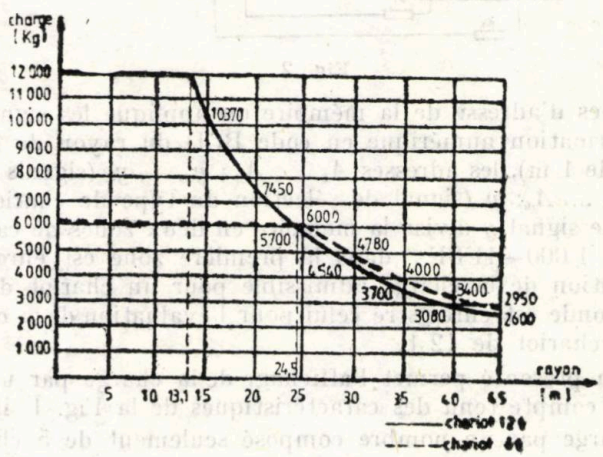

Fig. 1

En principe, le schéma de mesure proposé (Fig. 2), représente une machine à algorithme d'état ASM (Algorithmic State Machine), ou autrement dit, un automate séquentiel où l'algorithme de transition des états est introduit dans un circuit de type PROM, CI_1 (I 2716), ayant une capacité 2 Kx 8, un régistre type D à rôle de mémoriser l'état présent, CI_2 (MMC 4035), un démultiplexeur CI_3 (MMC 4051) et un circuit décodeur à 7 ségments D_1, ..., D_5 (MDE 2111) [1], [3].

Le rapport d'état, pour la programmation de la mémoire, est :

$$RS = \frac{y(y_6y_5y_4)x_6x_5x_4x_3x_2x_1x_0}{SY_6Y_5Y_4Y_3Y_2Y_1Y_0} .$$

Le mot de sortie de la mémoire O_0, ..., O_7 est divisé en O_0, ..., O_3 qui représente le mot de commande de l'affichage de la charge admissible (les signals notés avec Y_0, ..., Y_3), O_4, ..., O_6 qui représente le mot pour l'état suivant (les signals notés avec Y_4, ..., Y_6) et la sortie O_7 (le signal noté avec S) est utilisée pour la signalisation optique ou acoustique de la fin de la course du chariot de la grue.

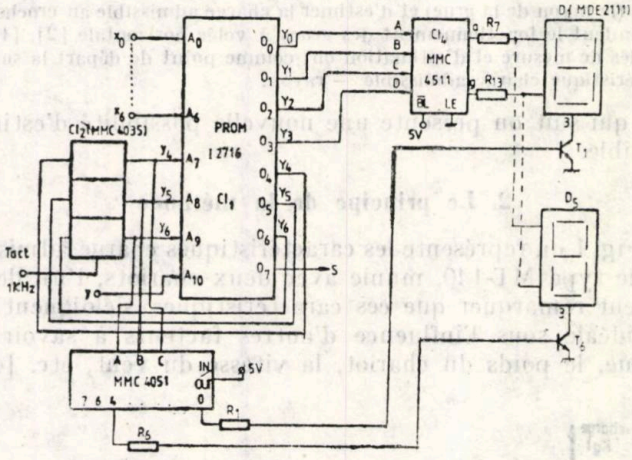

Fig. 2

Aux entrées d'adresse de la mémoire on applique les signals suivants : x_0, ..., x_6 (l'information numérique en code BCD du rayon de la grue, avec une résolution de 1 m), les adresses A_0, ..., A_6 ; y_4, ..., y_6 (signals de réaction), les adresses A_7, ..., A_9; y (signal de sélection du type de chariot 6 t, 12 t), l'adresse A_{10}. Le signal y divise la mémoire en deux zones de capacité 1Kx8, 0000—0FFF et 1 000—1FFF ; dans la première zone est enregistré l'algorithme d'évaluation de la charge admissible pour un chariot de 6 t, tandis que dans la seconde est enregistré celui pour l'évaluation de la charge admissible pour un chariot de 12 t.

Le schéma présenté permet l'affichage de la charge par un nombre de 8 chiffres, mais compte tenu des caractéristiques de la Fig. 1 il suffit l'affichage de la charge par un nombre composé seulement de 5 chiffres, la résolution de l'affichage étant de 1 Kg.

Afin de suivre le fonctionnement du schéma proposé on choisit en tant qu'exemple l'affichage de la charge admissible pour un rayon de 15 m, avec un chariot de 12 t. Dans ce cas la charge est de 10 370 Kg, $y=1$.

En utilisant le rapport d'état ci-dessus on peut représenter la succession des états de la manière suivante :

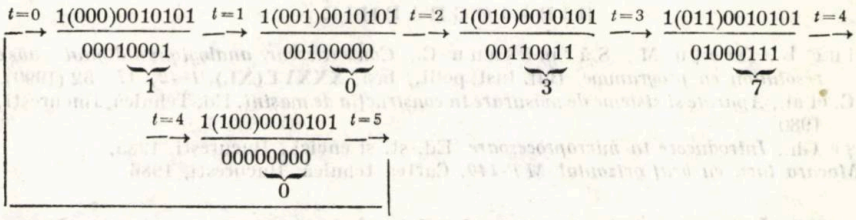

Dans tous les états ci-dessus $x_6x_5x_4, x_3x_2x_1x_0$ ont la valeur 15 parce que le tact du schéma (1 KHz) a une fréquence plus grande que celle de modification du rayon (celle-ci est d'environ 10 Hz).

Le procédé d'affichage utilisé est du type dynamique, l'allumage d'un seul affiche étant commandé en fonction de la combinaison des signals $y_4y_5y_6$ et l'affichage complète de la charge maximum est réalisé pendant la durée de 5 tacts.

À $t=0$ l'affichage D_1 (1-décimal) présente le chiffre le plus significatif de la charge, parce que $Y_3Y_2Y_1Y_0=0001$, $y_6y_5y_4=000$, donc la sortie „0" du multiplexeur CI_3 est 1 logique et en conséquence le transistor T_1 est commandé (Fig. 2).

Au tact $t=1$ l'affichage D_2 (0-décimal) présente le chiffre suivant, puisque $Y_3Y_2Y_1Y_0=000$, $y_6y_5y_4=001$, donc la sortie„1"du multiplexeur CI_3 est 1 logique et par conséquent le transistor T_2 est commandé. Les autres chiffres sont affichés de la même manière de sorte qu'au tact $t=5$ on revient à l'état initial.

Le processus d'affichage est continué de cette manière jusqu'à une nouvelle modification du rayon de la grue (les signals $x_6x_5x_4 \cdot x_3x_2x_1x_0$). Pour toutes les valeurs du rayon on obtient des successions d'états pareils à cellui présenté ci-dessus et à la fin on réalise le dictionnaire de l'inscription de la mémoire. Ainsi, pour la succession donnée, en éliminant la parantèse du numérateur, on a le dictionnaire d'inscription suivant :

$$D_{ins}=\frac{\text{Adresses}}{\text{Sorties}}\ ;\ \frac{415}{11}\ ;\ \frac{495}{20}\ ;\ \frac{515}{33}\ ;\ \frac{595}{47}\ ;\ \frac{615}{00}\ .$$

3. Conclusions

Le schéma analysé appartient à un appareil plus complexe qui permet la détermination de la valeur numérique du rayon et l'affichage de la charge admissible au crochet, conformément au rayon.

L'équipement a été testé sur l'appareil avec de bons résultats. Le schéma permet l'évaluation de la charge admissible au crochet de la grue à volée horizontale, la résolution de l'affichage étant de 1 Kg pour une résolution du rayon de 1 m.

Le schéma a une consommation réduite compte tenu qu'on a utilisé un procédé d'affichage dynamique.

Reçue le 7 avril 1990

Institut Polytechnique, Jassy,
Chaire de Mesures électriques

BIBLIOGRAPHIE

1. Breniuc L., Creţu M., Sărmăşanu C., *Convertisseur analogique—digital avec résolution en programme.* Bul. Inst. polit., Iaşi, **XXXVI (XL)**, *1—2*, 47—52 (1990).
2. Micu C. et al., *Aparate şi sisteme de măsurare în construcţia de maşini.* Ed. Tehnică, Bucureşti, 1980.
3. Toacşe Gh., *Introducere în microprocesoare.* Ed. şt. şi encicl., Bucureşti, 1985.
4. * * * *Macara turn cu braţ orizontal MT-140.* Cartea tehnică, Bucureşti, 1986.

ASUPRA ESTIMĂRII SARCINII ADMISIBILE LA CÎRLIG PENTRU MACARALELE CU BRAŢ ORIZONTAL

(Rezumat)

Se prezintă schema electrică utilizată pentru estimarea sarcinii admisibile maxime la cîrligul macaralelor cu braţ orizontal, funcţie de raza acesteia, folosind caracteristicile sarcină admisibilă — rază. Rezoluţia obţinută pentru afişarea sarcinii este de 1 Kg la un domeniu de măsurare de 12 t.

BULETINUL INSTITUTULUI POLITEHNIC DIN IAȘI
Tomul XXXVI (XL), Fasc. 3—4, 1990
Secția III
ELECTROTEHNICĂ. ENERGETICĂ. ELECTRONICĂ. AUTOMATIZĂRI

D.C. 621.313.33

THE POSSIBILITY OF THE SELF-CASCADED MACHINE RUNNING OF A SQUIRREL-CAGE INDUCTION MOTOR

BY

I. ANDRONE and V. BAHRIN

1. Introduction

It is well known the operation of two induction motors as a cascade-connected machine in wich those ones are electrically connected together and their rotors connected together mechanically [1], [2]. The combined unit has two running speeds corresponding to the sum and the difference of the pole-number of the individual motors. A two-motor set may be replaced by one alone — the H u n t motor. This motor, of essentially the same contruction as a normal induction one, comprises single stator and rotor windings; the different sections of the rotor winding of different pole-numbers are series connected; the stator winding appears as a high impedance (open-circuited) at the first pole-number, at wich the winding is supplied by a three-phase source and as a low impedance (short-circuit) at the second polen-umber; the H u n t motor has too two running speeds.

If the wound rotor of H u n t motor is replaced by the squirrel-cage one, the advantages are important. There is, in this meaning, a British Patent [3], and the interest in this type of machine has renewed by a need for motors of small rating to run at normal speeds from high frequency supplies and, also, when the machine rating is such that the bore diameter limits the number of stator slots. The running base of this type of motor is one of the rotor current sheet density harmonics.

The same performances were achieved through on purpose cuts of the two end rings of the rotor bars [4] of a squirrel cage. The cuts of the end rings of the squirrel-cage isn't a novelty [5], [6], but it was performed there for another purposes.

As was shown in [4] the cutting of one of the two end rings of a squirrel-cage with Q_2 bars is made in $\mu+p$ equal-distanced points; $\mu+p$ groups of q bars each are obtained namely:

$$\mu+p=\frac{Q_2}{p}. \tag{1}$$

The fundamental of the rotor current sheet density harmonic of its F o u r i e r 's series is

$$a^{(1)}(\theta_2, t)=-(1-k_{pq}^2)\frac{\sqrt{2}Q_2 I_{2a}}{2\pi R}\cos(p\theta_2-\omega_2 t+\psi_2), \tag{2}$$

having p pairs of poles. The harmonics of orders

$$\nu'=\frac{\mu+2p}{p}, \tag{3}$$

$$\nu''=\frac{\mu}{p} \tag{4}$$

in respect of p of positive and negative sequence are, respectively :

$$(5)\qquad a^{\frac{\mu+2p}{p}}(\theta_2, t)=k_{pq}k_{(\mu+2p)q}\frac{\sqrt{2}Q_2I_{2a}}{2\pi R}\cos[(\mu+2p)\theta_2-\omega_2 t+\psi_2],$$

$$(6)\qquad a^{\frac{\mu}{p}}(\theta_2, t)=k_{pq}k_{\mu q}\frac{\sqrt{2}Q_2I_{2a}}{2\pi R}\cos(\mu_2+\omega_2 t-\psi_2),$$

having $\mu+2p$ and respectively p pairs of poles. In the above relations θ_2 is the angular rotor coordinate, Q_2—the number of rotor bars, R—the rotor radius, $I_{2a}=E_2/Z_2$—the current of angular frequency ω_2 and $\psi_2=\arg[\underline{Z}_2]$; the factors k_{pq}, $k_{(\mu+2p)q}$ and $k_{\mu q}$ are given by :

$$(7)\qquad k_{pq}=\frac{\sin\frac{\pi pq}{Q_2}}{q\sin\frac{\pi p}{Q_2}}\qquad (8)\quad k_{(\mu+2pq)}=\sin\frac{\frac{\pi(\mu+2p)q}{Q_2}}{q\sin\frac{\pi(\mu+2p)}{Q_2}},$$

$$(9)\qquad k_{\mu q}=\frac{\sin\frac{\pi\mu q}{Q_2}}{q\sin\frac{\pi\mu}{Q_2}}.$$

The interest is now focused on the negative sequence harmonic (6) because the „second machine" of the internal cascade is rotor fed. The running speed of the machine due of this harmonic correspond to $\mu+p$ pairs of poles ; in this aim the stator winding must appears as a closed circuit with a sufficiently high winding factor for μ pairs of poles.

2. Speeds and Slips

The relations (2), (5) and (6) are the revolving waves ones. The angular speeds of these waves w.r.t. the rotor are determined by inspecting a certain value of each of them and their change of place on the rotor periphery; differentiating the constant argument $(\mu+2p)\theta_2-\omega_2 t+\psi_2=\text{const.}$ of the positive sequence harmonics, the angular speed w.r.t. the rotor is obtained :

$$(10)\qquad \Omega'_{2\nu}=\frac{d\theta_2}{dt}=\frac{\omega_2}{\mu+2p}=\frac{s\omega_1}{\nu' p}=\frac{s\Omega_1}{\nu'}=s\Omega_1\frac{p}{\mu+2p},$$

if $s=(\Omega_1-\Omega)/\Omega_1$ is the rotor slip w.r.t. the angular speed of the magnetic field of p pairs of poles and $\omega_1=2\pi p_1$ —the angular frecquency of the supplying network of stator winding which produce a revolving magnetic field with Ω_1 angular speed. In a similary way, the angular speed of negative sequence harmonics of the rotor current sheet w.r.t. the rotor is obtained as

$$(11)\qquad \Omega''_{2\nu}=-\frac{\omega_2}{\mu}=-\frac{s\omega_1}{\nu'' p}=-\frac{s\Omega_1}{\nu''}=-s\Omega_1\frac{p}{\mu}.$$

The rotor angular speeds of positive and negative sequence of the rotor current sheet harmonics w.r.t. the stator are:

$$\Omega'_{1\nu}=\Omega+\Omega'_{2\nu}\,;\qquad \Omega''_{1\nu}=\Omega+\Omega''_{2\nu}. \tag{12}$$

Taking account of (10) and (11), these speeds results:

$$\Omega'_{1\nu}=\frac{\Omega_1}{\nu'}\left[(1-s)\nu'+s\right]=\Omega_1\left(1-\frac{\mu+p}{\mu+2p}s\right), \tag{13}$$

$$\Omega''_{1\nu}=\frac{\Omega_1}{\nu''}\left[(1-s)\nu''-s\right]=\Omega_1\left(1-\frac{\mu+p}{\mu}s\right). \tag{14}$$

The ratio between the harmonic's speeds w.r.t. the stator and, respectively, w.r.t. the rotor define the slips of positive and negative harmonics namely:

$$s'_\nu=\frac{\Omega'_{1\nu}}{\Omega'_{2\nu}}=1+\frac{1-s}{s}\nu'=-\frac{\mu+p}{p}+\frac{\mu+2p}{sp}, \tag{15}$$

$$s''_\nu=\frac{\Omega''_{1\nu}}{\Omega''_{2\nu}}=1-\frac{1-s}{s}\nu''=\frac{\mu+p}{p}-\frac{\mu}{sp}. \tag{16}$$

The values of the rotor slip s which correspond to synchronous running of the machine w.r.t. the harmonic's speeds are determined putting $s'_\nu=s''_\nu=0$ or $\Omega'_{1\nu}=\Omega''_{1\nu}=0$. From these conditions the following values of s are obtained:

$$s'=\frac{\nu'}{\nu'-1}=\frac{\mu+2p}{\mu+p}=1+\frac{p}{\mu+p}>1, \tag{17}$$

$$s''=\frac{\nu''}{\nu''+1}=\frac{\mu}{\mu+p}=1-\frac{p}{\mu+p}<1. \tag{18}$$

The synchronous speeds of machine corresponding to the positive and negative sequence rotor current sheet harmonics are determinated, respectively, by:

$$\Omega'_{sc}=\Omega|_{s=s'}=(1-s')\Omega_1=-\frac{p}{\mu+p}\Omega_1=-\frac{2\pi f_1}{\mu+p}, \tag{19}$$

$$\Omega''_{sc}=\Omega|_{s=s''}=(1-s'')\Omega_1=\frac{p}{\mu+p}\Omega_1=\frac{2\pi f_1}{\mu+p}. \tag{20}$$

It is to be noted that the two synchronous speeds (19) and (20), which correspond to the two type harmonics of the positive and, respectively, negative sequence, are of opposite directions but of equals values and corresponding to the sum $\mu+p$ of the two pairs of poles because $\nu'p-p=\nu''p+p$.

Taking as reference of speeds the cascade synchronous speeds Ω'_{sc} and Ω''_{sc}, the slips s'_c and s''_c of the cascade w.r.t. these speeds are defined by the relations:

$$s'_c=\frac{\Omega'_{sc}-\Omega}{\Omega'_{sc}}=\frac{\mu+2p}{p}-\frac{\mu+p}{p}s, \tag{21}$$

$$s''_c=\frac{\Omega''_{sc}-\Omega}{\Omega''_{sc}}=-\frac{\mu}{p}+\frac{\mu+p}{p}s. \tag{22}$$

From (15) and (16) the factors $s'_v s$ and $s''_v s$ are determined and then were compared with (21) and (22). It results:

(23) $$s'_c = s'_v s,$$ (24) $$s''_c = s''_v s.$$

From (21), (22) and (23), (24) the important relationships between slips are determined:

(25) $$s'_c + s''_c = 2,$$ (26) $$s'_v + s''_v = \frac{2}{s}.$$

Graphical representation of the relationships between angular speeds and the slips are shown in Figs. 1 and 2.

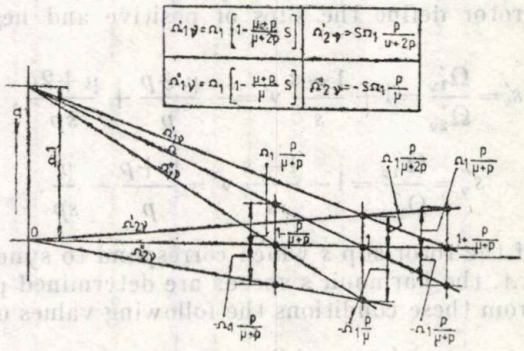

Fig. 1

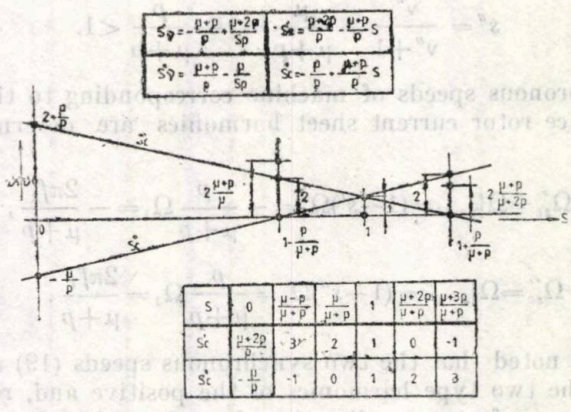

s	0	$\frac{\mu-p}{\mu+p}$	$\frac{\mu}{\mu+p}$	1	$\frac{\mu+2p}{\mu+p}$	$\frac{\mu+3p}{\mu+p}$
s'_c	$\frac{\mu+2p}{p}$	3	2	1	0	-1
s''_c	$-\frac{\mu}{p}$	-1	0	1	2	3

Fig. 2

3. The Currents

The electrical equivalent circuit diagram of squarrel-cage rotor machine, represented in Fig. 3, are modified as in Fig. 4, if the $\mu+p$ equal distanced cuts of one the two end rings are made.

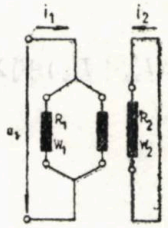

Fig. 3

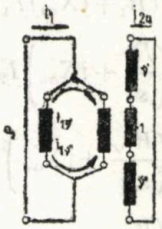

Fig. 4

The stator winding has two identical branches parallel connected and the rotor winding has three series connected ones. The magnetic total flux linked with the two stator, parallel connected branches, are the sum of total main magnetic flux and the leakage flux linkage :

$$(27) \qquad \Psi_{1t}^{(1)}=\Psi_1^{(1)}+\Psi_{\sigma 1}^{(1)}\,, \quad \Psi_{1t}^{(\nu')}=\Psi_1^{(\nu')}+\Psi_{\sigma 1}^{(\nu')}\,, \quad \Psi_{1t}^{(\nu'')}=\Psi_1^{(\nu'')}+\Psi_{\sigma 1}^{(\nu'')}\,.$$

In the relations (27) superscripts, between brackets, denotes the orders of harmonics and lower numbers is referred to the stator (1) and rotor (2). For the series connected rotor branches the total magnetic fluxes are :

$$(28) \qquad \Psi_{2t}^{(1)}=\Psi_2^{(1)}+\Psi_{\sigma 2}^{(1)}\,, \quad \Psi_{2t}^{(\nu')}=\Psi_2^{(\nu')}+\Psi_{\sigma 2}^{(\nu')}\,, \quad \Psi_{2t}^{(\nu'')}=\Psi_2^{(\nu'')}+\Psi_{\sigma 2}^{(\nu'')}\,.$$

The coils of the stator winding is in such a way connected that the magnetic fluxes of the fundamental harmonic are of the same phase and those of ν''th harmonic are of opposite phase; it is necessary, in the same time that the magnetic fluxes of ν'th harmonic linked with the two branches of stator winding to be of the same phase in each of those or to have a lower winding factor for series circuit for this order of harmonic.

Equations of tensions, relative to the circuit diagram in Fig. 4, taking into account the leakage inductances (lower subscript σ) are :

$$(29) \quad \begin{cases} u_1=R_1 i_1+L_{\sigma 1}\dfrac{\mathrm{d}i_1}{\mathrm{d}t}+\dfrac{\mathrm{d}\Psi_1^{(1)}}{\mathrm{d}t}\,, \quad 0=R_2 i_2+L_{\sigma 2}\dfrac{\mathrm{d}i_{2a}}{\mathrm{d}t}+\dfrac{\mathrm{d}\Psi_2^{(1)}}{\mathrm{d}t}+\dfrac{\mathrm{d}\Psi_2^{(\nu')}}{\mathrm{d}t}+\dfrac{\mathrm{d}\Psi_2^{(\nu'')}}{\mathrm{d}t}\,, \\ 0=R_{1\nu'} i_{1\nu'}+L_{\sigma\nu'}\dfrac{\mathrm{d}i_{1\nu'}}{\mathrm{d}t}+\dfrac{\mathrm{d}\Psi_1^{(\nu')}}{\mathrm{d}t}\,, \quad 0=R_{1\nu''} i_{1\nu''}+L_{\sigma\nu''}\dfrac{\mathrm{d}i_{1\nu''}}{\mathrm{d}t}+\dfrac{\mathrm{d}\Psi_1^{(\nu'')}}{\mathrm{d}t}\,, \end{cases}$$

where $i_{1\nu'}$ and $i_{1\nu''}$ are the currents through the primary winding of harmonics of orders ν', and respectively ν''.

The tensions, currents and magnetic fluxes in the four equations of system (29) have different angular frequencies : namely in the first equation the angular frequency is $\omega_1=2\pi f_1$, in the second, $\omega_2=s\omega_1$, in the 3rd and 4th the angular frequencies are $\omega_1'=s_1'\omega_2$ and $\omega_1''=s_1''\omega_2$ respectively.

If the rotor quantities reported to the stator side are used, the leakage and useful reactances are introduced, the equations (29) may be written in complex form :

$$
(30)\quad \begin{cases} \underline{U}_1=(R_1+jX_{\sigma 1})\underline{I}_1+jX_{u1}(\underline{I}_1+\underline{I}'_{2a}), \\ 0=\left(\dfrac{R'_2}{s}+jX'_{\sigma 2}\right)\underline{I}'_{2a}+jX_{u1}(\underline{I}_1+\underline{I}'_{2a})+jX'_{u\nu'}(\underline{I}'_{2a}+\underline{I}'_{1\nu'})+jX'_{u\nu''}(\underline{I}'_{1a}+\underline{I}'_{1\nu'}), \\ 0=\left(\dfrac{R'_{1\nu'}}{s'_\nu s}+jX'_{\sigma\nu'}\right)\underline{I}'_{1\nu'}+jX'_{u\nu'}(\underline{I}'_{2a}+\underline{I}'_{1\nu'}), \\ 0=\left(\dfrac{R'_{1\nu''}}{s''_\nu s}+jX_{\sigma\nu''}\right)\underline{I}'_{1\nu''}+jX'_{u\nu''}(\underline{I}'_{2a}+\underline{I}'_{1\nu''}). \end{cases}
$$

Based on the system (30), in Fig. 5 an equivalent circuit diagram is drawn.

Resolving the system (30) w.r.t. the currents and taking into account relations (21)...(25) the following expression of the current supply, for example, is obtained :

$$
(31)\quad \underline{I}_1=\frac{\underline{A}+\underline{B}s''_c+\underline{C}s''^2_c+\underline{D}s''^3_c}{\underline{E}+\underline{F}s''_c+\underline{G}s''^2_c+\underline{H}s''^3_c}\underline{U}_1.
$$

Similar expressions are obtained for the other currents. Geometrical locus (31) of current $\underline{I}_1$ at variable cascade slip $s''_c\in(-\infty,\infty)$, represented in rectangular coordinates, is a curve of 6th grade ; this fact leads to major difficulties in the relations handling and in the interpretation of the results. A major reduction can be made if the ν' th harmonic of positive sequence is neglected. In this case, using the notations :

$$
(32)\quad X_1=X_{u1}+X_{\sigma 1},\ X'_2=X_{u1}+X'_{u\nu''}+X'_{\sigma 2},\quad X'_3=X'_{u\nu''}+X'_{\sigma\nu''},
$$

the following expressions for the currents are obtained :

$$
(33)\quad \begin{cases} \underline{I}_1=\dfrac{1}{\underline{\Delta}}\underline{U}_1\left[\left(\dfrac{R'_2}{s}+jX'_2\right)\left(\dfrac{R'_{1\nu''}}{s''_\nu s}+jX'_3\right)+X'^2_{u\nu''}\right], \\ \underline{I}'_{2a}=-\dfrac{1}{\underline{\Delta}}\underline{U}_1\left[jX_{u1}\left(\dfrac{R'_{1\nu''}}{s''_\nu s}+jX'_3\right)\right],\quad \underline{I}'_{1\nu''}=-\dfrac{1}{\underline{\Delta}}\underline{U}_1X_{u1}X'_{u\nu''}, \end{cases}
$$

where

$$
(34)\quad \underline{\Delta}=(R_1+jX_1)\left(\frac{R'_2}{s}+jX'_2\right)\left(\frac{R'_{1\nu''}}{s''_\nu s}+jX'_3\right)+X^2_{u1}\left(\frac{R'_{1\nu''}}{s''_\nu s}+jX'_3\right)+X'^2_{u\nu''}(R_1+jX_1).
$$

If the relations (22) and (24), which described the slips s and s''_ν as functions of s''_c, are taking into account, the following expression for the supply current is obtained :

$$
(35)\quad \underline{I}_1=\frac{\underline{A}+\underline{B}s''_c+\underline{C}s''^2_c}{\underline{D}+\underline{E}s''_c+\underline{F}s''^2_c}\underline{U}_1,
$$

where :

$$
\underline{A}=(\mu+p)R'_2R'_{1\nu''}+j\mu R'_{1\nu''}X'_2,\quad \underline{B}=\mu(X'^2_{u\nu''}-X'_2X'_3)+j[(\mu+p)R'_2X'_3+pR'_{1\nu''}X'_2],
$$

(36) $$\underline{C}=p(X'^{2}_{u\nu}-X'_2X'_3),\quad \underline{D}=(R_1+jX_1)\underline{A}+\mu R'_{1\nu}X^2_{u1},$$
$$\underline{E}=(R_1+jX_1)\underline{B}+X^2_{u1}(pR'_{1\nu}+j\mu X'_3),\quad \underline{F}=(R_1+jX_1)\underline{C}+jpX^2_{u1}X'_3.$$

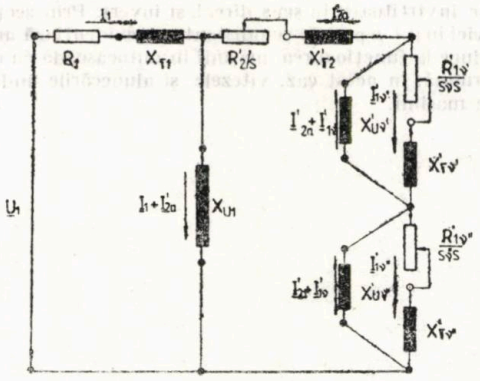

Fig. 5

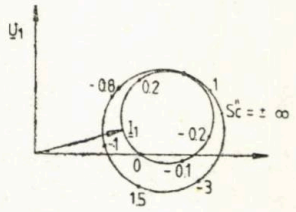

Fig. 6

The expression (35) describes the geometrical locus of the supply current at variation of s''_c as parameter. This geometrical locus is a duble circular curve of 4th grade in rectangular coordinates (Fig. 6).

If the expression (35) of the supply current of actual internal cascade of an induction motor is compared with the expression of supply current of cascade running of two machines [2], a great similitude is found.

One of the most important advantage of the single machine cascade running is a greater power factor compared with the two machine cascade running because in the first cas there is only one air-gap. The single machine cascade has also another advantages but has and disavantages and its utilisation is justified only after a study of concrete electromechanical operation.

Received, December 18, 1989

Polytechnic Institute, Jassy,
Department of Electrical Engineering
and Electrical Machines

REFERENCES

1. Richter R., *Mașini electrice*, (transl. from German). Vol. **IV**, Ed. Tehnică, București, 1960.
2. Gheorghiu I.S., Fransua A.S., *Tratat de Mașini Electrice*. Vol. **III**, Ed. Acad. R.S.R., București, 1971.
3. . . Patent Specification *1 155 743*, London (1969).
4. Androne I., Androne C., *Fonctionnement en cascade d'un moteur asynchrone à cage ayant un anneau sectionné*. Bull. ASE, *5* (1982).
5. Штурман Г.И., *Разомкнутые величьи клетки в короткозамкнутых асинхронных двигателях*. Электичество, *9* (1951).
6. Fransua A., Nicolaide A., Trifu C., *Mașini electrice uzuale*. Ed. Tehnică, București, 1973.

POSIBILITATEA DE FUNCȚIONARE ÎN AUTOCASCADĂ A MOTORULUI ASINCRON CU ROTORUL ÎN COLIVIE

(Rezumat)

Motoarele asincrone trifazate cu rotorul în colivie produc armonici ale densității liniare a solenației rotorice, reprezentînd unde învîrtitoare în sens direct și invers. Prin secționarea inelelor de scurt-circuitare a barelor coliviei în $\mu + p$ puncte echidistante se evidențiază armonica inversă cu μ perechi de poli care conduce la funcționarea mașinii în autocascadă cu o viteză corespunzătoare la $2(\mu + p)$ poli. Se determină, în acest caz, vitezele și alunecările undelor învîrtitoare cît și curenții din înfășurările mașinii.

BULETINUL INSTITUTULUI POLITEHNIC DIN IAŞI
Tomul XXXVI (XL), Fasc. 3—4, 1990
Secţia III
ELECTROTEHNICĂ. ENERGETICĂ. ELECTRONICĂ. AUTOMATIZĂRI

D.C. 621.394.9

SYNTHESIS OF A CMI CODER

BY

N.D. ALEXANDRU and IMAD FAYEZ MASHEH

1. Introduction

The CMI (Coded Mark Inversion) code is frequently used in digital communications, both at baseband and with modulation – demodulation. It was adopted by CCITT as an interface code at 139.264 Kbits/s [1]. Its power spectrum exhibits both a continuous part, which carries the information, and a discrete one (lines) [2].

The NRZ-L and CMI-coded signals are presented in Fig. 1 *a*, together with the clock signal. In the CMI coding a mark is represented alternatively by the logical levels L and H, while a space is represented by a LH transition in the middle of the bit interval (like the marks in the RZ coding). The state transition diagram, illustrating the coding rules, is represented in Fig. 1 *b*. Long strings of 1 s and 0 s are represented by rectangular waves with a fundamental frequency of $0.5R$ and respectively R, where R denotes the signaling frequency.

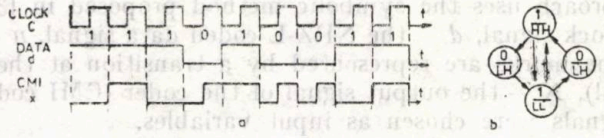

Fig. 1

The CMI coded signal is similar to a FSK signal with a square wave carrier and a modulation index of 0.5, which lacks phase continuity. We conclude that its spectrum will exhibit discrete components on signaling frequencies $0.5R$ and R and their harmonics. These are specific to a FSK signal with phase discontinuity, resulted from the reunion of two ASK signals.

An important advantage of this code regards the bit synchronization, considering the existence in its spectrum of the discrete components (lines) on the harmonics of $0.5R$ and the fact that it exhibits at least a transition at $1.5T$, where T is the duration of the bit interval. Unfortunately, the S/N ratio, necessary to ensure an imposed value of the error rate, must increase, taking into account the fact that the spectral lines affect the energetic budget of the signal.

2. Synthesis of the CMI Coder Regarded as a FSK Modulator

The waveforms specific to the CMI coder are illustrated in Fig. 2, together with a rectangular wave with the frequency $0.5R$, denoted by a. We observe that after an odd number of spaces there is a phase difference of 180° between the CMI and a signals. After an even number spaces, the rectangular wave with the fundamental frequency $0.5R$, representing the marks in the CMI signal, preserves its former phase value. This is equivalent with a PSK-type modulation of a square wave carrier by a modulating signal m. The fundamental frequency of the carrier is $0.5R$ (Fig. 2).

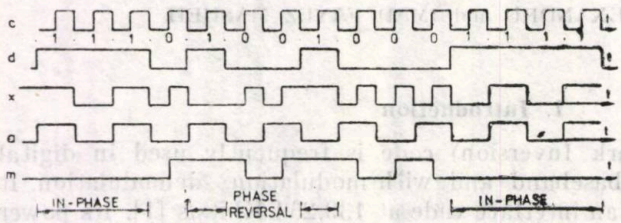

Fig. 2

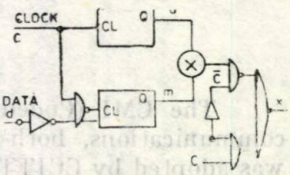

Fig. 3

We remark that the signal m can be obtained from the data bit stream $d(t)$ by a NRZ-S coding with the transitions taking place at the middle of the space intervals.

The CMI coding circuit results as in Fig. 3. The CMI signal is generated with a multiplexer which selects either the clock c when transmitting a space or the PSK-type signal p.

3. Synthesis of the CMI Coder with a Symbolic Method

This approach uses the symbolic method proposed in [3]. We denote by : c — the clock signal, d — the NRZ-L coded data signal, n — the NRZ-M coded data (the marks are represented by a transition at the beginning of the bit interval), X — the output signal of the coder (CMI coded data). The c, d and n signals were chosen as input variables.

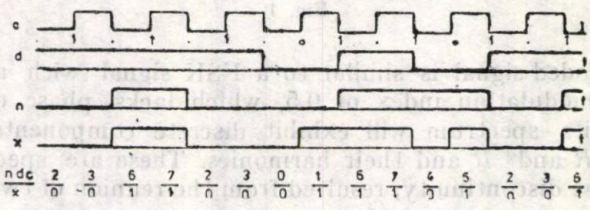

Fig. 4

The states describing the operation of the circuit were written in the octal code as ndc/X (s. Fig. 4). By grouping the allowed ($X=1$) and forbidden ($X=0$) states we get

$$X=\bigcup_{\substack{1:\,(1,5,6,7)\\0:\,(0,2,3,4)}}^{ndc}$$

where $\bigcup$ denotes the logical OR function. Grouping the allowed states according to their adjacencies, we get the implicants

		$n\ d\ c$	
X	4 1|5	$\varnothing\ 0\ 1$	$\bar{d}\cdot c$
	1 6|7	$1\ 1\ \varnothing$	$n\cdot d$

So,

(1) $$X = n\cdot d \bigcup \cdot\bar{d}\cdot c$$

and applying the de Morgan's theorems

(2) $$X = \overline{\overline{n\cdot d}\cdot\overline{\bar{d}\cdot c}}.$$

The coder diagram is represented in Fig. 5.

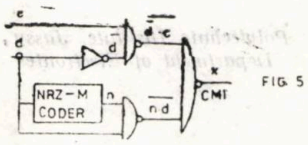

FIG. 5

Fig. 5

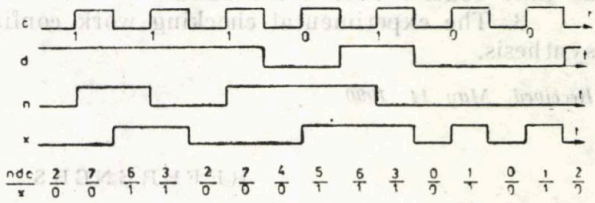

Fig. 6

Another possibility of implementation was investigated, starting with the waveforms in Fig. 6, which are similar to those from Fig. 4. The difference concerns the signal n which is also NRZ-M coded but exhibiting transitions in the middle of the mark intervals.

In a similar way,

$$X = \bigcup_{0\,:\,(0,2,4,7)}^{ndc}{}_{1\,:\,(1,3,5,6)}$$

		$n\ d\ c$	
X	4 1|5	$\varnothing\ 0\ 1$	$\bar{d}.c$
	2 1|3	$0\ \varnothing\ 1$	$\bar{n}\,c$
	6	$1\ 1\ 0$	$n\cdot d\cdot\bar{c}$

So,

(3) $$X = \bar{d}.c \bigcup \bar{n}.c \bigcup n.d.\bar{c}$$

or

(4) $$X = \overline{\overline{\bar{d}.c.}\ \overline{\bar{n}.c.}\ \overline{n.d.\bar{c}.}}$$

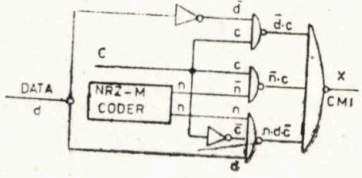

Fig. 7

The diagram of the coding circuit is represented in Fig. 7.

4. Conclusions

1. In a first approach, the CMI coder circuit was derived observing that a CMI signal exhibits signal elements which are rectangular waves with the frequencies $0.5R$ and R. This allowed us to consider it as a reunion of two ASK signals.

The spaces are represented like the marks in a RZ coding and the marks in the CMI waveform corresponding to a FSK signal of modulation signal 0.5 and square wave carrier with a fundamental frequency $0.5R$, which is PSK modulated by the NRZ-S coded data.

2. Remarking that in the CMI coding the marks are NRZ-M coded and using the symbolic method, two combinational logic circuits, operating as CMI coders, were synthesized.

3. The experimental checking work confirmed the correctitude of the synthesis.

Received, May 14, 1990

Polytechnic Institute, Jassy,
Department of Electronics

REFERENCES

1. * *. CCITT Recommandation G 703 : Interface at 139.264 Kbits/s, Red Book, Vol. III. 3, 1985.
2. Morgenstern G., *Zur Berechnung der spektralen Leistungsdichte von digitalen Basisband-Signalen.* Der Fernmelde Ingenieur, *12* (1979).
3. Reus N., *Tratarea simbolică a schemelor de comutaţie.* Ed. Acad., Bucureşti, 1971.
4. Alexandru N.D., Cotae P., *Telegrafie şi transmisiuni de date.* Instit. polit., Iaşi, 1987.
5. Alexandru N.D., *Contributions to the Study of Data Transmissions with FSK Modulation (Regarding Coding and Modulation)*, (in Romanian). Ph. D. Diss., Polyt. Inst., Jassy, 1981.
6. Alexandru N.D., Imad Fayez Masheh, *Sinteza decodorului CMI.* Jubilee Scient. Session, Nov. 10–12, 1988, IV, 327–330.

SINTEZA CIRCUITULUI CODOR CMI

(Rezumat)

Se studiază sinteza circuitului de codare CMI în mai multe variante. O primă schemă se obţine observînd că în semnalul CMI se pot identifica două frecvenţe, R şi $0,5R$, codorul CMI fiind un multiplexor care selectează fie tactul cu frecvenţa R, fie un semnal PSK cu frecvenţa purtătoare $0,5R$, modulat de secvenţa de date codată NRZ-S.

Alte scheme se obţin utilizînd circuite de codare diferenţială NRZ-M, cu tranziţia pe începutul sau pe mijlocul intervalului de bit.

BULETINUL INSTITUTULUI POLITEHNIC DIN IAŞI
Tomul XXXVI (XL), Fasc. 3—4, 1990
Secţia III
ELECTROTEHNICĂ. ENERGETICĂ. ELECTRONICĂ. AUTOMATIZĂRI

D.C. 621-523 ; 621.313.2

THREE-PHASE FULLY CONTROLLED BRIDGE CIRCUIT WITH LOW CONTENT OF HIGHER HARMONICS AT THE INPUT, FOR D.C. MOTOR DRIVE

BY

CLARISSA GÎTLAN and D. ALEXA

1. Introduction

In this paper a new circuit variant of three-phase fully controlled bridge with low content of higher harmonics at the input, for d.c. motor drive, is presented.

The reduction of the input higher harmonics current is obtained by the addition of the two rectifiers input currents, adequately dephased.

Finally the filter inductances L_1 and L_2 values are computed.

2. The Principle of Current Harmonics Reduction and the Calculus of L_1 and L_2

The schematic circuit, for a three-phase controlled bridge ford d.c. motor drive, is given in Fig. 1. It consists of two controlled rectifiers with parallel thyristors and two filter inductances, L_1 and L_2.

The two rectifiers thyristors are asimetrically controlled. According to Fig. 2 *c* and *d*, the control angles of these thyristors are equal to α_1 and α_2, respectively. The durations of the commutation processes are considered,

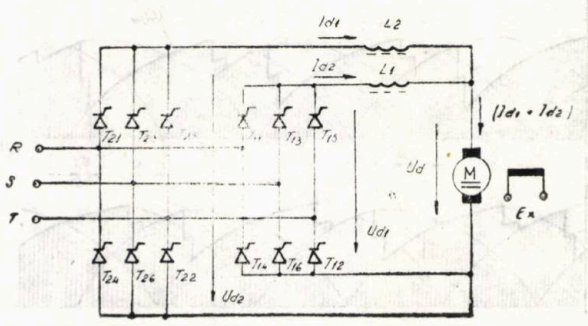

Fig. 1

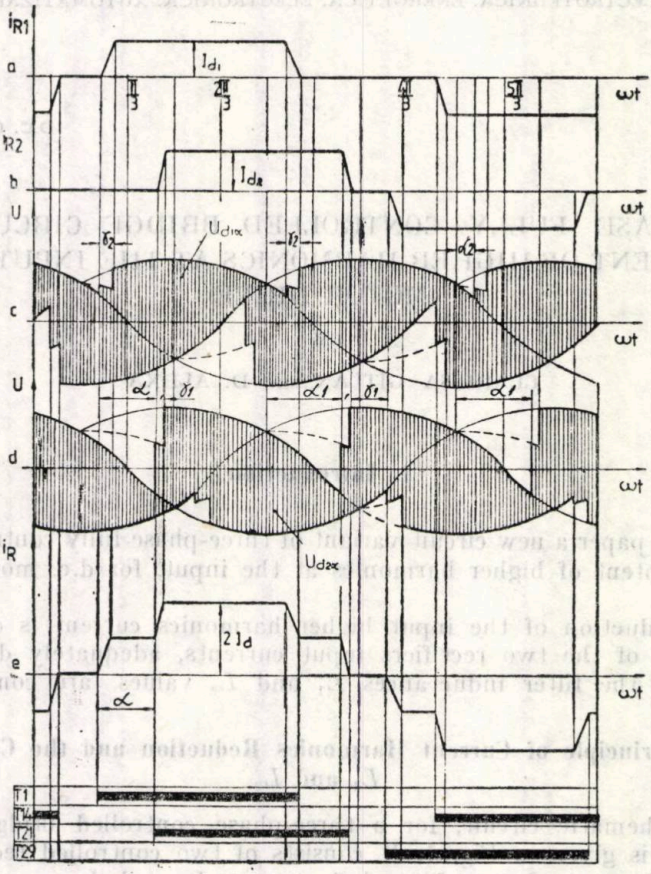
i_{R1}
a
I_{d1}
$\frac{\pi}{3}$
$\frac{2\pi}{3}$
$\frac{4\pi}{3}$
$\frac{5\pi}{3}$
ωt
i_{R2}
b
I_{d2}
U
$U_{d1\alpha}$
γ_2
α_2
c
U
α
γ_1
α_1
d
i_R
$U_{d2\alpha}$
$2I_d$
e
T1
T4
T2
T2'

Fig. 2

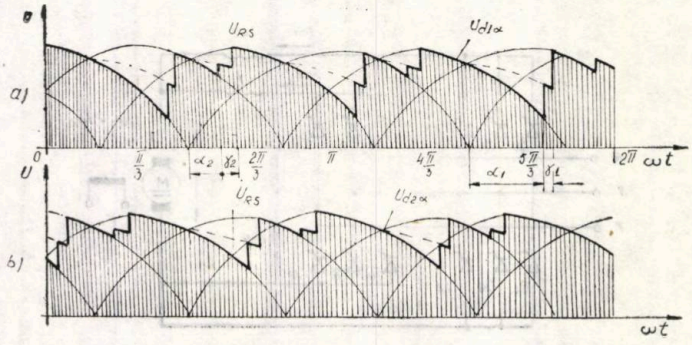
a)
U_{RS}
$U_{d1\alpha}$
0
$\frac{\pi}{3}$
α_2
γ_2
$\frac{2\pi}{3}$
π
$\frac{4\pi}{3}$
α_1
$\frac{5\pi}{3}$
γ_1
2π
ωt
U
b)
U_{RS}
$U_{d2\alpha}$
ωt

Fig. 3

denoted by γ_1 and γ_2, corresponding to angles α_1 and α_2, respectively. If $\alpha_1>\alpha_2$ then $\gamma_1<\gamma_2$ (γ is minimum for $\alpha=\pi/2$).

The hatched areas in these figures are equal to one another and represent the d.c. voltages $u_{1d\alpha}$ and $u_{2d\alpha}$ at the outputs of the rectifiers. The direct components $U_{1d\alpha}$ and $U_{2d\alpha}$ of these voltages will also be equal.

In ordre to change these direct components, the angles α_1 and α_2 must be changed, their difference being still constant.

The waveforms of d.c. voltages $U_{1d\alpha}$ and $U_{2d\alpha}$ obtained at the outputs of the rectifiers, considering the duration of the commutation process, are given in Figs. 3 *a* and *b*. The hatched areas in these figures are also equal to one another and represent the d.c. voltage $u_{1d\alpha}$ and $u_{2d\alpha}$ at the outputs of the rectifiers. The value of controlled direct voltage $U_{id\alpha}$ at the outputs of the two rectifiers, is :

$$U_{id\alpha}=\frac{3}{2\pi}\left[\int_0^{\alpha_1}\sqrt{6}U\cos\left(\omega t+\frac{\pi}{6}\right)\mathrm{d}(\omega t)+\int_{\alpha_1}^{\alpha_1+\gamma_1}\frac{3\sqrt{2}}{2}U\cos\omega t\,\mathrm{d}(\omega t)+\right.$$

$$+\int_{\alpha_1+\gamma_1}^{\frac{\pi}{3}+\alpha_2}\sqrt{6}U\cos\left(\omega t-\frac{\pi}{6}\right)\mathrm{d}(\omega t)+\int_{\frac{\pi}{3}+\alpha_1}^{\frac{\pi}{3}+\alpha_2+\gamma_2}\frac{3\sqrt{2}}{2}U\cos\left(\omega t-\frac{\pi}{3}\right)\mathrm{d}(\omega t)+$$

$$\left.+\int_{\frac{\pi}{3}+\alpha_2+\gamma_2}^{\frac{2\alpha}{3}}\sqrt{6}U\cos\left(\omega t-\frac{\pi}{2}\right)\mathrm{d}(\omega t)\right],$$

namely

$$U_{id\alpha}=U_{d0}\frac{\cos\alpha_1+\cos\alpha_2+\cos(\alpha_1+\gamma_1)+\cos(\alpha_2+\gamma_2)}{4}, \tag{1}$$

where

$$U_{d0}=\frac{3\sqrt{6}}{\pi}U.$$

All the rectifiers thyristors are conductive within time intervals equal to 1/3 of the supply voltage period, as can be seen in Fig. 2*f*.

The content in higher harmonics is very small. For instance the input currents of the two rectifiers, for phase R, are presented in Figs. 2 *a* and 2 *b*, and the total current i_R is given in Fig. 2 *e*.

Denoting the difference $\alpha_1-\alpha_2=\alpha$, the Fourier series of the total current i_R is :

$$i_R=8I_d\sum_{n=1}^{n=\infty}\frac{\left(\sin\frac{n\pi}{2}\right)^2\cos\frac{n\pi}{6}}{n\pi}\cos\frac{n\alpha}{2}\sin n\left(\omega t-\frac{\alpha_1+\alpha_2}{2}\right), \tag{2}$$

where n is the order of the higher harmonics and ω is the angular frequency of the supply network.

In order to simplify the control diagram the angle α can be chosen equal to $\pi/6$, the relative fundamental content of the supply current becoming in this case 0.986. If we take $\alpha=\pi/5$, the 5th harmonic can be eliminated, and for $\alpha=\pi/7$ the 7th harmonic can be eliminated [1].

Due to the filter inductances L_1 and L_2 the output currents of two rectifiers can be considered practically constant and equal to I_d.

The filter inductances values L_1 and L_2 can be calculated in accordance with the output rectified current limitation principle, at a required admissible value, in order to avoid the motor thermic charge and not to worsen the commutation ; it result :

$$(3) \qquad L>\frac{\pi}{3}\left(1-\frac{\sqrt{3}}{2}\right)\frac{Ud_0}{\omega(\Delta I_d)_{\text{adm.}}}=0.447\cdot10^{-3}\frac{Ud_0}{(\Delta I_d)_{\text{adm.}}},$$

where $(\Delta I_d)_{\text{adm}}$ is the admissible value.

On the other hand, in accordance with the average output rectified current limitation principle at a minimum, in order to avoid the converter function in breaked conduction, the inductances values may satisfy the inαquality :

$$(4) \qquad L>\frac{2-\sqrt{3}}{3}\cdot\frac{U_{d_0}}{\omega I_{d\min}}=0.285\cdot10^{-3}\frac{U_{d_0}}{I_{d\min}},$$

where : U_{d_0} represents the average value of rectified voltage ($\alpha=0$), ω — the angular frequency of the supply network, $I_{d\min}$ — the average rectified output minimum current (usually $I_{d\min}$ is the current when the motor is not loaded) [2].

Received, June 4, 1990

Polytechnic Institute, Jassy,
Department of Applied Electronics

REFERENCES

1. Alexa D, *Static Frequency Converter with Current Source Inverter and Low Content of Higher Harmonics at Input and Output*, AfE, **73**, 51—57 (1990).
2. Kelemen A., Imecs M., *Electronica de putere*. EDP, Buc., 1983.
3. Séguier G., *Power Electronic Converters*. North Oxford Academic Publ. Ltd., 1986.

CIRCUIT DE COMANDĂ PENTRU MOTORUL DE CURENT CONTINUU CU CONŢINUT REDUS ÎN ARMONICI SUPERIOARE LA INTRARE

(Rezumat)

Se prezintă circuitul de comandă al unui motor de c.c. cu conţinut redus în armonici superioare la intrare. Reducerea acestor armonici se obţine prin sumarea curenţilor de intrare în cele două redresoare corespunzător fazate. Se utilizează comanda asimetrică pentru tiristoarele ce echipează redresoarele. Se deduc formele de undă şi relaţiile de calcul pentru tensiuni în prezenţa fenomenelor de comutaţie precum şi valorile bobinelor de netezire L_1 şi L_2.

BULETINUL INSTITUTULUI POLITEHNIC DIN IAŞI
Tomul XXXVI (XL), Fasc. 3—4, 1990
Secţia III
ELECTROTEHNICĂ. ENERGETICĂ. ELECTRONICĂ. AUTOMATIZĂRI

D.K. 621.313.17 ; 621-8

ÜBER EINE METHODE DER ENTWERFUNG DER GESCHWINDIGKEITS-DIAGRAMME FÜR SCHRITTMOTOREN IM RAHMEN EINES ANTRIEBSSYSTEMS

VON

CRISTEA PAL und DOINA ZAMFIR

1. Einleitung

Die Verwendung der Schrittmotoren in einigen Anwendungen wie, die Industrie-Roboter, die Werkzeugmaschinen, die Zeichenapparate, die Drucker, fordert, daß die Anzahl der Schritte N zwischen zwei aufeinanderfolgenden Stellungen in einer minimalen Zeit durchlaufen wird. Diese Tatsache setzt die Erarbeitung einiger Geschwindigkeitsdiagramme voraus, mit Beschleunigungsphasen, Betrieb bei konstanter Geschwindigkeit und Bremsung mit maximalen Werten der zulässigen Beschleunigung, so daß die Funktionsstabilität des Systems nicht gefährdet sein wird. Auf der Charakteristik Moment — Frequenz der Schritte eines Schrittmotors kann man für einen Widerstandsmoment eine Geschwindigkeit Start-Stop nachweisen, für die nicht das Risiko besteht, Schritte zu verlieren [1].

Eine Reihe von theoretischen und experimentellen Versuchen haben gezeigt, daß ein Gesetz der exponentialen Variation der Geschwindigkeit die Positionierung in einer minimalen Zeit erlaubt [2], [3].

Die Verwendung der Mikrorechner in der Steuerung der Antriebssysteme mit Schrittmotoren versichert dem System eine erhöhte Flexibilität und bietet die Möglichkeit, der Erarbeitung des Steuerungs-Algorithmus mittels „Software" [4], [5].

Im Rahmen der Arbeit werden Aspekte hinsichtlich der Entwerfung der Geschwindigkeitsdiagramme ausgehend von den dem Mikrorechner gelieferten Daten, bzw. von der Anfangsgeschwindigkeit Start-Stop, von der maximalen Geschwindigkeit, der Anzahl der durchzuführenden Schritte, der Variation der Beschleunigung, dargestellt.

2. Geschwindigkeitsdiagramm : mathematisches Modell

Der Schrittmotor erlaubt eine Geschwindigkeit Start-Stop V_0 und eine maximale Geschwindigkeit V_M, die von dem Wert des Widerstandsmoment abhängen.

Die von dem Variationsdiagramm der Zeitabhängigen Geschwindigkeit eingeschlossene Fläche ist proportional mit der Winkelstellung. Aus Abb. 1 geht hervor, daß im Falle der Verwendung eines exponentialen Geschwindigkeitsprofils (*1*) in derselben Zeit t_c eine größere Anzahl von Schritten erzielt werden kann, unter Befolgung der Bedingung einer kleineren Beschleunigung ($a = \Delta V/\Delta t$) für große Geschwindigkeitswerte. Andererseits erhält man recht große Beschleunigungswerte zu Beginn und am Ende der Bewegung.

Im Falle der Verwendung eines geradlinigen Diagramms der Geschwindigkeit (2), so ist der maximale Wert der Geschwindigkeit $V_{2M} < V_{1M}$, weil im Punkt A das System einer großen Beschleunigung ausgesetzt ist (es findet eine plötzliche Veränderung der Geschwindigkeit statt).

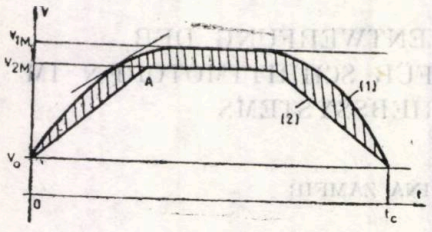

Abb. 1

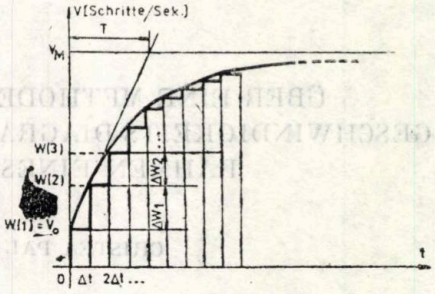

Abb. 2

Da die Beschleunigungsphase symmetrisch ist in Vergleiche zu der Bremsphase, werden wir das Studium nur auf die Beschleunigungsphase beschränken. Es wurde für eine Näherung in Stufen des idealen Geschwindigkeitsdiagramms (Abb.2), optiert, gemäß der Gleichung:

$$V(t) = V_0 + (V_M - V_0)(1 - e^{-\frac{t}{T}}), \tag{1}$$

worin: V_0 ist die Geschwindigkeit Start-Stop, V_M — die maximale dem Motor auferlegte Geschwindigkeit, T — die Zeitkonstante des Diagramms in der Beschleunigungsphase, V — die momentane Geschwindigkeit im Augenblick t. Durch Ableitung in Abhängigkeit von der Zeit erhält man:

$$\frac{dV}{dt} = \frac{V_M - V}{T}, \tag{2}$$

oder in endlichen Differenzen:

$$\Delta V = \frac{\Delta t}{T}(V_M - V). \tag{3}$$

Wird dem Geschwindigkeit $V(t_i)$ des Motors im Moment t_i, $W(I)$ und dem Geschwindigkeit $V(t_{i-1})$, $W(I-1)$ zugewiesen, dann kann man für $t_{i-1} = t_i - \Delta t$, schreiben:

$$W(I) = W(I-1) + \Delta W(I-1), \tag{4}$$

wo

$$\Delta W(I-1) = \frac{V_M - W(I-1)}{T/\Delta t}, \qquad W(1) = V_0. \tag{5}$$

Die Bestimmung des Verhältnisses $T/\Delta t$ wird unter der Bedingung der Minimalisierung des Geschwindigkeitsfehlers durchgeführt. Theoretisch wird die maximale Geschwindigkeit V_M bei $e^{-t/T} = 1$ erreicht, also für $t \to \infty$.

Wir nehmen einen Grenzfehler der Geschwindigkeit $P1,(0{,}01\,V_m)$, an, so daß die mittels der Durchführung des Schrittes N_A-1 (N_A ist die Anzahl der Beschleunigungsschritte) erreichte Geschwindigkeit die auferlegte Restriktion erfüllt :

$$\Delta V = V_M - W(N_A-1) \leqslant \frac{P1}{100}\cdot V_M. \tag{6}$$

Die Geschwindigkeit, die mit der Durchführung des Schrittes K erreicht wird, ist :

$$W(k) = W(k-1) + \frac{V_M - W(k-1)}{Q}, \quad Q \triangleq \frac{T}{\Delta t}. \tag{7}$$

Es kann bewiesen werden, daß :

$$\begin{aligned} W(k) &= V_0\left(1-\frac{1}{Q}\right)^k + \frac{V_M}{Q}\left[1+\left(1-\frac{1}{Q}\right)+\ldots+\left(1-\frac{1}{Q}\right)^k\right] = \\ &= V_0\left(1-\frac{1}{Q}\right)^k + V_M\left[1-\left(1-\frac{1}{Q}\right)^k\right]. \end{aligned} \tag{8}$$

Für $k=1$:

$$W(1) = V_0 + \frac{V_M - V_0}{Q}. \tag{9}$$

Es wird angenommen, daß die Beziehung (8) gültig ist für $k-1$ so daß :

$$\begin{aligned} W(k) &= W(k-1) + \frac{V_M - W(k-1)}{Q} = \frac{V_M}{Q} + \left(1-\frac{1}{Q}\right)W(k-1) = \\ &= \frac{V_M}{Q} + \left(1-\frac{1}{Q}\right)\left\{V_0\left(1-\frac{1}{Q}\right)^{k-1} + \frac{V_M}{Q}\left[1+\left(1-\frac{1}{Q}\right)+\left(1-\frac{1}{Q}\right)^{k-1}\right]\right\} = \\ &= V_0\left(1-\frac{1}{Q}\right)^k + \left[1-\left(1-\frac{1}{Q}\right)^k\right]; \end{aligned} \tag{10}$$

es folgt daß die Beziehung (7) ist bestätigt.

Der Geschwindigkeitsfehler nach der Durchführung des Schrittes $k=N_A-1$ ist :

$$\Delta V = V_M - W(N_A-1) = V_M\left(1-\frac{1}{Q}\right)^{N_A-1} - V_0\left(1-\frac{1}{Q}\right)^{N_A-1}. \tag{11}$$

Durch Auferlegung der Bedingung (6) folgt :

$$\left(1-\frac{1}{Q}\right)^{N_A-1} \leqslant \frac{V_M}{V_M-V_0}\cdot\frac{P1}{100} \quad \text{bzw.} \quad Q \leqslant \frac{1}{1-\left(\frac{V_M}{V_M-V_0}\cdot\frac{P1}{100}\right)^{\frac{1}{N_A-1}}}. \tag{12}$$

Es wird angenommen :

$$Q = \left[\frac{1}{1-\left(\frac{V_M}{V_M-V_0}\cdot\frac{P1}{100}\right)^{\frac{1}{N_A-1}}}\right]. \tag{13}$$

Die Konstante Q wird die Performanz den Beschleunigung—Bremsung des Motors bestimmen.

Das exponentiale Geschwindigkeitsprofil kann in folgenden Varianten erzielt werden (Abb. 3).

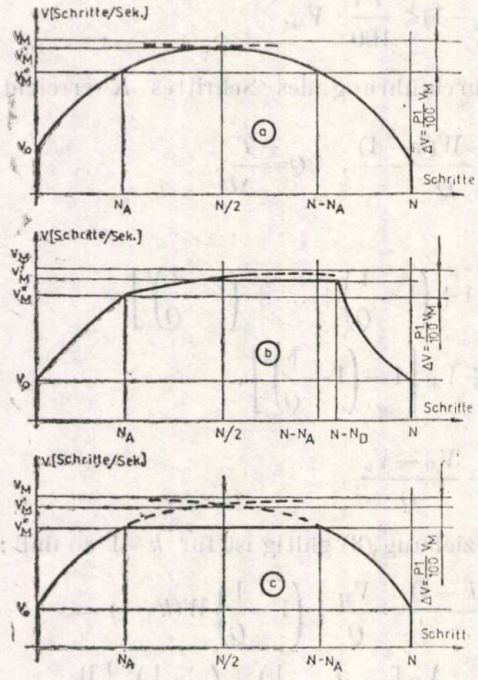

Abb. 3

Das symmetrische Profil mit zwei Phasen (Abb. 3 *a*) umfaßt die Beschleunigungsphase mit $N/2$ Schritten bis zur maximalen realen Geschwindigkeit V'_M (die Geschwindigkeit V_M kann nur theoretisch erreicht werden), gefolgt von einer Bremsung in $N/2$ Schritten. Nach der Durchführung von N_A Schritten wird die Geschwindigkeit V''_M erreicht, durch welche die der Geschwindigkeit des Motors auferlegte Genauigkeit versichert wird. Bis zur Durchführung von $N/2$ Schritten setzt die Beschleunigungsphase fort und hat, als Folge, die Abnahme des Geschwindigkeitsfehlers.

Das asymmetrische Profil mit drei Phasen (Abb. 3 *b*) umfaßt eine Beschleunigungsphase in $N/2$ Schritten bis zur maximalen realen Geschwindigkeit V'_M, ein Betrieb mit konstanter Geschwindigkeit bis zu $N-N_D$ Schritten, gefolgt von einer Bremsung in N_D Schritten. Bei den meisten Anwendungen ist $N_D=N_A$. Das Diagramm weist fortgeschrittenere Sicherheitsbedingungen beim Halten bei kleineren Werten der Beschleunigung auf, aber es hat den Nachteil großer Beschleunigungen bei hohen Geschwindigkeiten.

Das symmetrische Profil mit drei Phasen (Abb. 3 *c*) umfaßt eine Beschleunigungsphase in N_A Schritten, ein Betrieb mit konstanter Geschwindigkeit V'_M bis zu $N-N_A$ Schritten, gefolgt von einer Bremsung in N_A Schritten.

In allen der drei dargebotenen Fälle imponiert die Zeitkonstante der Beschleunigung—Bremsung mittels der Variablen $Q=T/\Delta t$, die von der Schrittanzahl der Beschleunigung—Bremsung und der der Geschwindigkeit auferlegten Präzision bestimmt ist.

3. Steuerungsalgorithmus. Organigramm

Um das Geschwindigkeitsdiagramm zu realisieren werden die Zeitintervalle zwischen zwei aufeinanderfolgenden Steuerungen des Motors bestimmt. Der Betrieb des Motors mit der Geschwindigkeit W (Schritte/Sekunde), erfordert die Ausarbeitung der Steuerungsimpulse in Intervallen $\nu=1/W$ (also, ein Steuerungsimpuls gelangt zum Motor nach einer Zeit $\nu=1/W$ Sekunden von der Aussendung des vorherigen Impulses).

Für das Zurücklegen von N Schritten werden die Geschwindigkeits-Vektoren $W(I)$ und die Vektoren der Zeitintervalle $\nu(I)=1/W(I)$ im Rahmen der Subroutine der Bestimmung des Geschwindigkeitsprofils (Abb. 4) berech-

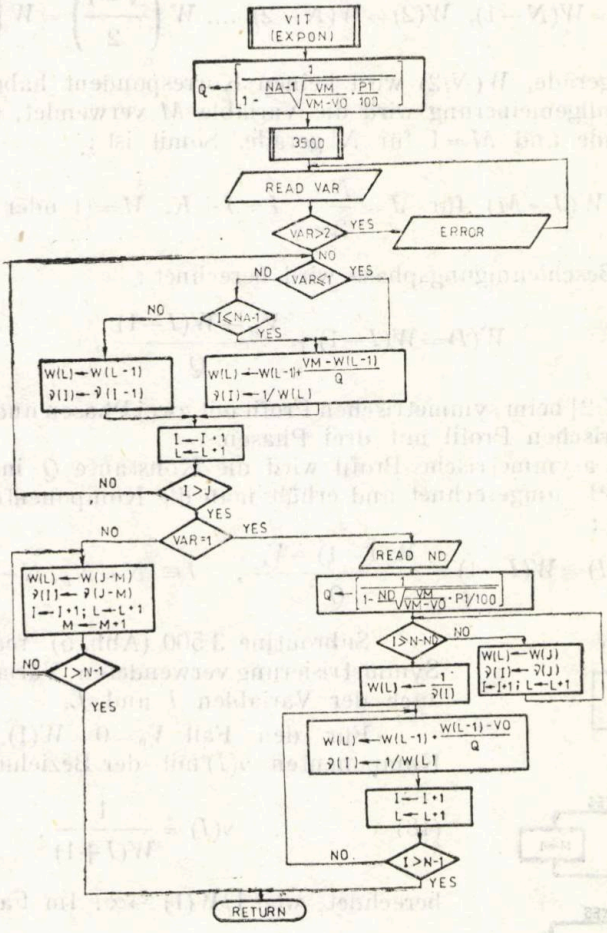

Abb. 4

net ; als bekannt werden die maximale Geschwindigkeit, V_M, die Anfangsgeschwindigkeit, V_0, die Geschwindigkeits-Präzision, $P1$, die Schrittanzahl der Beschleunigung, N_A und der Bremsung, N_D, angenommen.

Durch das Einführen der Variablen VAR wird der Typ des exponentialen Profils folgendermaßen ausgewählt : VAR=0 — symmetrisches Profil mit zwei Phasen; VAR=1 —asymmetrisches Profil mit drei Phasen; VAR= =2—symmetrisches Profil mit drei Phasen.

Für den Fall N ungerade wird der Vektor der Zeitintervalle ν eine gerade Anzahl von $N-1$ Komponenten haben.

Die symmetrischen Profile werden nur für die ersten $N/2$ Schritte berechnet, die zweite Hälfte der Bewegung wird von denselben Komponenten

beschrieben, aber in umgekehrter Richtung. Die den Schritten $(N/2+1)$, ..., $N-1$ entsprechenden Geschwindigkeiten werden wie folgt, erhalten:

Für N ungerade

$$(14) \qquad W(1)=W(N-1),\ W(2)=W(N-2),\ \ldots,\ W\left(\frac{N-1}{2}\right)=W\left(\frac{N-1}{2}+1\right).$$

Für N gerade, $W(N/2)$ wird keinen Korrespondent haben.

Zur Verallgemeinerung wird die Variable M verwendet, u. zw.: $M=0$ für N ungerade und $M=1$ für N gerade. Somit ist:

$$(15) \qquad W(I)=W(J-M) \text{ für } J=\frac{N}{2},\quad I=J+K,\ M=(1 \text{ oder } 0)+K,\ K>0.$$

In der Beschleunigungsphase wird berechnet:

$$(16) \qquad W(I)=W(I-1)+\frac{V_M-W(I-1)}{Q},$$

wobei $I\in[1, N/2]$ beim symmetrischen Profil mit zwei Phasen und $I\in[1,N_A-1]$ beim symmetrischen Profil mit drei Phasen.

Für das asymmetrische Profil wird die Konstante Q in Abhängigkeit von N_D und $P1$ umgerechnet und erhält man die Komponente W aufgrund der Beziehung:

$$(17) \qquad W(I)=W(I-1)-\frac{W(I-1)-V_0}{Q},\quad I\in[N-N_D,\ N-1].$$

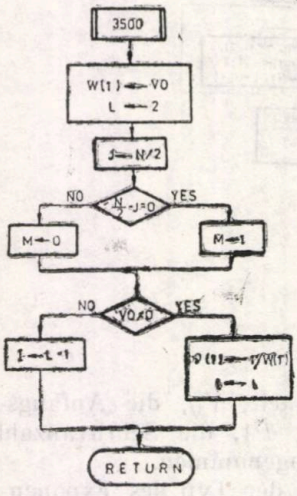

Abb. 5

Subroutine 3 500 (Abb. 5) realisiert die zur Symmetrisierung verwendeten Variablen M, sowie auch der Variablen I und L.

Für den Fall $V_0=0=W(1)$, werden die Komponenten $\nu(I)$ mit der Beziehung:

$$(18) \qquad \nu(I)=\frac{1}{W(I+1)},$$

berechnet, weil $1/W(1)\to\infty$. Im Falle $V_0\neq 0$:

$$(19) \qquad \nu(I)=\frac{1}{W(I)}.$$

Zur Verallgemeinerung:

$$(20) \qquad \nu(I)=\frac{1}{W(L)},\ \text{wobei } L=\begin{cases} I \text{ für } V_0\neq 0, \\ I+1 \text{ für } V_0=0. \end{cases}$$

4. Schlussfolgerungen

Die Positionierung eines Antriebsmechanismus mit Schrittmotoren setzt den Betrieb der Motoren gemäß eines bestimmten Geschwindigkeitsdiagramms voraus, mit Beschleunigungsetappen, Konstanthaltung der Geschwindig-

keit und Bremsung. Die Steuerung der Schrittmotoren mit geöffneter Schleife erfordert die Anwendung einiger Beschleunigungs-, Bremsungs-Techniken, um das Verlieren von Schritten zu vermeiden.

Erachtend die Vorzüge eines exponentialen Geschwindigkeitsdiagramms, wird die Ausarbeitungsmethode eines solchen Diagramms festgelegt ausgehend von den dem Mikrorechner gelieferten Anfangsdaten.

Das Diagramm wird während der Durchführung von $N-1$ Schritten realisiert, der erste vom Motor ausgeführte Schritt entspricht dem Startimpuls. Es werden praktisch $N-1$ Zeitintervalle zwischen den N Steuerungsimpulsen in Form eines Vektors mit $N-1$ Komponenten bestimmt. Die vom Motor erreichte Geschwindigkeit, dank der Durchführung des Schrittes I, ist in der entsprechenden Komponente des Vektors enthalten.

Eingegangen am 5. März 1990

Technische Hochschule, Jassy,
Lehrstuhl für Automatisierung

LITERATURVERZEICHNIS

1. Pal C., *Contribuţii la extinderea posibilităţilor de comandă numerică a sistemelor de acţionare electrică.* Dokt. Diss., TH, Jassy, 1981.
2. Auger M., *Procédé et dispositif pour commander l'accélération d'un moteur électrique pas à pas.* Brevet France, *8 504 373* (1986).
3. Pinchon D., *Sur le temps de réponse d'un système de positionement avec moteur pas à pas.* R.G.É., **71**, *1*, 51–55 (1982).
4. Pal C., *Structură hardware pentru comanda cu microcalculator a motoarelor pas cu pas.* II.ten Symp., „Strukturen, Algorithmen und Leitungsausrüstungen der industriellen Prozessen", Jassy, 1981.
5. Link W., *Das dynamische Verhalten des Schrittmotors bei schenellstmöglichen Positionierungsvorgängen.* AfE, **66** *1*, 19–27 (1983).

ASUPRA UNEI METODE DE GENERARE A GRAFICELOR DE VITEZĂ PENTRU MOTOARELE PAS CU PAS DIN CADRUL SISTEMELOR DE ACŢIONARE

(Rezumat)

Se prezintă unele aspecte privind generarea graficelor de viteză exponenţiale pentru motoarele pas cu pas din cadrul unui sistem de acţionare electrică, plecînd de la datele iniţiale furnizate microcalculatorului. Se consideră, în acest sens, viteza iniţială start-stop, viteza maximă, numărul de paşi de executat, variaţia acceleraţiei.

BULETINUL INSTITUTULUI POLITEHNIC DIN IAŞI
Tomul XXXVI (XL), Fasc. 3—4, 1990
Secţia III
ELECTROTEHNICĂ. ENERGETICĂ. ELECTRONICĂ. AUTOMATIZĂRI

D.K. 621.316.99

BEITRÄGE ZUM STUDIUM DES VERHALTENS DER ERDUNGEN IN BÖDEN MIT ERHÖHTEM WIDERSTAND BEI IMPULSEN

VON

RODICA OLĂH

1. Einleitung

Die Übergangprozeße der waagerechten Erdungen beim abfliessen des Blitzstromes können mit Hilfe der Gleichungen der langen homogenen Netzlinien, bei denen die Größen L, g, C und r gleich verteilt sind, studiert werden (Abb. 1).

Die Lösung dieser Gleichungen im Falle der Stromwelle in der „Rampenform", $i=at$, führt zu dem Impulswiderstandansdruck der Erdung [1]:

$$Z(0,t)=\frac{u(0,t)}{i(0,t)}=\frac{u(0,t)}{at}=\sqrt{\frac{r}{g}}\,\mathrm{cth}\sqrt{rg}\,l-\frac{c}{g^2lt}\left(1-\mathrm{e}^{-\frac{g}{C}t}\right)+$$

$$+\frac{2v^2L}{lt}\sum_{k=1}^{\infty}\frac{1}{(\delta^2+\omega^2k)}\left[1-\mathrm{e}^{-\delta t}\left(\frac{\delta}{\omega_k}\sin\omega_k t+\cos\omega_k t\right)\right]- \tag{1}$$

$$-\frac{4v^2\delta r}{lt}\sum_{k=1}^{\infty}\frac{1}{(\delta^2+\omega_k^2)}\left[1-\mathrm{e}^{-\delta t}\left(\frac{\delta}{2\omega_k}-\frac{\omega_k}{2\delta}\right)\sin\omega_k t+\cos\omega_k t\right],$$

in welcher:

$$\omega_k=\sqrt{\left(\frac{k\pi}{\tau}\right)^2-\sigma^2}, \tag{2}$$

während

$$\tau=\frac{1}{v} \tag{3}$$

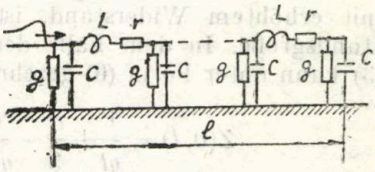

Abb. 1

stellt die Verbreitungszeit der Welle über die ganze Länge der Erdung mit der Geschwindigkeit $v=1/LC$ und

$$\delta=\frac{1}{2}\left(\frac{r}{L}+\frac{g}{C}\right), \tag{4}$$

$$\sigma=\frac{1}{2}\left(\frac{r}{L}-\frac{g}{C}\right) \tag{5}$$

sind der Dämpffaktor und bzw. der Distorsionskoeffizient.

Die Berechnung der Harmonische aus der Gleichung (1) ist schwierig, doch vereinfacht sich die Gleichung (1) in Einzelfällen, welches praktisch die meisten konkreten Fälle sind.

In dem Beiträge [2], [3] wurde der Fall der waagerechten Erdungen in Böden mit geringem Widerstand analysiert, deren Verhalten bei Impuls sich durch die Größen L und g charakterisierte.

In dem vorliegenden Beitrag wird die Möglichkeit der Verwendung einiger vereinfachten Gleichungen des Impulswiderstands, im Falle der Boden mit erhöhtem Widerstand bei dem auch die Kapazitätsbeilag beachtet wird, analysiert.

2. Berechnung des Impulswiderstands der langen waagerechten Erdungen im Böden mit hohem Widerstand

Im Falle in welchem der Bodenwiderstand so hoch ist, daß der Distorsionskoeffizient nicht wichtig ist, in der Gleichung (2) kann man σ^2 in Vergleich zu $(k\pi/\tau)^2$ vernachlassen und aus der Beziehung (2) folgt :

$$\omega_k = \frac{k\pi}{\tau} . \tag{6}$$

Wenn man eine Abweichung von 8% annimmt in der Berechnung der ersten Harmonische, erhält man :

$$\sqrt{1-\left(\frac{\sigma\tau}{\pi}\right)^2} = 0{,}92. \tag{7}$$

In diesem Falle ist $r/L \ll g/C$ und der Distorsionskoeffizient ist :

$$|\sigma| \cong |\delta| \approx \frac{g}{2C} = \frac{1}{2\varepsilon\varepsilon_0\rho} . \tag{8}$$

Aus den Beziehungen (3), (7) und (8) wird die größte Länge der Erdung festgesetzt für welche die Abweichung des Impulswiderstand nur durch die erste Harmonische beeinflußt ist :

$$l \leqslant 2{,}5\, v\varepsilon\varepsilon_0\rho. \tag{9}$$

So, die Abweichung aus der Berchnung von ω_k, in dem Falle der Böden mit erhöhtem Widerstand, ist im Zusammenhang mit der Impulswiderstandsgröße. In dem Falle der Erfüllung der Beziehung (9), der Ausdruck (3) kann unter Form (6) geschrieben werden und aus der Ausdruck (1) folgt :

$$\begin{aligned} Z(0,t) = {} & \frac{1}{gl} + \frac{rl}{3} - \frac{C}{g^2 lt}\left(1 - e^{-\frac{g}{C}t}\right) + \frac{Ll}{3t}\{1 - e^{-\delta t}[1 + 2F(\delta\tau - 3) - \\ & - 6F^2(\delta\tau - 1) + 4F^3\delta\tau]\} - \frac{2rl\delta\tau^2}{45t}\left\{1 - e^{-\delta t}\left[1 + F\left(\delta\tau - \frac{15}{\delta\tau}\right) - \right.\right. \\ & \left.\left. - 15F^2\left(2 - \frac{3}{\delta\tau}\right) + 10F^3\left(6 - \delta\tau - \frac{3}{\delta\tau}\right) - 15F^4(2 - \delta\tau) - 6F^5\delta\tau\right\}, \end{aligned} \tag{10}$$

wo :

$$F = \begin{cases} \dfrac{t}{2\tau} \text{ wenn } \dfrac{t}{2\tau} \leqslant 1 ; \\ \dfrac{t}{2\tau} - n \text{ wenn } \dfrac{t}{2\tau} > 1 ; \end{cases} \qquad n - \text{ganze Zahlen.}$$

Für die Zeit $t=0$ aus der Ausdruck (10) erhält man:

$$Z(0,0)=\sqrt{\frac{L}{C}}, \tag{11}$$

also die charakteristische Impedanz der Welle.

Für diskrete Werte von $t=n\tau$, in welchen n ganze Zahlen sind, aus dem Ausdruck (10) erhält man zwei Ausdrücke nämlich:

$$Z(0,t)=\frac{1}{gl}+\frac{rl}{3}+\frac{Ll}{3t}\left(1+\frac{1}{2}e^{-\delta t}\right)-\frac{C}{g^2lt}(1-e^{-\frac{g}{C}t})- \\ -\frac{2rl\delta\tau^2}{45t}\left(1+\frac{7}{8}e^{-\delta t}\right), \tag{12}$$

bei n — ungerade Zahlen, und

$$Z(0,t)=\frac{1}{gl}+\frac{rl}{3}+\frac{Ll}{3t}(1-e^{-\delta t})-\frac{C}{g^2lt}(1-e^{-\frac{g}{C}t})-\frac{2rl\delta\tau^2}{45t}(1-e^{-\delta t}), \tag{13}$$

bei n — gerade Zahlen.

Die Differenz zwischen den beiden Ausdrücken kann man dadurch erklären daß die wiederspiegelten Wellen vom Erdungsende gelengen an den Erdungsanfang nach einer Zeit $t=2\tau n$, verändert den Wert von Z.

Im Falle in welchem $\delta t\geqslant 3$, $e^{-\delta t}\to 0$; in der Gleichung (1) kann man $e^{-2\delta t}(\approx e^{-\frac{g}{C}t}=0)$ vernechlassen und erhält man aus dem Ausdruck (1)

$$Z(0,t)=\frac{1}{gl}+\frac{rl}{3}+\frac{Ll}{3t}-\frac{C}{g^2lt}-\frac{2rl\delta\tau^2}{45t}. \tag{14}$$

Die Amplitude der wiederspiegelten Oszillationen ist im diesem Falle umwichtig, also aus den Ausdrucken (11) und (12) direkt die Gleichung (14) folgt.

Beim Feststellen des Ausdrucks (14) aus der Beziehung (1) wurde angenommen daß die Pulsationen ω_k reale Werte darstellen, also in jeden Fallen wenn $k=[1,\infty)$,

$$\omega_k^2=\left(\frac{k\pi}{\tau}\right)^2-\sigma^2\geqslant 0, \tag{15}$$

welche einer Länge der Erdung

$$l\leqslant 2\pi v\varepsilon\varepsilon_0\rho \tag{16}$$

entspricht.

Ohne der Kapazität C und den Längewiderstand r zu beachten, aus der Beziehung (14) folgt:

$$Z(0,t)=\frac{1}{gl}+\frac{Ll}{3t}. \tag{17}$$

3. Beurteilung der Resultate und Schlussfolgerungen

In Abb. 2 wurde der Abhang zwischen dem Widerstand des Bodens ρ und der größten Länge der Erdung l, sowie die Hervorhebung der Zonen der Verwendung der vereinfachten Ausdrucken (12) ... (14) des Impulswiderstands der Erdung dargestellt. Der Impulswiderstand in der Zone I (Abb. 2),

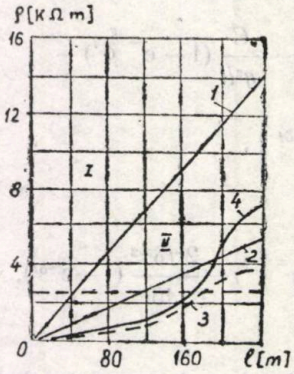

Abb. 2

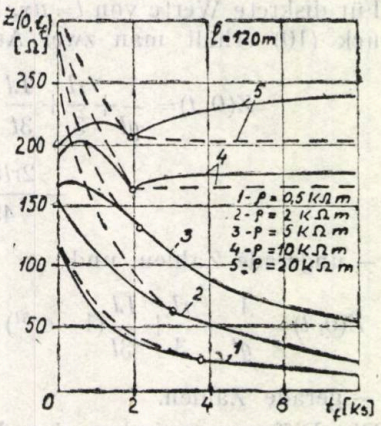

Abb. 3

welche durch die Ordonatenachse und Kurve (*1*), die der Gleichung $l=2{,}5v\varepsilon\varepsilon_0\rho$ entspricht, begrenzt ist, kann durch die Ausdrucke (12) und (13) errechnet werden. Im Falle $\delta t \geqslant 3$, kann man für die Zonen I und II (Abb. 2) den Ausdruck (14) verwenden. Die Zone II ist von der Ordonatenachse und Kurve (*2*), die der Gleichung $l=2\pi v\varepsilon\varepsilon_0\rho$ entspricht, begrenzt. Zum Vergleich wurde in Abb. 2 auch die Kurve (*3*) gezeichnet, welche der Kondition $l \leqslant 2\sqrt{\rho t}$ entspricht, für Böden mit geringen Widerstand [2]. Der Impulswiderstand in

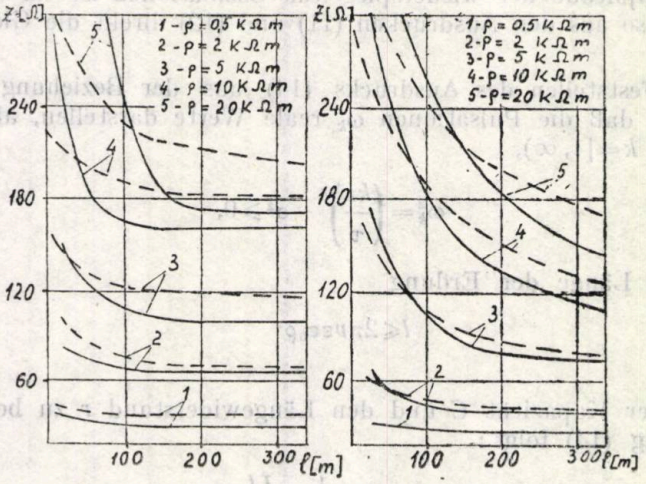

Abb. 4

der Zone *III* (Abb. 2), welche von der Linearformkurve $\rho = 2\,000\ \Omega m$ und Kurve (*3*) begrenzt ist, kann durch den Ausdruck (17) errechnet werden, also ohne den Kapazitätseffekt zu beachten. In Abb. 2 wurde auch die Kurve der größten realen Länge (*4*) dargestellt.

In Abb. 3 wurde der Zeitabhang des Impulswiderstands $Z(0, t_f) = f(t_f)_{\rho=\text{const.}}$ bei einer waagerechter Erdung von $l = 120$ m, für $\rho = 500 \ldots 20\,000\ \Omega m$, ohne den Längenwiderstand zu beachten, unter der Verwendung der ergebenen Ausdrucken dargestellt.

In Abb. 4 wurde der Abhang zwischen dem Impulswiderstand und der Länge der waagerechten Erdung $Z(0, t_f) = f(l)_{\rho=\text{const.}}$ für $\rho = 500 \ldots 20\,000\ \Omega m$ bei $t_f = 3\,\mu s$ (Abb. 4 *a*) und bei $t_f = 10\ \mu s$ (Abb. 4 *b*).

Die Kurve mit unterbrochener Linie bezieht sich auf die Situation in welcher die Kapazität C vernachlässigt wird.

4. Schlussfolgerungen

Aus der Beurteilung der festgesetzte Resultate ergeben sich die folgenden Schlußfolgerungen:

1. Im Böden mit geringem Widerstand ($\rho < 2\,000\ \Omega m$) und für Stoßströmen mit der Zeit des Frontes $t_f \geqslant 3\ \mu s$ kann man den Kapazitätseffekt vernachlässigen.

2. Der Kapazitätseffekt kann bei Böden mit großem Widerstand und umbesondere für $t_f < 3\ \mu s$ nicht vernachlässigt werden.

3. Die Verwendung der vereinfachten Gleichung (14) für die Berechnung des Impulswiderstands, mit Berücksichtigung der Kapazität, ist gültig in einem Bereich in welchem die Länge der Erdung und der Bodenwiderstand in Zusammenhang gebracht werden wie in Ausdruck (16).

4. Umsoviel der Wert des Bodenwiderstandes größer ist umsomehr wächst der Wert der Erdungslänge für welche die vereinfachte Gleichung (14) korrekt angesehen werden kann um ein geelignetes Verhalten der waagerechten Erdungen bei Impuls zu erhalten.

Eingegangen am 4. April 1990

Technische Hochschule, Jassy,
Lehrstuhl für Energetik

LITERATURVERZICHNIS

1. Анненков Б. З. *Расчет импульсного сопротивления противовесов.* Электричество, *2*, 19—23 (1970).
2. Oláh R., *Contribuţii la studiul comportării la impuls a prizelor de pământ orizontale în soluri cu rezistivităţi de valoare redusă.* Wiss. Tagung, TH, Jassy, 10—12. Nov. 1988, VIII. Abteilung, 333—336.
3. Oláh R., *Cu privire la calculul componentei inductive a rezistenţei prizelor de pământ în regim de impuls.* Wiss. Tagung, TH, Jassy, 10—12. Nov. 1988, VIII. Abteilung, 337—340.

CONTRIBUŢII LA STUDIUL COMPORTĂRII LA IMPULS A PRIZELOR DE PĂMÎNT ÎN SOLURI CU REZISTIVITATE DE VALOARE RIDICATĂ

(Rezumat)

Se analizează, pornind de la metoda cunoscută a modelării prizelor de pământ orizontale în regim de impuls prin scheme electrice cu parametrii uniform distribuiţi, posibilitatea utilizării unor relaţii simplificate de calcul a rezistenţei la impuls în cazul solurilor cu rezistivitate ridicată, la care se consideră şi parametrul capacitiv.

BULETINUL INSTITUTULUI POLITEHNIC DIN IAŞI
Tomul XXXVI (XL), Fasc. 3—4, 1990
Secţia III
ELECTROTEHNICĂ. ENERGETICĂ. ELECTRONICĂ. AUTOMATIZĂRI

C.D. 621.313.332

UN ALGORITHME DE CALCUL DU RÉGIME PERMANENT DU GÉNÉRATEUR ASYNCHRONE

PAR

VIRGIL ALEXANDRESCU, ROMULUS SFICHI, GH. CÂRŢINĂ, EUGEN VOINEA et VIOLETA ŢĂRANU

1. Introduction

L'utilisation avantageuse des machines asynchrones pour hydrogénérateurs à petite ou moyenne puissance est, de nos jours, bien connue et largement répandue. De plus, il paraît que les générateurs asynchrones à grande puissance vont jouer un rôle important à l'avenir dans les grands réseaux électriques [2], [3].

Le principal inconvénient du générateur asynchrone (GA) est représenté par une consommation assez élevée de puissance réactive, ce qui réclame l'installation des sources de compensation adéquates.

L'analyse des régimes permanents des réseaux électriques, auxquels sont raccordés des GA, doit constituer l'objet de nombreux études, y compris l'établissement du niveau optimal de compensation et l'encadrement en perspective de nouveaux GA. Cet impératif exige l'approfondissement du problème de la puissance réactive consommée par les GA. C'est justement dans ce but qu'on va proposer ci-dessous un algorithme itératif concernant le calcul du régime permanent du GA, en poursuivant tout d'abord la détermination de la puissance réactive demandée, qui dépend d'une façon sensible de divers facteurs tels que : la charge active, la valeur effective et la fréquence de la tension aux bornes du stator.

2. Algorithme proposé et résultats numériques

On expose brièvement dans l'annexe le schéma équivalent et les grandeurs qui regardent le régime permanent du GA. Dans ce qui suit on fera appel au schéma de la Fig. 1.

En appliquant au schéma de la Fig. 2 les tensions définies par les relations:

$$\underline{U}_1=\sqrt{3}\underline{U}_{1f}, \qquad \underline{U}_m=\sqrt{3}\underline{U}_{mf}, \qquad \underline{U}_2=\sqrt{3}\underline{U}_{2f}, \tag{1}$$

on obtient la multiplication par $\sqrt{3}$ des courants des branches et, par

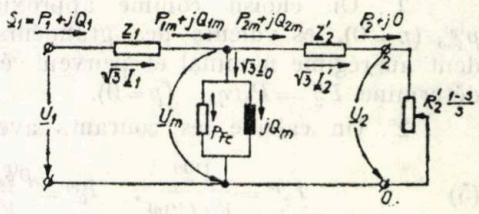

Fig. 1

conséquent, les puissances apparentes complexes spécifiées dans la Fig. 1 sont des puissances triphasées.

En tenant compte du sens positif choisi dans la Fig. 3, pour la circulation des puissances actives, il résulte :

$$P_1 = -P_{1g} < 0, \quad P_{1m} < 0, \quad P_{2m} = -P_{eg} < 0, \quad P_2 = -P_{mec} < 0 ; \tag{2}$$
$$Q_1 > 0, \quad Q_{1m} > 0, \quad Q_{2m} > 0.$$

La puissance réactive Q_1, absorbée par le GA, a deux composants : l'un de dispersion (Q_s) et l'autre d'aimantation (Q_m), ayant pour expressions :

$$Q_s = 3X_1 I_1^2 + 3X_2' I_2'^2, \tag{3}$$

$$Q_m = \frac{U_m^2}{X_m} = \sqrt{3}\, U_m I_m, \tag{4}$$

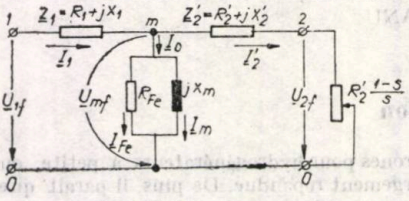

Fig. 2

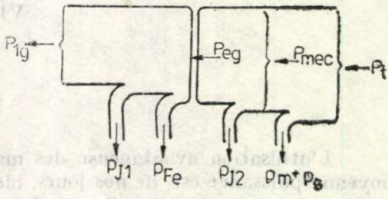

Fig. 3

de sorte que $Q_1 = Q_s + Q_m$.

Pour le GA, dont on connaît les données nominales P_n, U_n, $\cos\varphi_n$, η_{en} et les paramètres R_1, X_1, R_2', X_2', X_m, le calcul du régime permanent suppose à accepter les hypothèses suivantes :

a) grandeurs connues : la charge P_1, la tension U_1 et la fréquence f du réseau d'alimentation ;

b) dépendence proportionelle avec la fréquence des paramètres X_1, X_2' et l'indépendance de ceux-ci par rapport à la saturation ;

c) valeur constante du paramètre R_{Fe} ; à ce propos, on a constaté que l'approximation $R_{Fe} \simeq \infty$ est aussi satisfaisante ;

d) la tension $\underline{U}_1$ choisie pour origine de phase : $\underline{U}_1 = U_1 e^{j0}$;

e) grandeurs inconnues : Q_1, par ses composants Q_s et Q_m, η_e, s.

Quant à la valeur de X_m on peut la considérer fonction uniquement de la fréquence ou du régime si la courbe d'aimantation de la machine est connue. Cette courbe, qui représente la fonction $\Phi(I)$, se ramène à la forme $U_m(I_m)$ par des procédés habituels, en tenant compte aussi de la fréquence.

En notant par p le numéro de l'itération courante, l'algorithme itératif proposé comprend plusieurs pas de calcul, à savoir :

1°. On choisit comme approximations initiales $\underline{U}_m^{(p)}$, $U_2^{(p)}$, $Q_m^{(p)}$, $Q_s^{(p)}$, $p_{Fe}^{(p)}$, $(p=0)$, les valeurs des grandeurs $\underline{U}_m$, $\underline{U}_2$, Q_m, Q_s, p_{Fe} qui correspondent au régime nominal et peuvent être facilement calculées. De plus, on détermine $P_2^{(p)} = P_1/\eta_{en}$, $(p=0)$.

2°. On calcule les courants avec les formules :

$$\underline{I}_2'^{(p)} = \frac{P_2^{(p)}}{\sqrt{3}\,\underline{U}_2^{*(p)}}, \quad \underline{I}_0^{(p)} = \frac{p_{Fe}^{(p)} - jQ_m^{(p)}}{\sqrt{3}\,\underline{U}_m^{*(p)}}, \quad \underline{I}_1^{(p)} = \underline{I}_0^{(p)} + \underline{I}_2'^{(p)}, \tag{5}$$

où l'indice * signifie la conjuguée d'une grandeur complexe.

3°. On détermine des nouvelles valeurs pour les tensions $\underline{U}_m$ et $\underline{U}_2$:

$$\underline{U}_m^{(p+1)} = U_1 - \sqrt{3}\underline{Z}_1\underline{I}_1^{(p)}, \qquad \underline{U}_2^{(p+1)} = \underline{U}_m^{(p+1)} - \sqrt{3}\underline{Z}_2'\underline{I}_2'^{(p)}, \tag{6}$$

où l'on a noté par: $\underline{Z}_1 = R_1 + jX_1$, $\underline{Z}_2' = R_2' + jX_1'$.

4°. En utilisant les valeurs $U_m^{(p+1)}$, $I_1^{(p)}$, $I_2'^{(p)}$ on calcule:

a) les puissances $Q_m^{(p+1)}$, $Q_s^{(p+1)}$ à l'aide des formules (4) et (5);

b) les pertes:

$$p_{Fe}^{(p+1)} = \frac{(U_m^{(p+1)})^2}{R_{Fe}}, \quad p_{J1}^{(p)} = 3R_1(I_1^{(p)})^2, \quad p_{J2}^{(p)} = 3R_2'(I_2'^{(p)})^2; \tag{7}$$

c) les autres grandeurs:

$$P_2^{(p+1)} = P_1 - p_{J1}^{(p)} - p_{J2}^{(p)} - p_{Fe}^{(p+1)}, \quad \eta_{le}^{(p+1)} = \frac{P_1}{P_2^{(p+1)}}, \quad s^{(p+1)} = \frac{p_{J2}^{(p)}}{p_{J2}^{(p)} + P_2^{(p+1)}}; \tag{8}$$

e) on vérifie les conditions de convergence imposées simultanément aux grandeurs Q_m, Q_s, P_2:

$$|Q_m^{(p+1)} - Q_m^{(p)}| \leq \varepsilon_Q, \qquad |Q_s^{(p+1)} - Q_s^{(p)}| \leq \varepsilon_Q, \qquad |P_2^{(p+1)} - P_2^{(p)}| \leq \varepsilon_P. \tag{9}$$

Si ces conditions ne sont pas satisfaites, on reprend les calculs en partant du point 2°.

Les tests effectués sur différents types de GA ont prouvé une bonne convergence du processus itératif. Dans ce sens on présente quelques résultats concernant les deux types de GA, concentrés dans le Tableau 1.

Tableau 1

Données nominales et paramètres techniques pour deux type de GA

Type	P_n KW	U_n V	n_1 tours/min	cos φ_n	$p_{Fe\,n}$ KW	R_1 Ω	X_1 Ω	R_2' Ω	X_2' Ω	X_m Ω
1	1 200	400	600	0,83	17,55	0,00151	0,0171	0,00206	0,0193	0,383
2	800	400	500	0,87	6,2	0,00234	0,0165	0,00214	0,0166	0,518

En général, on a constaté que la convergence est réalisée en 3...5 itérations, en choisissant les erreurs $\varepsilon_Q = \varepsilon_P = 1 \ldots 2$ KVA. L'exemple numérique présenté dans le Tableau 2 met en évidence que la convergence est obtenue après 4 itérations, pour $\varepsilon_Q = \varepsilon_P = 1{,}5$ KVA.

Les fonctions $Q_1(U_1)$, qui représentent les caractéristiques statiques de charge réactive pour les deux types de GA du Tableau 1, obtenues en appliquant le même algorithme, sont représentées dans les Fig. 4 (GA du type *1*) et 5 (GA du type *2*). En tout les deux cas on a tracé les courbes qui correspondent aux différentes charges actives pour deux valeurs de la fréquence (1 — f=50 Hz; 2 — f=47 Hz).

Tableau 2

Résultats du calcul itératif pour le GA du type 1 dans le régime caractérisé par : $P_1 = -800$ KW $U_1 = 380$ V, $f = 50$ Hz

Itération	U_m V	U_2 V	Q_s Kvar	Q_m Kvar	P_2 KW
0	374,48	376,23	438,87	366,16	−842,3
1	356,55	354,34	198,98	331,93	−835,22
2	360,97	363,78	222,45	340,2	−837,96
3	360,07	361,82	214,18	338,5	−837,06
4	360,31	362,35	215,63	338,97	−837,23

On a remarqué aussi que l'utilisation de la courbe d'aimantation du GA au point *d* de l'algorithme, en vue de calculer la puissance Q_m, n'exerce pas une influence importante sur la rapidité de la convergence.

3. Conclusions

1. L'algorithme proposé a été testé pour divers types de GA dans plusieurs variantes du régime, attestant son efficacité par la convergence rapide et sûre du processus itératif.

2. On peut effectuer le calcul du régime permanent d'un réseau électrique contenant des GA, à une precision élevée, en utilisant l'algorithme présenté ci-dessus. Dans ce cas chaque itération concernant le régime du réseau, à l'aide de laquelle on détermine les tensions nodales, est suivie des calculs itératifs, par la méthode exposée, pour les noeuds auxquels sont connectés des GA.

Annexe

Le régime permanent de la machine asynchrone est décrit, conformément à la théorie technique, à l'aide du schéma équivalent monophasé de la Fig. 2, où l'on a spécifié les grandeurs ci-dessous : R_1, X_1 — la résistance et la réactance de dispersion du stator ; R'_2, X'_2 — la résistance qui correspond aux pertes Joule et la réactance de dispersion du rotor, rapportées au stator ; R_{Fe}, X_m — la résistance qui correspond aux pertes dans le fer du stator et la réactance d'aimantation ; $\underline{I}_1$, $\underline{I}'_2$, $\underline{I}_{Fe}$, $\underline{I}_m$, $\underline{I}_0$ — les valeurs effectives complexes des courants attachés aux diverses branches du schéma ; $s = (n_1 - n)/n_1$ — le glissement de la machine, défini en fonction de la vitesse synchrone n_1 et de la vitesse n du rotor ; $\underline{U}_{1f}$, $\underline{U}_{mf}$, $\underline{U}_{2f}$ — les valeurs effectives complexes des tensions de phase aux paires de bornes $1-0$, $m-0$, $2-0$.

Le régime de générateur sera possible si le rotor est entraîné par un moteur primaire (turbine) à une vitesse sursynchrone ($n > n_1$, $s < 0$), le stator étant connecté à un réseau électrique ou à une batterie de condensateurs. Dans ce cas le générateur asynchrone, en fournissant de la puissance active, consomme simultanément de la puissance réactive nécessaire aux circuits magnétiques de la machine.

Le bilan des puissances actives du générateur asynchrone est représenté dans la Fig. 3, où l'on a noté par : P_{1g} — la puissance utile, produite aux bornes du stator ; P_t — la puissance fournie par la turbine à l'arbre du générateur ; p_{J1}, p_{J2} — les pertes Joule du stator et, respectivement, du rotor ; p_{Fe} — les pertes dans le fer du stator ; $p_m + p_s$ — les pertes mécaniques et supplémentaires ; P_{eg} — la puissance transmise sur voie électromagnétique du rotor vers le

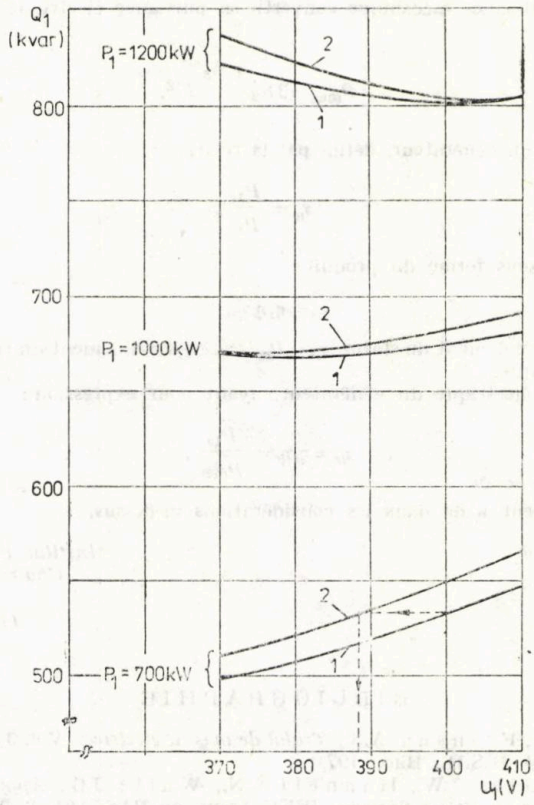
Q1
(kvar)
P1=1200kW
P1=1000kW
P1=700kW
800
700
600
500
370
380
390
400
410
U1(V)
1
2

Fig. 4

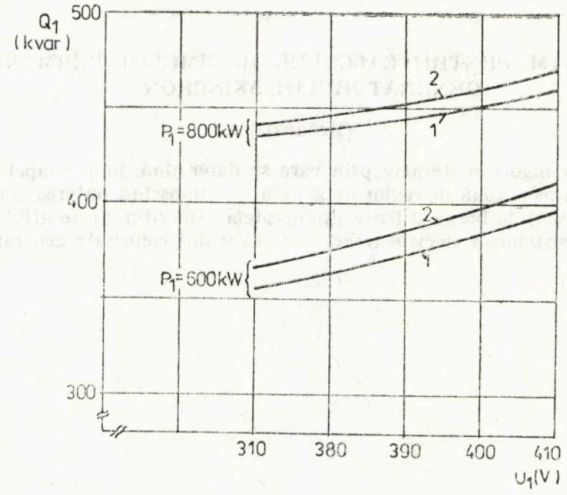
Q1
(kvar)
500
400
300
P1=800kW
P1=600kW
310
380
390
400
410
U1(V)
1
2

Fig. 5

stator ; P_{mec} — la puissance mécanique convertie en puissance électrique dans le rotor, qui a pour expression :

$$P_{mec}=3R_2'\frac{1-s}{s}I_2'^2. \tag{A.1}$$

Le rendement du générateur, défini par la relation :

$$\eta_g=\frac{P_{1g}}{P_t}, \tag{A.2}$$

on peut le calculer sous forme du produit :

$$\eta_g=\eta_s\eta_r\eta_m, \tag{A.3}$$

où $\eta_s=P_{1g}/P_{eg}$ est le rendement du stator, $\eta_r=P_{eg}/P_{mec}$ — le rendement du rotor, $\eta_m=P_{mec}/P_t$ — le rendement mécanique.

Le rendement électrique du générateur, ayant pour expression :

$$\eta_e=\eta_s\eta_r=\frac{P_{1g}}{P_{mec}}, \tag{A.4}$$

représente une grandeur utile dans les considérations ci-dessus.

Reçue le 18 avril 1990

Institut Polytechnique, Jassy,
Chaire d'Énergétique
et
IRE, Suceava

BIBLIOGRAPHIE

1. Gheorghiu I.S., Fransua A.S., *Tratat de mașini electrice.* Vol. 3, *Mașini asincrone.* Ed. Acad. R.S.R., Buc., 1971.
2. Mello F.P., Feltes J.W., Hannett L.N., White J.C., *Application of Induction Generators in Power Systems.* IEEE Trans. on PAS, **101**, 9, 3 385—3 393 (1982).
3. Фазылов Х. Ф., Аллаев К. Р., *Расчетный и экспериментальный анализ режимов электроэнергетических систем содержащих асинхронные генераторы.* Энергетика и транспорт, *6*, 33—41 (1989).

UN ALGORITM PENTRU CALCULUL REGIMULUI PERMANENT AL GENERATORULUI ASINCRON

(Rezumat)

Se prezintă un algoritm iterativ prin care se determină, în principal, puterea reactivă consumată de mașina asincronă în regim de generator, cunoscînd puterea activă debitată, valoarea efectivă a tensiunii la borne și frecvența acesteia. Algoritmul este util în calculul regimurilor permanente ale sistemelor electroenergetice la care sînt conectate generatoare asincrone.

BULETINUL INSTITUTULUI POLITEHNIC DIN IAŞI
Tomul XXXVI (XL), Fasc. 3—4, 1990
Secţia III
ELECTROTEHNICĂ. ENERGETICĂ. ELECTRONICĂ. AUTOMATIZĂRI

C.D. 621.311.21 ; 621.3.072.8

LE PROBLÈME DE L'ÉNERGIE RÉACTIVE DANS LES RÉSEAUX ÉLECTRIQUES AVEC DES MICROHYDROCENTRALES

PAR

GH. CÂRŢINĂ, ROMULUS SFICHI, VIRGIL ALEXANDRESCU et EUGENIU VOINEA

1. Introduction

La puissance réactive demandée par le générateur asynchrone (GAS), fonctionnant dans un régime permanent, est la somme de la puissance réactive de magnétisation, Q_m, et des puissances réactives de dispersion dans le stator et dans le rotor (Q_{s1}, Q_{s2}) :

$$Q=Q_m+Q_s=Q_m+Q_{s1}+Q_{s2}. \tag{1}$$

En principe, le problème de la consommation de la puissance réactive par machine asynchrone reste le même tant dans le régime de générateur, que dans celui de moteur. En considérant le caractère complexe des phénomènes, pour le calcul de la puissance réactive demandée par GAS, à partir des valeurs des puissances actives fournies (P_1), de la tension aux bornes (V_1) et de la fréquence du réseau (f_1), on peut utiliser l'algorithme et le programme de calcul présentés en [1]. Dans cette Note on présente, toutefois, les courbes de variation de la puissance réactive en fonction de la tension aux bornes et de la fréquence du réseau, pour différents types de générateurs asynchrones.

2. La compensation de la puissance réactive dans les réseaux avec des microhydrocentrales

Dans les microhydrocentrales on utilise, comme générateurs, des moteurs asynchrones de différentes puissances. La compensation de la puissance réactive dans les réseaux avec des microhydrocentrales représente un problème assez difficile. Du point de vue mathématique il s'agit d'un modèle d'optimisation des productions d'énergie réactive dont la fonction-objectif est le coût total actualisé.

Les composants des frais totaux actualisés sont : C_{PE} — le coût actualisé de la réduction des pertes d'énergie active ; C_{CE} — la réduction du coût actualisé des pertes de puissance active à la pointe de charge ; I — le coût des investissements dans les sources réactives.

Le bénéfice obtenu par la compensation de l'énergie réactive a donc pour expression :

$$(2) \qquad B=C_{PE}-C_{CE}-I=\sum_{i=1}^{n}(\theta\bar{q}_i r_i x_i-\lambda r_i x_i^2+\theta\bar{Q}_i R_i X_i-\lambda R_i X_i^2-a x_i),$$

où :

$$(3) \qquad \theta=2(G'\sigma'+\alpha)\,; \quad G'=10^{-3}\frac{u^2}{V_n^2}G\,; \quad a=\gamma u+\lambda p_c\frac{V_n^2}{u}\,; \quad \lambda=G'+\alpha\,;$$

$$\alpha=\frac{k_a\beta_a}{10^3}N_f\frac{u^2}{V_n^2}\,; \quad \sigma'=\left(1+2\,\frac{\sigma}{100}\right)k\beta.$$

Les symboles utilisés dans les relations ci-dessus ont les significations suivantes : $\bar{q}_i$, x_i — la valeur moyenne de la puissance réactive au noeud i, respectivement la puissance des condensateurs installés au noeud i ; $\bar{Q}_i$, X_i — la valeur moyenne de la puissance réactive circulant dans le tronçon i, respectivement la puissance des condensateurs installés en aval du noeud i ; r_i, R_i — les résistances électriques du transformateur installé au noeud i, respectivement du tronçon i ; β_a — le prix de revient du KWh perdu ; N_f — le nombre des heures de fonctionnement par année ; k_a — le coefficient d'actualisation (a — le taux d'actualisation) ; p_c — les pertes spécifiques d'énergie dans les condensateurs ; u — la puissance de l'unité standardisée de condensateurs ; β — un coefficient de corrélation ; γ — le prix de revient du Kvar installé dans les condensateurs ; G — le prix de revient du KW installé dans la centrale électrique de pointe ; $q_{i\max}$, $Q_{i\max}$ — les puissances réactives au maximum de charge ; σ — l'écart type de la variable aléatoire $q(t)$.

Dans la relation (2), le bénéfice est exprimé en fonction des valeurs moyennes des puissances réactives. Le modèle d'optimisation des productions d'énergie réactive contient, outre la fonction-objectif (2), les restrictions

$$(4) \qquad x_i\leqslant x_{i\max}, \quad \sum_{i=1}^{n}x_i\leqslant X_{\text{disp}}, \quad (i=\overline{1,n}),$$

où X_{disp} représente le nombre des unités de condensateurs disponibles.

L'algorithme de calcul utilise une méthode d'optimisation au long des axes de coordonnées, avec des pas d'exploration constants, égaux avec la valeur de l'unité standardisée de condensateurs (15 Kvar, 20 Kvar, ...).

Chaque itération a deux étapes :

a) le calcul de la variation du bénéfice pour les variations unitaires des variables x_i, $(i=\overline{1,\ n})$:

$$(5) \qquad \mu_i=\Delta B_i, \quad (i=\overline{1,n})\,;$$

b) la définition d'une séquence par :

$$(6) \qquad x_k^{(s+1)}=x_k^{(s)}+1 \quad \text{pour le noeud } k, \quad \Delta B_k=\max_i\{\Delta B_i\},$$

$$(7) \qquad x_i^{(s+1)}=x_i^{(s)}, \text{ pour le reste.}$$

Ces variations sont calculées à chaque itération de manière à maximiser le bénéfice. Le critère d'arrêt est atteint si :

a) la variation du gain devient nulle

$$\mu_i=\Delta B_i=0, \qquad (i=\overline{1,n})$$

et la compensation n'est plus économique ;

b) la compensation a atteint une limite technique (les relations (4)), où les valeurs imposées sont déterminées à partir d'autres critères.

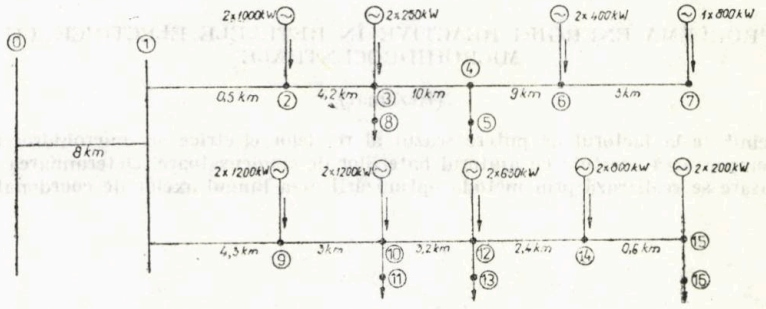

Fig. 1. — Schéma du réseau électrique étudié.

Pour le schéma de la Fig. 1 ont été analysées 6 variantes, présentées dans le Tableau 1. Dans le tableau, pour les six variantes sont présentées les économies d'énergie/année, le nombre des unités de compensation, le bénéfice/année, etc.

Tableau 1

Les caractéristiques	Les variantes de calcul					
	I	II	III	IV	V	VI
La section du conducteur, [mm²]	50	95	95	95	95	95
N_f, [h/année]	2 920	2 920	2 920	2 000	1 500	1 000
G, [lei/KW]	8 760	8 760	0	8 760	8 760	8 760
γ, [lei/Kvar]	175	175	0	175	175	175
β_a, [lei/KWh]	0,65	0,65	1	0,65	0,65	0,65
$\sum_{i=1}^{n} x_i$, $u=15$ Kvar	261	258	261	251	245	237
le bénefice / année, [10^3 lei]	1 111	493	569	377	314	252
ΔW, [MWh/année]	1 111	570	570	393	294	196

3. Conclusions

L'analyse de la compensation de l'énergie réactive dans les résea ux considérés atteste un niveau de compensation au dessous du niveau optimal.

Dans les réseaux électriques avec des microhydrocentrales, le niveau optimal de compensation s'approche du celui maximal.

L'exactitude du calcul est liée à celle des données d'entrée.

Reçue le 5 mai 1990

Institut Polytechnique, Jassy,
Chaire d'Énergétique
et
IRE, Suceava

BIBLIOGRAPHIE

1. * * * Contract de recherche scientifique, Inst. Polyt., Jassy, *2 230* (1988).
2. Cârţină Gh., *Modèle mathématique et méthode d'optimisation des productions d'énergie réactive dans un réseau électrique*. Bull. ASE/UCS, **73**, *1*, 27—31 (1983).

PROBLEMA ENERGIEI REACTIVE ÎN REŢELELE ELECTRICE CU MICROHIDROCENTRALE

(Rezumat)

Plecînd de la factorul de putere scăzut al reţelelor electrice cu microhidrocentrale se propune compensarea acestuia cu ajutorul bateriilor de condensatoare. Determinarea puterilor de compensare se realizează prin metoda optimizării de-a lungul axelor de coordonate.

BULETINUL INSTITUTULUI POLITEHNIC DIN IAŞI
Tomul XXXVI (XL), Fasc. 3—4, 1990
Secţia III
ELECTROTEHNICĂ. ENERGETICĂ. ELECTRONICĂ. AUTOMATIZĂRI

RECENZII

BOOK REVIEWS РЕЦЕНЗИЙ

BUCHANAN J., *CMOS/TTL Digital System Design*. McGraw-Hill Publishing Comp., New York, 1990, ISBN 0-07-008711-3.

In the last thirty years, digital electronic technology was widely developed, becoming increasingly faster. In the past, with the older slower logic families, designers were often able to neglect the electrical system without disastrous results. That is no longer possible. The need for speed requests very fast edges, very low noise margins, and other nonideal characteristics of the digital circuits which, carelesly used, invite disaster.

The book covers the most common problems that arise in very fast electronic circuit design using TTL and CMOS logic families and tries to give some clues for the electrical design of digital circuits.

In order to do this, the author points out in the first part of the book the most common problems that can be met in working digital circuits, giving a broad and detailed explanation of each of them. The reader becomes accustomized with notions as TTL and CMOS logic families, TTL and CMOS circuits, noise margins, fan-out constraints, inductance and transient current effect, crosstalk, transmission-line ringing, power-supply transients and ground upsets.

The second part includes a set of guidelines and design recommendations so that the problems described in the first part can be avoided. This part deals with major topics as : power, ground, reset and clock signal distribution, signal interconnections, system timing, delays and so on. The last chapter of the second part deals with an usually neglected topic : the unused inputs. The danger of allowing CMOS device inputs to float is noted and the destructive mechanism is described.

Throughout the book, practical engineering approximations are used rather than rigorous mathematical analysis. The goal is to develop a practical engineering estimate of the magnitude of any possible problem in an efficient and timely manner.

The book is structured in two parts and fourteen chapters. Every chapter deals with detailed information on a specific topic so that readers interested in some particular information can go directly to the chapter that deals with that particular information.

The book is highly recommended to computer and electronics engineers that use high speed TTL and CMOS logic devices and, beyond a good logic design, they also need a good electrical design for their devices.

Răzvan Voicu

SARKOWSKI H., *Messtechnik bei Electronikgeräten*. Export Verlag, Berlin, 1984, 189 S., ISBN 3-8169-0384.

Die Informationsexplosion hat den Park der Meßgeräte auf elektrischem Wege stark bereichert. Diese Tatsache zwang den Fachmann den Auftrag kontinuerlichen Studiums der neuen meßtechnischen Ausrüstung, sowohl analytisch als auch synthetisch, zu unternehmen.

Das vorliegende Buch behandelt den zweiten Gesichtspunkt, so daß sein Inhalt leicht lesbar und nutzvoll ist.

Der komplexe theoretische Anblick der Funktionierung dieser Meßgeräte ist weggelaßen und man betrachtet nur die Weise wie ein bestimmtes Gerät in einen bestimmten Meßzweck implementiert ist. Anders gesagt, das Buch gibt dem Fachmann mässige Angebote für die praktische Probleme die er auslösen muß.

Den zehn Kapitel entlang waren ausgesehen fast alle Meßmittel die dem Fachmann nutzbar sind (von klassischen Avometer, Wattmeter bis zum komplizierten, elektronischen Meß- und Prüfgeräte).

Ich würde empfehlen daß der Leser ins Durchlesen einigen Kapitel besonders sorgfältig zu sein.

Erstens, die Problematik des Einheitensystems. Die Einführung des Internationalen-Einheitensystems, (SI), hat die Benutzung elektrischen Meßeinheiten vom Praktiker viel erleichtert. Er muß trotzdem die Besonderheiten dieses Systems sich eignen, nämlich die die inkohärente Einheiten („die fremde Einheiten") betreffen und die Schreibung (Symbolisierung) der abgeleiteten Einheiten, im allgemeinen. Man könnte so einige schlechte Gewohnheiten entweder aus alten Büchern oder aus täglichen Routine geerbt, vermeiden.

Äusserst wichtig für Meßtechik sind die in siebenten Kapitel gegebene Anweisungen bezüglich des Verhaltens der Meßgeräte in Hochfrequenz.

Wird der Einfluß der Erdkapazitäten, bzw. der Leitungsinduktivitäten durch geeignete Verfahren, gemäß jeden Meßfall, nicht vermieden, dann können Meßergebnisse ganz illusorisch sein.

Endlich, die letzte drei Kapitel stellen eine gewisse Neuheit dar. Sie beschreiben nicht einige Meßgeräte, sondern Test-Geräte die etwas über logischen Zustände der Bauelementen digitaler Meßgeräte ausdrücken können. Also zeigen sie das Binär-Verhalten des Test-Objektes an, daher funktioniert er normal oder mangelhaft.

Diese elektronische Test-Geräte gehen von einfachen Logik-Tastköpfe, Logik-Klips oder Logik-Komparatoren aus und kommen bis komplizierten Logik-Analysatoren (Zeit-Analysatoren und Zustands-Analysatoren) oder die Methode der Signatur-Analyse an.

Die Geräte von ersten Typus gestatten das Mangel der einfachen IC-Bauelemente entdeckt werden können, während die der zweiten Typus machen dasselbe, aber für komplizierten VLSI-IC-Bauelemente, nämlich Mikroprozessoren.

Zum Beispiel, gelingt die Methode der Signatur-Analyse für einen Mikroprozessor (in gewisse Hardware- und Software-Bediengungen) eine binäre Konfiguration, an einen gewissen Knotenpunkt der Schaltung (auf 16 Bit, in Hexadezimal kodiert), feststellen. Im Normalfall der Funktionierung, diese Konfiguration stellt die echte Signatur für denjenigen Knotenpunkt der Schaltung dar. Falls für ein anderen Mikroprozessor (desselbe Typus) tritt eine andere Konfiguration auf, das heißt eine Fälschung ist geschehen und der Mikroprozessor mangelhaft ist. Es ist möglich daß der Mangel, durch die einfache Platinen-Austauschung, verschwindet.

Also, diese Signatur-Analyse kann Zeit und Geld ersparen sowohl in Ausnutzung als auch in Entwicklung elektrischer Meßsysteme.

Das Verdienst dieses Buches ist das daß ihm gelingt um einen großen Informationsinhalt in einen beschränkten Raum zusammenzupressen.

Die Sprache ist einfach und lapidar, so daß das Durchlesen des Buches in wenige Stunden ganz möglich ist.

Das Buch gestattet dem Techniker, dem Ingenieur sogar dem Studenten wie und mit welchen Meßmitteln gewisse elektrische Meßgrößen gemessen werden können, eventuel wie Mangel bei Digital-Meßmittel lokalisiert werden können.

P. Pogângeanu

VOGEL J., *Elektrische Antriebstechnik*. VEB Verlag Technik, Berlin, 1988, 416 S. ISBN 3-341-00489-0

The electric drives, widely used in economy, represent one of the most important consumers of electric power. The proper and scientifically-based choice of a driving system, is the aim of this book which is divided into six chapters and appendixes.

The first chapter presents the fundamental quantities of the motion which intervene in the driving system imposed by the working machine : power and torque, mechanical power, kinematic magnitudes (space, speed, acceleration, variation of acceleration vs. time) for the translation and rotational motions. The running conditions of the working machines and their classification according to these conditions are discussed.

The second chapter deals with the mechanical and adjustment characteristics, the running conditions of the electric driving machines, as well as with the friction and induction electromagnetic couplings. Some notes on the choosing of the electrical driving machines are to be found at the end of this chapter.

The third chapter deals with the determination of the power of the electric driving motor under heating conditions for various running conditions of the working machine, namely, intermittent duration, pulsatory and non-periodic loadings.

The fourth chapter presents the power electronic control of the electrical driving system.

The fifth chapter discusses the optimal control of the driving systems, referring to the adjustment of the speed and of the position for different electrical driving systems.

The sixth chapter presents the driving systems with various special electrical motors.

This book is intended for the specialists working in the field of design, controll and exploitation of the electrical driving systems.

Simona-Ana Caba

ZIMMERMANN R. u.a., *Das Technik — Wörterbuch Lichttechnik.* VEB Verlag Technik, Berlin, 1989, 428 S., ISBN 3-341-00722-9.

This dictionary in four languages (English, German, French and Russian) has been made on account of the development during the last years of the electric lighting in the industrialized countries, the reason being the increasing needs for new light sources and superior lighting systems, the new results of the researches on the physiology and psychology of sight as well as the concept of the rational usage of energy sources.

This work aims to help the research specialists, the engineers, technicians and designers from the lighting field. At the same time, it is useful for professors and students from universities, technical institutes, higher and specialized schools, for translators and people working in the documentation domain.

The dictionary contains about 11,000 words from the following domains : a) the base of the lighting technique ; b) the technique of light generation ; c) the measuring technique for light, irradiation and colour ; d) lighting technique ; e) radiation receivers.

To simplify the things, this paper uses a two-part recording system. The first part, the main one, contains alphabetically the English terminology (words and expressions) as well as the corresponding translations in the other languages. The second part contains the same words and expressions, alphabetically arranged, for each of the three other languages and the references to the corresponding number in the first part.

Mircea Oprişor

FRAIDON FRAMROZ MAZDA, *Power Electronics Handbook.* Butterworths & Co Ltd., London, 1990, 417 pp., ISBN 0-408-03004-4.

This handbook presents the components and circuits used in power electronic systems as well as their main applications. The content is composed from four parts as follows :

The first chapter describes shortly the manufacturing technologies of power semiconductors, the design and characteristics of the currently used components.

The second part presents the auxiliary elements and devices used in combination with power semiconductors, namely : a) the methods and elements used to eliminate the heat generated in the semiconductor junction with a view to maintain its working efficiency (chapter 2) ; b) small-power devices used to control the power semiconductors valves (chapter 3) ; c) the methods and components used to reduce the radio interferences generated by the power electronic circuits (chapter 4) ; d) the components and circuits used to protect the power valves from overvoltages and overcurrents (chapter 5).

The third part gives detailed information on the component and design of different circuits with power semiconductors, as follows : a) types of circuits with power semiconductors (chapter 6) ; b) basic power circuits used for static switching (chapter 7) ; c) circuits used to alternating voltage control (chapter 8) ; d) rectifier circuits with control on the a.c. part (chapter 9) ; e) circuits used to change directly the frequency of an alternating current source (chapter 10); f) existing forced switching systems (chapter 11); g) direct d.c.—d.c. convertors (chapter 12); h) d.c.-supplied invertors and frequency converters with intermediary d.c. circuit (chapter 13).

The fourth part describes the most frequently usages of power electronic circuits dealt with in the third part, namely, the control of the d.c. or a.c. electric machines and the control of the non-reactive loads from electrothermy, lighting and electrochemistry (chapter 14).

At the end of the book there is a glossary of 62 terms and expressions, a bibliography comprising 15 titles briefly commented upon and an extensive alphabetical index.

This book is intended for the engineers working in the converter domain as well as for the students designing such circuits.

Mircea Oprişor

GRAFIK W., *dBase III*, VEB Verlag Technik, Berlin, 1989, 240 S., ISBN 3-341-00703-2

Les réalisations technologiques — hardware, tout comme le développement des applications — software, ont déterminé une vraie explosion de l'utilisation de l'informatique et, surtout, de la microinformatique. En répondant aux intérêts d'un grand nombre d'utilisateurs, un nombre croissant d'auteurs concentrent leurs efforts dans cette direction.

Le livre de Grafik s'adresse à ceux qui, étant donnée leur profession ou par pure passion, veulent s'initier dans la création et l'exploitation des banques de données. En supposant un minimum de connaissances initialles, l'auteur aborde dans une succession bien graduée les problèmes fondamentaux des banques de données, spécialement du système dBASE III, conçu pour les microcalculateurs de 16 bits, et en opérant sur des calculateurs compatibles IBM. Il y sont expliquées les concepts de banque de données, structures de commande, expressions, fichiers, modifications et compléments de données et structures, entrées, sorties, éditeurs, opérations complexes, utilisations de dBASE III. Les annexes résument les fonctions dBASE, le travail dans le mode direct, extensions possibles pour dBASE III+.

La manière dont est écrit le livre — bien graduée, claire, attractive, avec de nombreux exemples — le récommande comme référence fondamentale tant pour les débutants que pour les avancés.

M. Antonescu

* * * *Wissensspeicher Ultraschalltechnik*. VEB Fachbuchverlag, Leipzig, 1987, 440 S., ISBN 3-343-00205-4.

Les nombreuses et spectaculaires applications offertes par l'utilisation des ultra-sons implique nécessairement l'existence des références de synthèse, où, auprès de la présentation de leurs bases théoriques, on doit y trouver leur description systématique. C'est ce que les auteurs de ce volume se sont proposés et en ont réussi à réaliser.

La partie concernant la physique des ultra-sons synthétise l'information théorique fondamentale relative à la propagation, aux grandeurs caractéristiques, à l'atténuation, à la diffraction, à l'écho, aux analogies électro-mécaniques, à la propagation non-linéaire. Ensuite un vaste chapitre est destiné à la présentation des méthodes de génération des ultra-sons.

Une fois ces connaissances implémentées, dans les chapitres suivants on traite en détail les applications dans les techniques de mesures, le contrôle non-destructif, la diagnose médicale, la localisation, la navigation et les applications de puissance.

Le livre finit avec nombre de chapitres concernant les références, mots-clefs et résumés des standardes d'intérêt dans le domaine.

Un livre plein d'information, fondé sur des éléments théoriques clairement formulés, avec de nombreuses applications, très variées, présentées sous une forme immédiatement accessible à l'utilisateur.

Un livre auquel le niveau scientifique des auteurs et l'expression concise et suggestive lui confèrent les vertues d'une véritable référence fondamentale.

M. Antonescu

KUTTRUFF H., *Physik und Technik des Ultraschalls*. S. Hirzel Verlag, Stuttgart, 1988, 415 S., ISBN 3-7776-0427-5.

Les nombreuses applications offertes par l'utilisation des ultrasons assurent pour le domaine de l'ultra-acoustique l'intérêt d'un public de plus en plus large, où les physiciens et les ingénieurs forment la majorité. C'est le motif pour lequel les cours relatifs à l'ultra-acoustique ne manquent pas de la formation de ces spécialistes.

Le livre de Kuttruff est tout d'abord didactique. L'auteur se propose et réussit à introduire le lecteur non-avisé dans le domaine de l'ultra-acoustique, afin que ensuite lui élargisse peu à peu son horizon théorique et puis le consolide par des applications.

Les dix-sept chapitres unissent d'une manière équilibrée et bien graduée la partie théorique à celle appliquée. Les premiers huit chapitres sont destinés à la présentation de quelques connaissances d'acoustique générale, radiation et diffraction des sons, génération, réception et absorbtion des ultra-sons, génération des hyperfréquences. Dans les sept chapitres suivants on résume les applications fondamentales en relation avec le traitement des signaux et les techniques de mesure, le contrôle non-destructif, la diagnose médicale, la microscopie ultra-sonore, la holographie et la tomographie acoustiques, la cavitation, les applications des ultra-sons à

forte intensité. Les derniers trois chapitres offrent aux lecteurs les références, résument la signification des symbôles et des mots-clefs utilisés.

Un matériel vaste, complet, équilibré, qui se distingue tant par la clarté que par la forme suggestive de la présentation. Un vrai cours fondamental dans le domaine, qui honore l'auteur et offre des connaissances solides au lecteur.

M. Antonescu

BURCKHARDT C.W. (Ed.), *18th International Symposium on Industrial Robots. Proceedings*. IFS Publications, 1988, ISBN 0-948507-97-7.

This volume is the result of the 18th International Symposium on Industrial Robots (ISIR), which took place in April 1988, in Switzerland. It is edited by Professor C.W. Burckhardt, Chairman of the International Scientific Committee of the 18th ISIR, who wrote the Foreword too.

The first group of two papers in the volume (Keynote Papers) presents the situation of robotics in the world and in Switzerland respectively. The period discussed is of the 1980's. Pointing out some difficulties in using and exploitation of robots, the authors present a few ideas to improve this matter of fact. In the first article, Professor D. Fabrizi, Chairman of the International Federation of Robotics (IFR), describes the organizational structures and objectives of IFR, too.

Two chapters in the book have the same name : *Applications* and *Assembly*. The articles relating to assembly underline some aspects. Thus, industrial robots penetrate in midle and small size batch production, e.g. in electronics industry. To do this, assembly robots have to be equipped with suitable sensors and a software flexible enough. In this way the detection of accurate positioning and the dimensional control of components can be achieved and the adaptability of the robot is increased. The adaptability is discussed in other papers too. For example, the part misalignment, a major problem in assembly, is analysed and a few strategies are proposed to solve it. About the software involved in assembly robots control some hierarchical models are developed. These systems can generate action procedures automatically using technics from Artificial Intelligence.

Under the name of *Mechanical Structures* there are some articles describing peculiar constructions of robots in order to obtain better performances. They contain a presentation of the design elements (with pictures of the robots), the advantages and disadvantages of each solution.

Two aspects, *Grippers* and *Sensors*, are treated in a distinct chapter. About grippers two interesting solutions are presented. The first is about electrostatic grippers and it outlines the theories behind electroadhesion and the use of such grippers specially in the textile industry. The second is about shape adaptiv grippers and it describes several ways to realize such a device. Three papers deal with sensors : the ultrasonic sensors and their use for objects locating and identification and the optical seam tracking sensors and their use in welding processes. The design for a high speed robot is the subject of one paper in this chapter too. This is an advanced research and the experiment, made on a robot capable of playing ping pong, is important for some general conclusions concerning the dynamical models and the control algorithms of future robots.

One of the ideas outlined in chapter *Applications in Industry* underline that it is profitable to consider the process to be automated as a whole and to design a flexible cell comprising one or several robots controlled by distributed software.

The *Connection between Robotics and CAD/CAM Systems* is presented in another chapter. By using some powerful software tools important advantages are obtained namely: the simplification of user's tasks, the possibility of an advanced simulation, an increased autonomy and adaptability of the entire workstation. *Economical Aspects and National Experience* is the title of the following chapter. The papers show, by economic arguments, the benefits of the investments in flexible automation and robots. The discussed examples are in automatic assembly, flexible manufacture and microengineering fields. The practical experience with robot applications in Poland is presented in another paper.

The last chapter, *Complex Systems and AI*, illustrates how different technics of Artificial Intelligence can improve the performances of robots. There are presented studies of using expert systems, knowledge aquisition and representation systems, rule-based knowledge systems and simulation software tools. Besides complex applications, specially of assembly type, we may note that AI is used with certain advantages in low level tasks such as the supervision of small flexible manufacturing cell or the replacement of classic PID controllers.

Comprising 45 papers the volume convers all the aspects of robotics and it is a valuable source for knowing the robotics situation in the world.

D. Pănescu

SCHILLER D., *Praktische NF-Verstärkertechnik*. Militär Verlag der DDR, Berlin, 1990, 128 S.

This book treats the field of audio techniques. It is addressed both to beginners as well as to those posessing some experience in this field. The book has a practical character and presents many practical circuits.

It starts with an extremely short introduction which presents the aim and reasons of the book.

Chapter 2, *Fundamentals of Audio Engineering*, introduces some elementary notions, such as audio range, level, dynamic range, distortion, power bandwidth, etc.

Chapter 3 is devoted to preamplifier and treats it in an elementary manner, easy-readable.

Chapter 4 treats the switching of signal sources. It presents the dual quadruple analogue switch TDA 1 029.

Chapter 5, *Ione and Volume Control*, presents passive and active circuits used for this purpose. Some examples using bipolar ICs are also given.

Chapter 6 presents the overloading of the amplifier and some associated measuring circuits.

Chapter 7, *Power Amplifier*, is the most important in the book. It treats different power stage configurations, from the simplest ones (class A and AB power stage) till the NOSFET and IC power amplifiers.

Chapter 8 discusses some practical measures which must be undertaken when constructing a power amplifier.

Chapter 9 is devoted to power amplifier supply.

This book though very concise, contains many application examples and indications which allow the user to construct the desired circuit. The information is accurate and presented at a rather elementary level.

This book should appeal to young enthusiasts interested in constructing power amplifiers.

N.D. Alexandru

* * * *Taschenbuch der Nachrichtentechnik*. Standard Elektrik Lorenz AG, Fachverlag Schiele & Schon, 1988, 477 S., ISBN 3-7949-0477-X.

This manual contains some very important notions and data connected with communications techniques and systems. It offers a global view of the new communications media and techniques. Although this is not a text book, it succeeds to provide the reader with some fundamental knowledge which allow him an easier access to the literature. About one third of the book contains concentrated information rallied in tables.

The first part, *Tables and General Hints*, contains different informations about SI units, universal and atomic constants, codes, levels, attenuation, white noise, radio frequencies, TV channels, technical documentation and many other related topics.

A second part, entitled *Devices and Components*, is a survey of the most important data about resistors, capacitors, semiconductor diodes, bipolar and field-effect transistors, other types of transistors, thyristors, diacs and triacs, integrated circuits and other devices and components.

In a third part, notions and data specific to acoustic and electro-acoustic conversion are displayed.

A fourth part deals with radio and TV, TV standards, videotext, digital audio tape recording, radio data transmission systems, satellite TV communication systems.

Part 5 contains, in a very abbreviated form, the main standards and standardization institutions for communications.

Part 6 treats the main communications techniques such as telephone networks, analogue and digital switching, ISDN, analogue and digital transmission techniques, telephone services.

Part 7 contains informations about communication channels, such as lines and cables, microwave systems, satellites and optical transmission.

Part 8 presents the communications in bureaus and production (CAD—CAE—CAM), telecontrol and data protection.

Part 9 deals navigation systems, including satellite systems and radar.

Part 10 presents some control systems used in the feroviar traffic.

In the last part problems of electric supply are treated in a concise form.

The book ends with an appendix which presents the authors of the book, the activity fields and delivery programs of SEL and an index of notions.

The book is very well-written and conveys a lot of information. It should appeal to students and every communication engineer as it offers a quick access to information concerning communication systems.

N.D. Alexandru

KRESS D., IRMER R., *Angewandte Systemtheorie. Kontinuierliche und zeitdiskrete Signalverarbeitung*. VEB Verlag Technik, Berlin, 1989.

This book presents in a very accurate manner the fundamentals of signals and systems. For a better understanding, the theory was presented in a compressed form and is illustrated with many practical examples.

Chapter 1 presents the theoretical fundamentals of signals and systems (signal processing in time-discrete systems, treatment of random signals using correlation theory and related techniques, etc.).

Chapter 2 is devoted to systems having idealized and elementary characteristics, such as low-pass, high-pass and band-pass filters, linear modulators and others.

Chapter 3 treats the problem of filters (fundamentals, transforms, analog and digital filters).

Chapter 4 is devoted to sampled systems (PCM, digital TV) and treats also the sampling of periodic signals.

Chapter 5 contains an in-depth treatment of noise which is considered both as an useful signal and as a perturbation.

Chapter 6 deals with the spectral analysis of signals using the discrete Fourier transform.

The book ends with an appendix which presents analogue resonators and acoustic surface-wave components.

The book is very well-written and conveys a lot of information. It should appeal to students and interested engineers requiring a thorough back-ground in signal and systems theory.

N.D. Alexandru

* * * *Mikroelektronik Datenbuch. Analoge integrierte Schaltkreise. Konsumguterelektronik.* Militar Verlag der DDR, Berlin, 1990.

This book is an integrated circuits catalogue. It starts with a survey of IC types, nominal and extreme values and measuring conditions of the parameters. It continues with insert and soldering safe measures and a list of abbreviations used in the catalogue. The introductory part ends with a short presentation of the IC packages.

The first part covers the field of analogue ICs for audio and radio equipment.

The second part treats the analogue ICs for TV receivers (IF sound and video amplifiers, vertical deflection circuit, horizontal and video combination, etc.).

The last part covers new developments such as multistandard decoders, signal conditioning and delay circuit, video combination circuit.

The catalogue, though rather concise, contains some application examples and indications, which allow the user to implement the desired circuit. The information is accurate and sufficient.

This book should appeal to all those interested in the design of TV and radio receivers as well as to students in radio engineering.

N.D. Alexandru

EISSLER M., KNAPPMANN R. J., *Praktischer Einsatz von Berührungslos arbeitenden Sensoren*. Expert Verlag, 1989, 404 S., ISBN 3-8169-0361-4.

This book deals with practical use of sensors and offers a global view of the field. A special attention is devoted to the use of proximity sensors and distance measurements. Problems of signal processing and adapting with control system are also dealt with, though not in a thor-

ough manner. Although this is not a text book, it provides the reader with some fundamental knowledge.

The first chapter is a short Introduction into this field. The second chapter, *Pneumatic Sensors*, is a short review of these types of sensors.

In the third chapter, *Introduction to Inductive, Capacitive and Magnetic Sensors*, notions and data specific to these sensors are displayed.

A fourth part deals with application examples for the sensors presented in chapter 3.

Chapter 5 is an introduction to optoelectronic sensors, while chapters 6 contains application examples for them.

Chapter 7 deals with fiberoptic sensors, while chapters 8 contains application exemples for them.

Chapter 9 treats the main types of ultrasound and microwave sensors. Chapter 10 contains informations about fundamentals of image-processing sensors.

Chapter 11 presents videosensors used in image analysis while chapter 12 deals with fundamentals and uses of laser for measurements.

Chapter 13 presents numerous exemples of measurements in the industry using sensors.

The book is well written and contains many valuable informations.

N.D. Alexandru

CASSING M. et al., *Electromagnetische Wandler und Sensoren*. Expert Verlag, 1989, 332 S., ISBN 3-8169-0157-3.

This book deals with different calculation procedures of circuits containing permanent magnets. It contains many examples in which the most important computer-aided procedures and design strategies are explained.

The first chapter is a short presentation of permanent magnets used in radio, TV and telephony applications.

The second chapter deals with the use of permanent magnets in linear and small-angle drives.

In the third chapter, *Magnetic Sensors*, notions and data specific to these sensors are displayed.

A fourth chapter deals with developing an integrated system using the M a x w e l l's equations. This is the most important chapter in the book.

Chapter 5 deals with specific magnetic systems and components used for linear actuators and positioning.

The book is well written and contains many valuable informations. It should appeal to all students and electronic engineers searching for a computer-aided solving of permanent magnet circuit problems and practical applications.

N. D. Alexandru

KAPUR N.J., *Mathematical Modelling*. J. Wiley & Sons, New York, 1988, ISBN 0-470-20088-x, ISBN 81-244-0006-x.

In this book the autor explains the basic principles of mathematical modelling and illustrates these with some simple examples through geometry, algebra, trigonometry and calculus. Each subsequent chapter deals with mathematical modelling through one or more specific techniques. Thus he considers mathematical modelling through ordinary differential equations of first and second order, through systems of ordinary differential equations, functional equations, integro-differential equations, through graph theory concepts, through linear and nonlinear programming, dynamical programming, calculus of variations, maximum principle and through maximum entropy principle.

In each chapter, mathematical models are chosen from physical, biological, social, economic, management and engineering sciences. The models deal with different concepts, but have a common mathematical structure. Thus different problems may be represented in the same form, only the interpretations are different. In the present book mathematical modelling is of primary importance and mathematical technique are of secondary importance one.

The book can be used by the students from mathematics, science, engineering and commerce departements, giving a panoramic view of applications of mathematics in science and technology, and also for special courses on mathematical models in biology and medicine and maximum entropy models in science and engineering.

T. Ganciu

SORRENTINO R., *Numerical Methods for Passive Microwave and Millimeter Wave Structures.* IEEE Press, 1989, X+485 pp., ISBN 0-87942-249-1.

A strong interest in numerical methods and CAD techniques is therefore growing again among researchers, working engineers and students ; most have easy and immediate access to computing facilities powerful enough to analyze rather complicated electromagnetic structures, design elaborate microwave circuits, etc.

It has appeared desirable to collect in one book the most significant contributions in the area of numerical methods and computer techniques in order to provide working engineers with background information on the most representative and useful numerical approaches to the solution of microwave and millimeter wave structures.

This book serve as a reference for students and beginners, since necessary information is scattered throughout the literature.

Owing to the great variety of numerical methods, this book cannot provide extensive information about each numerical method along with a detailed explanation of its variations, improvements, etc. The aim is mainly to introduce the reader to those numerical techniques which have a broad enough field of application and to provide him with a sufficient understanding to apply the methods at least to the solution of some simple problems. The material provided here is expected to be sufficient for a general understanding of the method and its possible applications and limitations. For further details the reader is referred to the reference lists of the reprint papers as well as to the additional reference lists provided in the introductions to the parts. Overview papers of Part 1 and tutorial papers of the specific parts are an extremely useful starting point for further study.

The book is divided into 11 parts. The first consists of overview papers and serves as an introduction and a general reference to numerical computation in the field of microwave and millimeter wave structures. Each subsequent part is devoted to a different numerical technique. Typically, each contains a tutorial paper or one or two historical papers that have contributed significantly to the development of that specific technique. Subsequent refinements, improvements, or extensions together with examples of applications are then illustrated by additional papers. Emphasis has been placed on problems involving modern planar and quasi-planar structures, but also more conventional structures have been considered. Very recent contributions are included to provide the reader with an up-to-date reference.

Each part starts with a brief introduction. This has the purpose, particularly when no overview paper is included, of setting in a historical perspective not only the reprint papers but also some cited papers which could not be included for reasons of space.

Each method has its own advantages and disadvantages, but it must be emphasized that more than one may be suitable for the solution of a given problem. An initial selection can be made on the basis of the structure or the problem to be solved. Choice must then be made in terms of several aspects, namely, accuracy, computing efficiency, memory requirements flexibility, and versatility. One of the purposes of the introductory part is to provide critical information about the various numerical approaches, which is crucial for making a well-reasoned choice of the method best suited for the problem at hand.

Numerical methods are presented, roughly, in the order of increasing analytical complexity, starting with the more numerically oriented methods. Parts 2 ... 5 are devoted to the least analytical but most versatile methods (finite-difference, transmission-line matrix, finite-element, and boundary-element methods, respectively). The method of lines, which combines a two-dimensional finite-difference procedure with an analytical formulation in the third direction, is presented in Part 6. The method of moments, which represents a wide variety of numerical techniques and is somewhat related to many other methods, is presented later, in Part 7. Techniques requiring a progressively increasing amount of analytical preprocessing are included in Parts 8 ... 10 (mode-matching and spectral-domain approach, respectively). Circuit formalisms for the analysis of planar structures and related numerical methods (planar waveguide model, planar-circuit approach, segmentation and desegmentation methods) are included in the final part.

Irinel Casian

BÜRGER E., *Dictionary of Information Science.* Elsevier Science Publishers, Amsterdam, 1988, 904 pp., (in 2 volumes), ISBN 0-444-98904-8

More and more industrial and economic activities are now carried out with the help of computers. Owing to its integrative character, informatics has turned out to be the decisive basic science in laying the foundations for the effective use of computer technology in all areas.

It is especially owing to the microcomputer that information-processing technology has entered all areas of life and can solve tasks on an undreamt-of scale. Software development has been speeded up by the use of scientific methods, techniques and aids of informatics such as more effective programming languages, software engineering and documentation. As a result, informatics has gained in importance as a basic subject matter in secondary schools, colleges and universities.

This dictionary has been compiled with all these developments and trends in mind and by making use of the appropriate international scientific literature in the original languages, especially books and journals in English, Russian, German and French, dealing with the state of the art and further development of informatics and applied computer science and engineering. It covers the general fundamentals of informatics such as computer architecture ; hardware and software components; systems engineering; interactive and batch processing ; fundamentals of software development (programming) such as conceptual formulation, program implementation, data acquisition and data management; hardware components such as circuits, memories, input/output devices, interfaces, data acquisition terminals, sensors and actuators ; transmission media and network controllers ; system reliability ; such as CIM, CAD, CAM, artificial intelligence, expert systems and databases.

The alphanumerical organisation of the entries enables the reader to translate from any one to any other of the four featured languages, by using the indexes.

This four-language reference book has been developed particularly for specialized scientists and engineers working in informatics. It should be of value to lecturers and students at universities, technical and engineering colleges, and other schools of higher education where tnformatics is being studied, and will also serve as a useful tool for translators and documenialists.

APPLEBY B. L., *Elsevier's Dictionary of Commercial Terms and Phrases* (in English, German, Spanish, French and Swedish). Elsevier Science Publishers, Amsterdam, New York, 1984, 1 084 pp., ISBN 0-444-42270-6.

The technical progress of the 20th century has led to revolutionary changes in the world of commerce, which have proceeded at an increasingly fast pace since the end of the second world war. Trade has become internationalized. Both the container and, later, the computer have made many long-established business routines absolute and necessitated the creation of new ones. Today's businessmen must be equipped with a knowledge of economics, finance, law and technology in order to be able to make the right kind of decision.

This work is an attempt to reflect the complexity of modern commerce. Terms have been selected from a wide range of fields, including economics, finance, banking, stock-broking, customs procedures, and shipping. Account has also been taken of the fact that not all countries in the world are at the same level of development and so a number of older terms relating to customs procedures and piece-goods shipping procedures have been retained. Unlike the majority of such works Swedish equivalents have been included as an acknowledgement of the importance of the Nordic countries in world trade.

Terms are given in English with their equivalents in German, Spanish, French and Swedish, thus covering the most important commercial languages in the non-Communist world. Finally, the large number of terms, over 10,000, should help to ensure that this work will become a major aid to translators, students, businessmen and all others who have to cope with financial and economic texts in a variety of languages.

WITTMAN A., KLOS J., *Dictionary of Data Processing. Including Applications in Industry, Administration and Business.* Fifth, Revised and Enlarged Edition, Elsevier Science Publishers, Amsterdam, New York, 1987, 358 pp., ISBN 0-444-98947-1.

The vocabulary in the field of electronic data processing continues to develop extremely rapidly. The great variety of hardware and software, the ability of computers to process and store millions of data within ever shorter periods of time and the increasing number of different applications, especially in the field of office automation, have proved to have a lasting effect on the vocabulary used in both the written and the spoken language.

In the fifth edition of the *Dictionary of Data Processing*, some 300 new terms and approximately 150 acronyms have been added in order to bring it up to date and keep place with these developments. The authors have retained the convenient, easy to use format of previous editions, i.e. a basic numbered listing of English American terms in alphabetical order, with the equi-

valents in German and French, plus separate indexes in German and French keyed to the basic table by number. The Dictionary of Data Processing has for many years been a valuable working tool for all those involved in the field of data processing, including systems engineers, computer scientists, technicians, translators, interpreters, and information scientists. This new enlarged edition will continue to be a useful reference.

YUNGUI CI, CHENGXI ZHANG, CHENGZHENG SUN (Ed.), *New Generation Computing, Recent Research*. Elsevier Sci. Publ., Amsterdam, New York, XVI+348 pp., 1990, ISBN 0-444-88730-X.

New Generation Computing and Supercomputing have attracted a large amount of research effort throughout the world. This book introduces some of the recent research carried out of China. It consists of forty-two papers covering five main areas : logic-based inference machines from sequential to parallel ; knowledge-based systems ; heuristic search in AI ; dataflow computer architecture ; and optimization techniques for supercomputing.

C o n t e n t s : *Introduction*. Logic Programming. Knowledge-Based Systems. Dataflow Computation. Problem Solving and Search. Supercomputing.

Sequential Prolog Systems. On Some Issues in Implementation of Prolog. Extending the WAM with Execution Mechanisms for Non-Logical Components of Prolog. Implementation and Management of Prolog Code Databases. Implementation and Management of Prolog Source Databases and Management of Prolog Source Databases. Implementation of Prolog Builtins in the WAM-PLUS. Designing the Architecture of a Prolog Machine Based on the WAM-PLUS. An Integrated Implementation of Database Operations. Clause Representations. An Efficient Type System for Prolog listof : A Pragmatic Consideration on setof. Partial Solution, An Incomplete Inference Way to Approximate to the Solution of Negated Goal.

Parallel Processing of Logic Programs. The OR-Forest Description. The PSOF Process Model. Parallel Execution of Negative Goals. Automatic Partition of Subgoals. Compile-Time Detection of ADN-Parallelisms. An Environment Sharing Scheme. An Algorithm for Environment Reduction. An OR-Forest-Based Parallel Abstract Machine.

Knowledge-Based Systems. Foundations for Knowledge Systems. On Knowledge Base System Architecture. The Knowledge Base System KBS-1. Design and Implementation of a Relational Knowledge Base Prototype Machine. Performance Evaluation of Relational Knowledge Base Prototype Machine. A Tool for Building Second Generation Expert System. Improving Expert System Behaviour. Knowledge Acquisition Mechanism. Attribute Theory in Learning System.

Dataflow Computation and Architecture. A Performance Evaluation Model for Static Dataflow Computers. An Ordered Model Combining Dataflow with Control Flow. Architecture of a Synchronous Dataflow System. A Multi-Microcomputer System for Simulating SDS-1. Macro-Dataflow Computational Model and its Simulation.

Heuristic Search and Statistical Inferences. Statistical Inference Method in Heuristic Search Techniques. The Computational Complexity. The Extraction of Global Information. The Comparison Between the Statistical Heuristic Search and A. Hierarchy and Heuristic Search.

Issues of Supercomputing. Parallel Execution of Non-DO Loops. Optimization for the Parallel Execution of Non-DO Loops under the LIM. Speedup Studies of the LIM for Non-Do Loops in Comparison with the SIM. Processor Self-Scheduling for Parallel Loops in Preemptive Environments. Approches to Decentralized Control of Job Scheduling for Homogeneous and Heterogeneous Parallel Computer Systems.

References. Index.

BUDIG P., *Drehzahlvariable Drehstromantriebe mit Asynchronmotoren*. Verlag Technik, Berlin, 1988, 296 S., ISBN 3-341-00487-4.

Elektrische Antriebe spielen als elektromechanische Energiewandler bei allen Transport- und Produktionsvorgangen eine wichtige Rolle. Von besonderer Bedeutung ist dabei ihre leichte Steuer- und Regelbarkeit, die es ermöglicht, den als Folge der technischen Rationalisierung steigenden Ansprüchen an die Flexibilität und Präzision der Antriebsaggregate gerecht zu werden.

Das vorliegende Buch von Prof. P.-K. B u d i g entstand in der Absicht, das Zusammenwirken von drehzahlgeregelten Drehstrommotoren und den sie speisenden Stromrichtern dar-

zustellen. In dem Buch werden elektrische Drehstromantriebe mit Asynchronmotoren aus systematischer Sicht behandelt.

Durch die verschiedenen Kombinationsmöglichkeiten von bestimmten Steuerungsmethoden und -strukturen mit bestimmten Motoren besteht eine relativ große Variantenzahl von Drehstrom-Antriebssystemen.

Bei der Drehzahlstellung von Drehstromantrieben erwachsen für den Anwender besonders daraus Probleme, daß er es hier mit nicht sinusförmigen Strömen und Spannungen zu tun hat, wodurch die Momente, Verluste und Netzrückwirkungen relativ schwierig zu beherrschen sind.

Das Buch wendet sich gleichermaßen an Entwickler und Projektanten drehzahlvariablen Drehstromantriebe wie an Studierende der Elektrotechnik in der Endphase ihrer Ausbildung.

D. Alexa

SCHÖNFELD R., HABIGER E., *Automatisierte Elektroantriebe*. Verlag Technik, Berlin, 1990, 524 S., ISBN 3-341-00701-6.

In den letzten Jahren ist das Gebiet der geregelten elektrischen Antriebe stark in Fluß gekommen. Umgekehrt hat in der Vergangenheit aber auch die Regelungstechnik durch Forderungen aus dem Bereich elektrischer Antriebe wesentliche Impulse erhalten, die dazu führten, daß neuartige Regelverfahren entwickelt und in die Praxis eingeführt werden konnten. Dabei war auch der Gesichtspunkt maßgebend, daß Antriebe — im Gegensatz z.B. zu verfahrenstechnischen Regelstrecken — wohlbekannte Strukturen und gut definierte dynamische Eigenschaften aufweisen.

In dem Buch von Prof. R. Schönfeld und Prof. E. Habiger werden elektrische Antriebe aus systematischer Sicht behandelt. Stoffauswahl und Darstellung sind auf Entwurf und Dimensionierung des Antriebssystems unter Einbeziehung der Rechentechnik und der Mikroelektronik ausgerichtet. Aus dieser Sicht gesehen ist das Buch ein Bindeglied zwischen Darstellungen der elektrischen Maschinen und der Leistungselektronik einerseits und der Steuerungs- und Automatisierungstechnik andererseits.

Das Buch richtet sich an Studenten, Projektanten und Betrieber automatisierter Elektroantriebe.

D. Alexa

SAHNER G., *Digitale Messverfahren*. VEB Verlag Technik, Berlin, 1990, 152 S., ISBN 3-341-00819-5.

The book of prof. Gerald Sahner is part of the fameous collection „Meßtechnik" of the Publishing House „Verlag Technik", Berlin, collection which has contributed in a substantial manner to the improvement of the metrological level, training specialists from many countries, including Romania.

Written in a very concise and clear style, this work offers for the reader a big amount of up-to-date practical and theoretical information, dealing with the field of technics and devices for digital measurement.

So, after the author introduces the reader in the basic theoretical problems of the digital measurement (in chapters 1 and 2), in chapters 3 and 4, the main part of the work, the author does a close and through analysis of A/D and D/A converters, with emphasis on dynamic and static errors.

In the last chapter, the author presents the main types of apparatus and devices for digital measurement, with emphasis on modern multimeters guided by microprocessor.

Through his contents and richness of topical information, the present book is a very useful working-aid for the specialists from industry and education.

M. Antoniu

GLASER W., *Lichtwellenleiter*. VEB Verlagtechnik, Berlin, 1990, 144 S., ISBN 3-341-00793-8.

The work of W. Glaser successfuly intends to present the field of optical-fibre systems, a very up-to-date and developing one.

With a very easy to understand and suggestive style, axed specialy on the physic phenomena than mathematical apparatus, the author present the fundamental problems of thelephony with optical-fibre systems and interfacing the computers and TV with such systems.

In this way, after be analysed in the first three chapters the qualities of the light as information-carrier, in the 4th chapter presents the main types of optical fibre systems, with emphasis on the principal damages that may occur (reflection and refraction possibilities).

Then, in the chapters 5 ... 8 is presented the problem of the blocks for processing information by optical means : light sources, (LED-s, LASER-s), sensors (photo-diodes, photo-transisstors), optical-coupling elements and atenuators.

In chapters 9 and 10 are presented some applications of up-to-date optical metrology ; a special attention is payed for the telephone without battery.

At last, the chapter 11 presents the actual tendencies in the developing of the optical metrology and telephony, with emphasis on optical devices with thin layers.

Drawing a conclusion, the present work is very interesting for telecommunication-engineers and for those dealing with optical metrology.

M. Antoniu

SPINDLER E., *Antennen : Anleitung zum Selbstbau*. VEB Verlag Technik, Berlin, 1990, 276 S., ISBN 3-341-00837-3.

The book, in a revised edition, is a very useful guideline for those enthusiasts who really want to build by themselves their own TV antennas. Due to the author's great experience in the field (almost any type of the antenna described in the book was practically constructed by the author himself) and to the great number of standards, norms, tables and nomograms included, the book contains the complete information necessary to build an antenna for any TV channel, in any norm or standard having the appropriate gain, beamwidth and input impedance.

The author organized the material in 7 chapters followed by 8 appendices. The first chapter presents the main topics regarding the antennas, such as : input impedance, radiation pattern, gain, front-to-back ratio, beamwidth, frequency band, etc. Then, the antenna basic properties and the main types of antennas are shortly described ; a special attention is given to the dipole antenna.

The second chapter (a very short one) gives the necessary information for choosing the optimal antenna type, taking into account the TV norm used and the needed frequency band and channel. The specific problems of a colour TV receiving are encountered at the end of the chapter.

The third chapter refers to the practical problems raised by the effective construction of an antenna, its mounting, its possible far-controled electrical rotation and its pattern alteration by simple electronic means.

The fourth chapter firstly presents the VHF Yagi antenna arrays with 1 to 22 elements. There are given the elements'dimensions and spacings for any TV channel and standard (CCIR, OIRT, American, English, French, etc.). The gain and the pattern in *E* and *H* planes are presented, too. The author presents, also, the criteria one must use in order to make a good choice.

The same things can be said about the second part of the chapter that deals with the UHF Yagi antenna arrays. The 6 to 35 element antenna arrays are presented. The construction of some largeband antennas (e.g. log-periodic dipole antennas) is described, along with the main advantages and disadvantages put by the use of these complicated antennas. Some special types of antennas (such as X-element antenna and corner-reflector antenna) are encountered in this chapter, too.

A special part is devoted to the parabolic-reflector antenna that is extensively used in satellite TV receiving ; a simple design method is given.

The last part of this chapter describes some special types of antennas : room-antenna, window-antenna, shorted VHF antenna, etc.

The fifth chapter presents the groups of antenna arrays (arrays of arrays) comprising identical or different-type arrays, as well as antenna amplifiers and switches.

The main TV antenna feed standard cables and their use in practical constructions are the subjects of the sixth chapter.

The seventh chapter is devoted to the satellite TV. A detailed receiver presentation is made and the parabolic reflector's design, construction and verifying are given ; a very useful limit error table is included. There are, also, presented some general problems of the microwave

theory and practice. The position of all the satellites transmitting TV programs, their channels and the TV norm used are indicated in a special table.

All the appendices are grouped in the final chapter (the eighth) of the book. It includes standard mechanical and electrical protection rules, the TV and FM-radio norm parameters used all over the world, the amateur-radio bands and the black-and-white and colour TV norm adopted by any country in the world.

As we have already said, this excellent book contains the complete information one needs to build by himself the desired TV antenna and it is, therefore, a very useful tool for technicians, radio-amateurs and engineers working in the field, as well as, for all those who wish to use a self-made performant TV antenna.

I. Bogdan

IOINOVICI A., *Computer-Aided Analysis of Active Circuits*. Marcel Dekker Inc., New York and Basel, 1990, XVI+591 pp., ISBN 0-8 247-8 126-0.

The problem of ever-growing complexities in circuit design is a challenging actual subject. Different computer programs have become available for the simulation, testing and layout design of microelectronic circuits. However, a good interpretation of computational results requires a thorough understanding of the underlying theories and algorithms. The designer must also be aware of the strengths and inherent limitations of each program. In many cases he has to modify an existing program or even write a new one.

The fact that microelectronic design has become such a complex multidisciplinary enterprise has a very strong impact on electrical and electronical engineering education : there is a great need to introduce high-level topics, usually considered as intangible for an undergraduate or a practicing engineer, in such a way as to make them comprehensible for any reader level. It was for the book under review to fill such an important gap in the existing literature on circuit analysis.

Computer-Aided Analysis of Active Circuits is an excellent treatise on this subject, and is exceptionally well suited for a two-semester course in basic circuit theory and computer-aided circuit analysis and design. It is written in a very clear style and includes numerous references and an extensive list of available market circuit simulation programs. Fundametal methods of circuit analysis such as loop equations, nodal and modified nodal equations, and state equations are explained using a computational, topological approach. Every method is illustrated by a number fully solved examples and each chapter includes an extensive set of proposed problems keyed to the subject matter discussed. The table of contents and the index are detailed and can be very helpful in locating specific subjects. Original easy-to-use programs for dc, ac, and transient analysis, based on the nodal and loop methods, as well as some relevant subroutines, are listed in the Appendices.

The present work is not only an outstanding textbook, but also an extremely valuable reference for graduate students and researchers. It provides the state-of-the-art for the methods presented as well as some of the author's very recent research results. Topics like an introduction to the centering statistical design and references to the MACSYMA program were included for the first time in a textbook.

Dr. A. I o i n o v i c i is first a teacher ; his flair for guiding the student is manifestly evident in the text. After a short introduction on active circuits and network elements in Chap. 1, beginning with Chap. 2, the author focuses the reader's attention to network topology, the key to computer-aided circuit analysis. The topological concepts and the methods of loop, nodal and modified nodal analysis are developed in an easy-to-follow, progressive, logical manner, by considering first, in Chap. 3, simple one-port resistive networks and then general resistive networks and, after a short discussion on computer-aided solution of circuit equations in Chap. 4, following on, in Chap. 5, by considering *RLC* networks consisting of two terminal elements and only lastly the general case of dynamic circuits containing all types of elements.

Chapter 6 is an excellent survey on dynamic circuit analysis by the state equations method.

In Chapter 7 the author gives a general overview of the state-of-the-art in computer-aided analysis of cyclically switching circuits, although his confessed intention was only to show how the two main methods studied in the preceding chapters, the modified nodal algorithm and the state equations algorithm, can be applied for solving practical circuits. Some of the most promising methods in computer-aided analysis of cyclically switching circuits were developed very recently by the author himself, based on the definition of a new circuit element called *alternor*.

Chapter 8 provides a general discussion on transfer functions, active circuits stability and active filters, while Chap. 9 is a short introduction in the topics of circuit sesitivities and optimization.

Although primarily addressed to the undergraduate students, I believe that this exemplary book will be an essential reading for practicing engineers, particularly circuit designers and authors of computer-aided design software, as well as for circuit theory researchers too.

Em. Savin

WINDISH G., *M - matrices in Numerical Analysis*. Teubner, Leipzig, 1989, 140 S., ISBN 3-322-00710-3.

This book is published in the series „Teubner - Texte zur Mathematik" (vol. 115). It is devoted to M -matrices, a subclass of matrices which can be expressed in the form $A = Is - B$, with $s > 0$, $B \geq 0$ and I — unit matrix. The term „M - matrix" (M i n k o w s k i matrix) was first used by A. O s t r o w s k i in a paper published in 1937 in reference to a work of M i n k o w s k i published in 1900.

The book concerns the role of M - matrices in Numerical Analysis. Succeeding the author's intentions, the book presents the fundametals of M - matrix theory in an accessible way and the intimate relationship between nonsingular M - matrices and the discretization of second order linear elliptic and parabolic problems by finite difference methods, finite element methods and the method of lines.

The book is divided into two main parts. In the first part (Chapters 2 and 3), the class of M - matrices is introduced and important M - matrix properties are discussed according to subsequent applications in discretization methods.

In the second part (Chapters 4...6) one deals with the basic properties of the continuous problems (i. e. elliptic and parabolic second order equations) reflected in discrete approximations by nonsingular M - matrices. This approach applies to inverse-monotonicity, nonnegativity and monotonicity of solutions, maximum principles and conservation laws.

The book is highly recommended to applied mathematicians, systemists and control engineers which are interested in numerical analysis and simulation.

M. Voicu

MAREK I., ZITNY K., *Matrix Analysis for Applied Sciences*. Teubner, Leipzig, 1983, 1986.

This book in two volumes is published in the series „Teubner-Texte zur Matematik" (vol. 60—1983, vol. 84—1986). It is a systematic text on matrix theory where the matrices are treated as representations of linear operators in finite-dimensional vector spaces. A deeper penetration of functional analysis into various disciplines of Mathematics and other branches of Science yielded the authors to show the matrix as the most elementary concept of functional analysis. Thus the book contains all standard topics of the matrix theory as well as some much modern parts as theory of generalized inverses. Illustrating the aim of the book, the heading lines of the chapter are very transparent and significant : Algebraic Preliminaries, Metric Spaces, Selected Topics from Functional Analysis, H i l b e r t Spaces, Elements of Mathematical Analysis, Spectral Analysis, R i e s z Operators with Rational Resolvent Functions, Normal Operators with Rational Resolvent Function, Complexification, J o r d a n Representation of Linear Operators, Variational Principles, D r a z i n's Pseudoinverse Operator, M o r e - P e n r o d e Operator.

The book is written in a very clear and rigorous style according to the following scheme : definition — lemma — proposition — theorem — remark — example.

The book is intended to a broad class of readers who have to solve problems for which matrix theory and elements of functional analysis are appropriate and useful. The explanation is autonomous and problems solved together with a large scale of exercices are good tools for a reader to get an inside into various applications. It is suited for graduate students and scientists which use mathematical models and system theoretic concepts and methods.

M. Voicu

GROEN J., SMIT E., EIJSVOOGEL J. (Eds.), *The Discipline of Curiosity. Science in the World.* Elsevier Science Publishers, Amsterdam, 1990, 180 pp., ISBN 0-444 88861-6.

In the 20 th Century, more than ever before, the world is being shaped by science. Science has an intrinsic value in trying to find out how the world ticks, and it has an enormous and increasingly social value too. The scientific enterprise of today provides the information for the society of tomorrow. Scientists have become leading actors in world history.

The discipline of curiosity, as science may be called, is not just a discipline of from, it is also a discipline of ends : political, moral, cultural and commercial ends. Science and technology have become features of daily life. In this book of interviews, fifteen opinion leaders (prominent figures from international politics, business, communication and science) give their vision on the changing role of science in society. They all agree that scientific information is essential, not just for the scientist. For with the recognition of its crucial importance comes the understanding that the scientific entreprise is, or should be, a concern to everybody. The scientist is a central figure and has to communicate with politicians, entrepreneurs and public at large.

The problems to be faced are manifold and include questions like : How should education policies be adjusted ? How to combat the danger of an unequal spread of knowledge within human societies? How to prevent groups getting excluded from democratic processes because they have not learnt to understand ? How do we get scientific information in a form that is adequate and comprehensible to the various groups of potential users ? Will the knowledge and technology gap between the industrialized countries and the Third World widen even further? What are the consequences of different cultures having different approaches to sciences? Those, and other questions come up for discussion in this book.

C o n t e n t s : Introduction. The Haves and Have Nots (D. H a l b e r s t a m, the observer). An African Dream (S. O g u n s e i t a n, the information gatherer). Coordination without Funds (F. M a y o r Z a r a g o z a, the diplomat). The Human Lemmings (A. K i n g, the activist). The Government catalysis (E. B l o c h, the science policy-maker), What Price Presearch ? (H. B e c k e r s, the industrial scientist). Breaking the Mould (H. Y a m a d a, the scientist Japan). East—West Mergers (T. O l t e a n, the communication analyst). We Must not Lead (R. B e r n h a r d t, the lawyer). The Black Hole of Consciousness Advances (K. S i e g b a n n, the physicist). The Communication Deficit (S. M i n o v a, the publisher). The Public Digestion (J. M a d d o x, the editor). About the People Interviewed. Index.

ELZAS M. S., ÖREN T. I., ZEIGLER B. P. (Eds.), *Modelling and Simulation Methodology in the Artificial Intelligence Era.* North-Holland, Elsevier Science Publishers B. V., Amsterdam, 1986, ISBN 0-444-70 130-3.

In the Artificial Intelligence era the Modelling and Simulation domain cannot exists without the research results of the former. Moreover, a real kinship exists between Artificial Intelligence, Modelling and Simulation. These are the main ideas which are reflected throughout this volume.

The book gives an overview of the state-of-the-art, presents new research results and shows future developments in these interdisciplinary fields. This is emerged from the third Working Conference organized ever to devote itself entirely to modelling and simulation methodology in July, 1984, at the Conference Center near to Wageningen Agricultural University in the Netherlands.

The book contains those papers which presented important ideas relevant to the main theme in a clear and readable manner and is divided into seven sections.

From a survey of the field and conceptual bases to the related tools and techniques, the structures for knowledge-based model processing, the symbolic processing in simulation, the variable structure and learning models, the AI in simulation quality assurance and AI techniques in modelling of organizational problems are introduced and presented in a graded manner.

Both the AI and Simulation comunity use models as the main way with which they convey their knowledge. Many ideas on how to proceed are presented in this book and in the work that is continually going on to improve the methodologies in these two computer-related fields of research. There are outlined an appraisal of the kinship between AI, Modelling and Simulation, a system knowledge definition and its implicants, the applicability of AI techniques to knowledge representation in Modelling and Simulation, and the implications of machine learning in simulation.

The structures for knowledge-based model processing are presented with help of the relations between AI enviroments and Modelling and Simulation support systems, the entity-based struc-

tures for model and experimental frame construction, the knowledge-based model storage and retrieval, the approach to model composition from existing models and the structuring of linear optimization problems. The model components for symbolic processing by knowledge-based systems, the possibilities for expert aids in system simulation, the applications of expert systems concepts to adaptive experimentation with models, the world view-based discrete event model simplification and the transformation of a discrete-event system into a logic programming formalism sketch the symbolic processing in simulation.

The problems associated with the modelling of systems with variable structure are solved based on the learning automata theory, the models with variable structure, the development of hierarchical, modular model specification languages and the use of explicit constraints to evaluate a potentially unique, neural model for single-interval concept manipulation. A renewed attention is done to the ever more important issues of model validation and quality assurance of simulation experiments which can originate as well from *a priori* advisory standpoints as from *a posteriori* certification points of view. There are also presented the AI techniques in the extremely hard modelling of the organizational problems like as the societal systems, the strategic-level gaming, the decision support in negotiating process, information systems and in the office form-flow systems.

The last section of the volume is concerned with some novel developments in the area of practical tools that make use of recent results in computer science, that are the production rule-based techniques to process modelling, the involvement of logic programming based on possible modification of Prolog for simulation and graphic interfaces for modelling systems.

The book is written in an unitary and a concise manner outlining the impact of the results of Artificial Intelligence research, on the one hand, and of the Modelling and Simulation research, on the other hand, in the daily practice in a multitude of computer related fields. As both fields are strongly based on models, the fact that these two areas are on the brink of a period of synergy comes as more or less logical consequence. This volume will be of interest to all who use the modelling and simulation techniques in their work, like as the modern control systems, pattern recognition or computer vision scientists.

Teodor Marcu

HANNEMAN H. W., *The Patentability of Computer Software*. Kluwer Law and Taxation Publishers, Deventer, 1985, ISBN 90-6 544-255-1.

The book represents a monograph which is concerned with the international patentability of computer-related inventions and provides a complete guide to this more and more important problem. A computer-related invention is sought as a computer or computer-aided apparatus/method operating under programmed control to perform a novel, non-obvious function, and which apparatus/method is susceptible of industrial applications. These inventions represent valuable achievements which are as expensive to produce as they are easy to copy. As a result of the computers development, the users of computer software also soon realized that software had an independent and often considerable economic value and thus an increasing need arose for the protection of software, too. So, the question whether and, if so, how software is to be protected have been under discussion for more than 30 years.

The object of this book is to review the possibilities of protecting the computer software by means of patent law and to provide an international guide as to where the borderline between patentable and unpatentable advances in computer software has been drawn.

The volume is structured in 14 chapters. An introductory chapter presents an overview of the various other legal and technical forms of protecting software such as the copyright law, the trade secret and the contract law, the trademark and the technical protection and the patent law, because a single method of protection of computer software which is optimum in all circumstances cannot be indicated. The relative merits of each of them and the allowable combinations are also included. After this, a chapter for the non-technical gives a simple explanation and provides a glossary of some of the jargon used by computer-people.

The backbone of this work is concerned with the development of the natural law, the case law, the decisional law, and the actual position regarding the computer software patentability. Thus, the possibilities of protecting software under the patent laws of all major industrialized countries are presented by means of the common law in the U. S. A., Great Britain, Canada and Australia, and by the position taken in the civil law in France, Germany, Austria, Switzerland, Japan, and the Netherlands, respectively. The patentability of computer-related inventions under the European Patent Convention and under several European national laws are also discussed.

Finally the book presents the general conclusions and some recommendations on how the law should be.

The volume is written in a rigorously and an unitary manner reflecting the difficult and complex borderline between computer technology and law, on the one hand, and the patent practice great experience of the author in a large multinational company, on the other hand. Both of these aspects have leaded to an urgent need for a comprehensive study on cases subject to judicial controversy in the field of the patentability of computer-related inventions. Thus, the book provides a very practical assistance both to those directly involved in the development and marketing of software and those called upon for advice in this area. It is also offered a pertinent analysis and some models to several Eastern Europe countries where computers programs are excluded from patentability by law.

Teodor Marcu

Coli tipo : 7,5

Tiparul executat sub cd. nr. 181
la S.C. „Dosoftei" S.A. Iași
Str. Sf. Lazăr, nr. 49

1991 AUG 14

40822

ISSN 0258-9109